October 2015

Prediction of the Optimum Binder Content of Open-Graded Friction Course Mixtures Using Digital Image Processing

Yolibeth Mejias De Pernia
University of South Florida, tewis@hotmail.ca

Prediction of the Optimum Binder Content of Open-Graded Friction Course Mixtures Using Digital Image Processing

by

Yolibeth Mejias de Pernia

A dissertation submitted in partial fulfillment
of the requirements for the degree of
Doctor of Philosophy in Civil Engineering
Department of Civil and Environmental Engineering
College of Engineering
University of South Florida

Major Professor: Manjriker Gunaratne, Ph.D.
Gangaram Ladde, Ph.D.
James Musselman, M.E.
Qing Lu, Ph.D.
Wilfrido Moreno, Ph.D.

Date of Approval:
September 15, 2015

Keywords: Asphalt Pavement, Pie Plate Visual Method, Perceptual Image Coding

DEDICATION

I dedicate my dissertation work to my family and friends. A special feeling of gratitude to my loving husband, Juan Pernia whose words of encouragement and push for tenacity ring in my ears. My kids Juan Jose, Carlos and Leonardo have never left my side and are very special.

ACKNOWLEDGMENTS

I would like to express my sincere gratitude to my advisor, Professor M. Gunaratne, whose direction and lasting encouragement have been truly inspiring.

A sincere thank you to my committee members, Professors Qing Lu, Wilfrido Moreno, Gangaram Ladde, and Mr. James Musselman, for offering their time and input in completing this dissertation. Their opinions and contributions are gratefully appreciated.

The greatest appreciation to everyone from the bituminous section of the FDOT State Material Office (SMO), especially my dearest friend, Susan Andrews, for their contributions in terms of expert knowledge, experience, and constructive advice through the course of this work.

I would also like to extend my heartfelt gratitude to John Metz, Menna Yassin and Yordanka Goodwin for their academic and professional advice.

Last but not the least; I would like to thank all my loved ones. Even when they were not physically with me during this time, I know in my heart that they were always supporting me from afar.

TABLE OF CONTENTS

LIST OF TABLES v

LIST OF FIGURES ix

ABSTRACT xv

CHAPTER 1: INTRODUCTION 1
1.1. Background 1
1.2. Problem Statement and Research Objectives 3
1.3. Contributions of the Research 5
1.4. Dissertation Outline 5

CHAPTER 2: LITERATURE REVIEW 7
2.1. OGFC Pavement Technology 7
2.1.1. Flexible Pavements 7
2.1.1.1. Dense-Graded Friction Course (DGA) 8
2.1.1.2. Open-Graded Friction Course (OGFC) 8
2.1.1.3. Gap-Graded Friction Course (SMA) 8
2.1.2. History of OGFC Mixtures 9
2.1.3. Proposed Benefits of OGFC Mixtures 10
2.1.3.1. Safety 10
2.1.3.2. Noise Attenuation 10
2.1.3.3. Performance of OGFC Mixtures 11
2.2. Design of OGFC Mixtures 12
2.3. Imaging Methods and Application in Asphalt Mixture Analysis 14
2.4. Human Visual System 19
2.5. Neural Networks 20

CHAPTER 3: EXPERIMENTAL METHODOLOGY 22
3.1. Phase I (Determination of OBC of OGFC Mixtures Using FM 5-588 Imaging Process)…. 22
3.1.1. Material Selection 24
3.1.2. Determination of OBC of OGFC Mixtures Using FM 5-588 24
3.1.3. FDOT Imaging Technology 29
3.1.4. Validation of FDOT Imaging Process 31
3.1.4.1. Clean Database 33
3.1.4.2. Check Data for Outliers 33
3.1.4.3. Estimate Correlation Coefficients 34
3.1.4.4. Regression Analysis 35

3.1.4.5. Interpretation of the Regression Statistics Table 38
3.1.4.6. Findings of the Validation Section 39
3.2. Phase II (Development of OBC Image-Based Prediction Method).....41
3.2.1. Digital Image Acquisition and Processing.....41
3.2.2. Development of a Model to Automate the FM 5-588 Method to Predict OBC.....46
3.3. Phase III (Development of Image–based Quality Control Tool (QCT)).....46
3.3.1. "How to Develop" the Image-Based Quality Control Imaging Parameters (QCIP).....47
3.3.2. "How to Evaluate" The Image-Based Quality Control Imaging Parameters (QCIP).....48

CHAPTER 4: DEVELOPMENT OF A PERCEPTUAL-BASED IMAGE MODEL 50
4.1. Image Analysis Procedures for Characterization of the Human Visual System 51
4.1.1. Image Contrast.....51
4.1.2. Visibility 51
4.1.2.1. Connectivity of Black Pixels 52
4.1.2.2. Number of Connected Black Pixels Regions 52
4.1.2.3. Orientation of Connected Black Pixels Regions.....52
4.1.3. Contrast Sensitivity.....52
4.1.3.1. Size Distribution of the Target.....53
4.1.3.1.1. Sizes (Areas) of Connected Black Pixels Regions 53
4.1.3.1.2. Perimeter per Connected Black Pixels Regions.....53
4.1.3.2. Spatial Frequency of the Target.....53
4.1.3.2.1. Uniformity Radial 53
4.1.3.2.2. Uniformity Angular 54
4.1.4. Frequency and Orientation Selectivity.....54
4.1.4.1. Inconsistency Coefficient.....54
4.1.4.2. Centroidal Distances 55
4.1.4.3. Form Factor.....55
4.1.5. Other Imaging Parameters Involved in Information Processing in the HVS 55
4.1.5.1. Compactness per Connected Black Pixels Regions.....57
4.1.5.2. Solidity.....57
4.1.5.3. Eccentricity 58

CHAPTER 5: QUALITY CONTROL MODEL 59
5.1. Measure and Analyze ABD Characterization to Provide Quantifying QCIP 59
5.1.1. Orientation 60
5.1.2. Spatial Distribution 61
5.1.3. Segregation 62
5.2. Statistical Verification of QCIP 63
5.2.1. Orientation 64
5.2.2. Spatial Distribution 64

5.2.3. Segregation 66
5.3. Assess Scientific Acceptability of Measure Criteria of the QC Results 66
5.3.1. Orientation 70
5.3.2. Spatial Distribution 70
5.3.3. Segregation 70

CHAPTER 6: NEURAL NETWORK-BASED PREDICTION MODEL 71

CHAPTER 7: SUMMARY OF FINDINGS 75
7.1. Phase I- Preliminary Assessment of the Asphalt Binder Content Determination 75
7.2. Phase II- Prediction of Optimum Asphalt Binder Content 75
7.3. Phase III- QC Test Results and Analysis 80
7.4. Implementation of the Neural Network-Based OBC Estimation 87

CHAPTER 8: CONCLUSIONS 89

CHAPTER 9: RECOMMENDATIONS FOR FUTURE WORK 91

REFERENCES 92

APPENDIX A: TABLE OF EXPERIMENTAL TEST PLAN 99

APPENDIX B: TRACKING OF THE EXPERIMENTAL PROCESS 103

APPENDIX C: DETERMINATION OF OBC TEST FOR OGFC MIXTURES 107

APPENDIX D: GENERAL INFORMATION BY MIX 114
D.1 General Information of Mix A 114
D.2 General Information of Mix B 116
D.3 General Information of Mix C 118
D.4 General Information of Mix D 120
D.5 General Information of Mix E 122
D.6 General Information of Mix F 124
D.7 General Information of Mix G 126
D.8 General Information of Mix H 128
D.9 General Information of Mix I 130
D.10 General Information of Mix J 132
D.11 General Information of Mix K 134
D.12 General Information of Mix L 136
D.13 General Information of Mix M 138
D.14 General Information of Mix N 140
D.15 General Information of Mix O 142
D.16 General Information of Mix P 143
D.17 General Information of Mix Q 146
D.18 General Information of Mix R 148

D.19 General Information of Mix S 150

APPENDIX E: COMPARISON OF LABVIEW AND MATLAB RESULTS 152

APPENDIX F: RESULTS OF ASPHALT CONTENT CORRELATIONS 171

APPENDIX G: GRNN PREDICTION MODEL TABLES 194

APPENDIX H: STEPS FOR USING THE AUTOMATED OBC PREDICTION MODEL 199

APPENDIX I: STATISTIC TABLES 214

APPENDIX J: COPYRIGHT PERMISSIONS 237

LIST OF TABLES

Table 1 Problems encountered with OGFC mixtures 12

Table 2 Categorization of OGFC mix designs based on the OBC determination method 13

Table 3 OGFC gradations used for the study 25

Table 4 Coefficients of correlation for all the mixtures used for the study 34

Table 5 Results of the combined regression analysis. 36

Table 6 Summary output of the combined regressions for mix A 36

Table 7 Comparison of results of simple regression versus multiple regression for all the mixtures used for the study 38

Table 8 Regression statistic table for mix J 39

Table 9 Comparison of results of individual regression versus combined regression 41

Table 10 Imaging parameters that represent the visual transfer process used for the study. 58

Table 11 Statistical "t-test" for the QC parameters 65

Table 12 Evaluation of scientific acceptability of measurement properties based on reliability and validity ratings. 66

Table 13 Internal consistency values 69

Table 14 One-dimensional sample set of training and testing input data and predicted output data. 77

Table 15 Multi-dimensional sample set of training and testing input data and predicted output data. 79

Table 16 Quality control parameter results for (a) orientation (Δ_f), (b) spatial distribution (*SD*), and (c) segregation (*S*) results for sample sets for mixtures "A" to "S" 81

Table 17 Results of parameters for defective pies sets 82

Table A1 Experimental test plan.....99

Table B1 Tracking of experimental process for granite NS315 mix designs.....103

Table B2 Tracking of experimental process for granite GA553 mix designs 104

Table B3 Tracking of experimental process for oolitic 87339 mix designs.....105

Table B4 Tracking of experimental process for oolitic 87145 mix designs.....106

Table D1 Aggregate and binder type for mix A 114

Table D2 FDOT OGFC gradation specifications for mix A.....114

Table D3 Aggregate and binder type for mix B 116

Table D4 FDOT OGFC gradation specifications for mix B.....116

Table D5 Aggregate and binder type for mix C 118

Table D6 FDOT OGFC gradation specifications for mix C.....118

Table D7 Aggregate and binder type for mix D 120

Table D8 FDOT OGFC gradation specifications for mix D.....120

Table D9 Aggregate and binder type for mix E.....122

Table D10 FDOT OGFC gradation specifications for mix E 122

Table D11 Aggregate and binder type for mix F 124

Table D12 FDOT OGFC gradation specifications for mix F 124

Table D13 Aggregate and binder type for mix G 126

Table D14 FDOT OGFC gradation specifications for mix G.....126

Table D15 Aggregate and binder type for mix H 128

Table D16 FDOT OGFC gradation specifications for mix H.....128

Table D17 Aggregate and binder type for mix I.....130

Table D18 FDOT OGFC gradation specifications for mix I 130
Table D19 Aggregate and binder type for mix J.....132
Table D20 FDOT OGFC gradation specifications for mix J 132
Table D21 Aggregate and binder type for mix K 134
Table D22 FDOT OGFC gradation specifications for mix K.....134
Table D23 Aggregate and binder type for mix L.....136
Table D24 FDOT OGFC gradation specifications for mix L 136
Table D25 Aggregate and binder type for mix M.....138
Table D26 FDOT OGFC gradation specifications for mix M 138
Table D27 Aggregate and binder type for mix N 140
Table D28 FDOT OGFC gradation specifications for mix N.....140
Table D29 Aggregate and binder type for mix O 142
Table D30 FDOT OGFC gradation specifications for mix O.....142
Table D31 Aggregate and binder type for mix P 144
Table D32 FDOT OGFC gradation specifications for mix P 144
Table D33 Aggregate and binder type for mix Q 146
Table D34 FDOT OGFC gradation specifications for mix Q.....146
Table D35 Aggregate and binder type for mix R 148
Table D36 FDOT OGFC gradation specifications for mix R.....148
Table D37 Aggregate and binder type for mix S 150
Table D38 FDOT OGFC gradation specifications for mix S 150
Table G1 Data base for the granitic and oolitic materials using GRNN model 194
Table G2 Training, testing and predicting data base for the granitic and oolitic materials using GRNN model.....196

Table I1 *t*-values for various values of *df* confidence intervals 214

Table I2 T-test values for various spatial distribution values of *df* confidence intervals.....215

Table I3 One-sample test for various values of *df* confidence intervals 226

LIST OF FIGURES

Figure 1 Types of flexible pavements. 8

Figure 2 FDOT mix design image references 14

Figure 3 Flowchart of the study overview....23

Figure 4 Gradation curves for Nova-Scotia source aggregate (A-E) 25

Figure 5 Gradation curves for Georgia source aggregate (F-J)....26

Figure 6 Gradation curves for Florida source aggregate (K-P)....26

Figure 7 Gradation curves for Florida source aggregate (Q-S)....27

Figure 8 Steps followed for the pie plate preparation according to FM 5-588 including: (a) material preparation, (b) batch preparation, (c) mixture/pie plate's preparation, and (d) visual inspection to estimate OBC 28

Figure 9 Sample aggregate batching sheet (for mix K)....30

Figure 10 Pie plate and custom bracket 31

Figure 11 Typical calibration dot matrix unit 31

Figure 12 Comparison of digital imaging results for mix A - Labview versus Matlab 32

Figure 13 Percent of asphalt binder prediction using simple regression for mix A....37

Figure 14 Percent of asphalt binder prediction using combined regression for mix A.....37

Figure 15 Mix J trial 1.1 at 5.8%AC (a) %AC versus %black area, (b) %AC versus %Connected black area.....40

Figure 16 Sequences of steps followed for the enhancement procedure 42

Figure 17 Pixel connectivity schemes (a) 4-neighbor connectivity next pixels, (b) 4-neighbor connectivity corner pixels and (c) 8-neighbor connectivity. 44

Figure 18 Representation of (a) tracing of regions of black pixels connected and (b) labelling of regions of black pixel connected by color and numbers. 45

Figure 19 Sequences of steps followed for the pre-processing the pie plate digital images 46

Figure 20 Synthetic computer-generated images of (a) steps to create ellipses representing the connected black pixel regions of a PPS (b) uniformly distributed PPS, (c) slid (unevenly distributed) PPS, (d) properly placed PPS, (e) incorrectly placed PPS, (f) appropriately mixed PPS, and (g) inappropriately mixed PPS 49

Figure 21 Representation of black pixels on a pie plate image for connected black pixels (a) color label, (b) orientation relative to the center of the pie plate image, (c) individual areas, (d) traced perimeters, (e) label with numbers, (f) illustration of sections of radial segregation and angular mesh. 56

Figure 22 Example of convex hull of a connected black pixels area 57

Figure 23 Representation of connected black pixels on a pie plate image for SABD identification of the orientation relative to the center of the pie plate image 61

Figure 24 Representation of connected black pixels on a pie plate image for SABD identification for the location in the angular mesh. 62

Figure 25 Representation of connected black pixels on a pie plate image for SABD identification illustrating sections of segregation. 63

Figure 26 Calculation of Cronbach's alpha for all the mixtures considered in this study. 68

Figure 27 Neural network flowchart for (a) multi-dimensional, (b) one dimension....73

Figure 28 Neural network estimated AC for predicted versus actual for (a) one dimension training data, (b) one dimension testing data (c) multi-dimension training data, (d) multi-dimension testing data. 78

Figure 29 Optimum binder content prediction for multi dimension GRNN validation prediction model. 80

Figure 30 Distribution orientation parameter (θ_f) for (a) an acceptable quality of a real pie plate image and (b) a slide synthetic pie plate image. 84

Figure 31 Bar chart representing spatial distribution (*SD*) of connected black pixel areas of a sample set (Mixture A) and a computer-generated set of pie plate 85

Figure 32 Segregation results for predetermined AC contents for all of the samples testing in this research....86

Figure D1 Gradation curves for mix A 115

Figure D2 Gradation curves for mix B....117

Figure D3 Gradation curves for mix C.....119
Figure D4 Gradation curves for mix D.....121
Figure D5 Gradation curves for mix E.....123
Figure D6 Gradation curves for mix F.....125
Figure D7 Gradation curves for mix G.....127
Figure D8 Gradation curves for mix H.....129
Figure D9 Gradation curves for mix I.....131
Figure D10 Gradation curves for mix J.....133
Figure D11 Gradation curves for mix K.....135
Figure D12 Gradation curves for mix L.....137
Figure D13 Gradation curves for mix M.....139
Figure D14 Gradation curves for mix N.....141
Figure D15 Gradation curves for mix O.....143
Figure D16 Gradation curves for mix P.....145
Figure D17 Gradation curves for mix Q.....147
Figure D18 Gradation curves for mix R.....149
Figure D19 Gradation curves for mix S.....151
Figure E1 Labview versus Matlab digital image results -mix A.....152
Figure E2 Labview versus Matlab digital image results -mix B.....153
Figure E3 Labview versus Matlab digital image results -mix C.....154
Figure E4 Labview versus Matlab digital image results -mix D.....155
Figure E5 Labview versus Matlab digital image results -mix E.....156
Figure E6 Labview versus Matlab digital image results -mix F.....157

Figure E7 Labview versus Matlab digital image results -mix G 158
Figure E8 Labview versus Matlab digital image results -mix H 159
Figure E9 Labview versus Matlab digital image results -mix I.....160
Figure E10 Labview versus Matlab digital image results -mix J.....161
Figure E11 Labview versus Matlab digital image results -mix K 162
Figure E12 Labview versus Matlab digital image results -mix L.....163
Figure E13 Labview versus Matlab digital image results -mix M.....164
Figure E14 Labview versus Matlab digital image results -mix N 165
Figure E15 Labview versus Matlab digital image results -mix O 166
Figure E16 Labview versus Matlab digital image results -mix P.....167
Figure E17 Labview versus Matlab digital image results -mix Q 168
Figure E18 Labview versus Matlab digital image results -mix R 169
Figure E19 Labview versus Matlab digital image results -mix S.....170
Figure F1 Mix A %black area versus %binder contents 171
Figure F2 Mix A %connected black area versus %binder contents.....171
Figure F3 Mix B %black area versus %binder contents 172
Figure F4 Mix B %connected black area versus %binder contents 172
Figure F5 Mix C %black area versus %binder contents 173
Figure F6 Mix C %connected black area versus %binder contents 173
Figure F7 Mix D %black area versus %binder contents 174
Figure F8 Mix D %connected black area versus %binder contents.....174
Figure F9 Mix E %black area versus %binder contents.....175
Figure F10 Mix E %connected black area versus %binder contents.....175

Figure F11 Mixtures NS315 %black area versus %binder contents.....176
Figure F12 Mixtures NS315 %connected black area versus %binder contents 176
Figure F13 Mix F %black area versus %binder contents 177
Figure F14 Mix F %connected black area versus %binder contents.....177
Figure F15 Mix G %black area versus %binder contents.....178
Figure F16 Mix G %connected black area versus %binder contents 178
Figure F17 Mix H %black area versus %binder contents.....179
Figure F18 Mix H %connected black area versus %binder contents 179
Figure F19 Mix I %black area versus %binder contents 180
Figure F20 Mix I %connected black area versus %binder contents.....180
Figure F21 Mix J %black area versus %binder contents.....181
Figure F22 Mix J %connected black area versus %binder contents.....181
Figure F23 Mixtures GA553 %black area versus %binder contents.....182
Figure F24 Mixtures GA553 %connected black area versus %binder contents.....182
Figure F25 Mix K %black area versus %binder contents.....183
Figure F26 Mix K %connected black area versus %binder contents 183
Figure F27 Mix L %black area versus %binder contents.....184
Figure F28 Mix L %connected black area versus %binder contents.....184
Figure F29 Mix M %black area versus %binder contents.....185
Figure F30 Mix M %connected black area versus %binder contents.....185
Figure F31 Mix N %black area versus %binder contents.....186
Figure F32 Mix N %connected black area versus %binder contents 186
Figure F33 Mix O %black area versus %binder contents.....187

Figure F34 Mix O %connected black area versus %binder contents 187
Figure F35 Mix P %black area versus %binder contents 188
Figure F36 Mix P %connected black area versus %binder contents 188
Figure F37 Mixtures 87339 %black area versus %binder contents.....189
Figure F38 Mixtures 87399 %connected black area versus %binder contents 189
Figure F39 Mix Q %black area versus %binder contents.....190
Figure F40 Mix Q %connected black area versus %binder contents 190
Figure F41 Mix R %black area versus %binder contents.....191
Figure F42 Mix R %connected black area versus %binder contents.....191
Figure F43 Mix S %black area versus %binder contents 192
Figure F44 Mix S %connected black area versus %binder contents 192
Figure F45 Mixtures 87145 %black area versus %binder contents.....193
Figure F46 Mixtures 87145 %connected black area versus %binder contents 193

ABSTRACT

Florida Department of Transportation (FDOT) has been using Open Graded Friction Course (OGFC) mixture to improve skid resistance of asphalt pavements under wet weather. The OGFC mixture design strongly depends on the Optimum Binder Content (OBC) which represents if the mixture has sufficient bonding between the aggregate and asphalt binder. At present, the FDOT designs OGFC mixtures using a pie plate visual draindown method (FM 5-588). In this method, the OBC is determined based on visual inspection of the asphalt binder draindown (ABD) configuration of three OGFC samples placed on pie plates with pre-determined trial asphalt binder contents (AC). The inspection of the ABD configuration is performed by trained and experienced technicians who determine the OBC using perceptive interpolation or extrapolation based on the known AC of the above samples. In order to eliminate the human subjectivity involved in the current visual method, an automated method for quantifying the OBC of OGFC mixtures was developed using digital images of the pie plates and concepts of perceptual image coding and neural network (NN). Phase I of the project involved the FM-5-588 based OBC testing of OGFC mixture designs consisting of a large set of samples prepared from a variety of granitic and oolitic limestone aggregate sources used by FDOT. Then the digital images of the pie plates containing samples of the above mixtures were acquired using an imaging setup customized by FDOT. The correlation between relevant digital imaging parameters and the corresponding AC was investigated initially using conventional regression analysis. Phase II of the project involved the development of a perceptual image model using human perception metrics considered to be used in the OBC estimation. A General Regression Neural Network (GRNN) was used to uncover the

nonlinear correlation between the selected parameters of pie plate images, the corresponding AC and the visually estimated OBC. GRNN was found to be the most viable method to deal with the multi-dimensional nature of the input test data set originating from each individual OGFC sample that contains AC and imaging parameter information from a set of three pie plates. GRNN was trained by 70% and tested by 30% of the database completed in Phase I. Phase III of the project involved the configuration of a quality control tool (QCT) for the aforementioned automated method to enhance its robustness and the likelihood of implementation by other agencies and contractors. QCT is developed using three quality control imaging parameters (QCIP), orientation, spatial distribution, and segregation of ABD configuration of pie plate specimens (PPS) images. Then, the above QCIP were evaluated from PPS images of a variety of independent mixture designs produced using the FDOT visual method. In general, this study found that the newly developed software (GRNN-based) provides satisfactory and reliable estimations of OBC. Furthermore, the statistical and computer-generated results indicated that the selected QCIP are adequate for the formulation of quality control criteria for PPS production. It is believed that the developed QCT will enhance the reliability of the automated OBC estimation image processing-based methodology.

CHAPTER 1: INTRODUCTION

1.1. Background

In the US, there are several methods employed for designing open-graded friction course (OGFC) mixtures based on the estimation of optimum binder content (OBC). There are (i) compacted specimens method, (ii) absorption calculation method, and (iii) visual determination method [1]. The methods currently use by several Department of transportation (DOT) agencies (Alabama, Arizona, Florida, Georgia, Kansas, Kentucky, Mississippi, Missouri, Nebraska, Nevada, New Jersey, New Mexico, North Carolina, South Carolina, Tennessee, Texas, Virginia, and Wyoming) and four national organizations (American Society for Testing and Materials (ASTM), the Federal Highway Administration (FHWA), the National Asphalt Pavement Association (NAPA), and the National Center for Asphalt Technology (NCAT)).

The visual OBC determination procedures of the above agencies involve more or less similar general steps. In this process, uncompacted asphalt mixtures are prepared at varying trial asphalt binder contents (AC) specific to the aggregate and binder types and placed in clear pie plates for visual inspection of the bottom of the pie plates for the asphalt binder draindown (ABD) configuration [2]. The preparation of pie plate samples requires heating of the mixture at a specified temperature for a specified period of time. The binder grades, time and temperature at which the mixture is prepared, varies by procedure [1]. The inspection of the ABD for each procedure, however is always performed by trained and experienced technicians who determine the OBC based on perceptive interpolation or extrapolation from the prescribed AC. The need to

resolve the constantly encountered inconsistency issues in predicted OBC results is essential to assure the accuracy of the OGFC mixture design.

The Florida Department of Transportation (FDOT) has been using OGFC mixtures on Florida's high speed asphalt pavement facilities since the early 1970's [3]. OGFC is a porous pavement surface type consisting primarily of coarse aggregate with few fines, thereby permitting water to pass freely through it, in contrast to more traditional dense graded asphalt pavement surfaces. The increased permeability of OGFC mixtures reduces the hydroplaning potential of the pavement under wet weather conditions. In addition, OGFC surfaces also reduce the splash and spray behind vehicles and improve the surface reflectivity during wet-weather conditions [4].

In Florida, all asphalt mixtures are designed by the contractors and submitted to FDOT for review and verification, with the exception of OGFC mixtures. OGFC mixtures are designed by the FDOT's State Materials Office using Florida design Specification in Section 337 [5] and the Florida Method FM 5-588 - *Determining the Optimum Asphalt Binder Content of an Open-Graded Friction Course Mixture Using the Pie Plate Method* [2]. FM 5-588 is based on the 1974 Federal Highway Administration (FHWA) OGFC Design Procedure [6]. In the FM 5-588, the OBC is determined based on *visual assessment* of ABD on three pie plates with three pre-determined trial asphalt binder content AC. The OBC is adjudged to be the binder content at which the sample displays sufficient bonding between the mixture and the bottom of the pie plate without evidence of excessive ABD [2]. This method allows the OBC to be interpolated between the three trial AC presented on the pie plates.

While FM 5-588 has proven to be an effective method of designing OGFC mixtures, the OBC estimates of even similarly qualified technicians have proven to be highly variable at times since human subjectivity is introduced into the visual inspection of the ABD on the pie plates. In

order to eliminate this inherent subjectivity and make the OBC determination more repeatable and accurate, an automated procedure is needed to determine the OBC of OGFC mixtures. While previous research has involved in-depth analysis of a design method to determine the ACs from images of asphalt mixtures in general [7], only limited information is available on imaging which determine accurate OBC values. Hence, the objective of this research was to use a digital imaging process in conjunction with concepts of perceptual image coding and NN to estimate the OBC of OGFC mixtures in an automated manner.

The investigation was divided into three phases. Phase I involved the use of the conventional FM 5-588 to test nineteen OGFC mixtures designs which generated an extensive set of samples from granitic and oolitic limestone aggregate sources and the subsequent imaging of the corresponding pie plates using FDOT's customized imaging setup. In addition, statistical analysis was performed to correlate a set of relevant and basic image parameters derived from the pie plate images to the AC of the pie plates. Phase II of the investigation involved further analysis of image parameter and visual OBC estimates from Phase I to develop a perceptual image model based on applicable metrics of the human vision system (HVS) and neural networks (NN) to predict the OBC values in an automated manner. Phase III involved the configuration of a quality control tool (QCT) for the aforementioned automated method to enhance its robustness and the likelihood of implementation by other agencies and contractors. QCT is developed using three quality control imaging parameters (QCIP), orientation, spatial distribution, and segregation of ABD configuration of pie plate specimens (PPS) images.

1.2. Problem Statement and Research Objectives

In the US, twenty-percent of the Department of Transportation (DOT) agencies have standard procedures for designing open-graded friction course (OGFC) mixtures based on the

estimation of optimum binder content (OBC). Approximately ten percent of the aforementioned agencies currently use the visual determination procedure for estimating the OBC of OGFC mixtures. They are Florida (FM 5-588), Georgia (GDT 114), Nevada (Nev. T760C), New Jersey (NJDOT B-7) and South Carolina (SC-T-90) [1].

Currently, however, FDOT use a pie-plate *Visual Determination* method (FM 5-588) based on a FHWA method to design OGFC mixtures. In this method, the OBC is determined solely based on visual assessment of binder draindown on three pie plates with trial binder contents. The OBC is selected at the binder content where the sample displays sufficient bonding between the mixture and the bottom of the pie plate without evidence of excessive asphalt binder draindown [2]. While previous research has involved in-depth analysis of a design method to determine the percent asphalt content from images [7] there is limited information comparing the results of different mixtures design methods determining an accurate OBC.

The goal of this research was to provide FDOT with guidance in terms of refining the existing imaging process for FM 5-588 by developing an automated visual standard test methods for directly and quantifying the OBC for OGFC mixtures. To achieve the above goal, the following objectives are identified for this work:

- Identify all of the significant image parameters that impact the prediction of the binder content of pie-plates.
- Develop a correlation between the relevant image parameters and the OBC of OGFC mixtures in an accurate manner.
- Develop a software package to execute the OBC estimation of OGFC mixtures using digital images of the pie plates.

- Develop a software package to execute the quality control process for digital images based OBC determination.

1.3. Contributions of the Research

An automatic digital test methods for directly quantifying the OBC for OGFC mixtures using parallel processing, Perceptual image coding and neural networks is developed. It avoids the disadvantages of traditional method (FM 5-588) which predicts OBC subjectively. The research has the following impacts:

- Evaluation of the OBC asphalt mixture using the automated method will save a lot testing time.
- Investigation of the possibility of applying innovative concepts of machine vision to simulate the technicians' perception of the asphalt binder drain-down.
- Development of a methodology for complete automation of the FM 5-588 process thereby minimizing the subjectivity involved in its current version and rendering it to be more reliable.
- Developing a quality control parameters based on image processing which would be a viable tool for future design of OGFC mixtures.

1.4. Dissertation Outline

This dissertation is organized into nine chapters with the following specific contents:

- Introduction – This chapter includes a background of OGFC mixture design. The background is followed by the problem statement, research objectives, contributions of the research and the dissertation outline.
- Literature Review – This chapter is divided into five distinct sections. The first section details the various concepts useful for understanding the flexible pavement design principles and best practices associated with OGFC pavement technology. The second discusses the proposed benefits of OGFC mixtures. The third section addresses the design of OGFC mixtures. The

fourth section presents the imaging techniques, perceptual image coding and human vision system using 2D image analysis as well as their application in many areas of visual information processing. The fifth section describes the use of neural network analysis in prediction models in a variety of fields.

- Experimental Methodology – This chapter presents a description of the research methodology.
- Development of the Perceptual-Based Image Model – This chapter identifies the human vision systems (HVS) parameters relevant to the asphalt binder draindown (ABD) characterization of the OGFC samples in pie plates.
- Neural Network-based Prediction Model – This chapter presents the results of the neural network- based prediction model that relates the HVS parameters to the OBC values.
- Quality Control Model – This chapter presents the image analysis procedures that provide quantification relevant to the image-based quality control imaging parameters (QCIP) of the ABD of the pie plate specimen.
- Summary of Findings – Presents a summary of findings in this study.
- Conclusions – Deductions gathered from the most relevant analysis of results are presented in this section.
- Recommendations for Future Work –Directions for future work are provided in this section based on conclusions and analysis completed in this dissertation.

CHAPTER 2: LITERATURE REVIEW

This chapter is divided into five distinct sections. The first section details OGFC pavement technology. The second section illustrated the design of OGFC mixtures. The third section present a brief description of the imaging technics and their application in asphalt mixture analysis. The fourth section discusses the human vision system and the fifth section shows a brief description of the neural network.

2.1. OGFC Pavement Technology

These section details the various concepts useful for understanding the flexible pavement design principles and best practices associated with OGFC pavement technology. Although the primary focus of this research is on the determination of the OBC of the OGFC pavement types, flexible pavements technologies in general have also been explored.

2.1.1. Flexible Pavements

A flexible pavement is a relatively thin surface of asphalt constructed with a bituminous treated surface or a relatively thin surface of hot-mix asphalt (HMA) over one or more unbound base courses resting on a subgrade. FHWA defines a flexible pavement as a "*pavement structure composed of asphalt concrete layers constructed on unbound aggregates or stabilized bases*" [8]. The flexible pavement is called "flexible" since the total pavement structure bends (flexes) to accommodate traffic loads. The components of a traditional flexible pavement typically requires asphalt binder (3-8%), mineral aggregate (85-95%), air voids (2-20%), and sometimes (optional) modifiers/additives [9]. There are various types of asphalt concrete mixtures that combine asphalt cement binder with coarse and fine aggregates. Figure 1 shows the types of flexible pavements.

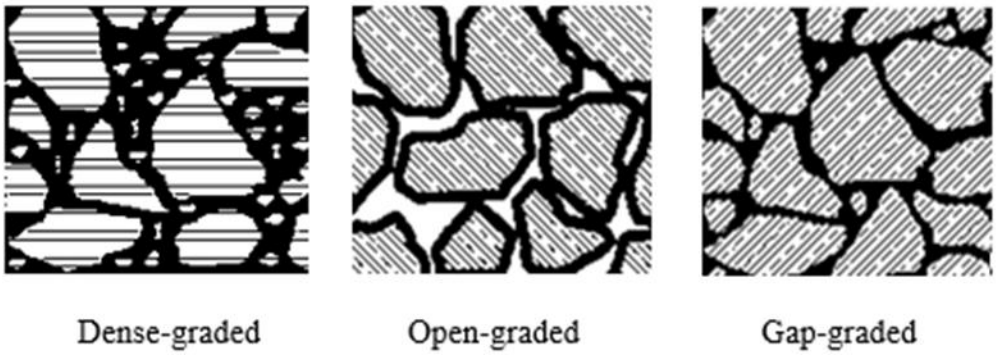

Figure 1 Types of flexible pavements.

2.1.1.1. Dense-Graded Friction Course (DGA)

Dense graded asphalt (DGA) is a mixture of evenly distributed aggregate from smallest to largest size and the binder. It is a well graded mixture typically used for all traffic conditions [9].

2.1.1.2. Open-Graded Friction Course (OGFC)

Open graded friction courses are a type of asphalt mixtures containing only a small portion of fine aggregate, creating a pavement with a relatively large percentage of air voids. They are primarily composed of single size coarse aggregate, and generally have a high asphalt content [9].

In Florida, OGFC mixtures are designed and constructed following Section 337 of the FDOT specification manual and OGFC mixtures are being used in multi-lanes with a design speed greater or equal to 50 mph using two sources of aggregates; granite and Oolitic limestone. The OBC percentages used in common practice are 5.5 to 7.0 percent for granite sources and 6.5 to 7.5 percent for Oolite sources. This range of OBC together with 15 to 25 percent voids allows surface water to enter the pavement structure and then quickly drain through and out of it [5].

2.1.1.3. Gap-Graded Friction Course (SMA)

Stone Mastic (Matrix) Asphalt (SMA) is a mixture of mid-size aggregate and the binder. It is considered to be a gap graded HMA and is typically used for surface courses on high volume highways to improve rut resistance and durability [9].

2.1.2. History of OGFC Mixtures

In 1944, California was the first state in the United States to begin using OGFC on its pavement network after making experimental variations to a maintenance practice called chip seals [10]. Subsequently, in the 1970's, the use of OGFC mixtures gained popularity across the country in response to the FHWA's program to improve skid resistance on roadways [11]. The first OGFC mix design method was published in 1974 by the FHWA [10], then modified in 1980 and further modified in 1990 [11]. The previously mentioned modified design method was based primarily on the surface capacity and absorption properties of the aggregate.

Florida has been using open-graded mixes since the early 1970's to improve skid resistance of asphalt pavements under wet weather [12]. On high-speed multi-lane road designs, OGFC mixtures are specified to allow the runoff water to be drained away from the tire pavement contact area [3 and 12]. For highways with a design speed of 35 mph or greater, three friction course mixtures are specified in FDOT's design manual: FC-5, FC-9.5, and FC-12.5 [13]. Of these, FC-12.5 and FC-9.5 are dense graded mixtures that are placed at approximate thicknesses of 1 1/2" and 1.0", respectively. FC-5, which is an open-graded mixture, is placed at an approximate thickness of 3/4" [13]. FC-5 mixture requires aggregates to be 100 percent polish-resistant crushed granite or crushed Oolitic limestone. If granite is used as the aggregate, hydrated lime in terms of one percent by weight of the total dry aggregate is added to the mixture. Fiber stabilizer additives, either mineral or cellulose, are also needed in the FC-5 mixture regardless of the aggregate type. Mineral fibers are added at a dosage rate of 0.4 percent by total mixture weight, and cellulose fibers are added at a dosage rate of 0.3 percent by total mixture weight.

In Europe, the aggregate standards are higher than in the United States [10] and OGFC mixtures are called Porous European Mixtures (PEM). European countries have started using

PEMs in the early 1960's. For example, the United Kingdom uses PEM in military airfield runways [14]; France uses PEM only on roadways with relatively high design speeds (50 mph) [15], and the Netherlands now uses PEM in the entire highway network [15]. There is a primary difference between OGFC mixtures and PEM: PEM air void content is 18-22% whereas it is 15% for OGFC, which in turn makes PEM more permeable than OGFC mixtures [16].

2.1.3. Proposed Benefits of OGFC Mixtures

The proposed benefits of OGFC pavements range from key environmental benefits to safety benefits. Some of the benefits associated with OGFC pavements include but are not limited to: utilization of technology to provide additional storm-water management measures, reduction in noise levels, increased visibility and improved safety for drivers and pedestrians due to reduced tire splash/spray in wet weather.

2.1.3.1. Safety

A major benefit of OGFC mixtures is that they can provide improvement in road safety for both drivers and pedestrians due to the potential for increased skid resistance especially when there is heavy precipitation and excess runoff conditions [4]. The surface course of OGFC mixtures exhibits properties that may prevent hydroplaning on roadway surfaces because water is allowed to percolate through the pavement surface. In addition, spray and splash are controlled thus improving driver visibility with the reduction of glare on the road surfaces, specifically during wet and dark conditions [4]. For the above reasons, over a period of five years (from 2007 to 2012), FDOT has placed over 195,000 tons of open-graded surface mixtures [17].

2.1.3.2. Noise Attenuation

The high air-voids trap road noise and because of the trapping of the noise, the tire-road noise is reduced by up to 50-percent [18]. Several studies in Europe and North America have found

that OGFC mixtures can help in reducing the noise generated by the tire and road interaction. A 2004 study by the Colorado DOT found that air voids and noise had a linear indirect relationship. The test concluded that, after testing 19 sites, OGFC pavement were the quietest pavements [19]. Furthermore, a study conducted by the University of Florida concluded that when a porous surface course were placed in sections of the US-27 in Florida, a noise level between 97 and 99 decibels (dB) which corresponds to that of a power mower was observed [20].

2.1.3.3. Performance of OGFC Mixtures

Although OGFC mixtures can provide numerous benefits to the highway industry, in a survey by [11] of OGFC use and performance in the United States a number of drawbacks were found. The most common problems with OGFC mixtures were raveling, stripping of existing underlying pavement, and winter maintenance issues. Raveling is the most common distress identified in OGFC mixtures [21] and it occurs in pavements when particles of aggregate still coated with the binder lose adherence to the pavement mixture. Loss of adherence to the pavement occurs due to excessive aging of the asphalt binder or inadequate asphalt binder contents [11]. Table 1 shows problems encountered with OGFC mixtures as reported in [1 and 11].

There are two types of raveling; short term, and long term. Short-term raveling can be intensified by placing the OGFC mixture at too low of a temperature, incomplete seating of aggregates during compaction, and in areas having low asphalt binder content as a result of asphalt binder drainage [22]. Long-term raveling is the result of segregation of the binder from the aggregate due to gradual asphalt binder drainage over time. The nature of OGFC mixtures can lead to the asphalt binder draining down and out of the mixture. This could result due to gravity, transportation of the mixture, or construction practices. The above conditions result in a low binder content of the OGFC mixture closest to the wearing surface, causing dislodging of the aggregate

under the action of traffic [22]. To prevent drainage from occurring in OGFC mixtures, fibers are recommended. The fibers aid in stabilizing the asphalt binder during production and placement [21].

Stripping occurs in pavements when the aggregate and binder become separated due to the presence of water that compromises the bond between the aggregate and binder as a consequence of inadequate drainage [1 and 11].

Table 1 Problems encountered with OGFC mixtures [1 and 11].

	Agency	Typical Problems Encountered
International	Austria	Raveling
	Germany	Raveling
	France	Raveling
	The Netherlands	Raveling & Rapid Aging
	Spain	Raveling & Pore Clogging
	United Kingdom	Pore Clogging & Rapid Aging
United States	Alaska	Ice Removal
	Colorado	Stripping
	Hawaii	Raveling
	Idaho	Pore Clogging
	Iowa	Ice Removal
	Kansas	Ice Removal
	Louisiana	Raveling
	Maine	Ice Removal
	Maryland	Raveling
	Minnesota	Raveling & Pore Clogging
	Rhode Island	Raveling
	South Dakota	Pore Clogging
	Tennessee	Stripping & Ice Removal
	Virginia	Stripping

2.2. Design of OGFC Mixtures

The OGFC mixture design was developed by the Federal Highway Administration (FHWA) [6] and later modified twice by FHWA through research at the National Center for Asphalt Technology (NCAT) [4 and 8]. Consequently, the new NCAT drain-down test method

was created [4]. The above method was used to calculate the degree of drain-down according to FHWA procedures [6].

FDOT uses Florida method FM 5-588 [2] to select the OBC by the visual inspection approach. However, other State DOTs and agencies use different approaches such as (1) compacted specimens and (2) absorption calculation to determine the OBC of OGFC mixtures. Table 2 shows the agencies that use this design procedure and the respective tests adopted by them for the determination of OBC [1, 7 and 23].

In the compacted specimens' procedure, OBC is determined by evaluating compacted specimens having a range of asphalt binder contents, similar to a typical asphalt mixture design procedure [23]. In the Absorption calculation procedure, the binder content is calculated based on the oil absorption value of the aggregate [23]. Finally, in the visual determination procedure, as described in the Introduction, OBC is determined by evaluating the asphalt binder drainage at the bottom of the pie plate by means of visual inspection (Figure 2) [2].

Table 2 Categorization of OGFC mix designs based on the OBC determination method [1, 7 and 23].

Compacted Specimens	Absorption Calculation	Visual determination
ASTM	FHWA	FLORIDA DOT
NAPA	ALABAMA DOT	GEORGIA DOT *
NCAT	ARIZONA DOT	NEVADA DOT
GEORGIA DOT*	GEORGIA DOT *	NEW JERSEY DOT
KANSAS DOT	KENTUCKY TC	SOUTH CAROLINA DOT
NEW MEXICO DOT	WYOMING DOT	
NORTH CAROLINA DOT		
MISSISSIPPI DOT		
MISSOURI DOT		
NEBRASCA DOT		
TENNESSE DOT		
TEXAS DOT		
VIRGINIA DOT		
* USE A COMBINATION OF MIX DESIGNS PROCEDURES		

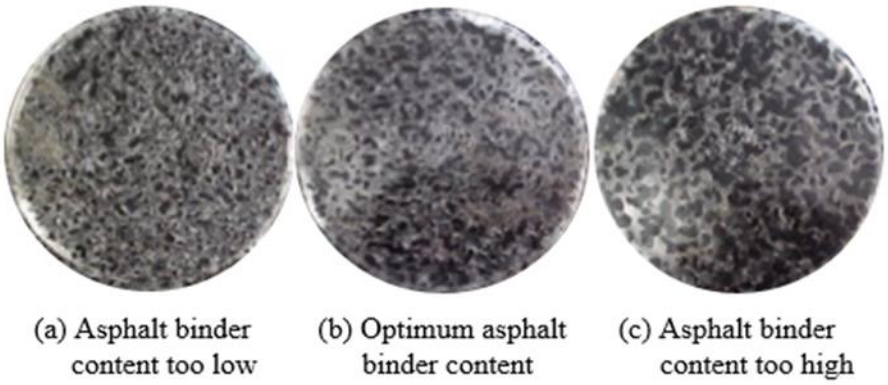

Figure 2 FDOT mix design image references [2].

2.3. Imaging Methods and Application in Asphalt Mixture Analysis

A pavement Mean Profile Depth (MPD) measuring technique was developed [24] with a photometric stereo technique for image capturing with four light sources in a controlled environment. Gray scale intensity distribution of the pavement surface image was used to recover the surface in three dimensions using an iterative global integration technique. MPD measured by a manual dial gauge was correlated with the MPD evaluated from the recovered surface. In this method [24], the color variation of the asphalt surface was not considered during image processing. Since the same gray scale intensity can be obtained from different texture conditions with color, the applicability of the above method in MPD determination is questionable.

A digital Sand Patch Test (SPT) was developed [25] using digital image analysis. In the image analysis, the application of "lacunarity analysis" is used to determine the particle sizes from a digital image of a pavement surface. The SPT investigation also concluded that the reproducibility of SPT is very low but it is still adequate for use in correlations between the average particle size obtained from image processing and the mean texture depth measured by the SPT method.

Another image based macrotexture measuring method was developed in the research documented in [26]. In this method, the Canny edge detection technique of digital image processing was considered for measuring the macrotexture of asphalt pavements. Pavement surface texture coarseness distributions were estimated from the edge profiles of the digital images. Aggregate size was measured by the chord length of edge boundaries using an edge detection pixel count method. During image data collection, the illumination condition was not controlled and image acquisition time varied from morning to afternoon at various times of the year in spite of the general knowledge that image quality varies with illumination. Mean aggregate size obtained from image analysis was statistically correlated with the sensor measured texture readings from a laser profilometer.

A macrotexture (MPD) measuring technique was developed [27] using Aggregate Image Measurement System (AIMS). AIMS was used in the laboratory to measure the macrotexture of aggregate surfaces by analyzing the images of cores from the actual pavements collected from five locations in Texas. The Circular Texture Meter (CTM) was used for measuring macrotexture in the field. Statistical analysis was performed for establishing a correlation with different segment lengths in the MPD calculation. It was suggested that AIMS could be used instead of a CTM for macrotexture measurement.

Recently, a Digital Imaging System (DIS) which is capable of generating the surface texture in three dimensions to identify pavement distresses using high definition images was developed [28]. Although DIS can capture high definition images, it does not provide any friction information about the pavement surface. Considering all these factors, emerging imaging technologies have been introduced for friction measurement by researchers during the last decade

to assure safety and easy operation without requiring lane closure during friction evaluation operations.

A new method was developed by Amarasiri *et al*, 2012 [29] to measure concrete pavement macrotexture on wheel paths using the reflection properties of the concrete pavement surface. In this method, a concrete pavement image was digitally formed for a given light source and camera position using the Bidirectional Reflection Distribution Function (BRDF). BRDF indicates the reflectance property of any surface. Digital images generated from a BRDF model of a concrete surface were compared with the images of concrete samples under identical optical and camera settings. The comparison showed a close resemblance between two images thereby validating the method.

Pavement wearing due to traffic was induced by gradual polishing of the artificial surface in different stages with digital images generated at every stage. On the other hand, concrete samples were also gradually polished in the laboratory and images were captured for analysis.

The above research [29] has established that friction on concrete pavement surfaces can be monitored based on quantifying the brightness of pavement images assuming that the color of concrete pavements remains unchanged. However, when extending this technology to asphalt pavements, the color variation of asphalt pavement needs to be addressed since color changes in asphalt pavements are significant even in the short-term as the aggregates get exposed due to traffic induced wear. In order to use the surface image brightness to quantify frictional variation in asphalt pavements, new filtering approaches have been introduced [30].

A novel method was developed by Peterson *et al*, 2009 [31] for threshold optimization for images collected from contrast enhanced concrete surfaces for air void characterization. In this method, the characterization of the air-voids of hardened concrete relies on "contrast

enhancement" step to make air-voids appear white and aggregate and paste appear black. A Visual Basic script program was developed and employed to analyze contrast enhanced surfaces and perform air void content calculations.

A new method has also been developed for crack detection from pavement images, called the “Crack-Tree” method [32]. This method consists of three steps in which the first step is the geodesic shadow-removal with an algorithm developed to remove the pavement shadows while preserving the cracks. The second step is the development of the crack probability map using tensor voting, which enhances the connection of the crack fragments with good proximity and curve continuity. Finally, the last step is the construction of a graphic model by sampling crack seeds from the crack probability map. In practice, different cracks or crack fragments may show different widths. In the above work [32], the researchers focus on detecting the location and shape of the crack curves, but not the crack width.

Another automated pavement distress detection using advanced image processing techniques has been developed in [33]. In the above work, a self-adaptive image processing method is proposed for the extraction and connection of break points of cracks in pavement images. The algorithm first finds the initial point of the crack and then determines the crack’s classification into transverse, longitudinal and alligator types. Different search algorithms are employed for different types of cracks. Then the algorithm traces along the crack pixels to find a break point and subsequently connects the identified crack point to the nearest break point in a particular search area. The nearest point then becomes the new initial point and the algorithm continues the process until reaching the end of the crack. The experimental results show that this connection algorithm is very efficient in maximizing the accuracy of crack identification.

Finite element modeling of geomaterials using digital image processing has been developed in [34]. “The above research presents a digital image processing method based finite element method for the two-dimensional mechanical analysis of geomaterials by taking into consideration their material non-homogeneities and microstructures. The method includes theories and techniques of digital image processing, the principles of geometry vectorization, and the techniques of automatic finite element mesh generation in the conventional finite element method. Digital imaging techniques are used to acquire the non-homogeneous distributions of geomaterials (soils, rocks, asphalt concrete and cement concrete) in the digital format. Digital image processing algorithms are developed to identify and classify the main homogeneous material types and their distribution structures that form the non-homogeneity of a geomaterial in the image. The interfaces of the main homogeneous material types are vectorized to form the internal material geometric structure and sub-regions. The vectorized digital images are used as inputs for finite element mesh generations using automatic mesh generation techniques. Lastly, the conventional finite element methods are employed to carry out the computation and analysis of geomechanical problems by taking into account the actual internal non-homogeneity of the geomaterial. Using asphalt concrete as an example, this research provides a detailed demonstration of the proposed digital image processing based finite element method. The research also applies the new method to the mechanical analysis of the Brazilian indirect tensile test in rock mechanics and pavement engineering. The numerical results show that this new digital image process based finite element method can take into account the material non-homogeneities in the geomechanical analysis.”

A digital planar image analysis based method for detecting aggregate gradation in asphalt mixtures from planar images has been developed in [35]. The purpose of this study was to finalize an effective analysis of asphalt road section images for automatically extracting aggregate

gradation without the need for physically separating the binder from the aggregate. The proposed methodology allows the user to estimate the aggregate gradation that otherwise would need to be established via specially equipped laboratory and time-consuming tests that also bring about health risks for the operators due to the use of solvents and other hazardous materials.

2.4. Human Visual System

Perceptual approaches have been widely used in many areas of visual information processing. Pylyshyn [36] explain how humans see and visualize and that seeing is different from thinking. It is emphasized that to see is not to create an inner replica of the world one is observing or thinking about or visualizing [36]. In other words, it is emphasized that both seeing and visualizing are different from thinking (and from each other), and that humans' intuitive views about seeing and visualizing rest largely on uncertainties [36]. Specifically, Pylyshyn [36] explains the visual system, the connection between vision and cognition, symbolic representations of percepts, and focuses on problems within one of the most highly developed areas in cognitive science, i.e. visual perception. Pylyshyn [36] traces the relation between the study of vision, the study of mental imagery, and the study of thinking more generally. Specially, the message in the last chapters of Pylyshyn [36] is that, apart from what it feels like to visualize or to examine a mental image in one's mind's eye, imagining and visualizing are a form of reasoning [36].

Numerous other studies have shown that the use of Human Vision System (HVS) techniques have been used to develop design quantification of values, perceptual based image codes, efficacy of human vision code and the use of vision human model and neural networks to reverse engineer networks fields [37-41]. Albanesi and Guerrini [37] adopted a human visual system (HVS) - based model on wavelet technique for tuning the target visual quality to define arbitrarily shaped regions of interest. Wang, Lee, and Chang [38] propose a systematic procedure

to design a quantization table based on the human visual system model for the baseline JPEG coder. Höntsch, and Karam [39] have focused on developing methods to minimize mathematically tractable, easy to measure, distortion metrics. Watson [40] considered the schemes for neural representation of visual information to express explicit image codes. In Thorpe *et al*, 2000 [41] show that the speed of image processing achieved by the human visual system is incompatible with conventional neural network approaches that use standard coding schemes based on firing rate of biological neurons. In the Thorpe *et al*, 2000 [41] results are summaries that demonstrate a number of advantages of such coding schemes.

2.5. Neural Networks

Artificial neural networks (ANN) have emerged as a result of simulation of biological nervous system, such as the brain, on a computer [42]. ANNs have been used intensively for solving regression and classification problems in many fields. In short, neural networks (NN) are nonlinear processes that perform learning and classification and their ability to learn by example makes ANN very flexible and powerful [42].

Recently NN have been used in many areas that require computational techniques such as pattern recognition, optical character recognition, outcome prediction, problem classification, including system modelling, fault diagnosis and control, financial forecasting, weather forecasting, indoor environment and hydrology [43-48]. In materials science and engineering fields, researchers have used neural network techniques to develop prediction models for mechanical properties of materials [43], road crack condition [44] etc. For instance, Haque and Sudhakar [43], have used ANN for the prediction of fracture toughness in microalloy steel, corrosion fatigue behavior and fatigue crack growth in dual-phase (DP) steel. The above mentioned authors report that the ANN back-propagation model with Gaussian activation function exhibited excellent

agreement with the experimental results. Yang [44] performed road crack condition modeling using recurrent Markov chains and ANN where ANN provided a more appropriate and applicable methodology for modeling the pavement deterioration process with respect to cracks [44].

In medical science fields, Generalized Regression Neural Network (GRNN) and Radial Basis Function (RBF) have been used for heart disease diagnosis [45]. In the Hannan *et al*, 2010 [45] research, neural network have been used to prescribe the medicine for heart disease. The results of the above evaluation showed that GRNN and RBF can be applied successfully for prescription of medicine for the patients with heart disease.

Numerous other studies have shown that the use of neural network techniques provide comparable or improved prediction accuracies compared to existing methods in application in weather forecasting, indoor environment and hydrology fields [46-48]. Lee and He [46] adopted the GRNN to predict wind speeds with more accuracy than the traditional one-year linear step-series-based model. Popescu *et al*, 2004 [47], shows that the results of their studies regarding the applications of the NN to the propagation path loss prediction in indoor environment showed good agreement with the measurements [47]. Furthermore, Kişi investigated the GRNN technique in model of reference evapotranspiration (ET0) obtained using the FAO Penman-Monteith equation [48].

CHAPTER 3: EXPERIMENTAL METHODOLOGY

This section describes how the study was conducted. The steps that are involved in this process are identified in the flowchart in Figure 3. Experimental Test Plan is found in Appendix A and Tracking of the Experimental Process are found in Appendix B. Phase I and II were previously documented in Gunaratne and Mejias de Pernia, 2014 [49], Gunaratne and Mejias de Pernia, 2015 [50] and Mejias de Pernia *et al*, 2015 [51]. Phase I[1] involves the selection of material and preparation of the specimen following FM 5-588 (Appendix C). Phase II involves the development of the image-based OBC prediction method and Phase III involves the QCT development process as shown in Figure 3(a), (b) and (c) respectively.

A description of the steps involved in this study is presented in this section in three sub-sections. (i) Phase I (Determination of OBC of OGFC Mixtures Using FM 5-588 Imaging Process), (ii) Phase II (Development of OBC Image-Based Prediction Method) and (iii) Phase III (Development of QCT).

3.1. Phase I (Determination of OBC of OGFC Mixtures Using FM 5-588 Imaging Process)

Phase I is described by sections (i) Material selection, (ii) Determination of OBC of OGFC mixtures using FM 5-588, (iii) FDOT imaging technology, and (iv) Validation of FDOT imaging technology as shown in Figure 3(a).

[1]Portions of this chapter were previously published in [49-51]. Permission is included in Appendix J.

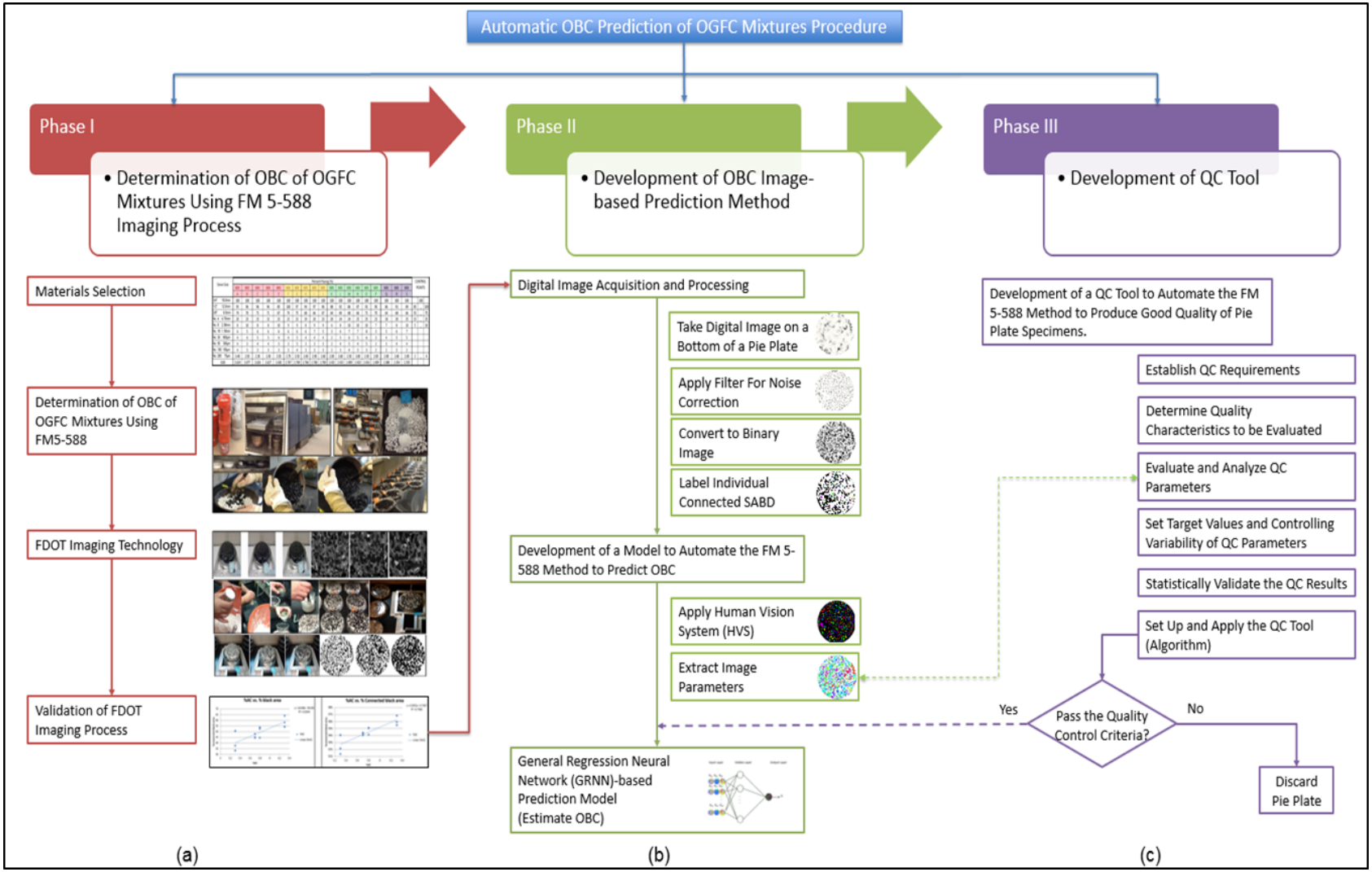

Figure 3 Flowchart of the study overview.

3.1.1. Material Selection

The aggregate gradation and the porosity of OGFC mixtures are critical to producing a mixture that will have the necessary structural (strength) and functional (permeability) performance characteristics required for satisfactory field performance [52]. The aggregate gradation should allow for a large percentage of coarse aggregate for control of the porosity of the asphalt mixtures, and an adequate fine aggregate content to prevent the void structure from closing [52]. In this investigation, two different granitic aggregate sources and two different oolitic limestone aggregate sources were used to create the tested OGFC mixtures. The granitic mixtures were identified as mixtures A-J and the oolitic limestone mixtures identified as mixtures K-S. More specifically, the aggregate sources for Nova Scotia Granite, Georgia Granite, White Rock Quarries limestone and Titan American limestone were labeled as A-E, F-J, K-P, and Q-S, respectively [49-51].

In total, nineteen different OGFC gradations were generated and tested using the PG 67-22 asphalt binder which comprised a total of 228 samples prepared from 120 granitic and 108 oolitic limestone aggregate sources [49-51]. Hydrated lime was added at a rate of 1.0% by weight of aggregate for each granitic mixture, and mineral fiber at a rate of 0.4% by total mixture weight for all mixtures, as defined in the FDOT specifications [5]. Table 3 shows the aggregate gradations used for the study. Figure 4 to Figure 7 includes the gradation curves for each mixture.

3.1.2. Determination of OBC of OGFC Mixtures Using FM 5-588

The 1974 FHWA design procedure [6] established the OBC of OGFC mixtures based on the surface capacity (Kc) of the aggregate and optimized the gradation to established standards. Then, the mixing temperature was set based on samples placed in Pyrex glass pie plates, which were subsequently placed in an oven at varying temperatures to assess the ABD. With time and

experience, FDOT modified the FHWA procedure to design OGFC mixtures based on standardized aggregate types and gradations, and determined the OBC based on pie plate samples.

Table 3 OGFC gradations used for the study.

Sieve Size	Nova Scotia Granite					Georgia Granite					White Rock Quarries Limestone						Titan America Limestone			CONTROL POINTS
	Percent Pasing (%)																			
	MIX A	MIX B	MIX C	MIX D	MIX E	MIX F	MIX G	MIX H	MIX I	MIX J	MIX K	MIX L	MIX M	MIX N	MIX O	MIX P	MIX Q	MIX R	MIX S	
3/4" 19.0mm	100	100	100	100	100	100	100	100	100	100	100	100	100	100	100	100	100	100	100	100
1/2" 12.5mm	95	96	96	96	85	100	97	94	97	96	88	92	86	87	92	90	86	91	89	85 - 100
3/8" 9.5mm	74	70	71	71	67	74	75	68	66	67	64	69	68	66	71	70	64	68	66	55 - 75
No. 4 4.75mm	20	23	15	15	23	23	23	19	20	23	20	24	24	25	25	23	18	20	25	15 - 25
No. 8 2.36mm	8	10	8	8	10	9	9	8	9	9	6	8	10	10	10	7	7	8	10	5 - 10
No. 16 1.18mm	6	5	6	6	6	6	6	6	7	5	3	6	7	7	8	3	5	6	7	
No. 30 600µm	4	4	5	5	4	4	5	4	4	4	2	5	6	5	6	3	4	5	5	
No. 50 300µm	4	3	4	4	3	3	5	3	3	3	2	4	5	4	5	2	3	4	4	
No. 100 150µm	4	3	3	3	3	3	4	3	3	3	2	3	4	3	3	2	2	3	2	
No. 200 75µm	3.40	2.50	2.30	2.30	2.50	2.70	2.50	2.40	2.90	2.60	2.00	2.60	2.50	3.00	2.30	2.00	2.00	2.60	2.00	2 - 4

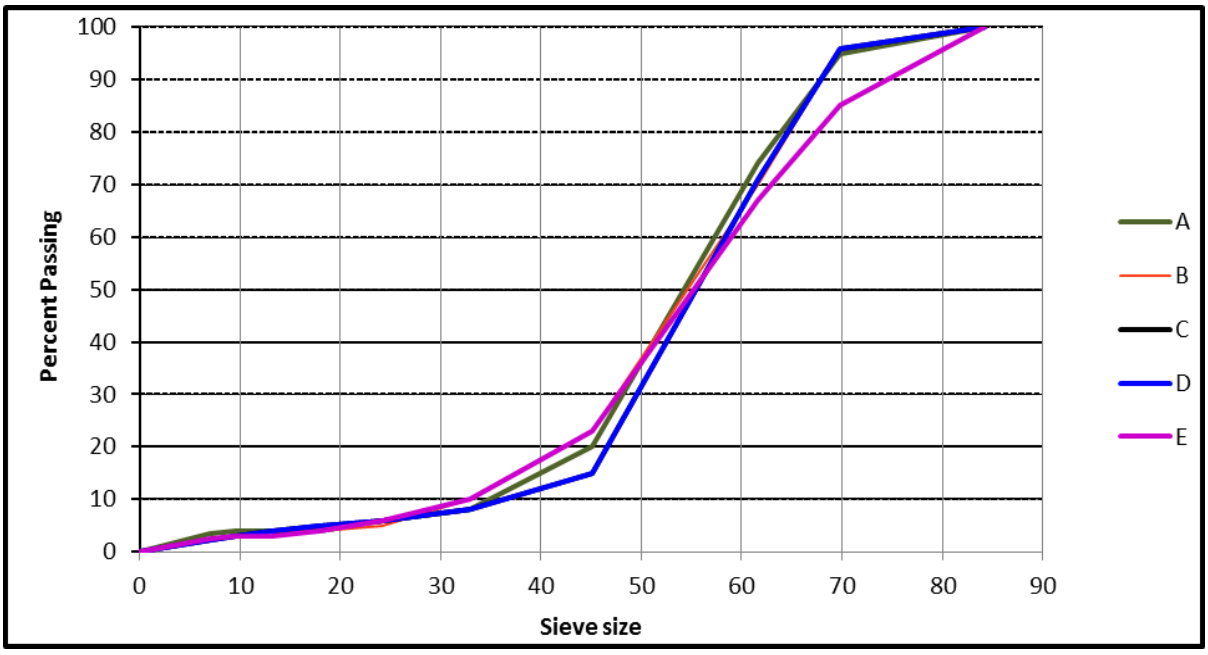

Figure 4 Gradation curves for Nova-Scotia source aggregate (A-E).

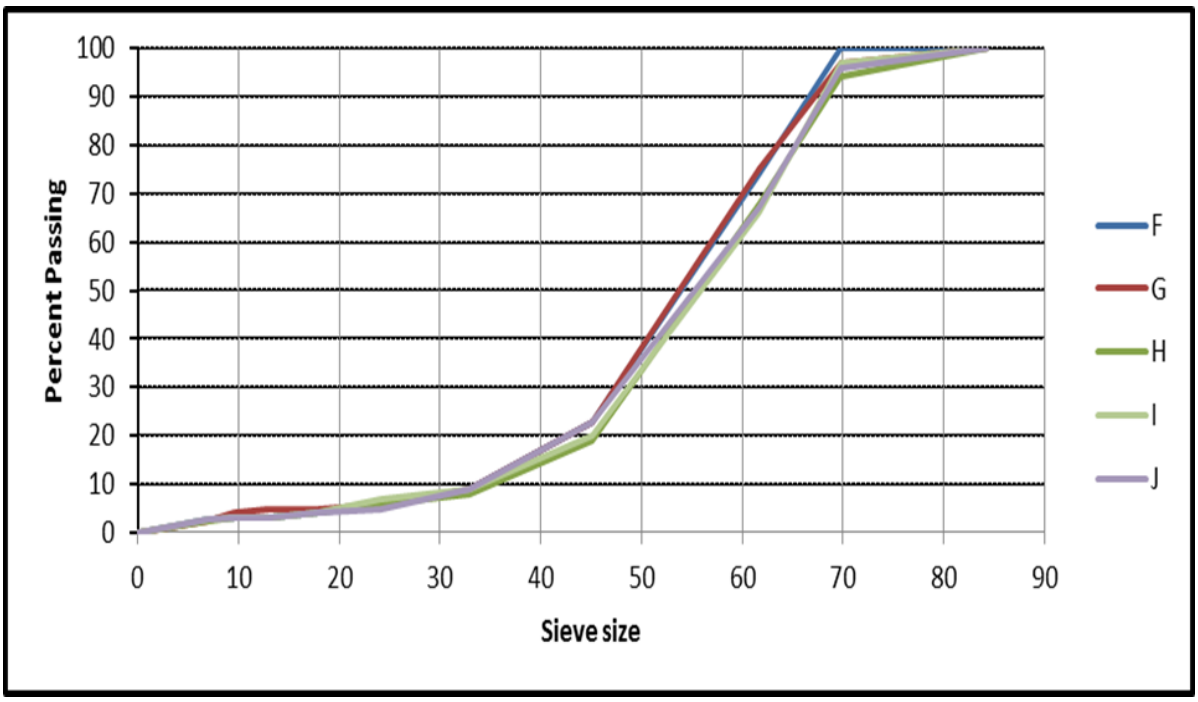

Figure 5 Gradation curves for Georgia source aggregate (F-J).

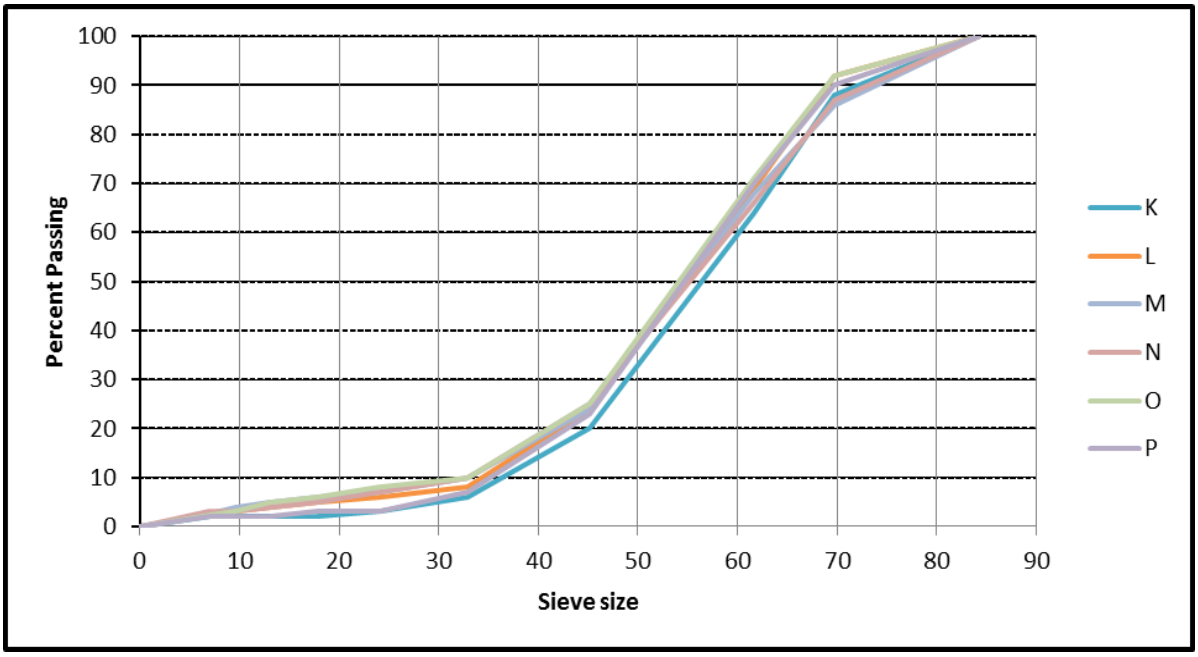

Figure 6 Gradation curves for Florida source aggregate (K-P).

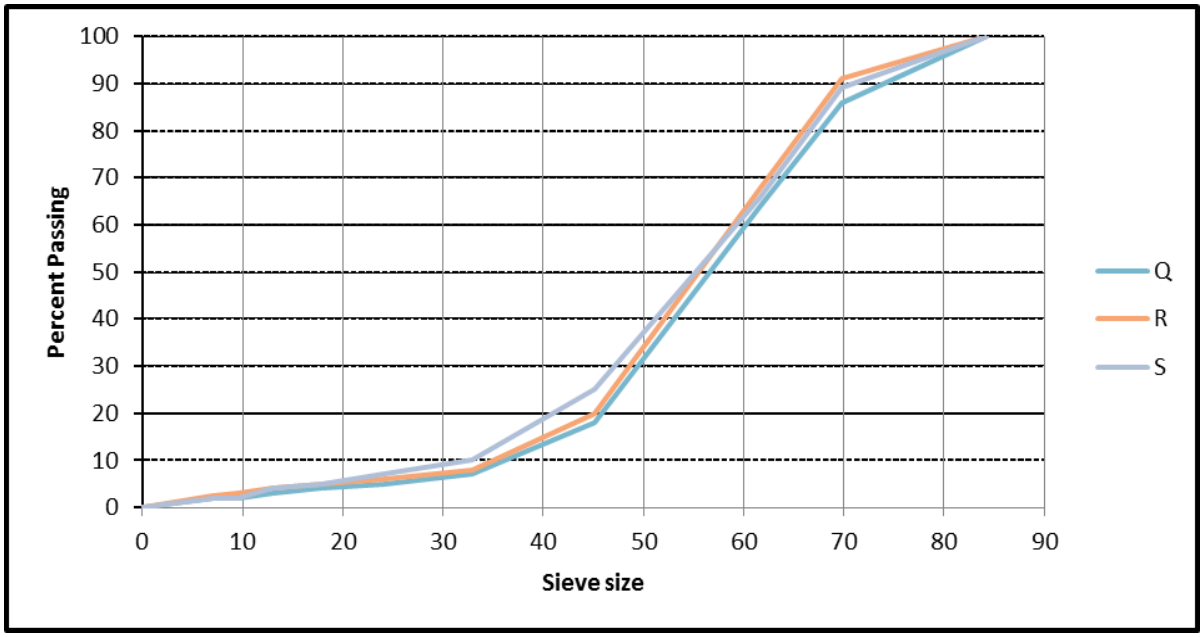

Figure 7 Gradation curves for Florida source aggregate (Q-S).

The complete material aggregate, binder and gradation for all the mixes are shown in Appendix D.

Currently, FM 5-588 requires the preparation of OGFC samples placed in pie plates at three pre-determined trial AC chosen based on the aggregate type: 5.3%, 5.8% and 6.3% for granitic aggregate, and 5.8%, 6.3% and 6.8% for oolitic limestone aggregate. The next step requires visual inspection of the bottom of the pie plates for the ABD distribution [2 and 6]. This inspection is performed by trained and experienced technicians who determine the OBC based on perceptive interpolation or extrapolation from the above specified AC, guided by documented references shown in Figure 2.

For this research, each OGFC mixture was tested in triplicates to account for the random distribution of the aggregate and interstices within each aggregate mixture and random sample preparation errors. The appropriate amount of materials was acquired in order to prepare triplicates with each mixture and additional triplicate mixtures corresponding to the visually determined OBC

as shown in Figure 8(a). AASHTO Method T2 [53] and FM 1-T 248 [54] were used to sample and prepare the materials for testing. Upon sampling, the aggregates were dried overnight at 110°C and then sieved in Gilson TS-1 bulk sieve shakers.

Laboratory aggregate "batches" were produced at the three predefined trial AC corresponding to the aggregate type as shown in Figure 8(b). Next, the uncompacted mixtures were placed in nine-inch clear glass circular pie plates and conditioned in an oven at 320°F (160°C) for one hour. Figure 8(c) shows the steps followed for the pie plate preparation according to FM 5-588. Once the pie plates cooled down to the room temperature, they were inverted for the subsequent visual determination of the OBC as shown in Figure 8(d).

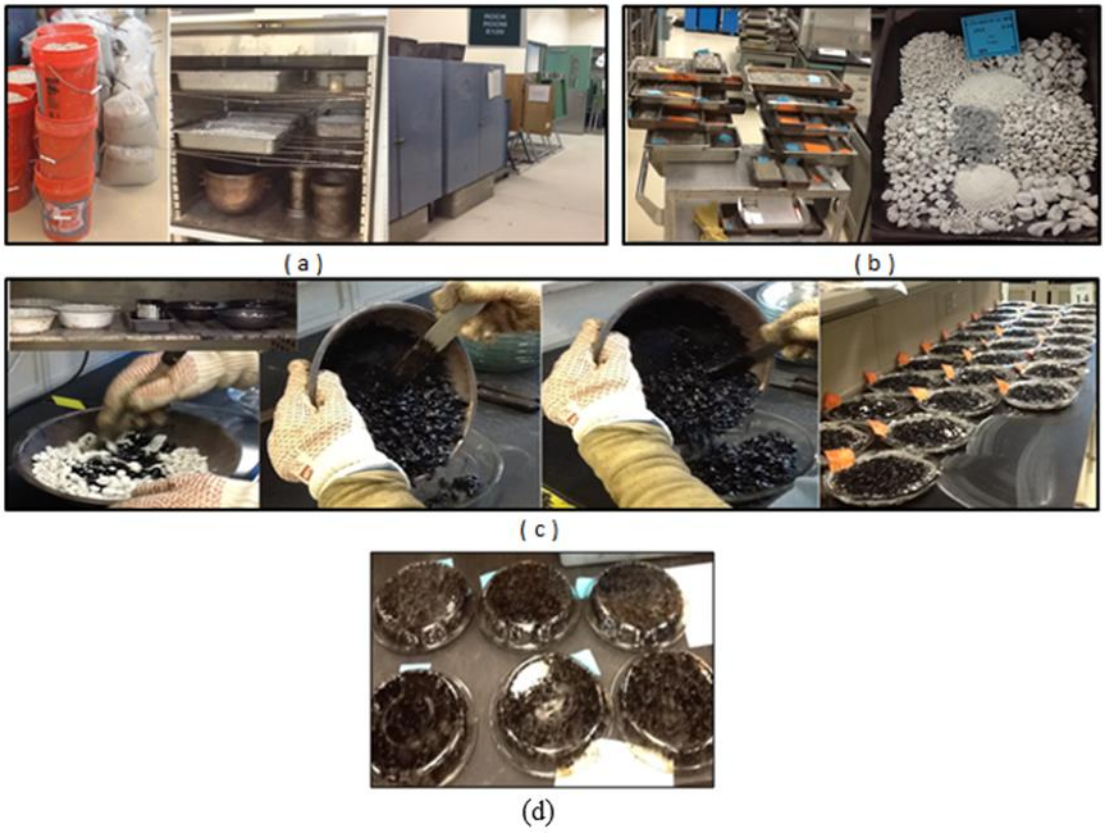

Figure 8 Steps followed for the pie plate preparation according to FM 5-588 including: (a) material preparation, (b) batch preparation, (c) mixture/pie plate's preparation, and (d) visual inspection to estimate OBC.

Finally, the three additional OGFC samples were also prepared at the visually determined OBC's. A sample batch sheet is shown in Figure 9.

3.1.3. FDOT Imaging Technology

FDOT's customized imaging system developed to automate the FM 5-588 method consists of a standard digital camera attached to a custom made aluminum bracket (Figure 10) oriented at 35° to the horizontal to minimize glare on the surface during the image acquisition. A preliminary computer program developed by FDOT was used to calibrate the pie plate image [7]. A "dot matrix" calibration unit with a fixed spacing was used in the above setup to calibrate the specific software for the camera angle and simulate an image perspective of a 90° bird's eye view. The known dimensions of the bracket leg are used to convert pixel values into actual distances during image processing [7].

A "dot matrix" calibration unit with a fixed spacing was used in the above setup to calibrate the specific software for the camera angle and simulate an image perspective of a 90° bird's eye view of a given pattern on 2D images (Figure 11) [55].

The preliminary program developed by FDOT was used to perform the initial image analysis tasks [7]. FDOT's image analysis program is based on Labview software. This software extracted the circular (9" diameter) section from the image of a pie plate for analysis of the binder area. A color threshold which reduces a grayscale image to a binary image was used to identify the image pixels corresponding to the binder in the pie plate image. Based on the selected threshold, a pixel analysis was conducted to calculate the total area of the binder. Thresholding is the simplest segmentation method for images and is used to separate out regions of an image corresponding to objects which one wishes to analyze [7]. This separation is based on the variation of intensity between the object pixels and the background pixels [56].

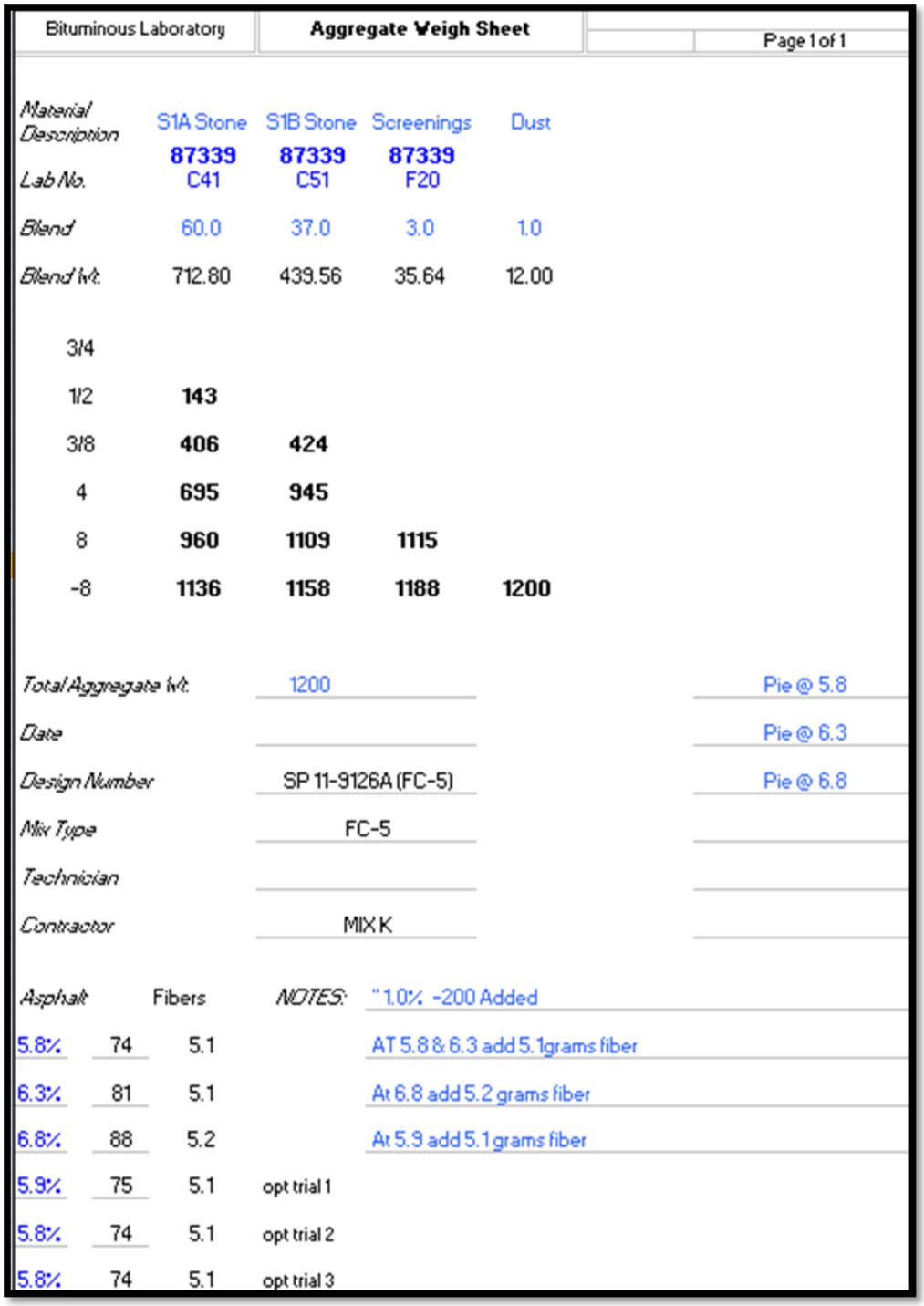

Bituminous Laboratory	Aggregate Weigh Sheet			Page 1 of 1
Material Description	S1A Stone	S1B Stone	Screenings	Dust
Lab No.	87339 C41	87339 C51	87339 F20	
Blend	60.0	37.0	3.0	1.0
Blend Wt.	712.80	439.56	35.64	12.00
3/4				
1/2	**143**			
3/8	**406**	**424**		
4	**695**	**945**		
8	**960**	**1109**	**1115**	
-8	**1136**	**1158**	**1188**	**1200**

Total Aggregate Wt.	1200	Pie @ 5.8
Date		Pie @ 6.3
Design Number	SP 11-9126A (FC-5)	Pie @ 6.8
Mix Type	FC-5	
Technician		
Contractor	MIX K	

Asphalt		Fibers	*NOTES:*	"1.0% -200 Added
5.8%	74	5.1		AT 5.8 & 6.3 add 5.1grams fiber
6.3%	81	5.1		At 6.8 add 5.2 grams fiber
6.8%	88	5.2		At 5.9 add 5.1 grams fiber
5.9%	75	5.1	opt trial 1	
5.8%	74	5.1	opt trial 2	
5.8%	74	5.1	opt trial 3	

Figure 9 Sample aggregate batching sheet (for mix K).

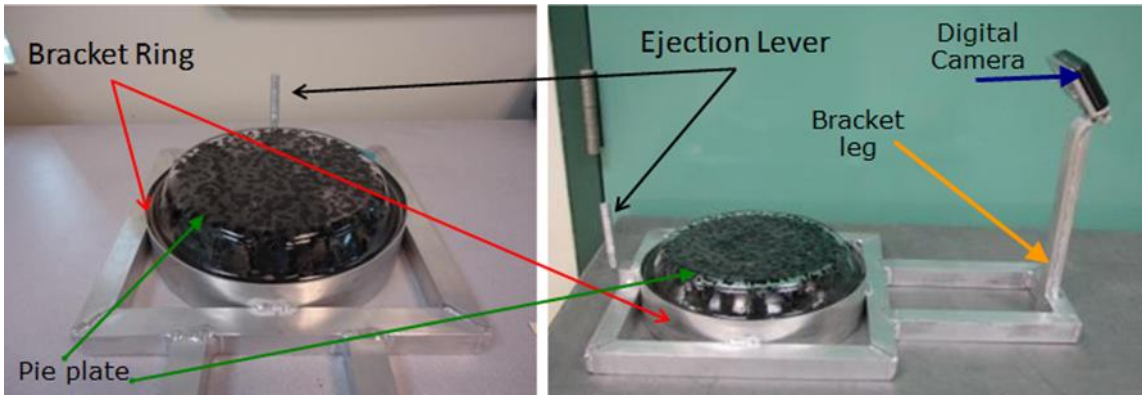

Figure 10 Pie plate and custom bracket (courtesy of FDOT [6]).

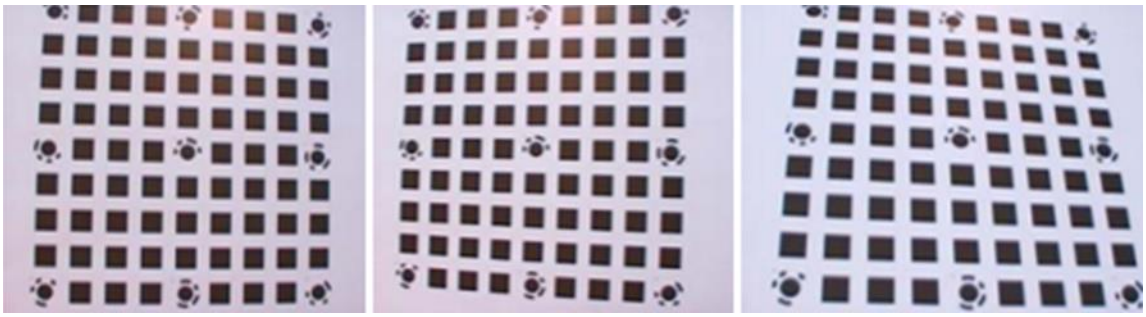

Figure 11 Typical calibration dot matrix unit [52].

It must be noted that image analysis was accomplished using two different methods; (1) the Labview program provided by FDOT State Material Office (SMO), and (2) the Matlab software developed by the author. As seen in Figure 12, the estimates of the binder area in each pie plate image obtained from the above two sources are in perfect agreement. Moreover, Appendix E (Figures E1 to E19) provides test results from the above two methods (i.e. Labview versus Matlab) obtained in this module for all of the mixtures tested in this research.

3.1.4. Validation of FDOT Imaging Process

Statistical analysis to validate the preliminary Florida pie plate test image processing method. Many statistical analyses attempt to find a pattern in a data series, based on an assumption about the nature of the data.

For the database, two image processing parameters (percent black pixel area and connectivity of black pixels), generated during the statistical analyses in Phase I were completed following the next steps: a) clean database, b) check data for outliers, c) estimate correlation coefficients, d) develop a regression analysis, e) interpreted the regressions statistical tables and f) gathered the finding of the validation section.

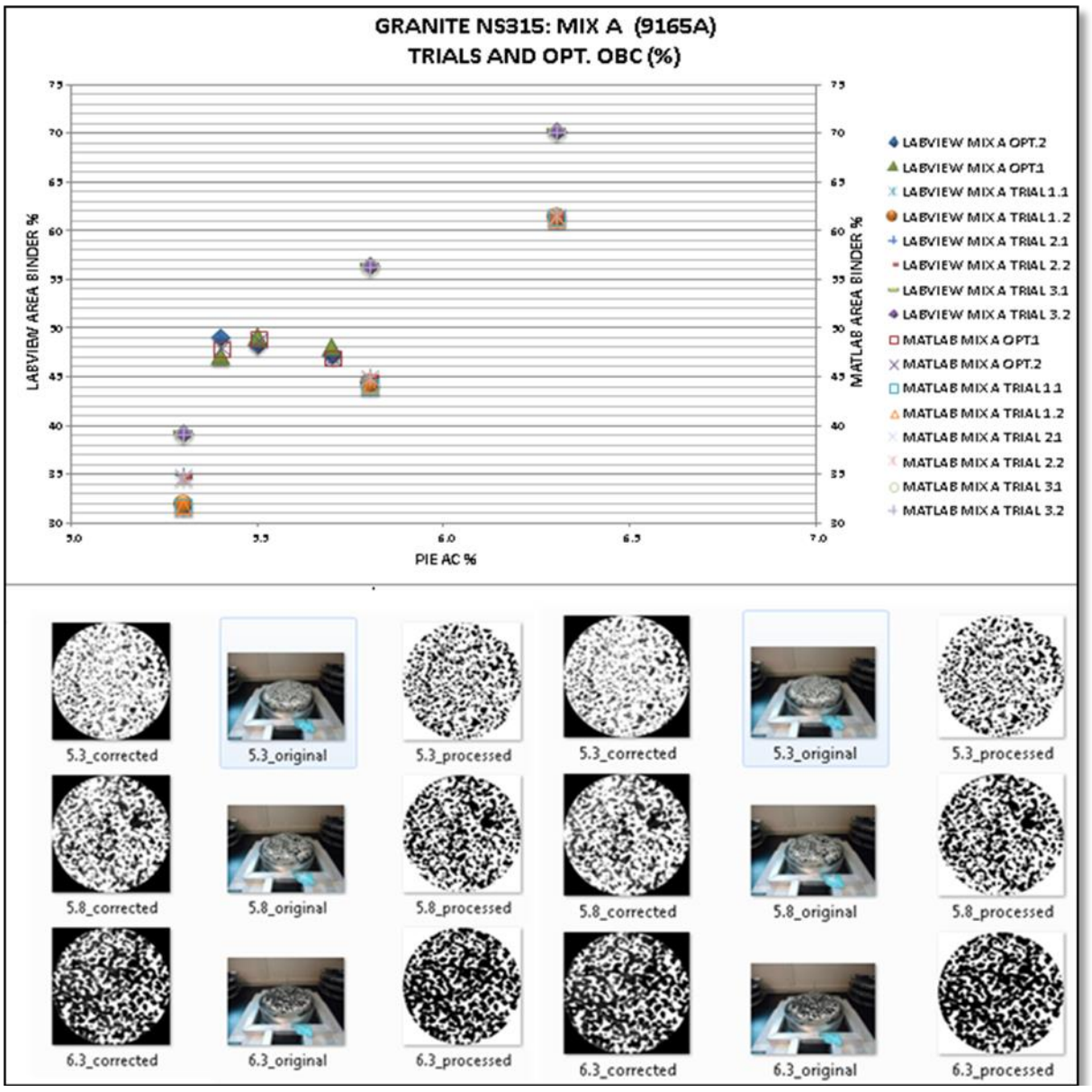

Figure 12 Comparison of digital imaging results for mix A - Labview versus Matlab.

3.1.4.1. Clean Database

'Cleaning' is the process of removing those data points which are either (a) obviously disconnected with the effect or the assumption that defines the pattern or (b) obviously erroneous by virtue of sub-standard measurement. The cleaning of the database was performed by checking the data against the original data to generate a reliable database, when the data was checked against the original data to verify that they had been entered correctly, it was observed that no errors were found in the database.

3.1.4.2. Check Data for Outliers

To avoid biased results, the data set was checked for both univariate outliers (outliers with respect to one variable alone) and multivariate outliers (outliers with respect to a combination of variables). Outlier detection in a Microsoft Excel worksheet is demonstrated on the sample set of mixture J (24 numeric values), completed in a several steps outlined below [51].

The first step in identifying outliers is to pinpoint the statistical center of the range. To perform pinpointing, one starts by finding the 1st and 3rd quartiles. A quartile is a statistical division of a data set into four equal groups, with each group making up 25 percent of the data. The top 25 percent of a collection is considered to be the 1st quartile, whereas the bottom 25 percent is considered the 4th quartile.

In Excel, one can easily obtain quartile values by using the QUARTILE function. This function requires two arguments: a range of data and the quartile number one wants.

The next step is taking these two quartiles, calculating the statistical 50 percent of the data set by subtracting the 3rd quartile from the 1st quartile. This statistical 50 percent is called the interquartile range (IQR). Statisticians generally agree that IQR*1.5 can be used to establish a reasonable upper and lower fence:

The lower fence is equal to the 1st quartile – IQR*1.5.

The upper fence is equal to the 3rd quartile + IQR*1.5.

The final results of final upper and lower fences for all of the mixtures was “normal” indicating "no outliers"

3.1.4.3. Estimate Correlation Coefficients

The correlation coefficient (Multiple R) is defined as the measurement of how strong a linear relationship exists between two numeric variables *x* and *y*. The correlation coefficient is always a number between -1.0 and +1.0. If the correlation coefficient is close to +1.0, then there is a strong positive linear relationship between *x* and *y*. If the correlation coefficient is close to -1.0, then there is a strong negative linear relationship between *x* and *y*. The closer to zero the correlation coefficient is the less of a linear relationship between *x* and *y* exists [51].

The correlation coefficient (multiple R) for all the mixtures was a number between 0.38 and +0.97 (Table 4) indicating the existence of a strong positive linear relationship between *x* (asphalt binder content) and *y* (image processing parameter).

Table 4 Coefficients of correlation for all the mixtures used for the study.

GRANITE			OOLITE		
	Mix	Multiple R		Mix	Multiple R
NS315	A	0.95			
	B	0.91	**87339**	K	0.89
	C	0.95		L	0.98
	D	0.97		M	0.94
	E	0.97		N	0.79
GA553	F	0.90		O	0.38
	G	0.84		P	0.88
	H	0.92	**87145**	Q	0.95
	I	0.92		R	0.95
	J	0.86		S	0.82

3.1.4.4. Regression Analysis

Regression analysis was used to generate mathematical expressions for the relationships between the classification parameters and asphalt binder content. The regression tool was used to estimate the model parameters [51]. The regression tool determined the coefficients (β_i) that yield the smallest residual sum of squares of errors, which is equivalent to the greatest correlation coefficient squared, R^2, in Equation (1) or (2).

- Regression analysis of percent black pixel area versus asphalt binder content and connectivity of black pixels versus asphalt binder content

$$\hat{y} = \beta 1 + \beta 2\, x + u \quad (1)$$

where: $\hat{y}$ = Predicted asphalt binder content percentages; $\beta 1$, $\beta 2$ = Regression coefficients corresponding to the independent variables; x = Percent black pixel area or connectivity of black pixels; and u = Error.

As seen in the Table 5, when all the mixtures are considered, there is only a marginal improvement in R^2 values in the correlations with the asphalt binder contents when percent black pixel area is replaced by the connectivity of black pixels. Hence the author sought to use a combined model of both the above variables to predict the asphalt binder content of mixtures.

- Regression analysis of predicted asphalt binder content versus combination of percent black pixels area and connectivity of black pixels

$$\hat{y} = \beta 1 + \beta 2\, x_2 + \beta 3\, x_3 + u \quad (2)$$

where: $\hat{y}$ = Predicted asphalt_binder content; $\beta 1$, $\beta 2$, $\beta 3$ = Regression coefficients; x_2 = Percent black pixel area; x_3 = Connectivity of black pixels; and u = Error.

Table 5 also shows the results of the combined regression analysis using Equation (2) for all the considered mixtures.

Table 5 Results of the combined regression analysis.

Mix	Single regression R^2 results for		Multiple regression R^2 results for
	Black area percent	Connectivity of black pixels	Black area percent and Connected black pixels
NS315	0.76	0.73	0.76
GA553	0.61	0.66	0.80
87339	0.70	0.70	0.70
87145	0.74	0.80	0.81

Table 6 provides a summary of the results from combined regression analysis for mix A.

Table 6 Summary output of the combined regressions for mix A.

SUMMARY OUTPUT						
Regression Statistics						
Multiple R	0.893022419					
R Square	0.79748904					
Adjusted R Square	0.778202282					
Standard Error	0.181427856					
Observations	24					
ANOVA						
	df	*SS*	*MS*	*F*	*Significance F*	
Regression	2	2.722095924	1.361047962	41.34904568	5.22047E-08	
Residual	21	0.691237409	0.032916067			
Total	23	3.413333333				
	Coefficients	*Standard Error*	*t Stat*	*P-value*	*Lower 95%*	*Upper 95%*
Intercept	3.571419302	0.911845774	3.916692279	0.000792717	1.675132206	5.467706398
% Area Black Pixels	0.029265431	0.003746481	7.811444548	1.20452E-07	0.021474197	0.037056666
Connectivity of black pixel	0.840392025	1.126587506	0.745962494	0.463959205	-1.502474949	3.183258999

The results of the multiple regression analysis depicted by Equation (2) in terms of the predicted asphalt binder content against the actual asphalt binder content in mix A are shown in

Figure 13 and Figure 14 indicates that a multiple regression model that uses both percent black pixel area and the connectivity of black pixels on the pie plates shows an increase in the R^2 value.

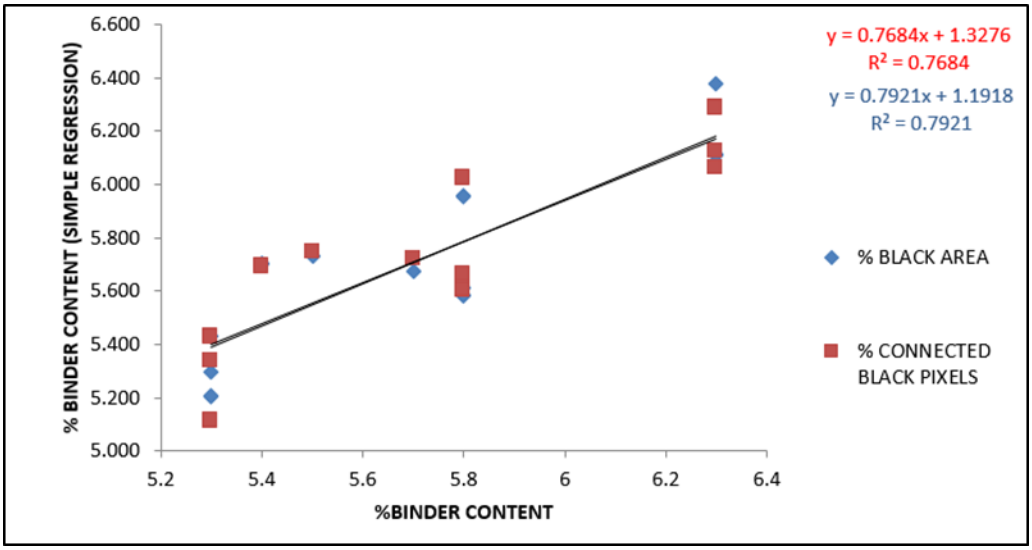

Figure 13 Percent of asphalt binder prediction using simple regression for mix A.

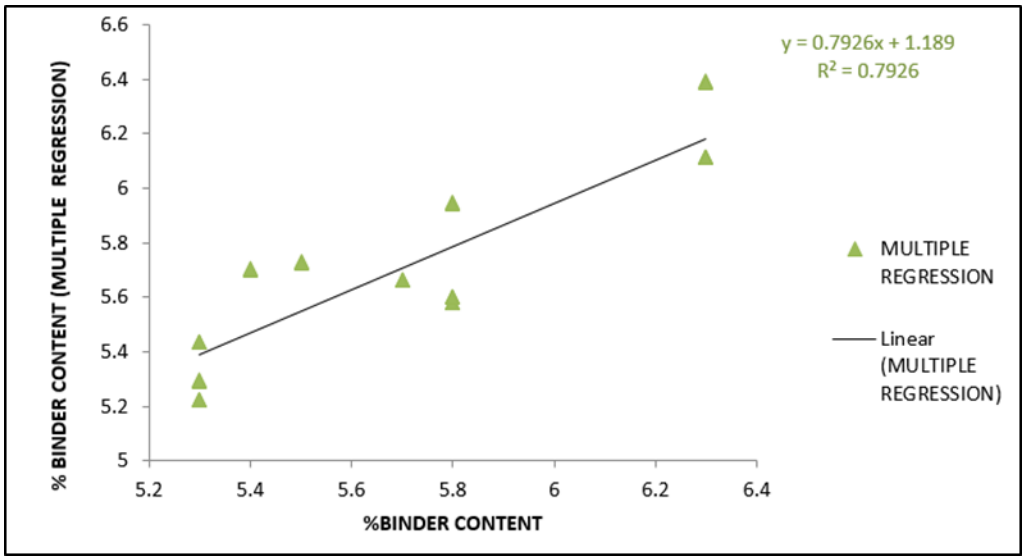

Figure 14 Percent of asphalt binder prediction using combined regression for mix A.

The simple regression models for percent black pixel area and connectivity of black pixels in Figure 13 account for 76.84% and 79.21% of the variance, while the combined regression model in Figure 14 accounts for 79.26% of the variance. The more variance that is accounted for by the

regression model the closer the data points will fall to the fitted regression line. Theoretically, if a model could explain 100% of the variance, the fitted values would always equal the observed values and, therefore, all the data points would fall on the fitted regression line. Therefore, the more parameters that one can add to the model the closer to the variance the values will be, providing more accurate asphalt binder percent predictions.

A summary of the improvement of the predictive models based on the use of combined regression for all mixtures is shown in Table 7.

Table 7 Comparison of results of simple regression versus multiple regression for all the mixtures used for the study.

MIX	Single regression R^2 results for		Multiple regression R^2 results for	Black area percent vs. Black area percent and Connectivity of black pixels difference			Connected black pixels percent vs. Black area percent and Connectivity of black pixels difference		
	Black area percent	Connectivity of black pixels	Black area percent and Connected black pixels						
NS315	0.76	0.73	0.76	NO CHANGE	-	%	INCREASED BY	2.0	%
GA553	0.61	0.66	0.80	INCREASED BY	13.5	%	INCREASED BY	9.6	%
87339	0.70	0.70	0.70	NO CHANGE	-	%	NO CHANGE	-	%
87145	0.74	0.80	0.81	INCREASED BY	4.5	%	INCREASED BY	0.6	%

3.1.4.5. Interpretation of the Regression Statistics Table

Sample regression statistics for mix J are shown in Table 8 in which R Square (R^2) is of the greatest interest. Table 8 gives the overall goodness-of-fit measures, $R^2 = 0.781$.

Adjusted R^2 is defined as follows:

$$R^2 = R^2 - (1-R^2)*(k-1)/(n-k) = 0.781 - 0.219*2/21 = 0.78 \quad (3)$$

$R^2 = 0.781$ means that 78.1% of the variation of y_i around $\hat{y}$ (its mean) is explained by the repressors' x_{2i} and x_{3i}.

The standard error in Table 8 refers to the estimated standard deviation of the error term u in Equation (3). It is sometimes called the standard error of the regression and it equals

to $\sqrt{SSE/(n-k)}$, where SSE is sum of squared errors of prediction, n is number of observations used in the regression and k is the number of repressors including the intercept.

Table 8 Regression statistic table for mix J.

		Explanation
Multiple R	0.884	R = square root of R^2
R Square	0.781	R^2
Adjusted R Square	0.760	Adjusted R^2 used if more than one x variable
Standard Error	0.178	This is the sample estimate of the standard deviation of the error u
Observations	24	Number of observations used in the regression (n)

3.1.4.6. Findings of the Validation Section

The above described statistical techniques have been implemented in Excel and Matlab to derive the required correlations for all the mixes. For example, Figures 15(a) and (b) shows the statistics for two correlations that have been developed by the author for the Trial 1.1 of mix J [49 and 51].

It can be seen that the correlation is very satisfactory with respect to the connected black area versus percent AC (%AC) plots. For example, the overall goodness-of-fit measurement, R^2, increases from 0.65 to 0.755 between the percent black-area parameter versus percent AC to the black pixel connectivity parameter versus percent AC. The complete results of this analysis for all the mixes are shown in Appendix F (Figures F1 to F47 and Table F1). However, it can be seen from the plots in Appendix F that R^2 values did not improve markedly for all the mixes when percent black pixels parameter was replaced by the black pixel connectivity parameter. Hence the author sought to use both variables to predict the asphalt content of the mixes using combined regression seen in Equation (2).

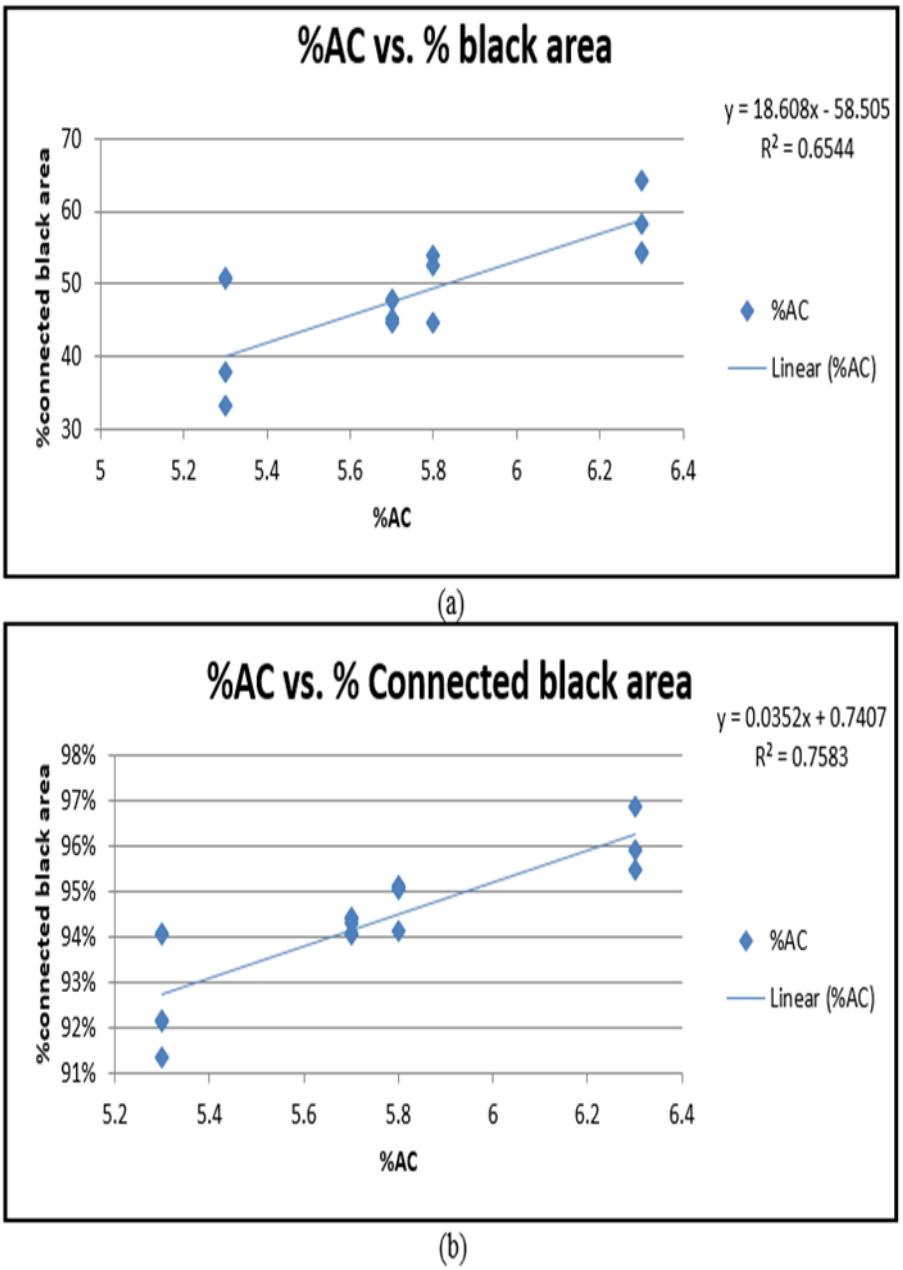

Figure 15 Mix J trial 1.1 at 5.8%AC (a) %AC versus %black area, (b) %AC versus %Connected black area.

Table 9 demonstrates the comparison summary of the results from both types of regression for a number of mixes.

Table 9 Comparison of results of individual regression versus combined regression.

	R^2					
MIXES	%AREA	% CONNECTED	DIFFERENCE	COMBINED REGRESION	CHANGE FROM INDIVIDUAL VARIABLES	CHANGE FROM INDIVIDUAL VARIABLEs TO COMBINED
MIX J	0.65	0.73	8%	0.78	INCREASED BY 8%	INCREASED BY 13%
87339	0.70	0.70	0%	0.70	N/A 0%	N/A -
GA553	0.61	0.66	5%	0.80	INCREASED BY 5%	INCREASED BY 19%
87145	0.74	0.80	6%	0.81	INCREASED BY 6%	INCREASED BY 7%
NS315	0.76	0.73	-3%	0.76	DECREASED BY -3%	DECREASED BY -

3.2. Phase II (Development of OBC Image-Based Prediction Method)

Phase II is described by sections (i) Digital image acquisition and processing, (ii) Development of a model to automate the process to predict OBC, and (iii) General regression neural network (GRNN)-based prediction model to estimate OBC.

3.2.1. Digital Image Acquisition and Processing

In these next step, digital images of all pie plate samples were acquired using the setup described in the previous section. Then, Plaster of Paris was added to each pie plate to enhance the contrast, as shown in Figure 16(a) for the subsequent visual inspection and a new (post-enhancement) set of digital images of the pie plates were also acquired. A sample set of such digital images is shown in Figure 16(b). In order to enrich the database with more extensive data that could be used in modeling the random errors possibly committed in image capturing, a second set of the post-plastered digital images (immediate after the first set was taken without moving the pie plate from the custom bracket) was also acquired from the pie plates, yielding a total of 456 digital images for all the mixtures [50].

A research study by Zelelew, Papagiannakis, and Masad, 2008 [57] introduced an automated digital image processing technique for analyzing the internal structure of asphalt mixtures from CT images. Such innovations for easing the complexity of processing and analysis

of the captured images have become acceptable techniques for basic image processing. *Matlab*^{TM} was used to implement the different stages of this technique in the current research based on (i) removing the random noise in the image; (ii) converting the grayscale image into a binary image using an appropriate threshold value; (iii) finding the connected components (groups of black pixels) in each image, denoted as "regions"; (iv) assigning a unique label to each identified region; and (v) computing geometric properties of each labeled region [50].

In the next step, the digital images were preprocessed for quality enhancement to facilitate precise analysis and more accurate interpretation of results at the analysis stage. Important tasks in preprocessing include filtering for removal of noise introduced during image acquisition, emphasizing of specific features relevant to the analysis, and converting the original grayscale images into binary images for analytical convenience. Digital images are often corrupted with noise or undesired features originating from various sources depending on the ambient conditions at the time of digital image acquisition. In this investigation, the only likely sources of noise were non-uniform lighting and scratches or other marks on the bottom of the glass pie plates. To remove the random noise in the image the median filter (*medfilt2*) was applied.

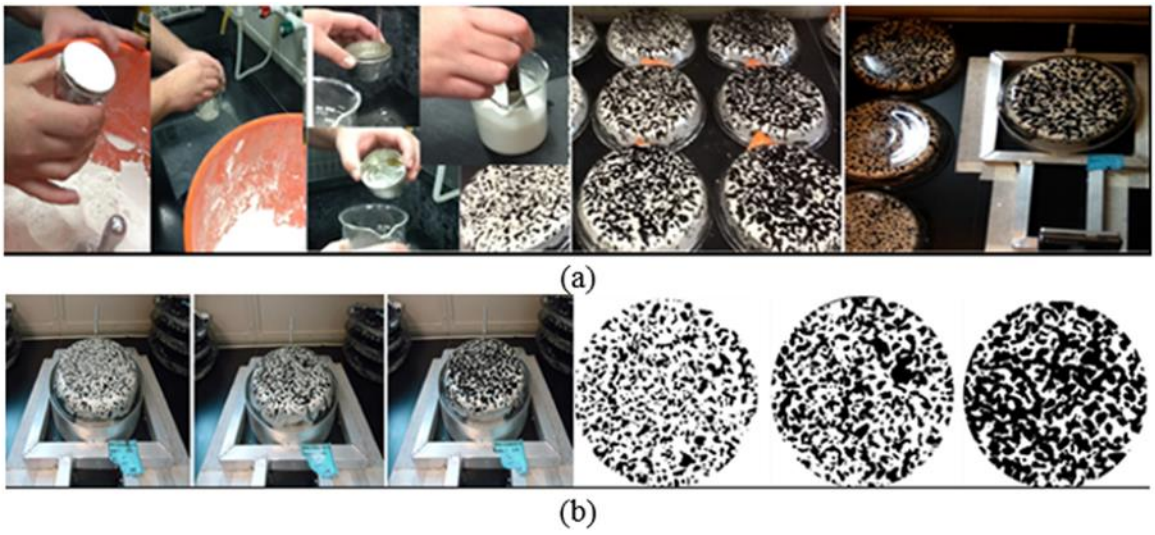

Figure 16 Sequences of steps followed for the enhancement procedure.

The final step of pre-processing involved image enhancement using a thresholding technique to convert the grayscale images with gradually varying intensities from black to white into binary images consisting of only black and white pixels. Thresholding is the simplest segmentation method for digital images and it is used to separate out regions of an image corresponding to objects which one wishes to analyze. This separation is based on the variation of intensity between the object pixels and the background pixels [55]. A color threshold which reduces a grayscale image to a binary image is used to identify the image pixels corresponding to the asphalt binder. In this study, the *im2bw* function outputs a binary image for an input grayscale image by replacing all the pixels in the input image with intensities greater than the selected thresholding level with the value of 1 (white) and all the other pixels with the value of 0 (black) [56]. After filters are applied, the connected black pixels are grouped into regions.

The grouping of connected black pixels into regions was accomplished using the Adjacency Searching Method [58], allowing the connected black pixel regions which are considered to represent the ABD, to be evaluated further. A brief discussion of the Adjacency Searching Method is found next.

A pixel *p* at coordinates of *(i, y)* has four *horizontal* and *vertical* neighbors whose coordinates are given by *(i+1, j), (i-1, j), (i, j+1), (i, j-1).* This set of pixels, called the 4-connected next neighbors of *p*, is denoted by Figure 17(a) and each pixel is a unit distance from *(i, j).* The 4-connected diagonal neighbors of *p* have coordinates *(i+1, j+1), (i+1, j-1), (i-1, j+1), (i-1, j-1)* and are denoted by Figure 17(b). These points, together with the 4-neighbors, are called the 8-connected of *p*, denoted by Figure 17(c). The location of 8-connected for each applicable pixel is carried out as follows.

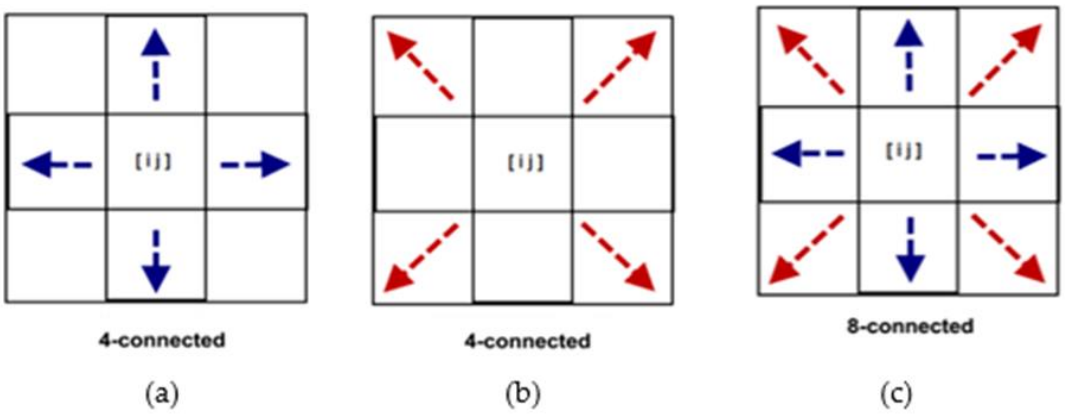

Figure 17 Pixel connectivity schemes (a) 4-neighbor connectivity next pixels, (b) 4-neighbor connectivity corner pixels and (c) 8-neighbor connectivity.

First, the searching algorithm finds the initial black pixel of an image and starts the search within the previously defined search area and the prioritized (next or diagonal) directions. The basic rule for the searching algorithm is to follow the adjoining black pixels until there is no other black pixel in the prioritized directions. The algorithm will finally count and label the number of pixels next and diagonal to the pixel *p*. The search algorithm is summarized below:

- From the binary image, find the initial black pixel *p* [49 to 51].
- Start counting from *p* the pixels with the same color (black) next to *p* to the right, left, top and bottom to find 4-connected next neighbors
- Follow the black pixels in the four directions until no other black pixel is found next to *p*
- Label the pixel *p* with the number of the pixel visited last
- Return to the initial black pixel *p* again and now start counting from *p* the pixels with the same color (black) next to it to the top right corner, top left corner, bottom right corner and bottom left corner to find 4-connected diagonal neighbors
- Follow the black pixels in the four diagonal directions until no other black pixel is found diagonal to *p*

- Add the count of the 4- connected next neighbors and the 4-connected diagonal neighbors to find 8-connected neighbors
- Determine the presence of a break point (where no more black pixel is found)
- Repeat the process for the each image.

Then, a labelling operation is performed to change the pixel intensities of regions of black pixels to unique integers (*bwlabel*) as shown in Figure 18(a) and, subsequently, a color map function is implemented to apply RGB color visualizing label of the regions (*label2rgb*) as shown in Figure 18(b).

The geometric properties of each labeled region are then calculated (*regionprops*). These include the area, equivalent diameter and centroid. Once the processing of the images is completed, the algorithm proceeds to the analysis for the determination of orientation, spatial distribution and segregation [50]. Figure 19 shows the steps used in this study for pre-processing the pie plate digital images.

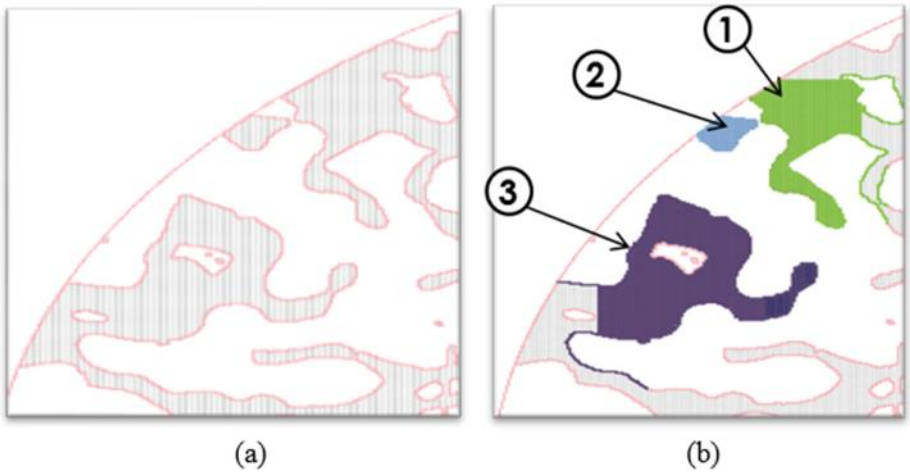

Figure 18 Representation of (a) tracing of regions of black pixels connected and (b) labelling of regions of black pixel connected by color and numbers.

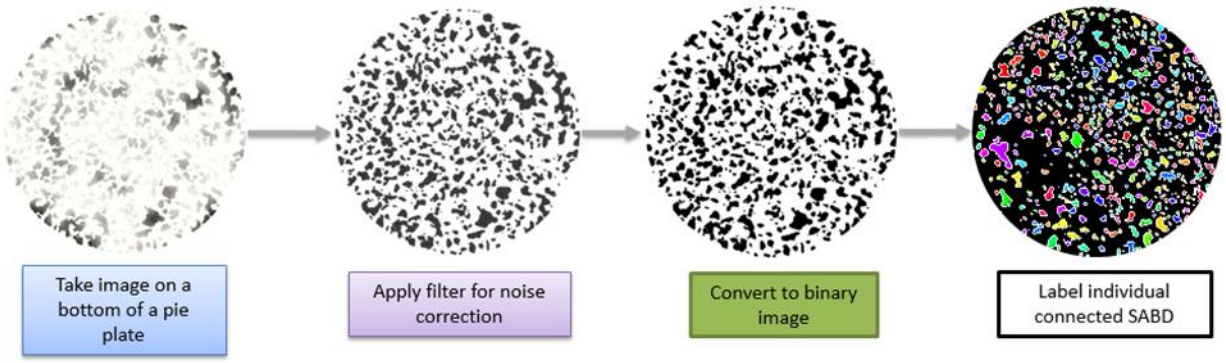

Figure 19 Sequences of steps followed for the pre-processing the pie plate digital images.

3.2.2. Development of a Model to Automate the FM 5-588 Method to Predict OBC

To accomplish the automation of the FM 5-588 procedure to accomplish the main objective of the research (OBC prediction), the author analytically modeled the perceptual transfer process which involves the two modes of information processing i.e. visual processing and neural processing. Creation of this perceptual process consist on two task: (i) visual processing using the human vision system, and (ii) neural processing using general regression neural network. The above process is described in detail in the forthcoming Chapter 4.

3.3. Phase III (Development of Image–based Quality Control Tool (QCT))

This section gives a detailed discussion of the QCT development process as shown in Figure 3(c). This section is intended to provide (i) "How to develop" and (ii) "How to evaluate" the image-based quality control imaging parameters (QCIP) to be used in the QCT [50].

The (i) "How to develop" section describes the procedure of producing pie plates of OGFC mixtures currently followed by FDOT using FM 5-588. Meanwhile, the (ii) "How to evaluate" section describes methods of identifying and analyzing the ABD characterization by means of the previously identified QCIP. The above analysis is based on the findings of past research studies on aggregate characterization. This section also describes the statistical validation of the QCIP including setting up of the target value and acceptable tolerance for each QC parameter following

the measure evaluation criteria [59] that provide a scientific basis for the selection of target values and acceptable tolerances.

3.3.1. "How to Develop" the Image-Based Quality Control Imaging Parameters (QCIP)

In FDOT, QC check standards are currently unavailable for the production of pie plates using FM 5-588. Consequently, in this study, guidelines for checking the production quality of the pie plates were set up by inspecting more than 228 production PPS and consulting with the FDOT Materials office collaborators consisting of the project managers, laboratory technicians, and engineers [60]. The algorithm used for formulating the QCT redefines connected black pixel regions as ellipses with clearly demarcated major and minor axes. An example of an acceptable pie plate image where each of the black pixels regions are modified as ellipses is shown in Figure 20(a) [51, 59 and 60].

Based on the FDOT Materials Office collaborators' judgment, a pie plate would become unacceptable due to the following three reasons [60]:

- If the PPS has been "slid," "moved," or "glided" during the placing of the mixture from the mixing bowl into the pie plate or during the removal of the pie plate from the oven, the ABD's will show a definitive alignment at a specific angle. An example of an image of a pie plate with such a "slide" is shown on the right side of Figure 20(c), while an image of a pie plate with "no slide" is shown on the left side of Figure 20(b).
- If the PPS has been "dropped," "dumped," or "forced into place" during the placing of the mixture from the mixing bowl into the pie plate, the ABD will be displayed as an uneven distribution over the bottom surface of the pie plate. An example of an "unevenly distributed" ABD is shown on the right side of Figure 20(e), while an 'evenly distributed" ABD is shown on the left side of Figure 20(d).

- If the PPS has been left with “aggregate particles not thoroughly coated” or with “large conglomerates of fines particles” during the mixing of the aggregate batch and free-standing asphalt binder in the mixing bowl, then when the mixture is transferred from the mixing bowl into the pie plate, ABD will exhibit an irregular distribution causing segregation on the outside or the inside of the pie plate. An example of an image of an “incorrectly mixed and segregated” pie plate is shown on the right side of Figure 20(g), while a ‘non-segregated” pie plate image is shown on the left side of Figure 20(f). Following constant communication with FDOT collaborators regarding the PPS production, the current lightly adopted visual QC checks were reviewed and a set of three relevant, definitive and measurable QCIP that would represent the technician’s visual QC checks in a more systematic and objective manner, were selected from the broad set of imaging parameters described in the forthcoming sub-section 3.3.2. These three parameters address the following specific properties of ABD of PPS; (i) orientation, (ii) spatial distribution, and (iii) segregation [60].

3.3.2. “How to Evaluate” The Image-Based Quality Control Imaging Parameters (QCIP)

To accomplish the measurement of the relevant QC parameters, the author analytically modeled the ABD characterization by means of past aggregate characterization researchers studies [61 to 69]. The quality control ABD characterization provides quantifying parameters of the surface appearance of pie plates highly relevant to QC of the ABD configuration of a pie plate specimen. The measurement task is divided into three different group of QC parameters relevant to the design of the QC tool; (i) orientation, (ii) spatial distribution, and (iii) segregation of ABD in pie plate specimen. The above process is explained in detail in the forthcoming Chapter 5.

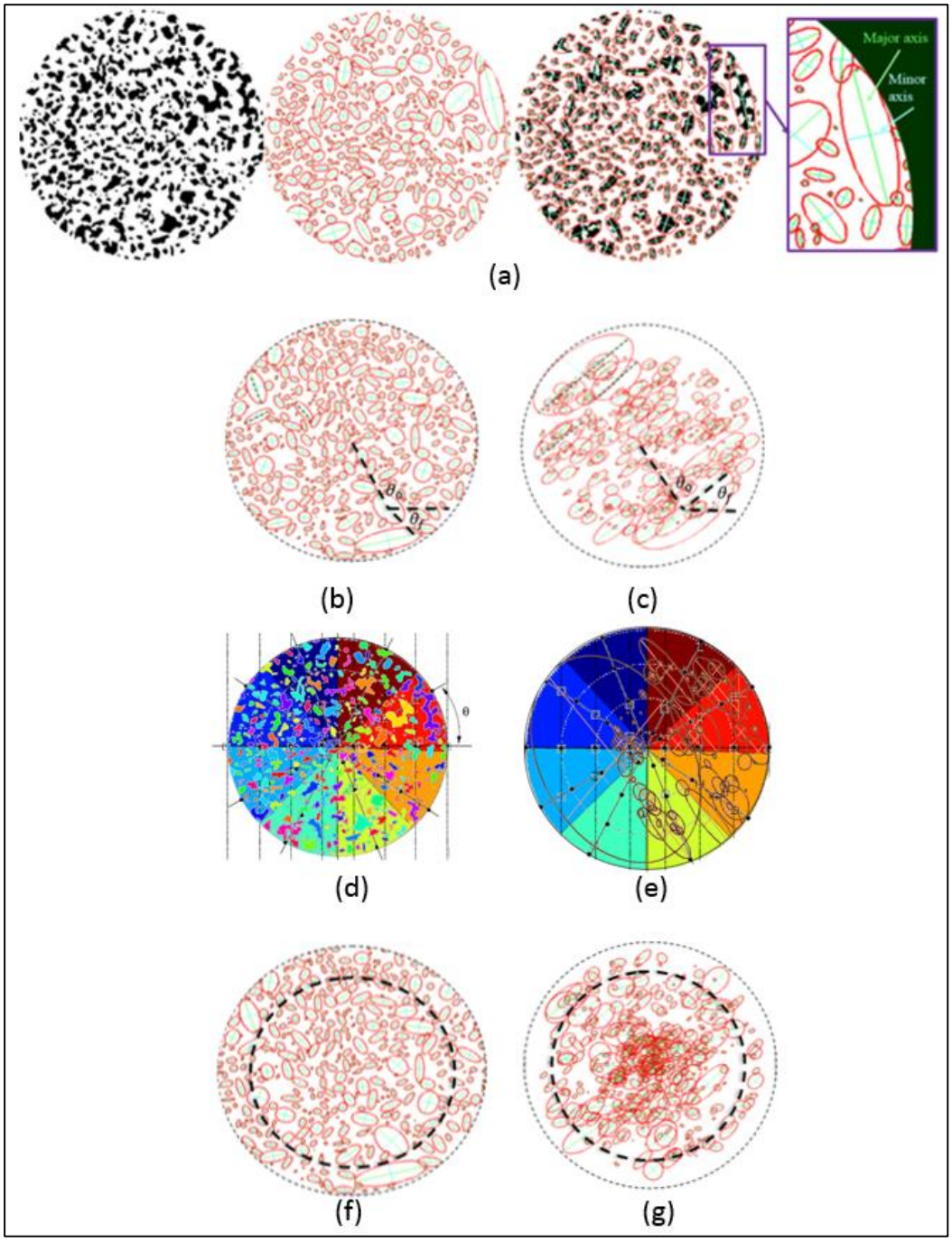

Figure 20 Synthetic computer-generated images of (a) steps to create ellipses representing the connected black pixel regions of a PPS (b) uniformly distributed PPS, (c) slid (unevenly distributed) PPS, (d) properly placed PPS, (e) incorrectly placed PPS, (f) appropriately mixed PPS, and (g) inappropriately mixed PPS.

CHAPTER 4: DEVELOPMENT OF A PERCEPTUAL-BASED IMAGE MODEL

To accomplish the automation of the FM 5-588 procedure, the authors analytically modeled the perceptual transfer process which involves the two modes of information processing i.e. visual processing and neural processing, performed by the technicians in executing the existing FM 5-588 methodology. In general, a perceptual transfer function consists of an optical transfer function and a neural transfer function [36]. In this investigation, the above functions will be referred to as processes since mathematical functions are not employed to represent them. To develop a quantifiable optical transfer process in this investigation, the human (technician) visual system (HVS) properties involved in the OBC determination were examined first and an exhaustive set of relevant imaging parameters associated with the digital images of pie plates was derived. The above imaging parameters were then used in designing a neural transfer process that would determine the corresponding OBC, with minimum human intervention. This is achieved by training an appropriate neural network based on the extensive experimental results available from the visually executed FM 5-588. The neural network specifically trained for the types of aggregate and binder used in the training dataset is expected to transfer the imaging parameters extracted from pie plate images of any other mixtures having similar constituents to the corresponding OBC estimates in an automated manner [49 and 50].[2] Hence such a neural network would minimize the need for human involvement which introduces subjectivity.

[2]Portions of this chapter were previously published in [49, and 50]. Permission is included in Appendix J.

4.1. Image Analysis Procedures for Characterization of the Human Visual System

Modeling of the HVS as performed in computer vision and image processing is based on specific parameters derived from psycho-physical experiments [36]. The image analysis procedures presented in this section describe the particular set of image-based parameters that were presumed to represent the optical transfer process undergone by technicians who evaluate the ABD in pie plates, based on the surface appearance of pie plates. Consultation with the FDOT technicians and the authors' subsequent comparative study of the pie plate samples corresponding to trial ACs and those of the additional samples prepared at the visually adjudged OBC, led to the identification of several applicable imaging parameters. Based on their respective roles in the visual transfer process and the relevant applications in image enhancement, these parameters can be categorized into five distinct aspects of visual perception that are involved in identification of image targets by humans: (i) image contrast (ii) visibility (iii) contrast sensitivity (iv) frequency and orientation selectivity and (v) other imaging parameters involved in information processing.

4.1.1. Image Contrast

Contrast is the ability of the HVS to detect the difference in luminance between two or more stimuli. The relevant stimuli in the pie plate images are (i) the black pixel areas representing asphalt and (ii) the white pixels representing plaster of Paris. Hence the percent black pixels area of the entire pie plate (PBA) (Equation (4)) would be the most appropriate basic parameter to represent the contrast in pie plates as observed by the evaluator.

$$PBA = \frac{number\ of\ black\ pixels}{total\ number\ of\ pixels} * 100 \quad (4)$$

4.1.2. Visibility

Based on the study of visual masking concepts [36], the visibility of the target (asphalt regions in the images represented by black pixels) in contrast to the mask (rest of the image) can

be represented by the following parameters: connectivity of black pixels, number of connected black pixels and orientation of the connected black pixels regions.

4.1.2.1. Connectivity of Black Pixels

Connectivity of black pixels (CC) indicates the number of other black pixels connected to each black pixel in a pie plate image. This parameter is calculated by the adjacency searching method (subsection 3.2.1) [58]. The basic rule for the searching algorithm is to follow the adjoining black pixels until there is no other black pixel in the prioritized directions (lateral, longitudinal and diagonal). The above algorithm will finally count and label the number of black pixels next and diagonal to any given black pixel [*ij*], as illustrated in Figure 17.

4.1.2.2. Number of Connected Black Pixels Regions

In order to estimate the above parameter, specific color labels were assigned to the connected black pixels regions using the *BWlabel* syntax [56]. Figure 21(a) shows the representation of each connected black pixel region by a different color label.

4.1.2.3. Orientation of Connected Black Pixels Regions

This parameter can be computed by determining the orientation between a designated x-axis of the pie plate image and the major axis of the individual connected black pixel region [61]. Figure 21(b) shows the orientations of connected black pixel regions relative to the center of the pie plate image expressed in terms of an angle ranging from -90 to +90 degrees. For the ensuing analysis, the individual orientation values were averaged for each pie plate. The orientation parameter could be used in the future as a quality control indicator.

4.1.3. Contrast Sensitivity

The contrast sensitivity of HVS depends not only on the relative luminance between the background and the stimulus (black pixel regions) as expressed by the above contrast and visibility

factors but also on many other secondary factors, such as the size distribution and spatial frequency of stimuli objects [36]. In order to account for effects of the above factors in the evaluation of ABD which is presumed to be executed based on observation of the black pixel regions of the pie plates, the following additional factors were considered.

4.1.3.1. Size Distribution of the Target

4.1.3.1.1. Sizes (Areas) of Connected Black Pixels Regions

The sizes of connected black pixels regions were obtained as shown in Figure 21(c) and labeled with individual numbers as shown in Figure 21(e). The individual areas values were averaged for each pie plate.

4.1.3.1.2. Perimeter per Connected Black Pixels Regions

To determine the perimeter per connected black pixels region, the contour length of each black pixel region (Figure 21(d)) in the pie plate image was traced first and the average perimeter of the black pixel regions in the pie plate calculated.

4.1.3.2. Spatial Frequency of the Target

4.1.3.2.1. Uniformity Radial

Uniformity radial (U_R) parameter indicates the uniformity of the distribution of the target (connected black pixel regions) in the radial direction of the pie plate. It is calculated by separating the specimen into two sections (outer and inner) in the radial direction and estimating the distribution of the target in each section, as illustrated in Figure 21(f) [59 and 62]. U_R is calculated using Equation (5):

$$U_R = \left[\frac{Average\ Connected\ black\ pixel\ regions\ in\ the\ outer\ section}{Average\ Connected\ black\ pixel\ regions\ in\ the\ inner\ section} - 1\right] * 100 \quad (5)$$

A U_R value of zero indicates that no segregation occurs in the radial direction, while a positive value indicates that segregation occurs in the outer section of the pie plate image.

Conversely, a negative U_R indicates that segregation occurs in the inner section of the pie plate image [62]. This is one parameter (U_R) that could also be used as a quality control indicator.

4.1.3.2.2. Uniformity Angular

Uniformity angular (U_A) parameter indicates the uniformity of the distribution of the target (connected black pixel regions) in the tangential direction of the pie plate. It is calculated by dividing the pie plate image into an angular grid at 30° intervals from 0° to 360° and estimating the distribution of the target in each segment using Equation (6) [59 and 62] as illustrated in Figure 21(f)):

$$U_A = \left[\frac{connected\ black\ pixel\ areas\ of\ regions\ in\ the\ considered\ 30°\ section}{total\ \ connected\ black\ pixel\ areas\ in\ the\ pie}\right] * 100 \qquad (6)$$

For the ensuing analysis, the individual uniformity angular values by section were averaged for each pie plate. This parameter (U_A) could be used in the future as a quality control indicator.

4.1.4. Frequency and Orientation Selectivity

Studies on the frequency and orientation selectivity of the HVS reveal the existence of neurons that are sensitive to orientation, size, form, and spatial frequency, or in other words, how dissimilar the target area. The dissimilarity is measured by the parameters of Inconsistency Coefficient, centroidal distance, form factor and other imaging parameters involved in information processing in the HVS [59].

4.1.4.1. Inconsistency Coefficient

The inconsistency coefficient (I) characterizes each connected black pixels region in a pie plate image by comparing its minor and major axis with the average major axis/minor axis of other connected black pixels regions of the same pie plate. It is expressed by Equation (7) [56 and 63]:

$$I = \frac{Ax_{min}}{Ax_{max}} = \frac{(minor\ axis\ of\ individual\ connected\ black\ pixel\ region)}{(major\ axis\ of\ individual\ connected\ black\ pixel\ region\ )} \qquad (7)$$

The individual inconsistency coefficient values were averaged for each pie plate. The higher the value of average I, the less similar the connected black pixel regions are.

4.1.4.2. Centroidal Distances

Centroidal distances of each connected black pixel region are determined by measuring the distance from the centroid of each connected regions to the center of the pie plate image as shown in Figure 21(c) [50 and 63]. The individual centroidal distance values were averaged for each pie plate.

4.1.4.3. Form Factor

Form factor (*FF*) describes the geometrical irregularity of target areas (e.g., connected black pixels region) with respect to a circle, for which FF=1. It is expressed by the following equation [64 and 65]:

$$FF = \frac{4\pi A}{P^2} = \frac{4\pi(area\ of\ individual\ connected\ black\ pixel\ region)}{(perimeter\ of\ individual\ connected\ black\ pixel\ region)^2} \quad (8)$$

For the ensuing analysis, the individual form factor values were averaged for each pie plate.

4.1.5. Other Imaging Parameters Involved in Information Processing in the HVS

Perceptive estimates made based on visual observation are primarily driven by past experiences of observers such as the technicians involved in the visual OBC determination. While visually processing the characteristics of the trial pie plates of known ACs, the technicians would interpolate the binder content of the most favorable sample, i.e., OBC, using their past experience with an additional set of pie plate image characteristics not included in the above categories. The authors have identified the following three parameters to be in this category.

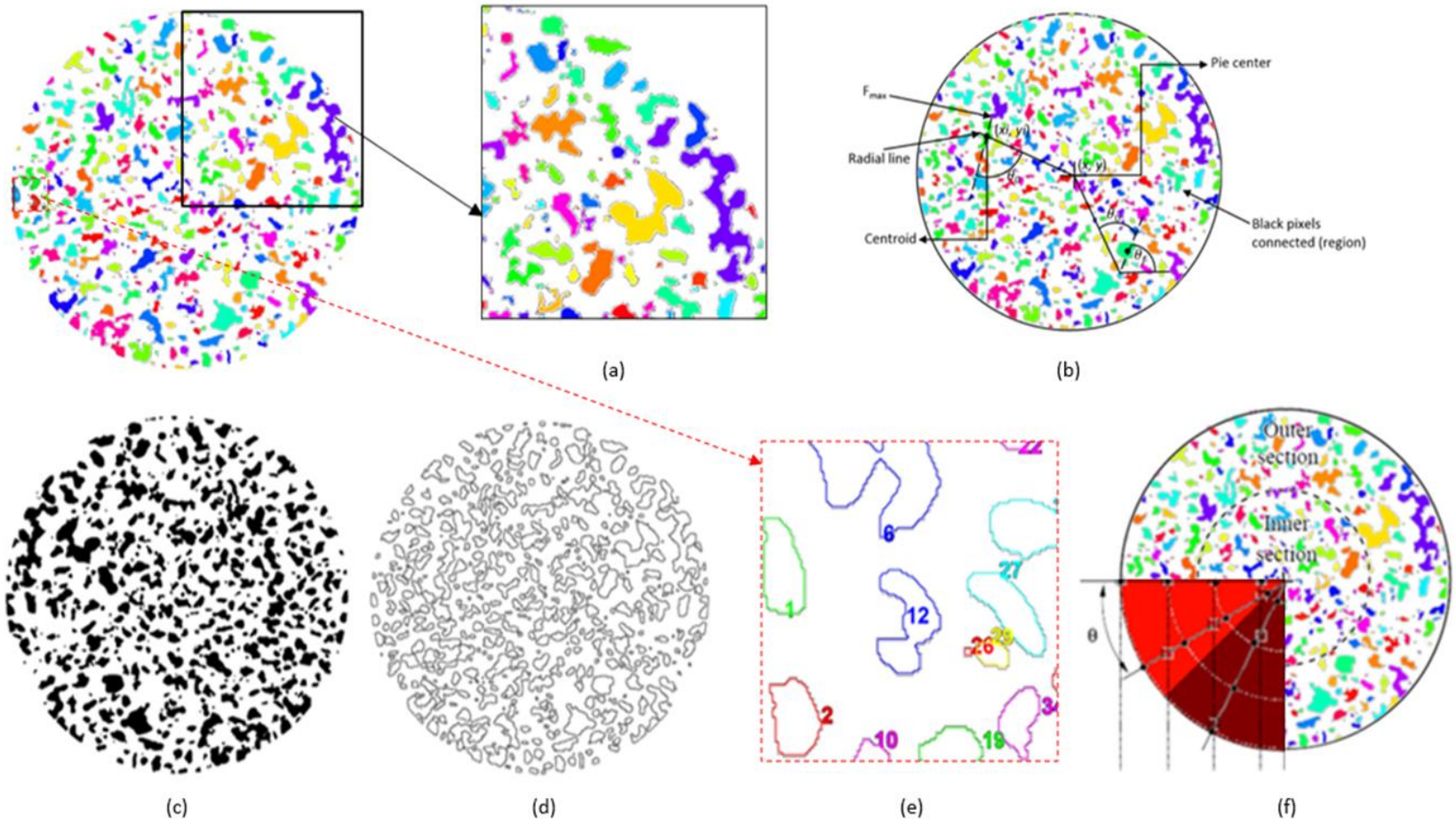

Figure 21 Representation of black pixels on a pie plate image for connected black pixels (a) color label, (b) orientation relative to the center of the pie plate image, (c) individual areas, (d) traced perimeters, (e) label with numbers, (f) illustration of sections of radial segregation and angular mesh.

4.1.5.1. Compactness per Connected Black Pixels Regions

Compactness (*C*) is a measure of the ruggedness of the connected black pixel regions as expressed by Equation (9) [35]. This parameter represents a lesser or higher level of complexity of the contour of each black pixel area region.

$$C = \frac{(square\ of\ the\ perimeter\ of\ an\ individual\ connected\ black\ pixel\ region)}{(area\ of\ the\ individual\ connected\ black\ pixel\ region)} \quad (9)$$

Authors' scrutiny of the additional samples prepared at the OBC after the OBC of each mixture was determined by the technicians revealed that, in judging how close the AC of a given pie plate is to OBC, the evaluators would also look for the presence of black pixel regions that are not rugged. For the ensuing analysis, the individual compactness values were averaged for each pie plate.

4.1.5.2. Solidity

Solidity (*SLD*) is the measure of the density of any connected black pixel region which specifies the proportion of the pixels in the convex hull (Figure 22) circumscribing a connected black pixel region [56] and computed as:

$$SLD = \frac{(Actual\ connected\ black\ pixel\ region)}{(Convex\ hull\ area\ of\ each\ connected\ black\ pixel\ region)} \quad (10)$$

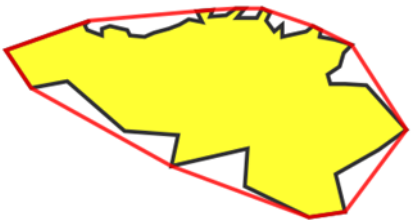

Figure 22 Example of convex hull of a connected black pixels area.

In judging how close the AC of a given pie plate is to OBC, the evaluators would look for black pixel regions to have solid appearances. A solidity value of 1 implies that the given

connected black pixel region is entirely solid. The individual solidity values were averaged for each pie plate.

4.1.5.3. Eccentricity

This parameter specifies the eccentricity of the ellipse bearing the same second moment of area as the considered connected black pixel region. The eccentricity has the usual definition of ratio of the distance between the foci of the above ellipse and its major axis length [56]. For the ensuing analysis, the individual eccentricity values were averaged for each pie plate.

Finally, an information vector **X** containing the averages of each of the above imaging parameters (Table 10) that are assumed to constitute the visual transfer function was set up for each pie plate sample (Figure 21) [66 and 67]. Then **X**, the corresponding asphalt binder contents and the estimated OBC values were used to develop the neural transfer function as described in Chapter 6. The GRNN prediction model are found in Appendix G.

Table 10 Imaging parameters that represent the visual transfer process used for the study.

	Parameters	*HVS category*
1	PERCENT OF BLACK PIXELS OF PIE PLATE	Contrast
2	CONNECTIVITY OF BLACK PIXELS	Visibility
3	NUMBER OF REGIONS OF PIE PLATE	
4	AVERAGE ORIENTATION	
5	AVERAGE AREA OF REGIONS	Contrast Sensitivity
6	AVERAGE PERIMETER	
7	UNIFORMITY_RADIAL	
8	AVERAGE UNIFORMITY_ANGULAR	
9	AVERAGE INCONSISTENCY COEFFICIENT	Frequency and Orientation Selectivity
10	AVERAGE CENTROID DISTANCE	
11	AVERAGE FORM FACTOR	
12	AVERAGE COMPACTNESS	Information Processing in the HVS
13	AVERAGE SOLIDITY	
14	AVERAGE ECCENTRICITY	

CHAPTER 5: QUALITY CONTROL MODEL

The author's research developments in digital imaging processing to quantify the ABD on pie plates has resulted in the possibility of increased contractor involvement in the design and acceptance of OGFC mixtures designs. As a result, questions have arisen as to whether the results of QC tests of PPS production carried out by contractors should be incorporated into the acceptance criteria currently used by FDOT in addition to the proposed imaging processing algorithm presented in Chapter 4. In order to address these questions, the primary objective of this chapter is to develop the QCT to be implemented through the database generated during the Phases I and II of this study and accomplish the evaluation of the relevant QC parameters that would indicate the quality of the pie plate specimens[3].

The development of QCT is divided in three sections; (i) Evaluate and analyze ABD characterization by means of past aggregate characterization researchers studies [61 to 69] to provide bases for quantifying the image-based quality control imaging parameters (QCIP) of the surface appearance of pie plates highly relevant to QC of the ABD configuration of the pie plate specimen; (ii) statistical verification of QCIP, and (iii) assess scientific acceptability of measure criteria (reliability and validity) of the QC results.

5.1. Measure and Analyze ABD Characterization to Provide Quantifying QCIP

Findings from one of the most complete studies [68] on defining internal aggregate parameters derived from images were used to analyze the ABD regions of the PPS digital images.

[3]Portions of this chapter were previously published in [50]. Permission is included in Appendix J.

The steps of redefining the ABD regions into ellipses is shown in Figure 20(a). Major and minor axes of ABD regions are essential for quantifying the QCIP. The major axis of a given ABD region is the line joining two pixels on the boundary contour that are the farthest apart and the length of that line is defined as the major axis length. On the other hand, the minor axis is the longest line perpendicular to the major axis that can be inscribed within that ABD region and its length is the minor axis length. For each ABD region, the aforementioned QCIP are calculated.

5.1.1. Orientation

The set of orientation parameters of each ABD region can be defined using two criteria; (i) the orientation angle of the major axis with respect to the horizontal axis (θ_f) and (ii) the orientation angle of the major axis relative to the line joining the centroid of the region to the pie plate center (θ_o) [61-62, 68-69]. Figure 23 shows the orientation of connected black pixel (ABD) regions of the PPS image expressed using both the above criteria and calculated using equations (11) and (12) respectively.

$$\theta_f = tan^{-1}\frac{(y_i - y_j^c)}{(x_i - x_j^c)} \tag{11}$$

$$\theta_o = cos^{-1}\frac{(x_j^c - x^p) + \tan\theta_f * (y_j^c - y^p)}{\sqrt{1 + (\tan\theta_f)^2} + \sqrt{(x_j^c - x^p)^2 + (y_j^c - y^p)^2}} \tag{12}$$

where x_j^c and y_j^c are the coordinates of the centroid of the labeled region j; x^p and y^p are the coordinates of the center of the pie plate; x_i and y_i are the coordinates of the surface pixel at the outer intersection of a given ABD ellipse and its major principal axis. It must be noted that when $\theta_f = 90^\circ$, θ_o must to be calculated using $\theta_o = cos^{-1}(y_j^c - y^p)$.

The next step is the determination of the directional distribution of ABD by calculating the vector magnitude (Δ_f), which quantifies the average anisotropy of orientation parameter θ_f [66, 68-69]. The aforesaid directional distribution of the ABD vector magnitude is calculated using

Equation (13) [65 and 68]. The results of directional distribution of the ABD indices (Δ_f) for all PPS tested in Phase I are presented in the forthcoming Summary of Findings chapter (Chapter 7).

$$\Delta_f = \frac{1}{M} * \sqrt{(\sum_{i=1}^{M} \cos 2\theta_f)^2 + (\sum_{i=1}^{M} \sin 2\theta_f)^2} \quad (13)$$

where Δ_f is the directional distribution of the ABD vector magnitude for the orientation, and M is the number of θ_f values in a given pie plate.

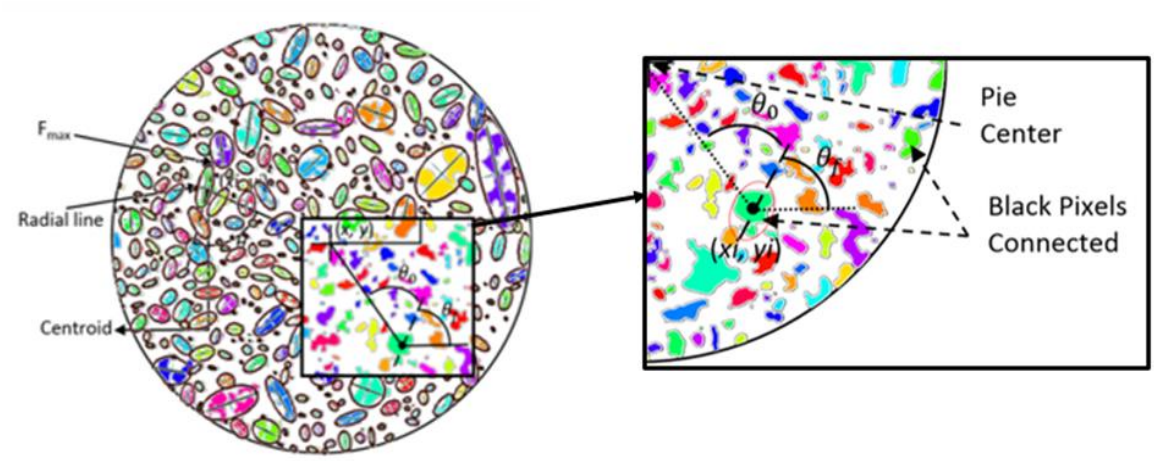

Figure 23 Representation of connected black pixels on a pie plate image for SABD identification of the orientation relative to the center of the pie plate image.

5.1.2. Spatial Distribution

The spatial distribution (*SD*) is calculated by first dividing the PPS image into wedge sections as illustrated in Figure 24. Thirty degree sections were considered to be the optimum in this study and thus 12 wedge shaped sections covered the entire cross section of each PPS. Then, an algorithm was developed to evaluate the percentage of ABD with centroids within each section ($SD_{section}$), using Equation (14) [50, 62, 63, 66 and 67]. The presumption underlying the eventual analysis is that, if the ABD regions are evenly distributed in the PPS, then different sections should have more or less identical ABD areas. The pie plate spatial distribution (SD) parameter was calculated as the standard deviation of the $SD_{section}$ in the twelve sections

computed using Equation (15). The results of the $SD_{section}$ parameter by section and by pie plate for all PPS tested in Phase I are presented in the forthcoming Summary of Findings chapter (Chapter 7).

$$SD_{section} = \left[\frac{connected\ SABD\ regions\ in\ the\ \theta{=}30^{\circ}\ section}{total\ \ connected\ SABD\ regions\ in\ the\ pie\ plate}\right] * 100 \quad (14)$$

$$SD = Standard\ Deviation\ (SD_{section\ 1-12}) \quad (15)$$

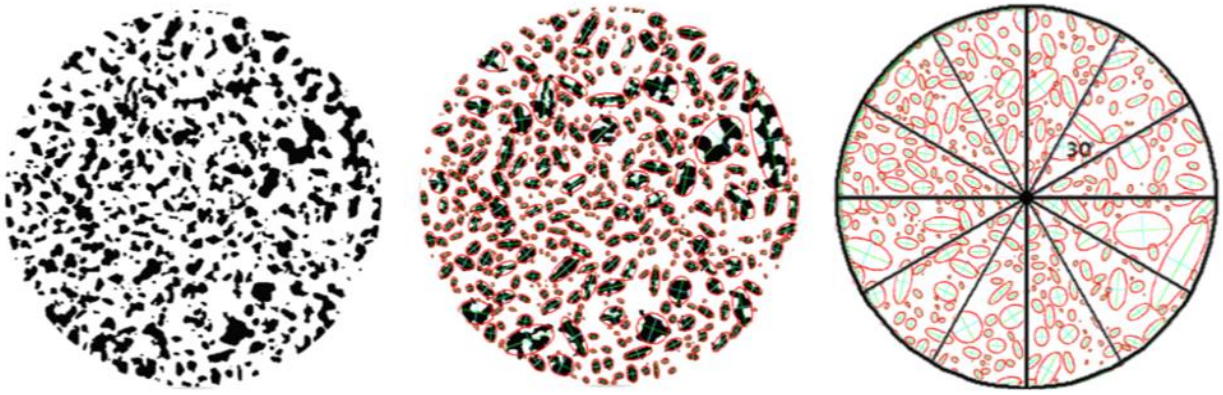

Figure 24 Representation of connected black pixels on a pie plate image for SABD identification for the location in the angular mesh.

5.1.3. Segregation

Segregation (S) is calculated by first dividing each PPS into two sections in the radial direction; the outer section (S_o) and the inner section (S_i) of the PPS image which are of equal areas as illustrated in Figure 25 [61-63 and 69].

The parameter S is evaluated by determining the percent of ABD regions with centroids within each of the two sections, using Equation (16) and the ratio of the ABD regions (inner/outer) is evaluated using Equation (17).

$$S_{o\ or\ i} = \left[\frac{Connected\ SABD\ regions\ in\ the\ outer\ or\ inner\ section}{Connected\ SABD\ regions\ \ in\ the\ pie\ plate}\right] * 100 \quad (16)$$

$$S = \left[\frac{Connected\ SABD\ regions\ in\ the\ inner\ section}{Connected\ SABD\ regions\ \ in\ the\ outer\ section} \right] \quad (17)$$

The algorithm then plots (in the form of column chart) the percentage of SABD regions in each section [69]. The tabulated results are presented in the forthcoming Summary of Findings chapter (Chapter 7).

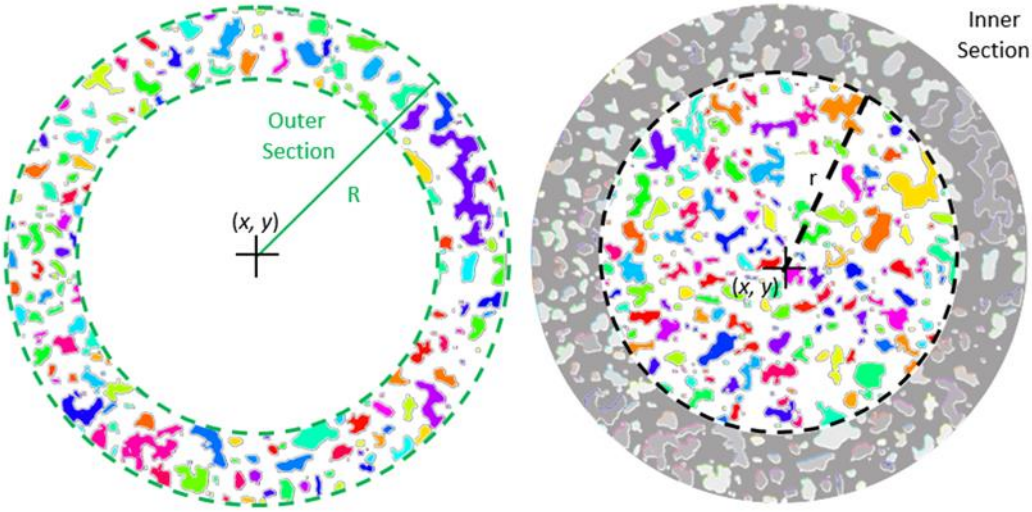

Figure 25 Representation of connected black pixels on a pie plate image for SABD identification illustrating sections of segregation.

5.2. Statistical Verification of QCIP

The quality of the output consists of two key components; target value and variability [70]. Target value is the goal set for a certain characteristic and variability describes how much a process varies from item-to-item [70]. For example, on a particular pie plate, the orientation of the ABD should be well distributed instead of being in the same direction. Quality control actions and considerations should be based on objective evidence and not subjective opinion. This does not mean that experience and expertise are not valuable but rather that they should be used to determine what measurements to consider and how to improve the process. Furthermore, all the pie plate samples (PPS) used in this study had satisfied the visual quality checks routinely performed by the FDOT technicians. Thus, the above PPS provided a basis for verifying the applicability of the QCIP

selected by the authors. Consequently, a statistical study was performed on the QCIP computed for all the PPS tested in Phase I of the study.

The three imaging parameters (measures) defined above which are considered as potential QC parameters for the QCT were evaluated by the authors against the two scientific acceptability of measure criteria; reliability and validity. Reliability demonstrates that the measure data elements are repeatable, producing the same results a high proportion of the time when assessed in the same population in the same time period and/or that the measure score is precise and validity demonstrates that the measure data elements are correct and/or the measure score correctly reflects the quality of care provided, adequately identifying differences in quality [71].

5.2.1. Orientation

Theoretically, the values of the orientation parameter Δ_f (equation (13)) range from 0 to 1 with 0 representing a completely random distribution of ABD regions and 1 representing ABD regions that are perfectly aligned in one direction. Table 11(a) shows the statistical t-test results for Δ_f parameter obtained from the PPS samples tested in Phase I. Statistical tables used for the evaluation of the results are found in Appendix I. Based on the t-test, it was found that the mean difference of the Δ_f parameters within all PPS is 0.119 at a significant level of 99.9%.

5.2.2. Spatial Distribution

Theoretically, the value of $SD_{section}$ for each section should be 8.33 for a perfectly uniform distribution of ABD in the 12 sections of the pie plate. Table 11(b) shows the statistical t-test results for the pie plate spatial distribution ($SD_{pie\ plate}$) parameter for PPS produced in Phase I. Based on the results, it can be seen at a confidence level of 95% that the standard deviation of the spatial distribution (equation (5)) is within 0 and 1.52 for acceptable pie plates. Appendix I shows the completed generated results of the SPSS for the spatial distribution parameter.

Table 11 Statistical "t-test" for the QC parameters.

(a) One-Sample Statistics Statistical t-test for the orientation (Δ_f) parameters

	N	Mean	Std. Deviation	Std. Error Mean
Δ_f	342	.1191	.05243	.00284

	Test Value = 0					
					95% Confidence Interval of the Difference	
	T	df	Sig. (2-tailed)	Mean Difference	Lower	Upper
Δ_f	42.018	341	.000	.11912	.1135	.1247

(b) One-Sample Statistics Statistical t-test for the spatial distribution ($SD_{pie\ plate}$) parameter

	N	Mean	Std. Deviation	Std. Error Mean
$SD_{pie\ plate}$	342	1.0514	.27431	.01483

	Test Value = 0					
					95% Confidence Interval of the Difference	
	T	df	Sig. (2-tailed)	Mean Difference	Lower	Upper
$SD_{pie\ plate}$	70.885	341	.000	1.05143	1.0223	1.0806

(c) One-Sample Statistics Statistical t-test for the segregation (S_{ratio}) parameters.

One-Sample Statistics

	N	Mean	Std. Deviation	Std. Error Mean
Inner	342	48.3616	7.00167	.37861
Outer	342	51.6384	7.00167	.37861
Ratio	342	.9703	.25737	.01392

One-Sample Test

	Test Value = 0					
					95% Confidence Interval of the Difference	
	T	df	Sig. (2-tailed)	Mean Difference	Lower	Upper
Inner	127.736	341	.000	48.36161	47.6169	49.1063
Outer	136.390	341	.000	51.63839	50.8937	52.3831
Ratio	69.720	341	.000	.97028	.9429	.9977

5.2.3. Segregation

Theoretically, both the outer and inner segregation parameters (S_o and S_i) must be equal to 50 for an even distribution with no segregation in either the outer section or the inner section. In other words, the ratio (S_{ratio}) of the ABD area (inner/outer) (Equation (17)) must be equal to 1.0 for an evenly distributed ABD in a pie plate. Table 11(c) shows the statistical t-test results of the segregation parameters for the pie plates used in Phase I. It was found at a confidence level of 99% that for the pie plates produced in Phase I, the S_{ratio} has a mean value of 0.97.

5.3. Assess Scientific Acceptability of Measure Criteria of the QC Results

To ratify the QC results (target and ranges values), the data set was evaluated for scientific acceptability of measure properties (reliability and validity) [71] following the "Evaluation of Scientific Acceptability of Measure Properties" based on reliability and validity ratings as shown in Table 12.

Table 12 Evaluation of scientific acceptability of measure properties based on reliability and validity ratings [71].

Validity Rating	**Reliability Rating**	**Pass *Scientific Acceptability of Measure Properties* for initial Endorsement***	
High	**Moderate-High**	**Yes**	Evidence of reliability and validity
	Low	No	Represents inconsistent evidence--reliability is usually considered necessary for validity
Moderate	**Moderate-High**	**Yes**	Evidence of reliability and validity
	Low	No	Represents inconsistent evidence--reliability is usually considered necessary for validity
Low	Any rating	No	Validity of conclusions about quality is the primary concern. If evidence of validity is rated low, the reliability rating will usually also be low. Low validity and moderate-high reliability represents inconsistent evidence.

* A measure that does not pass the criterion of *Scientific Acceptatbility of Mesure Properties* would not be recommended for endorsement.

The first step in evaluating reliability and validity is to recognize the type of validity and the forms of reliability and how to measure them. The two main types of validity are Internal and External validity. Internal Validity is concerned with the degree of certainty that observed effects

in an experiment are actually the result of the experimental test. Internal validity is enhanced by increasing the control of these other variables. External Validity, in the other hand is concerned with the degree to which research findings can be applied to the real world, beyond the controlled setting of the research.

The four forms of reliability are Inter-Observer, Test-Retest, Parallel-Forms or Alternate-Forms, and Tests for Homogeneity or Internal Consistency. "Inter-Observer Reliability is used to assess the degree to which different observers agree when measuring the same phenomenon simultaneously. Test-Retest Reliability compares results from an initial test with repeated measures later on, the assumption being that the if the measurement is reliable there will be close agreement over repeated tests if the variables being measured remain unchanged. Parallel-Forms or Alternate-Forms Reliability is used to assess the consistency of the results of two similar types of test used to measure the same variable at the same time. Tests for Homogeneity or Internal Consistency, in the other hand is concerned with the measurement which would reflect the homogeneity of the results. This can be tested using several methods, the split-half form, Chronbach's alpha, or Cohen's kappa." For this study the Chronbach's alpha was used to obtain the lower bound on reliability using equation (18). Commonly-accepted rule of thumb is that Cronbach's alpha of 0.7 (some say 0.6) indicates acceptable reliability and 0.8 or higher indicates good reliability.

One can easily obtain Chronbach's alpha values by using the following function provided in the Real Statistics Resource Pack in Excel:

CRONALPHA(R1, *k*) = Cronbach's alpha for the data in range R1 if $k = 0$ (default) and Cronbach's alpha with *k*th item (i.e. column) removed if $k > 0$.

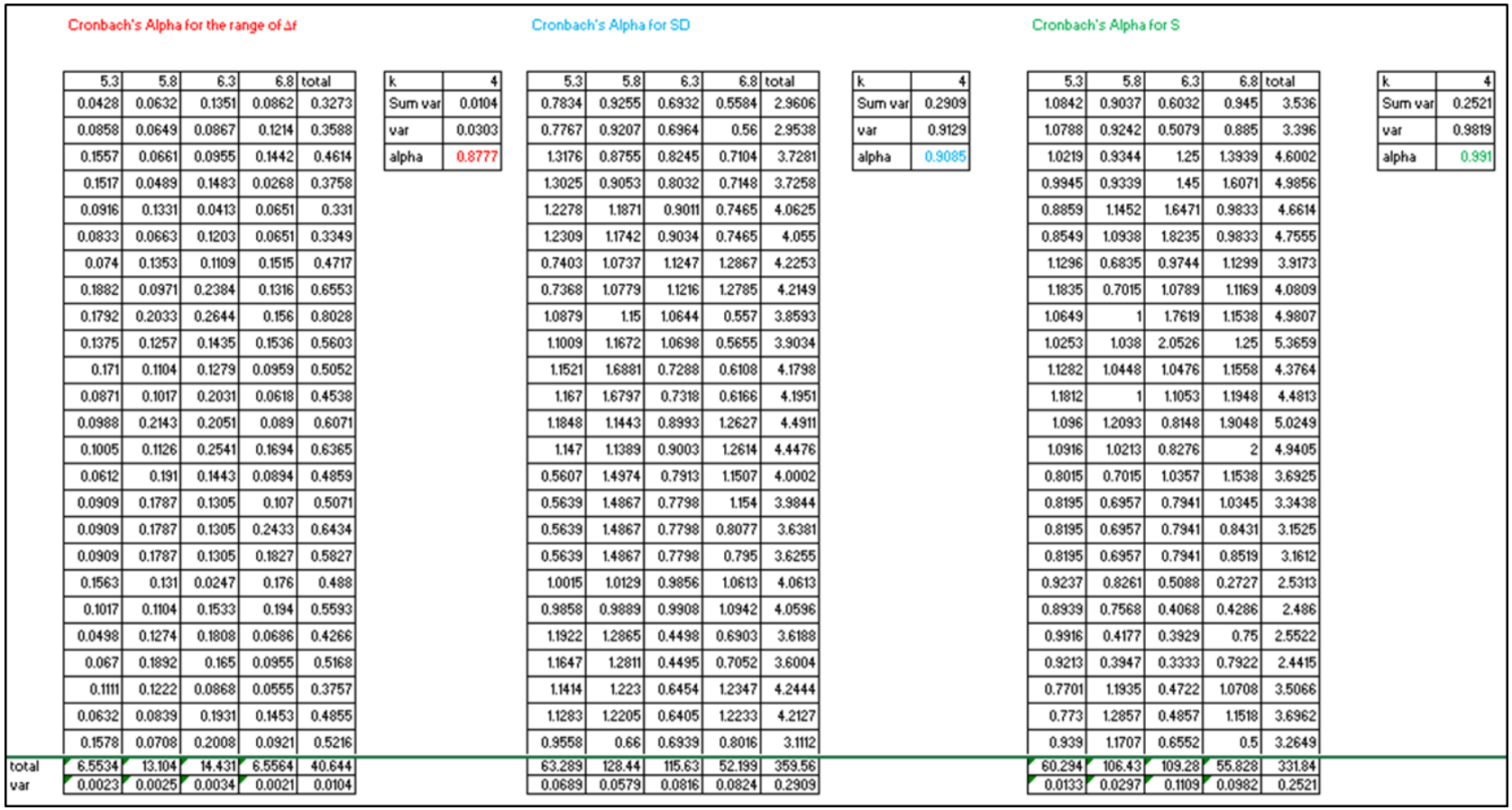

5.3	5.8	6.3	6.8	total
0.0428	0.0632	0.1351	0.0862	0.3273
0.0858	0.0649	0.0867	0.1214	0.3588
0.1557	0.0661	0.0955	0.1442	0.4614
0.1517	0.0489	0.1483	0.0268	0.3758
0.0916	0.1331	0.0413	0.0651	0.331
0.0833	0.0663	0.1203	0.0651	0.3349
0.074	0.1353	0.1109	0.1515	0.4717
0.1882	0.0971	0.2384	0.1316	0.6553
0.1792	0.2033	0.2644	0.156	0.8028
0.1375	0.1257	0.1435	0.1536	0.5603
0.171	0.1104	0.1279	0.0959	0.5052
0.0871	0.1017	0.2031	0.0618	0.4538
0.0988	0.2143	0.2051	0.089	0.6071
0.1005	0.1126	0.2541	0.1694	0.6365
0.0612	0.191	0.1443	0.0894	0.4859
0.0909	0.1787	0.1305	0.107	0.5071
0.0909	0.1787	0.1305	0.2433	0.6434
0.0909	0.1787	0.1305	0.1827	0.5827
0.1563	0.131	0.0247	0.176	0.488
0.1017	0.1104	0.1533	0.194	0.5593
0.0498	0.1274	0.1808	0.0686	0.4266
0.067	0.1892	0.165	0.0955	0.5168
0.1111	0.1222	0.0868	0.0555	0.3757
0.0632	0.0839	0.1931	0.1453	0.4855
0.1578	0.0708	0.2008	0.0921	0.5216
6.5534	13.104	14.431	6.5564	40.644
0.0023	0.0025	0.0034	0.0021	0.0104

k	4
Sum var	0.0104
var	0.0303
alpha	0.8777

5.3	5.8	6.3	6.8	total
0.7834	0.9255	0.6932	0.5584	2.9606
0.7767	0.9207	0.6964	0.56	2.9538
1.3176	0.8755	0.8245	0.7104	3.7281
1.3025	0.9053	0.8032	0.7148	3.7258
1.2278	1.1871	0.9011	0.7465	4.0625
1.2309	1.1742	0.9034	0.7465	4.055
0.7403	1.0737	1.1247	1.2867	4.2253
0.7368	1.0779	1.1216	1.2785	4.2149
1.0879	1.15	1.0644	0.557	3.8593
1.1009	1.1672	1.0698	0.5655	3.9034
1.1521	1.6881	0.7288	0.6108	4.1798
1.167	1.6797	0.7318	0.6166	4.1951
1.1848	1.1443	0.8993	1.2627	4.4911
1.147	1.1389	0.9003	1.2614	4.4476
0.5607	1.4974	0.7913	1.1507	4.0002
0.5639	1.4867	0.7798	1.154	3.9844
0.5639	1.4867	0.7798	0.8077	3.6381
0.5639	1.4867	0.7798	0.795	3.6255
1.0015	1.0129	0.9856	1.0613	4.0613
0.9858	0.9889	0.9908	1.0942	4.0596
1.1922	1.2865	0.4498	0.6903	3.6188
1.1647	1.2811	0.4495	0.7052	3.6004
1.1414	1.223	0.6454	1.2347	4.2444
1.1283	1.2205	0.6405	1.2233	4.2127
0.9558	0.66	0.6939	0.8016	3.1112
63.289	128.44	115.63	52.199	359.56
0.0689	0.0579	0.0816	0.0824	0.2909

k	4
Sum var	0.2909
var	0.9129
alpha	0.9085

5.3	5.8	6.3	6.8	total
1.0842	0.9037	0.6032	0.945	3.536
1.0788	0.9242	0.5079	0.885	3.396
1.0219	0.9344	1.25	1.3939	4.6002
0.9945	0.9339	1.45	1.6071	4.9856
0.8859	1.1452	1.6471	0.9833	4.6614
0.8549	1.0938	1.8235	0.9833	4.7555
1.1296	0.6835	0.9744	1.1299	3.9173
1.1835	0.7015	1.0789	1.1169	4.0809
1.0649	1	1.7619	1.1538	4.9807
1.0253	1.038	2.0526	1.25	5.3659
1.1282	1.0448	1.0476	1.1558	4.3764
1.1812	1	1.1053	1.1948	4.4813
1.096	1.2093	0.8148	1.9048	5.0249
1.0916	1.0213	0.8276	2	4.9405
0.8015	0.7015	1.0357	1.1538	3.6925
0.8195	0.6957	0.7941	1.0345	3.3438
0.8195	0.6957	0.7941	0.8431	3.1525
0.8195	0.6957	0.7941	0.8519	3.1612
0.9237	0.8261	0.5088	0.2727	2.5313
0.8939	0.7568	0.4068	0.4286	2.486
0.9916	0.4177	0.3929	0.75	2.5522
0.9213	0.3947	0.3333	0.7922	2.4415
0.7701	1.1935	0.4722	1.0708	3.5066
0.773	1.2857	0.4857	1.1518	3.6962
0.939	1.1707	0.6552	0.5	3.2649
60.294	106.43	109.28	55.828	331.84
0.0133	0.0297	0.1109	0.0982	0.2521

k	4
Sum var	0.2521
var	0.9819
alpha	0.991

Figure 26 Calculation of Cronbach's alpha for all the mixtures considered in this study.

Thus for the data (all the mixtures considered in this study), we can obtain the results shown in Figure 26 using CRONALPHA(B4:F118) for the QCIP gives the following: CRONALPHA(B4:F118) Δ_f =.8777, CRONALPHA(B4:F118)$_{SD}$ =.0.9085, and CRONALPHA(B4:F118)$_S$ = .991. As you can see from Figure 26, Cronbach's alpha values indicates acceptable reliability for all of the QCIP.

$$\alpha = \frac{K}{K-1}\left(1 - \frac{\sum_{i=1}^{K}\sigma_{Y_i}^2}{\sigma_X^2}\right) \tag{18}$$

where K is a sum of components (observed test scores), σ_X^2 is the variance of the observed total test scores, and $\sigma_{Y_i}^2$ is the variance of component i for the current sample.

Statistical analysis would also play a major role in the examination of statistical results that would be used to establish target values and acceptable tolerances of the QCIP. Using the statistical results derived from a supplementary simulation study developed by the authors, target values and acceptable tolerances were found for each QC parameter and based on them, guidelines for the use of QCIP were formulated. Table 13 shows the internal consistency values.

Table 13 Internal consistency values [71].

Cronbach's alpha	Internal consistency
$\alpha \geq 0.9$	Excellent
$0.9 > \alpha \geq 0.8$	Good
$0.8 > \alpha \geq 0.7$	Acceptable
$0.7 > \alpha \geq 0.6$	Questionable
$0.6 > \alpha \geq 0.5$	Poor
$0.5 > \alpha$	Unacceptable

In the expanded study, a sample set of computer-generated defective pie plates were produced using a computer algorithm to supplement a limited number of defective pie plates prepared by FDOT staff. In both sets of defective pie plates; computer-generated and those

prepared by FDOT staff, the SABD areas were represented by ellipses. Then, QCIP of both sets were evaluated. The statistical results of this set of defective pie plates and all PPS tested in Phase I are presented in the forthcoming Summary of Findings chapter (Chapter 7).

5.3.1. Orientation

Based on the results presented in the forthcoming Summary of Findings chapter (Chapter 7) and the scientific acceptability of measure criteria [71], the authors propose that the range of Δ_f of 0 to 0.25 be considered as the range for acceptable orientation of ABD in a pie plate sample.

5.3.2. Spatial Distribution

Based on the results presented in the forthcoming Summary of Findings chapter (Chapter 7) and the scientific acceptability of measure criteria [71], the authors propose that if the standard deviation of the *SD* values of the 12 sections of the pie plate is less than 1.52, the spatial distribution will be considered acceptable for a pie plate.

5.3.3. Segregation

Based on the results presented in the forthcoming Summary of Findings chapter (Chapter 7) and the scientific acceptability of measure criteria [71], the authors propose that the S_{ratio} (inner/outer) range of 0.51 to 1.34 be considered acceptable for a pie plate.

CHAPTER 6: NEURAL NETWORK-BASED PREDICTION MODEL

FM 5-588 procedure is executed for each mixture with three pie plates and their trial AC's known to the technicians. Then, the technicians use the above values and their visual perception of ABD in pie plates to estimate the OBC based on the ABD. Therefore, the input to the envisioned OBC prediction mechanism would consist of three parallel sets of information vectors (X_k, k=1, 3) corresponding to each mixture. Each vector contains the imaging parameters described in Chapter 4, which are presumed to model the visual transfer process, and the corresponding three AC. Due to the vast extent of the input information and the complex relationship between the input data and the output y (OBC), a trained neural network was determined to be the most viable method of achieving the automated OBC prediction.

The function of the neural network is to discover the nonlinear perceptive control function that relates the parameters included in the above three vectors (X_k) to a single OBC value y. This is facilitated by training an appropriate neural network with the information presented in the training input vectors ($\mathbf{X_k}$) assembled using the experimental data gathered from the majority of mixtures tested in Phase I. The authors determined that this process can be successfully accomplished by a General Regression Neural Network (GRNN). GRNN approximates any arbitrary function between input and output vectors by executing the function estimation directly from training data [42]. GRNN is based on nonlinear regression theory for function estimation. The training set comprises **m** values of an input vector $\mathbf{X_k}$ with a single output value y. It must be noted that in the current investigation, each $\mathbf{X_k}$ is a set x_j (j=1,n) values containing imaging

parameters and asphalt binder contents while y is the OBC corresponding to each $\mathbf{X_k}$. Therefore, the GRNN must have n number of input nodes (neurons) and one output node (Figure 27(a)).

The estimation of the expected value of y is based on the following generalized conditional probability [42]:

$$E(y|X) = \frac{\int_{-\infty}^{\infty} y\, f(X,y)dy}{\int_{-\infty}^{\infty} f(X,y)dy} \tag{19}$$

where $f(\boldsymbol{X}, y)$ is the joint probability density function of $\boldsymbol{X}$ and y. For problems involving numerical data such as the current one, Equation (19) can be simplified to the following form:

$$\hat{Y}(\mathrm{X}) = \frac{\sum_{i=1}^{n} Y_i h_i}{\sum_{i=1}^{n} h_i} \tag{20}$$

$$h_i = e^{\left[-\frac{D_i^2}{2\sigma^2}\right]} \tag{21}$$

$$D_i{}^2 = (X - X_i)^T (X - X_i) \tag{22}$$

where: $\boldsymbol{X_i}$ and Y_i are input and output values of the i^{th} training sample ($i=1,m$) and D_i, which is the squared distance between the point of prediction (particular $\boldsymbol{X}$) and the i^{th} training sample $\boldsymbol{X_i}$.

It can be seen that Equation (21) specifies a normally distributed weight, around the assumed mean of $\boldsymbol{X_i}$ and a standard deviation of σ, that can be attached to the output of the i^{th} training sample. One realizes that the above weight decreases with D_i. Typically, h_i can be the output of a hidden layer neuron. Thus, instead of employing training weights like in other neural networks, (e.g. backpropagation neural network (BPNN)), the GRNN assigns the target value (Y_i) directly to the weights from the training set. This regression method yields the estimated value of y, which minimizes the squared error [42]. GRNN incorporates a one-pass learning algorithm with a parallel structure, which is commonly described as a memory-based algorithm that provides estimates of continuous variables and converges to the underlying nonlinear regression surface

between y and X. Even with sparse data, the algorithm provides smooth transitions from one observed value $(x_j)_i$ to another [42].

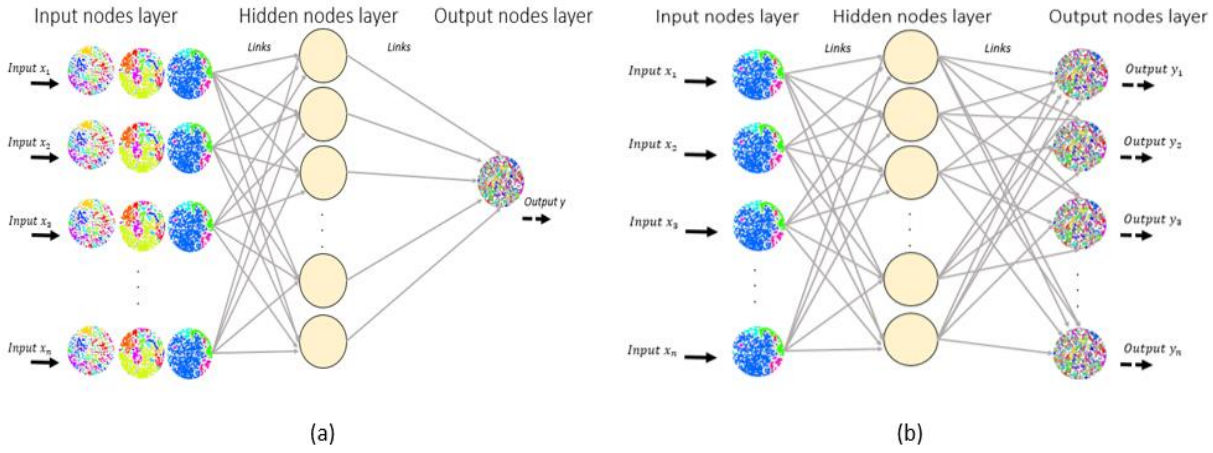

Figure 27 Neural network flowchart for (a) multi-dimensional, (b) one dimension.

A GRNN, like other probabilistic neural networks, needs only a fraction of the training samples a BPNN would need, to converge to the underlying function that would constitute the input and output data [42]. The additional knowledge needed to obtain a satisfactory fit is relatively small and can be done without additional input by the user. The above characteristics makes GRNN an ideal tool to implement estimates of systems that involve a complex relationship between a relatively large vector of input data such as $\mathbf{X_k}$ and the output *y*, as in the current OBC determination problem. The architecture of the GRNN used in this research consists of three layers; input layer, hidden layer and output layer. Two case studies are presented to illustrate the effectiveness of GRNN in this investigation. The first case study illustrates the exploration of the relationship between the relevant HVS parameters and the AC of pie plate mixtures using a one dimensional GRNN (Figure 27(b)). On the other hand, the second case study demonstrates the prediction of the OBC based on the relevant HVS parameters of pie plate mixtures by using a multi-dimensional GRNN (Figure 27(a). The values of imaging parameters discussed in Chapter 4 and the ACs are posed in 3 parallel vectors ($\boldsymbol{X_k}$, *k=1,3*) containing elements x_{kj} (*k=1,3* and *j=1,n*)

each corresponding to one of a trial set of three pie plates with one common OBC estimate y. This exercise is performed m times ($i=1,m$) during training of the GRNN.

The analysis/output for the training, testing and predicting neural network model generates a results file where the data was tabulated in the forthcoming summary of findings chapter (Chapter 7).

CHAPTER 7: SUMMARY OF FINDINGS

7.1. Phase I- Preliminary Assessment of the Asphalt Binder Content Determination

This phase of the study was performed to verify the accuracy of the existing FDOT method[4] by repeating the measurements using Matlab and Labview [51].

The results indicate the following: (1) The correlation between the percent black pixel area of the pie plate images and the asphalt binder content is not adequately defined for the former parameter to be used as a stand-alone parameter for accurate estimation of the asphalt binder content, (2) A regression analysis that employs both percent black pixel area and connectivity of black pixels seems to predict the asphalt binder content more accurately for all the mixtures considered in this study. The improved accuracy of the combined regression analysis involving both parameters identified above suggests that such estimation could be further improved by combining other relevant digital image based classification parameters. Based on these results the objective of the next phase was identified. Consequently, the author envision the possibility of using innovative imaging concepts and tools employed in machine vision and other cognitive sciences which would be more relevant to modeling the uncertainty arising from human judgment.

7.2. Phase II- Prediction of Optimum Asphalt Binder Content

This phase of this study was performed to investigate the accuracy of the GRNN method by repeating two predictions previously made using two different regression models [51]. First, the asphalt binder contents of pie plates were predicted using one imaging parameter (PBA) using

[4] Portions of this chapter were previously published in [51]. Permission is included in Appendix J.

a one dimensional GRNN prediction model (Figure 27(b)). Table 14 shows the sample set of input and output data used for one dimensional training. In the second case, asphalt binder contents of pie plates were predicted from the entire set of imaging parameters using a multi-dimensional GRNN prediction model (Figure 27(a)). The information from the pie plate imaging parameters from 228 samples and the corresponding OBC data is posed to the GRNN in three parallel vectors as discussed in chapter 6. Table 15 shows the sample set of input and output data used for multi-dimensional sample set of training and testing input data and predicted output data.

For both cases, the data sample consisted of three trials each of nineteen mixture designs. Seventy percent of the data was used to train the GRNN by feeding the imaging parameters and the known asphalt binder contents. The remaining data was used for testing the GRNN. Figure 28 shows the results of (a) predicted and actual asphalt binder contents of training data, and (b) predicted and actual asphalt binder contents of testing data, for the one dimensional GRNN prediction model. Similarly, Figure 28(c) and (d) show the corresponding results for the multi-dimensional case. Figure 29 shows the results of OBC prediction using the multi-dimensional GRNN prediction model [51]. It is noted that multi-dimensional GRNN model has an improved correlation (R^2 = 0.99) compared to its one dimensional counterpart (R^2 = 0.96). Furthermore, it was observed that both GRNN prediction models of asphalt binder content are significantly better than the corresponding versions obtained by the author using simple linear regression analysis where the R^2 values were 0.78 and 0.84 respectively [51].

Table 14 One-dimensional sample set of training and testing input data and predicted output data.

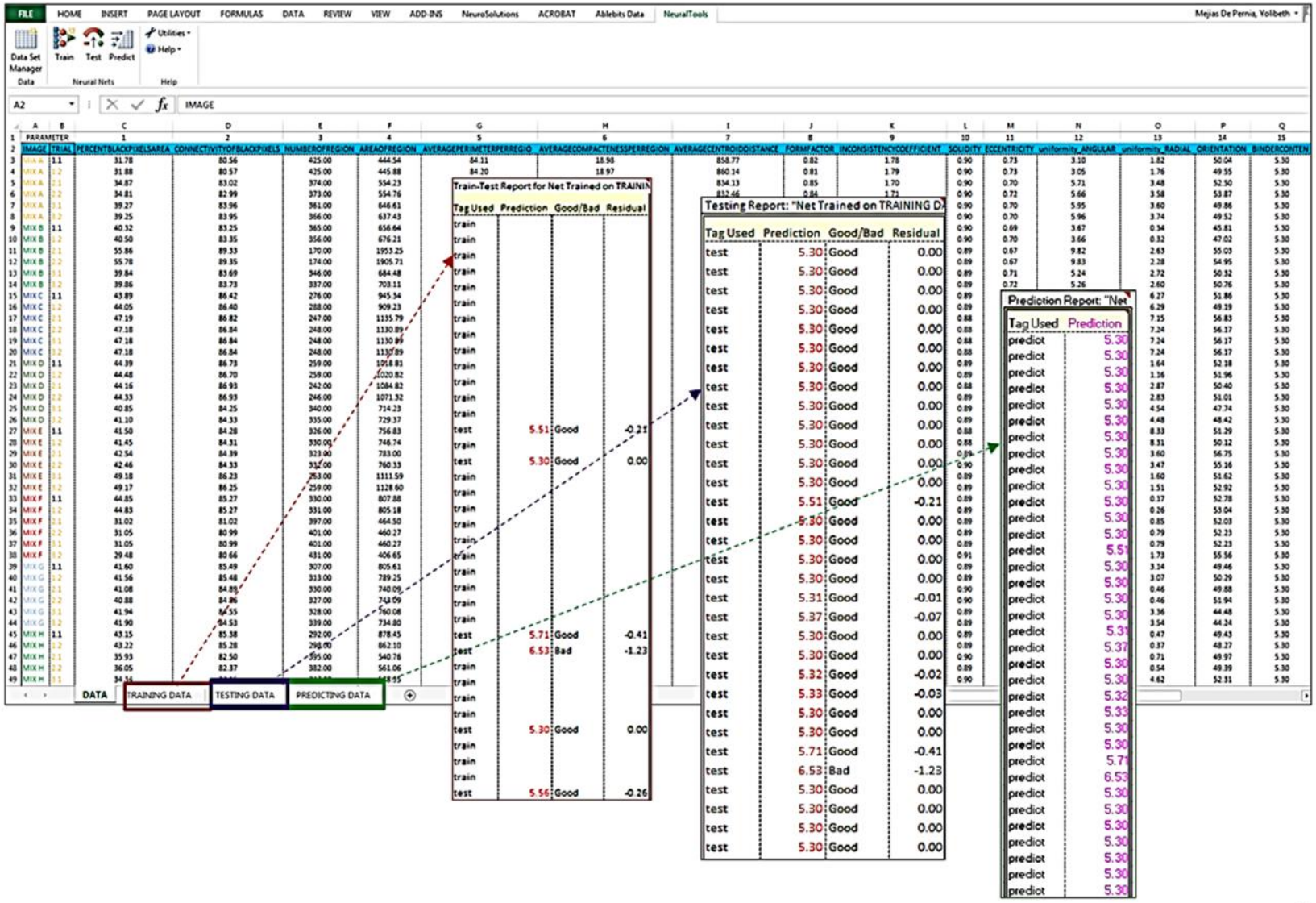

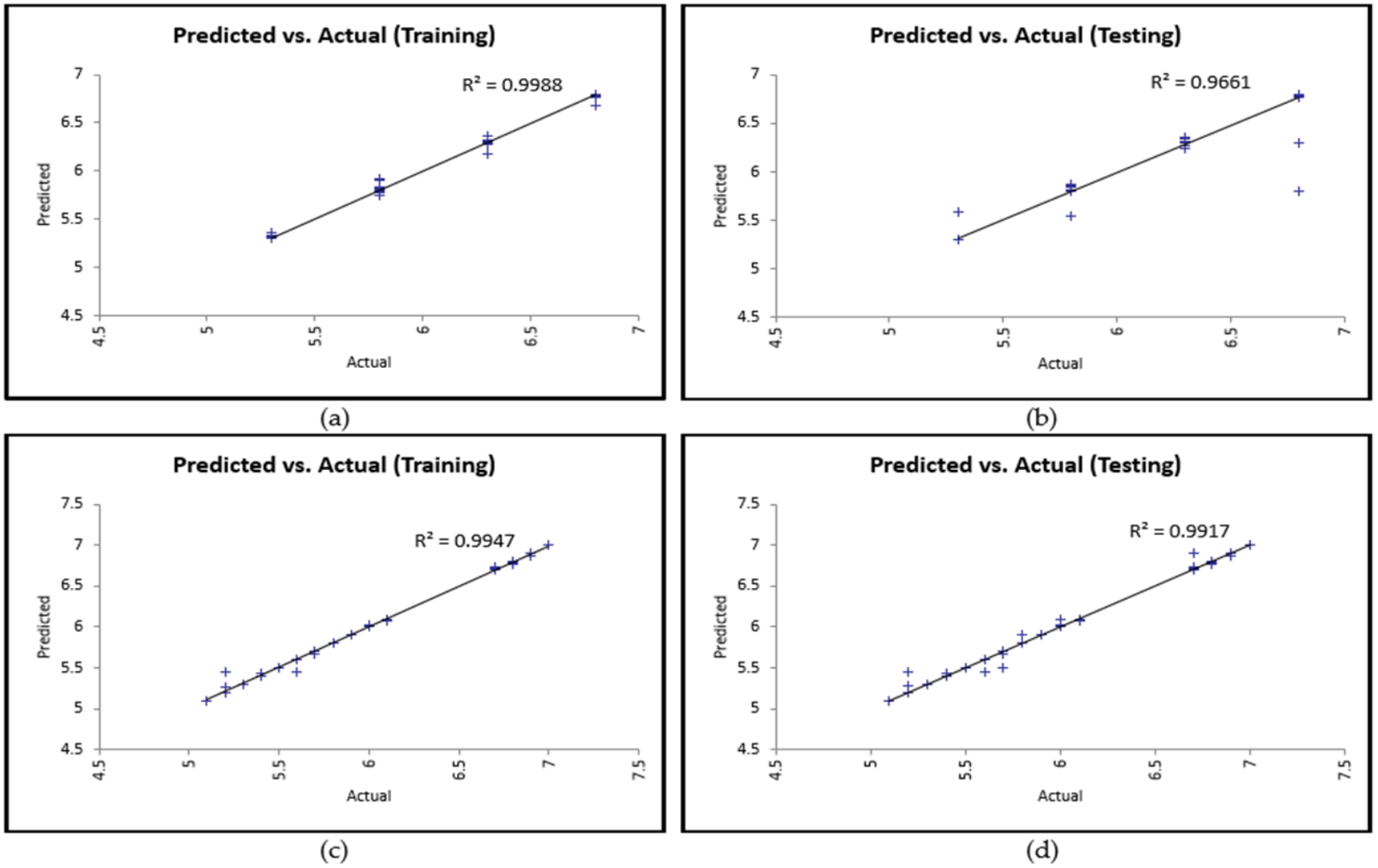

Figure 28 Neural network estimated AC for predicted versus actual for (a) one dimension training data, (b) one dimension testing data (c) multi-dimension training data, (d) multi-dimension testing data.

Table 15 Multi-dimensional sample set of training and testing input data and predicted output data.

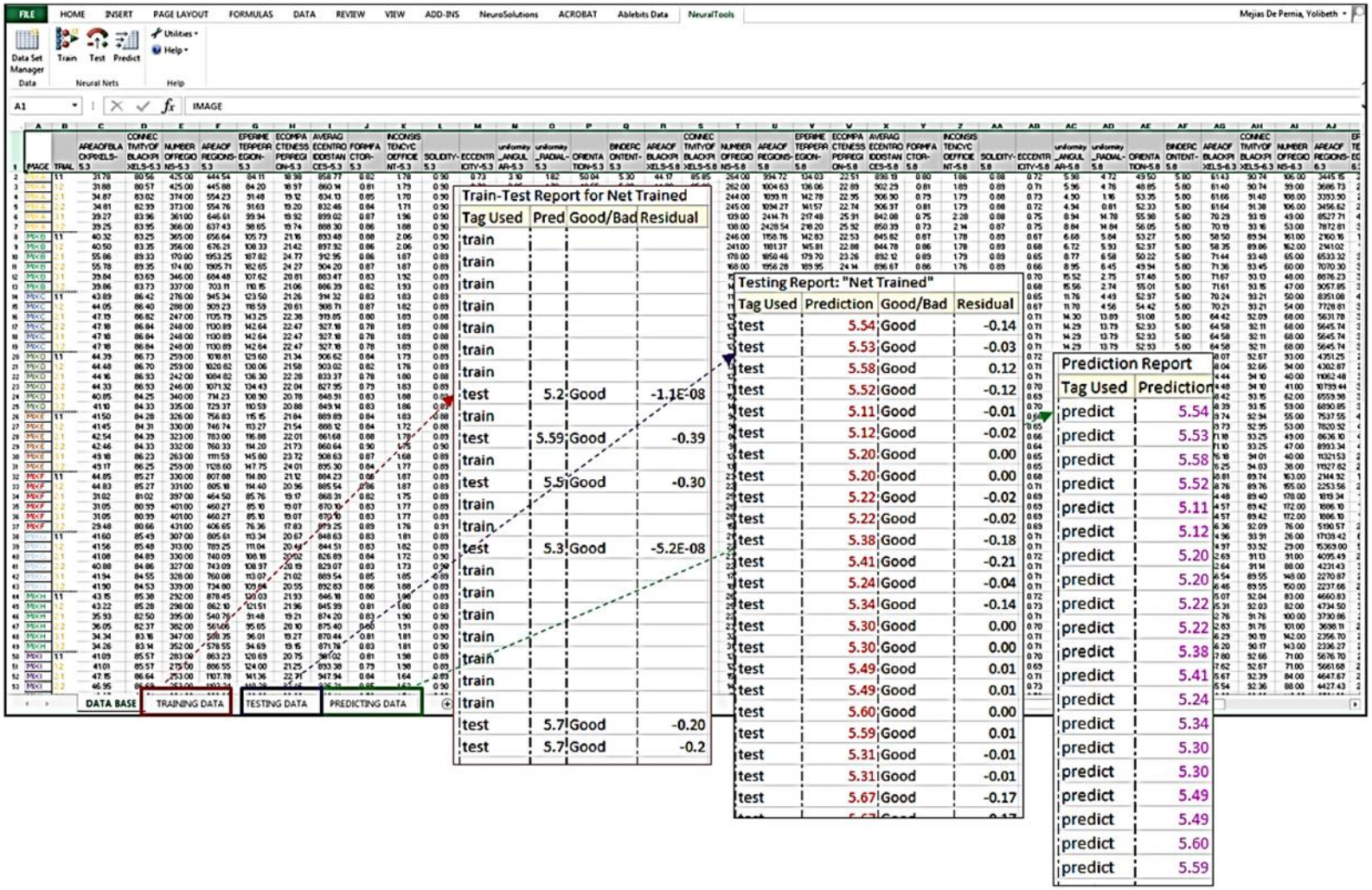

Train-Test Report for Net Trained

Tag Used	Pred	Good/Bad	Residual
train			
train			
train			
train			
train			
train			
train			
test	5.2	Good	-1.1E-08
train			
test	5.59	Good	-0.39
train			
test	5.5	Good	-0.30
train			
train			
test	5.3	Good	-5.2E-08
train			
train			
train			
train			
train			
train			
test	5.7	Good	-0.20
test	5.7	Good	-0.2

Testing Report: "Net Trained"

Tag Used	Prediction	Good/Bad	Residual
test	5.54	Good	-0.14
test	5.53	Good	-0.03
test	5.58	Good	0.12
test	5.52	Good	-0.12
test	5.11	Good	-0.01
test	5.12	Good	-0.02
test	5.20	Good	0.00
test	5.20	Good	0.00
test	5.22	Good	-0.02
test	5.22	Good	-0.02
test	5.38	Good	-0.18
test	5.41	Good	-0.21
test	5.24	Good	-0.04
test	5.34	Good	-0.14
test	5.30	Good	0.00
test	5.30	Good	0.00
test	5.49	Good	0.01
test	5.49	Good	0.01
test	5.60	Good	0.00
test	5.59	Good	0.01
test	5.31	Good	-0.01
test	5.31	Good	-0.01
test	5.67	Good	-0.17

Prediction Report

Tag Used	Prediction
predict	5.54
predict	5.53
predict	5.58
predict	5.52
predict	5.11
predict	5.12
predict	5.20
predict	5.20
predict	5.22
predict	5.22
predict	5.38
predict	5.41
predict	5.24
predict	5.34
predict	5.30
predict	5.30
predict	5.49
predict	5.49
predict	5.60
predict	5.59

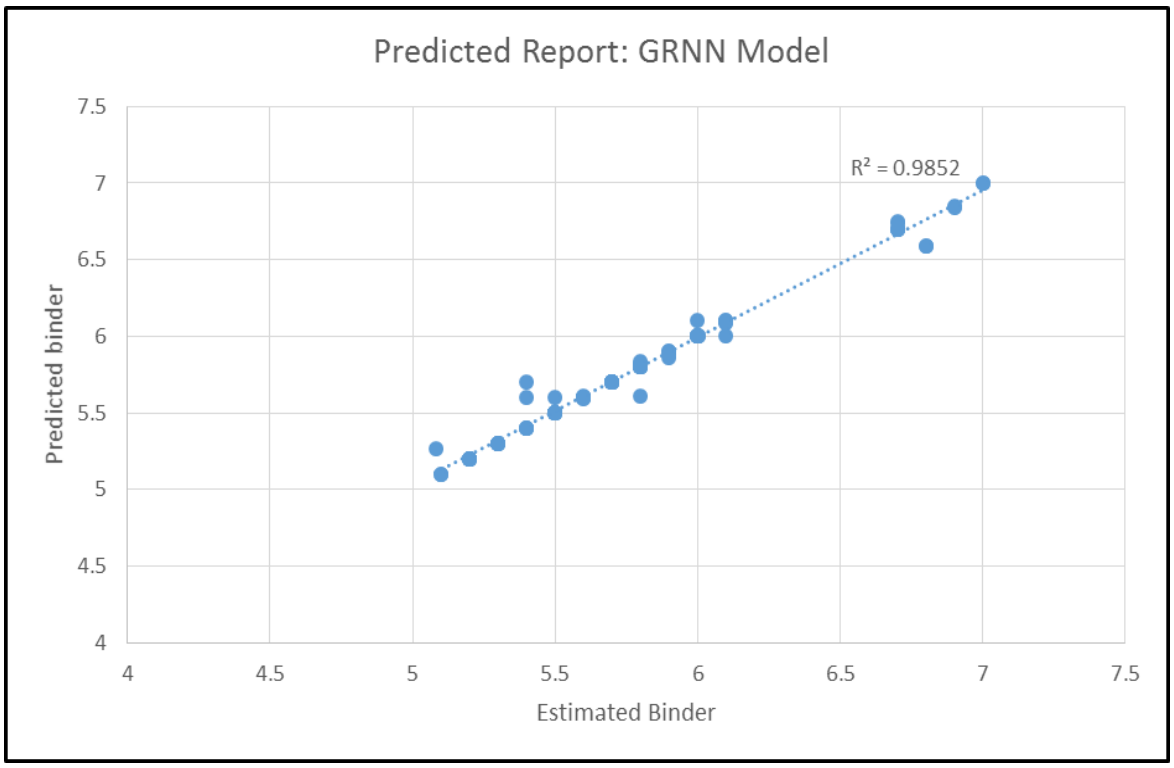

Figure 29 Optimum binder content prediction for multi dimension GRNN validation prediction model.

Steps for using the automated OBC prediction model are listed in Appendix H.

7.3. Phase III- QC Test Results and Analysis

On evaluating each of the QCIP for PPS in the database created in Phase I, the favorable conclusions drawn from the results in Tables 16 and 17 regarding the acceptability of the corresponding PPS were also compared to the conclusions reached from the general observation of PPS of each mixture. Complete agreement of the conclusions seen in this exercise verified the applicability of the derived QCIP. In addition, it also verified the accuracy of the algorithm developed by the author in detecting the orientation, spatial distribution and segregation of the ABD regions of the PPS.

Table 16 Quality control parameter results for (a) orientation (Δ_f), (b) spatial distribution (*SD*), and (c) segregation (*S*) results for sample sets for mixtures "A" to "S."

IMAGE NAME	PERCENT AC	Directional Distribution (Δ_f)	Spatial Distribution (SD) by sections of 30 degrees											Spatial Distribution (SD) standard deviation	INNER	OUTER	Segregation (S)	Ratio (inner/outer)
MIX A TRIAL 2.1 5.3 %	5.3	0.16	10.54	9.56	8.11	7.76	8.25	9.43	9.31	8.01	6.11	6.08	8.48	8.36	1.32	50.54	49.46	97.86	1.02
MIX A TRIAL 2.1 5.8 %	5.8	0.07	8.92	10.21	7.39	8.46	8.93	9.40	7.77	7.86	7.58	7.59	8.28	7.63	0.88	48.31	51.69	107.02	0.93
MIX A TRIAL 2.1 6.3 %	6.3	0.10	7.86	7.37	8.83	8.39	9.63	9.25	8.88	7.97	7.83	6.72	8.42	8.85	0.82	55.56	44.44	80.00	1.25
MIX B TRIAL 1.1 5.3 %	5.3	0.07	8.78	8.80	7.84	7.94	8.61	8.76	7.52	7.14	9.66	8.15	7.67	9.13	0.74	53.04	46.96	88.52	1.13
MIX B TRIAL 1.1 5.8 %	5.8	0.14	9.06	7.32	7.95	7.64	6.73	7.70	7.56	8.84	10.01	10.18	8.06	8.94	1.07	40.60	59.40	146.32	0.68
MIX B TRIAL 1.1 6.3 %	6.3	0.11	6.99	8.18	7.19	9.05	6.95	7.29	7.96	8.03	9.25	10.17	9.13	9.81	1.12	49.35	50.65	102.63	0.97
MIX C TRIAL 1.1 5.3 %	5.3	0.10	7.93	6.50	7.97	9.27	7.45	9.13	9.83	9.35	9.02	9.41	7.91	6.24	1.18	52.29	47.71	91.24	1.10
MIX C TRIAL 1.1 5.8 %	5.8	0.21	7.73	6.06	7.04	7.13	9.25	8.15	9.25	9.32	8.77	9.92	8.90	8.49	1.14	54.74	45.26	82.69	1.21
MIX C TRIAL 1.1 6.3 %	6.3	0.21	8.14	8.92	7.92	8.15	7.99	7.73	7.72	9.05	10.50	8.93	7.91	7.03	0.90	44.90	55.10	122.73	0.81
MIX D TRIAL 1.1 5.3 %	5.3	0.16	7.51	9.07	8.42	8.80	9.28	8.88	8.70	6.91	8.03	6.33	9.80	8.28	1.00	48.02	51.98	108.26	0.92
MIX D TRIAL 1.1 5.8 %	5.8	0.13	7.52	7.99	7.03	8.13	7.94	6.87	9.84	9.85	9.25	8.54	7.84	9.21	1.01	45.24	54.76	121.05	0.83
MIX D TRIAL 1.1 6.3 %	6.3	0.02	7.73	8.16	7.66	9.33	10.03	9.41	8.78	7.76	7.31	7.18	9.31	7.35	0.99	33.72	66.28	196.55	0.51
MIX E TRIAL 1.2 5.3 %	5.3	0.15	7.55	7.62	9.62	9.20	7.89	7.47	7.16	9.35	9.22	7.96	7.57	9.39	0.93	47.17	52.83	112.00	0.89
MIX E TRIAL 1.2 5.8 %	5.8	0.18	7.99	8.20	8.31	7.07	8.05	8.27	8.47	9.22	9.79	8.52	8.06	8.05	0.67	51.19	48.81	95.35	1.05
MIX E TRIAL 1.2 6.3 %	6.3	0.07	8.62	8.60	8.03	8.22	7.47	7.77	8.85	9.01	9.74	8.34	7.28	8.08	0.69	42.22	57.78	136.84	0.73
MIX I TRIAL 3.2 6.3 %	6.3	0.14	6.01	6.42	8.04	8.17	8.58	9.82	10.63	10.26	8.79	8.04	7.58	7.66	1.40	35.16	64.84	184.44	0.54
MIX L TRIAL 3.2 5.8 %	5.8	0.11	8.08	8.25	8.16	7.81	7.37	7.24	8.68	8.98	8.37	9.50	9.73	7.84	0.77	49.19	50.81	103.30	0.97
MIX L TRIAL 3.2 6.3 %	6.3	0.10	8.64	7.92	7.58	7.33	7.92	8.49	6.36	7.86	8.59	9.81	10.02	9.16	1.05	47.09	52.91	112.38	0.89
MIX L TRIAL 3.2 6.8 %	6.8	0.06	8.11	7.73	9.05	7.92	8.80	7.57	7.52	8.73	7.89	9.26	8.97	8.45	0.62	54.44	45.56	83.70	1.19
MIX M TRIAL 3.2 5.8 %	5.8	0.12	8.47	7.74	7.33	9.86	7.29	8.32	8.54	8.73	8.20	8.14	9.14	8.25	0.72	46.90	53.10	113.21	0.88
MIX M TRIAL 3.2 6.3 %	6.3	0.07	9.38	7.06	7.40	8.20	7.22	7.77	8.53	7.79	8.80	9.29	9.01	9.56	0.88	51.33	48.67	94.81	1.05
MIX M TRIAL 3.2 6.8 %	6.8	0.18	8.73	9.37	7.52	7.01	7.46	7.95	8.08	9.56	8.58	8.57	8.06	9.12	0.80	46.00	54.00	117.39	0.85
MIX N TRIAL 3.2 5.8 %	5.8	0.12	9.69	8.62	10.99	8.53	8.56	7.78	7.27	7.58	7.40	8.48	8.19	6.89	1.13	51.80	48.20	93.05	1.07
MIX N TRIAL 3.2 6.3 %	6.3	0.09	7.89	7.17	7.72	8.32	7.80	8.68	7.48	8.33	8.19	8.94	8.42	11.07	1.00	55.07	44.93	81.59	1.23
MIX N TRIAL 3.2 6.8 %	6.8	0.15	8.69	6.21	9.38	9.29	6.93	7.03	9.24	8.71	9.20	9.99	8.29	7.04	1.22	53.53	46.47	86.82	1.15
MIX O TRIAL 3.2 5.8 %	5.8	0.09	9.09	8.34	8.95	6.36	7.21	9.72	7.44	7.79	8.58	11.10	8.68	6.74	1.33	51.19	48.81	95.34	1.05
MIX O TRIAL 3.2 6.3 %	6.3	0.09	7.14	8.16	7.95	9.15	6.77	8.82	7.51	9.23	8.40	9.32	9.26	8.31	0.87	52.68	47.32	89.82	1.11
MIX O TRIAL 3.2 6.8 %	6.8	0.08	8.27	8.86	8.35	9.05	8.79	9.65	8.89	7.84	6.56	7.70	8.60	7.44	0.84	53.20	46.80	87.96	1.14
MIX S TRIAL 3.2 5.8 %	5.8	0.11	8.82	6.82	8.23	7.47	7.43	9.86	10.47	7.78	8.17	8.60	8.37	7.96	1.02	56.03	43.97	78.46	1.27
MIX S TRIAL 3.2 6.3 %	6.3	0.13	11.07	9.60	9.01	9.15	7.01	8.18	8.21	5.61	8.03	8.12	6.91	9.09	1.42	47.77	52.23	109.34	0.91
MIX S TRIAL 3.2 6.8 %	6.8	0.15	9.34	9.77	7.34	8.70	8.16	6.62	8.88	9.64	7.11	7.53	7.45	9.45	1.10	49.83	50.17	100.67	0.99

(a) (b) (c)

Table 17 Results of parameters for defective pies sets.

IMAGE NAME	PERCENT AC	Δ_f	Section by 30 degrees												Standard Deviation	INNER	OUTER	Segregation	Ratio (inner/outer)
MIX 13497 TRIAL 1.1 5.8 %	5.80	0.13	7.26	8.23	9.63	7.47	9.42	7.72	9.31	8.31	5.89	8.28	10.44	8.04	1.23	54.29	45.71	84.210472	1.19
MIX 13497 TRIAL 1.1 6.3 %	6.30	0.17	9.31	7.96	6.36	7.93	7.83	7.07	7.88	9.77	10.03	9.50	9.68	6.48	1.32	51.9	48.1	92.694004	1.08
MIX 13497 TRIAL 1.1 6.8 %	6.80	0.13	7.29	12.18	14.97	7.67	5.99	7.81	6.53	9.48	7.29	7.21	7.77	5.79	2.69	45.98	54.02	117.47565	0.85
MIX 13497 TRIAL 2.1 5.8 %	5.80	0.04	7.86	9.31	8.02	7.46	7.27	7.84	8.42	9.04	11.43	8.53	6.41	8.13	1.26	53.38	46.62	87.341716	1.14
MIX 13497 TRIAL 2.1 6.3 %	6.30	0.09	7.85	8.31	5.22	7.19	9.10	7.01	8.64	10.09	12.62	8.57	6.85	8.56	1.65	51.96	48.04	92.463708	1.08
MIX 13497 TRIAL 2.1 6.8 %	6.80	0.17	10.04	8.89	8.14	6.42	7.53	8.12	8.56	6.67	10.36	8.46	7.96	8.85	1.17	48.42	51.58	106.52167	0.94
MIX 13560 TRIAL 1.1 5.3 %	5.30	0.09	5.86	7.52	7.01	7.73	7.72	7.81	12.11	11.60	6.91	8.12	9.52	8.09	1.86	51.85	48.15	92.857083	1.08
MIX 13560 TRIAL 1.1 5.8 %	5.80	0.31	8.24	9.31	8.71	8.22	7.66	8.54	8.65	7.06	7.43	7.43	10.08	8.67	0.86	32.05	67.95	211.99986	0.47
MIX 13560 TRIAL 1.1 6.3 %	6.30	0.11	10.03	9.31	7.88	7.41	6.21	8.09	6.90	7.98	8.66	9.71	9.30	8.30	1.17	38.16	61.84	162.06886	0.62
MIX 13560 TRIAL 2.1 5.3 %	5.30	0.23	8.13	8.65	10.38	10.76	9.97	8.40	7.91	7.12	6.82	6.93	8.12	6.77	1.39	44.15	55.85	126.49564	0.79
MIX 13560 TRIAL 2.1 5.8 %	5.80	0.12	7.41	7.19	7.46	8.54	7.47	9.67	9.28	8.45	10.27	9.50	7.87	6.89	1.12	45.63	54.37	119.14886	0.84
MIX 13560 TRIAL 2.1 6.3 %	6.30	0.16	9.24	8.59	9.76	7.66	8.21	6.23	7.04	7.81	8.02	9.46	8.17	9.82	1.10	42.59	57.41	134.78252	0.74
MIX 13560 TRIAL 3.1 5.3 %	5.30	0.10	7.74	9.32	9.16	7.03	6.49	7.16	7.60	7.88	8.62	13.29	7.76	7.96	1.77	50.74	49.26	97.071067	1.03
MIX 13560 TRIAL 3.1 5.8 %	5.80	0.09	7.27	7.58	8.36	7.60	6.53	9.35	9.25	8.01	9.44	8.28	8.78	9.56	0.97	27.38	72.62	265.21722	0.38
MIX 13560 TRIAL 3.1 6.3 %	6.30	0.10	8.16	8.39	8.13	6.60	6.16	7.07	9.78	11.73	7.93	9.78	9.14	7.12	1.58	46.67	53.33	114.28564	0.88
MIX 13561 TRIAL 1.1 5.3 %	5.30	0.21	7.68	8.78	7.88	8.07	8.22	7.62	9.74	8.38	9.81	8.92	8.30	6.63	0.89	43.66	56.34	129.03217	0.78
MIX 13561 TRIAL 1.1 5.8 %	5.80	0.07	7.64	6.37	10.27	9.82	8.53	8.31	7.50	7.02	7.76	8.13	10.27	8.37	1.24	54.78	45.22	82.547116	1.21
MIX 13561 TRIAL 1.1 6.3 %	6.30	0.13	8.13	9.33	8.74	7.61	7.21	7.38	7.28	7.85	9.24	8.86	8.02	10.32	0.97	46.69	53.31	114.17315	0.88
MIX 13561 TRIAL 2.1 5.3 %	5.30	0.15	7.47	9.34	10.71	8.91	10.03	7.38	7.32	7.66	7.70	6.87	8.57	7.84	1.19	50.76	49.24	97.003682	1.03
MIX 13561 TRIAL 2.1 5.8 %	5.80	0.21	8.20	9.47	9.71	8.42	7.87	8.43	8.73	8.38	8.99	7.26	6.61	7.93	0.87	39.31	60.69	154.38586	0.65
MIX 13561 TRIAL 2.1 6.3 %	6.30	0.16	8.35	6.83	9.00	9.37	8.35	6.85	7.07	7.68	6.86	7.51	11.09	11.03	1.53	50.73	49.27	97.122239	1.03
MIX 13561 TRIAL 3.1 5.3 %	5.30	0.11	7.09	9.61	8.70	10.02	7.90	8.68	7.86	8.35	8.08	8.43	7.70	7.57	0.84	51.49	48.51	94.222161	1.06
MIX 13561 TRIAL 3.1 5.8 %	5.80	0.16	7.01	8.11	7.43	8.90	9.73	9.42	9.40	8.16	7.60	8.56	9.66	5.69	1.24	47.04	52.96	112.56537	0.89
MIX 13561 TRIAL 3.1 6.3 %	6.30	0.32	8.37	9.38	9.34	9.24	8.18	8.53	7.65	8.04	8.31	8.20	7.03	7.73	0.71	29.6	70.4	237.83768	0.42

(a) (b) (c)

Since all of the PPS generated in Phase I were acceptable, the above mentioned supplementary set of PPS consisting of computer-generated defective PPS and poor quality PPS created by FDOT were used to demonstrate that the author's algorithm can also identify the inferior quality of those PPS images. The graphical comparisons of all three QCIP obtained from both types of PPS are shown in Figures 30-32.

Based on the results of the above comparisons, the following conclusions can be drawn.

The directional distribution (Δ_f) representing each ABD region of a correctly placed PPS and a computer-generated defective PPS are shown in Table 16(a) and 17 (a) respectively. Therefore, the first QC parameter, orientation, which is based on Δ_f indicate uniformity of ABD orientation within the PPS in acceptable pie plates. A sample of the results for the QC parameter, orientation, is shown in Figure 30. Furthermore, based on Table 17, the values of Δ_f for correctly placed PPS range from 0 to 0.25 and it can be concluded that orientations of all ABD regions in PPS tested in Phase I are randomly distributed, and not aligned along any one particular direction. The above observations agree with the observation-based acceptable quality of the pie plates with respect to orientation. On the other hand, the defective PPS where the ABD regions were clearly aligned in one direction indicated values of Δ_f greater than 0.25. The above results seem to justify the consideration of the acceptable range of Δ_f to be 0-0.25 [71].

The results for the second QC parameter, the spatial distribution (*SD*), are plotted in the form of a column chart. An example of such a plot for the images of mix "A" tested in Phase I and a defective computer-generated pie plate image are shown in Figure 31. Based on Tables 16(b) and 17(b), all standard deviations values of the *SD* parameter for the sample mixture "A" lie between 0 and 1.52. Meanwhile, for the defective pie plate image, the above value is 2.69. The

above result seems to justify the consideration of the acceptable range of the standard deviation of the SD parameter to be 0-1.52 [71].

A sample of the results for the third QC parameter, segregation, is shown in Figure 32. Based on Tables 16(c) and 17(c), S_i and S_o values of 50% would indicate that the distribution of ABD within each section (inner and outer) is precisely the same and therefore no segregation had occurred in the PPS tested in Phase I. Based on the range of acceptability of S values for inner and outer sections and that of the S_{ratio} to be between 0.73 and 1.34 [62], the results show no evidence of segregation in some of the PPS images analyzed in this study. On the other hand, the defective PPS consistently produced values of S_{ratio} of less than 0.73 and greater than 1.34. Hence it can be concluded that the above specified acceptability range for the S_{ratio} seems to be reasonable [71].

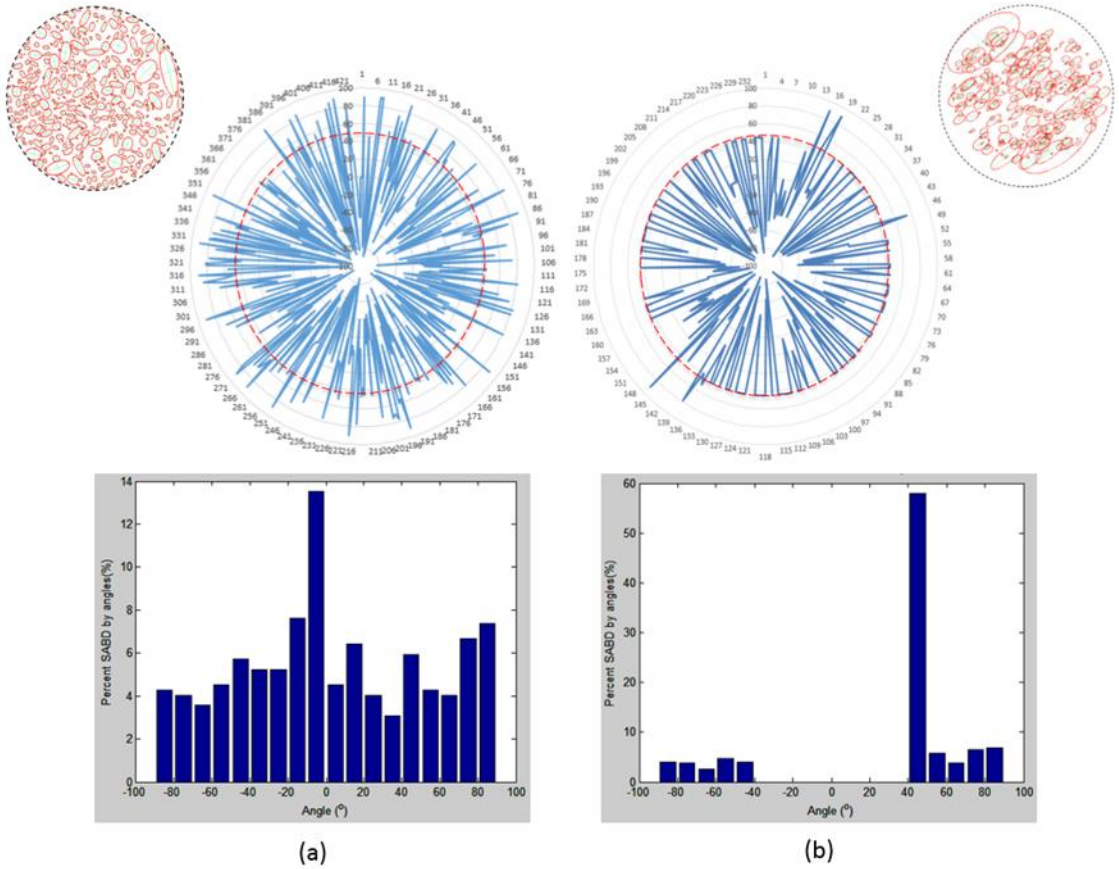

Figure 30 Distribution orientation parameter (θ_f) for (a) an acceptable quality of a real pie plate image and (b) a slide synthetic pie plate image.

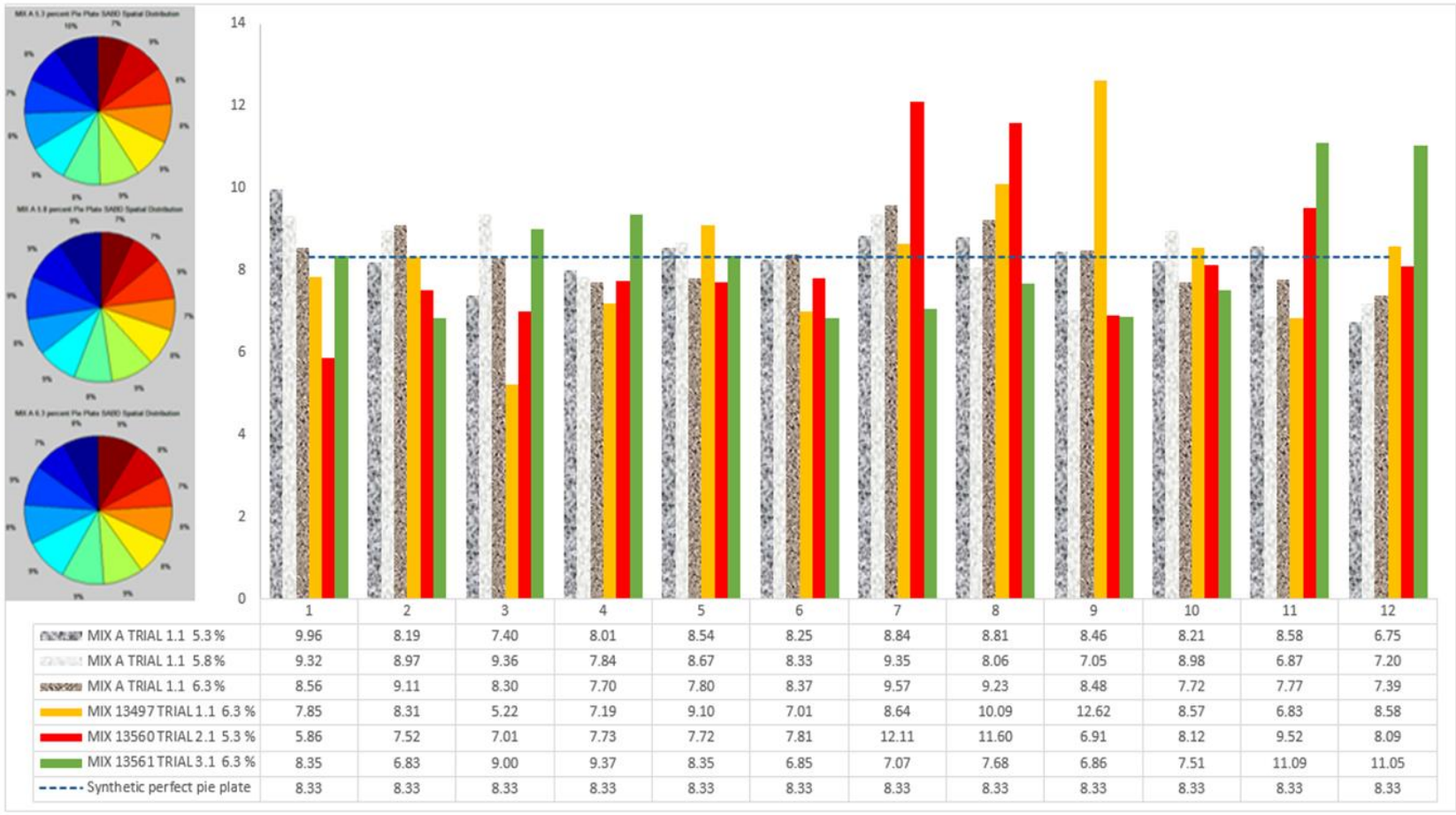

	1	2	3	4	5	6	7	8	9	10	11	12
MIX A TRIAL 1.1 5.3 %	9.96	8.19	7.40	8.01	8.54	8.25	8.84	8.81	8.46	8.21	8.58	6.75
MIX A TRIAL 1.1 5.8 %	9.32	8.97	9.36	7.84	8.67	8.33	9.35	8.06	7.05	8.98	6.87	7.20
MIX A TRIAL 1.1 6.3 %	8.56	9.11	8.30	7.70	7.80	8.37	9.57	9.23	8.48	7.72	7.77	7.39
MIX 13497 TRIAL 1.1 6.3 %	7.85	8.31	5.22	7.19	9.10	7.01	8.64	10.09	12.62	8.57	6.83	8.58
MIX 13560 TRIAL 2.1 5.3 %	5.86	7.52	7.01	7.73	7.72	7.81	12.11	11.60	6.91	8.12	9.52	8.09
MIX 13561 TRIAL 3.1 6.3 %	8.35	6.83	9.00	9.37	8.35	6.85	7.07	7.68	6.86	7.51	11.09	11.05
Synthetic perfect pie plate	8.33	8.33	8.33	8.33	8.33	8.33	8.33	8.33	8.33	8.33	8.33	8.33

Figure 31 Bar chart representing spatial distribution (*SD*) of connected black pixel areas of a sample set (Mixture A) and a computer-generated set of pie plate.

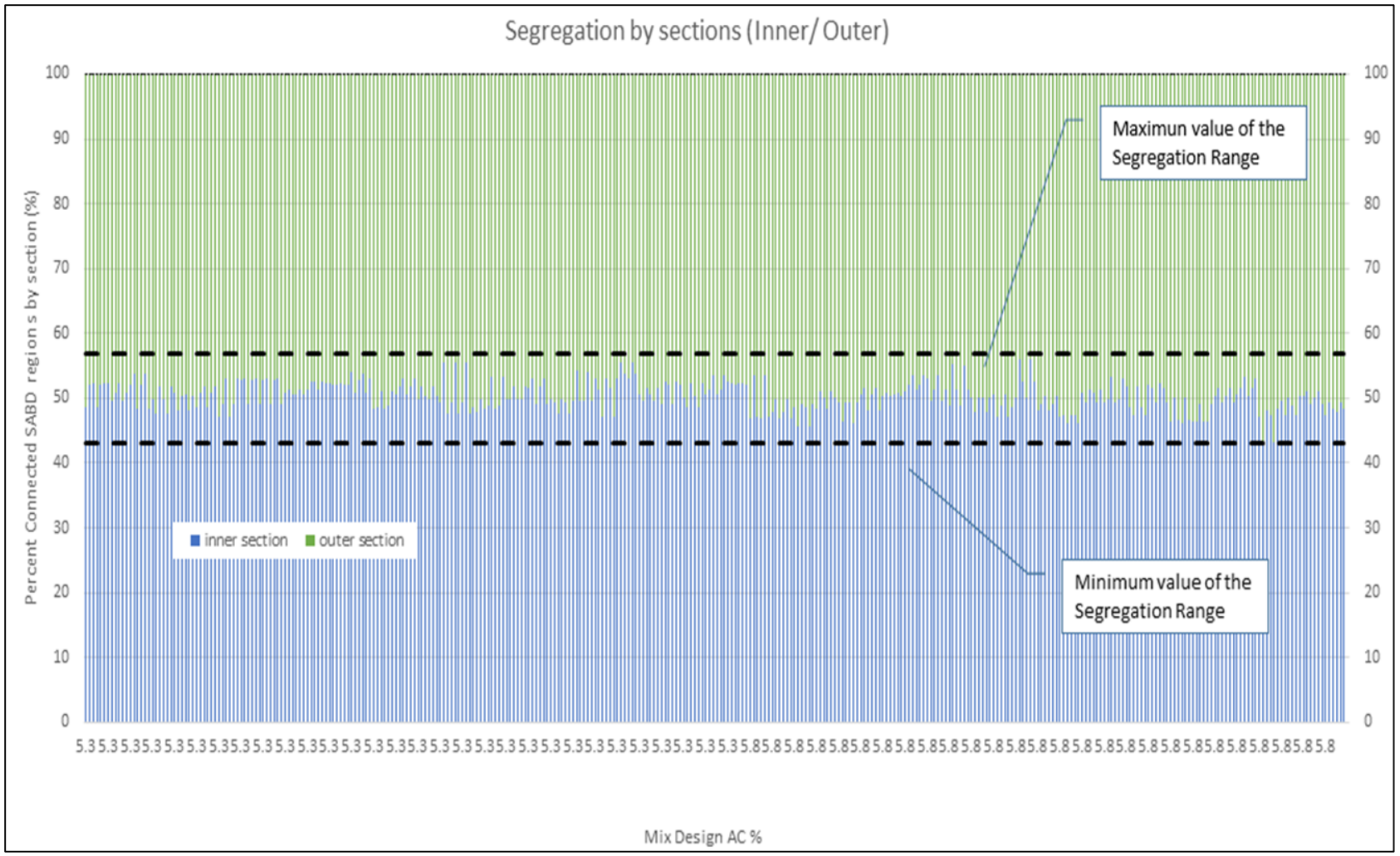

Figure 32 Segregation results for predetermined AC contents for all of the samples testing in this research.

7.4. Implementation of the Neural Network-Based OBC Estimation

The input data vector $\mathbf{X_k}$ contains three trial asphalt binder contents values *specific* to the aggregate and binder types that are predetermined by the agency. Therefore, when any given GRNN is trained by an adequate number of samples of each aggregate type, the GRNN would automatically recognize the aggregate type of any new mixture design based on the specific asphalt binder contents values in the input vector $\mathbf{X_k}$. As an example, for this research the nominal maximum aggregate size was 12.5 mm. If this aggregate size blend is to be substituted by 9.5 mm nominal maximum aggregate size, then before the automated OBC determination process is executed, three phases of in-house testing must be carried out by FDOT. The first phase of testing consisting of an adequate number of pie plates tests must be performed following the FM5-588 to create a new database for the new size blend study as in Phase I of the current study. Then, in the second phase, a comprehensive database of visual OBC estimates and the corresponding imaging parameters for pie plates prepared using the new aggregate must be compiled as in Phase I of the current study. In the final phase of testing, the neural network developed in Phase II of the current study must be re-trained with the modified dataset that also incorporates the trial asphalt binder contents, OBC estimates and the imaging parameters from the newly compiled database.

The above logic can also be extended to include different binder types as well by assuming that an appropriately trained GRNN would also recognize the binder type based on the specific trial asphalt binder content values that are predefined by the agency and previously exposed to the GRNN.

Hence the extension of the proposed neural network model to include a variety of additional types of aggregate and binders requires the building of a database that must be trained with an adequate number of mixture designs containing all possible types of aggregates and

binders and the corresponding specific trial asphalt binder contents values. Such a database can be set up conveniently by using the FM 5-588 to test all types of desired aggregate and binder types at pre-determined trial asphalt binder contents values relevant to those aggregate and binder types. Appendix C shows the steps that must be followed to use the software generated by the author that can automatically predict the OBC of OGFC mixtures using a multi-dimensional GRNN.

CHAPTER 8: CONCLUSIONS

In order to eliminate the human subjectivity involved in the current FM 5-588 (pie plate) method, an automated test method for the direct estimation of the optimum asphalt binder content (OBC) of OGFC mixtures was developed using the analysis of pie plate images and concepts of perceptual image coding and NN. The investigation consisted of three distinct phases where Phase I involved the testing of a large set of OGFC samples prepared from granitic and oolitic limestone aggregate sources using FM-5-588 and the subsequent imaging of the corresponding pie plates. Phase II of the investigation was focused on the formulation of (i) a perceptual image model based on specific imaging parameters which utilize a combination of human visual metrics that model human perceptive effects involved in estimating the OBC, and (ii) a Generalized Regression Neural Network (GRNN) that would discover the nonlinear relationship among the above imaging parameters, the corresponding trial ACs and the OBC. The designed neural network was trained using a major part of the data collected from the tested OGFC mixtures that consisted of the ACs and the relevant imaging parameters and the visual OBC estimates. Then the GRNN-based OBC predictions performed on an independent part of the same database showed that the model provides satisfactory estimation of OBC values not previously presented to the GRNN. The research also demonstrated that, even with respect to predicting ACs using imaging parameters, a higher accuracy can be obtained from a trained GRNN compared to regression models. An added attractive feature of the neural network method is that it can conveniently incorporate parameters which are difficult to be included in analytical equations. Phase III of the investigation involved the development of an image-based tool for quality control of pie plate samples for FM5-588

procedure for OBC determination of OGFC mixtures. This algorithm evaluates the selected QCIP of pie plate images prior to executing image-based OBC prediction method developed in Phase II and ensures high reliability of results. The results of Phase III prove that QCT could be used in OGFC pie plate specimen production method for more effective selection of good quality specimens. The experimental results show that this algorithm is very efficient in maximizing the accuracy of OBC estimation.

CHAPTER 9: RECOMMENDATIONS FOR FUTURE WORK

After accomplishing the envisioned objectives of the current research study, the investigators recommend the future research directions listed below:

- The GRNN based OBC estimations can be compared with the corresponding visual estimations of the FDOT technicians, for a number of independent OGFC mixtures, to verify the automated method.
- Future efforts can be focused on testing different OGFC mixtures to verify that this automation can be extended to other types of aggregates, binders (polymer modifiers and rubber) used by FDOT.

REFERENCES

[1] B. J. Putman, "Evaluation Of Open-Graded Friction Courses: Construction, Maintenance, and Performance," Report No. FHWA-SC-12-04. South Carolina Department of Transportation In Cooperation with: US Department of Transportation, South Carolina, 2012.

[2] Florida Department of Transportation, "Determining the Optimum Asphalt Binder Content of an Open-Graded Friction Course Using the Pie," FDOT, 2009. [Online]. [Accessed 10 10 2012].

[3] N. M. Jackson, Choubane B., and Musselman, J. A. "A preliminary Evaluation of FC-5 and FC-6 Friction Courses in Florida," Pavement Evaluation Conference, Roanoke, VA, 2002.

[4] National Center for Asphalt Technology (NCAT), "Design, Construction and Performance of New Generation of Open-Graded Friction Course Mixes," Research Synopsis-NCAT, Report No. 00-01, 2001.

[5] Florida Department of Transportation, "Florida Department of Transportation Specifications-Section 337," FDOT, 2010. [Online]. Available: http://www.dot.state.fl.us/specificationsoffice/implemented/specbooks/2010bk.shtm. [Accessed 9 10 2013].

[6] R. W. Smith, Rice, J. M., and Spelman, S. R. "Design of Open-Graded Asphalt Friction Courses," Federal Highway Administration Offices of Research and Development, Washington, D.C., 20590, January 1974 Interim Report.

[7] Florida Department of Transportation, "Test method for Image-based determination of Optimum Asphalt Content of FC-5 mixtures," FDOT State Material Office, 2012.

[8] Federal Highway Administration, "Asphalt mix design," U.S. Department of Transportation, 16 February 1998. [Online]. Available: http://isddc.dot.gov/OLPFiles/FHWA/010475.pdf. [Accessed 2 22 2013].

[9] Pavia Services, "Pavement Interactive," Pavement Interactive.org, 2012. [Online]. Available: http://www.pavementinteractive.org. [Accessed 7 11 2012].

[10] G. Huber, "Performance Survey on Open-Graded Friction Course Mixes, NCHRP Synthesis of Highway Practice 284," Washington, D.C, 2000.

[11] P. Kandhal, "Design, Construction, and Maintenance of Open-Graded Asphalt Friction Courses," National Asphalt Pavement Association. Information Series 115, 2002.

[12] Florida Department of Transportation, *Standard Specification for Road and Bridge Construction,* Tallahassee, Fla, 2004.

[13] Florida Department of Transportation, "Flexible Pavement Design Manual," Pavement Management Office. Document No. 625-010-002-G, 2008.

[14] L. Hwee and Guwe, W. "Performance Related Evaluation of Porous Asphalt Mix Design," Kuala Lumpur, Malaysia, 2004.

[15] C. Nielsen, "Durability of Porous Asphalt - International Experience," *Danish Road Directorate,* vol. 41, no. ISBS 8791177901, 9788791177903, pp. 27, 2006.

[16] D. Watson, Johnson, A., and Jared, D. "Georgia Department of Transportation's Progress in Open-Graded Friction Course Development," vol. Transportation Research Record No. 1616, 1998.

[17] V. Hafeli, "Open Graded Friction Courses (OFGC)," Ajax Paving Industries of Florida, 2012. [Online]. Available: http://www.worldofasphalt.com/Education/General/Handouts/Files/W23%20Open%20Graded%20Mixes%20for%20Friction%20Courses%20and%20Porous%20Pavements%20-%20Vince%20Hafeli.pdf. [Accessed 4 9 2014].

[18] National Asphalt Pavement Association (NAPA), "Thin Hot Mix Asphalt Surfacing," National Asphalt Pavement Association, Lanham, MD, 1995.

[19] D. Hanson, and James, R. "Colorado DOT Tire/Pavement Noise Study," Colorado Department of Transportation, Colorado, 2004.

[20] B. Birgisson, Roque, R., Varadhan, A., Thai, T., and Jaiswal, L. "Evaluation of Thick Open-graded and Bonded Friction Course for Florida," University of South Florida-FDOT Report 4504-968-12, 3 2006. [Online]. Available: http://www.dot.state.fl.us/research-center/Completed_Proj/Summary_SMO/FDOT_BC354_81_rpt.pdf. [Accessed 4 24 2014].

[21] Transportation Research Board, "Performance Survey on Open-Graded Friction Course Mixes, NCHRP Synthesis of Highway Practice 284," National Research Council, Washington, D.C, 2000.

[22] J.M.M. Molenaar, and Molenaar, A.A.A. "An Investigation into the Contribution of the Bituminous Binder to the Resistance to Raveling of Porous Asphalt," Barcelona, Spain, 2000.

[23] L.C. Kline, and Putman, B.J. "Comparison of Open Graded Friction Course (OGFC) Mix Design Procedures in the United States," vol. 90th Annual Meeting, no. CD-ROM, 2011.

[24] A. Gendy, and Shalaby, A. "Mean Profile Depth of Pavement Surface Macrotexture Using Photometric Stereo Techniques," *Journal of Transportation Engineering,* vol. 133, no. 7, pp. 433-440, 2007.

[25] S N. Goodman, Hassan, Y., and Abd El Halim, O. "Digital Sand Patch Test: Use of Digital Image Analysis for Measurement of Pavement Macrotexture," in *TRB,* Washington, DC, 2010.

[26] R. Elunai, Chandran, V., and Gallagher E. "Asphalt Concrete Surface Macrotexture Determination From Still Image," Vols. 12, no 3, pp. 857-869., 2011.

[27] A. Razaei, Hoyt, D., and Martin, A. "Simple Laboratory Method for Measuring Pavement Macrotexture," *Transportation Research Board,* no. 2227, pp. 146-152, 2011.

[28] International Cybernetics Corporation (ICC), "Digital Imaging Systems," International Cybernetics Corporation, 2012. [Online]. [Accessed 11 1 2012].

[29] S. Amarasiri, Gunaratne, M., and Sarkar, S. "Use of digital image modeling for evaluation of concrete pavement Macrotexture and wear." *ASCE,* vol. 138, no. 5, pp. 589-602, 2012.

[30] R. Ravi, and Gunaratne, M. "Application of Digital Image Analysis for Friction Evaluation of Asphalt Pavements," 2011.

[31] K. Peterson, Carlson, J., Sutter, L., and Van Dam, T. "Methods for Threshold optimization for images collected from contrast enhanced concrete surfaces for air-void system characterization.," *Material Characterization,* vol. 60, no. 7, pp. 710-715, 2009.

[32] Q. Zou, Cao, Y., Li, Q., Mao, Q., and Wang, S. "CrackTree: Automatic crack detection from pavement images," *Pattern Recognition Letters*, vol. 33, no. 3, pp. 227-238, 2012.

[33] Y. Sun., Salari E., and Chou, E. "Automated Pavement Distress Detection Using Advanced Image Processing Techniques," Department of Civil Engineering and Electrical Engineering of the University of Toledo, Toledo, Ohio, 2009.

[34] Z.Q.Yue, Chen S., and Tham, L.G., "Finite element modeling of geomaterials using digital image processing," *Computers and Geotechnics*, vol. 30, no. 5, pp. 375-397, 2003.

[35] L. Bruno, Parla, G., and Celauro, C. "Image analysis for detecting aggregate gradation in asphalt mixture from planar images," *Construction and Building Materials*, vol. 28, no. 1, pp. 21-30, 2012.

[36] Z. Pylyshyn, "Seeing and visualizing: It's not what you think," 2003. Massachusetts Institute of Technology., Chap 1 pp. 22-27, Chap 2 pp. 15-22, Chap 4 pp. 12-22, Chap 5 pp. 13-21, and 24-33, Chap 6 pp. 7-36, Chap 7 pp. 22-33, and Chap 8 pp. 1-24.

[37] M. G. Albanesi and Guerrini, F. "An HVS-based adaptive coder for perceptually lossy image compression," *Pattern Recognition*, no. 36, pp. 997 – 1007, 2003.

[38] C.-Y. Wang, Lee, S.-M., and Chang, L.-W. "Short communication Designing JPEG quantization tables based on human visual system," *Signal Processing: Image Communication*, no. 16, pp. 501-506, 2001.

[39] I. Höntsch and Karam, L. J. "Locally Adaptive Perceptual Image Coding," *IEEE Transactions on Image Processing*, vol. 9, no. 9, 2000.

[40] A. B. Watson, "Efficiency of a model human image code," *US National library of Medicine. National Institutes of Health*, vol. 4, no. 12, pp. 2401-17, 1987.

[41] S. J. Thorpe, Delorme, A., Van Rullen, R., and Paquier, W. "Reverse Engineering of the Visual System using Networks of Spiking Neurons," *IEEE International Symposium on Circuits and System*, no. 4, pp. 405-408, 2000.

[42] D. F. Specht, "A General Regression Neural Network," *IEEE transactions on neural Networks*, vol. 2, no. 6, pp. 1045-9227, 1991.

[43] M. E. Haque and Sudhakar, K. V. "ANN based prediction model for fatigue crack growth in DP steel," *Fatigue and Fracture of Engineering Materials and Structures*, no. 23, pp. 63-68, 2001.

[44] J. Yang, *Road crack condition performance modeling using recurrent Markov chains and artificial neural networks*, Graduate Theses and Dissertations. http://scholarcommons.usf.edu/etd/1310, 2004.

[45] S. A. Hannan, Manza, R. R., and Ramteke, R. J. "Generalized Regression Neural Network and Radial Basis Function for Heart Disease Diagnosis," *International Journal of Computer Applications* , vol. 7, no. 13, pp. 0975 – 8887, 2010.

[46] C.-Y. Lee and He, Y.-L. "Wind Prediction Based on General Regression Neural Network," in *Second International Conference on Intelligent System Design and Engineering Application*, IEEE DOI 10.1109/ISdea.2011.143617, 2012.

[47] I. Popescu, Constantinou, P., Nafornita M., and Nafornita, I. "Generalized regression neural network prediction model for indoor environment," in *Computers and Communications: Ninth International Symposium on Mobile Radio communications Laboratory*, Greece, Proceedings. ISCC 2004, 2004.

[48] Ö. Kişi, "Generalized regression neural networks for evapotranspiration modelling," *Hydrological Sciences Journal*, vol. 51, no. 6, pp. 1092-1105, 2006.

[49] M. Gunaratne and Mejias de Pernia, Y. "Final Report BDV25 - TWO 820-1," FDOT, Gainesville, 2014.

[50] M. Gunaratne and Mejias de Pernia, Y. "Final Report BDV25 - TWO 820-2," FDOT, Gainesville, June 2015.

[51] Y. Mejias de Pernia, Gunaratne, M., Nash, T., and Musselman, J. "Preliminary assessment of Asphalt binder content of open-graded friction course (OGFC) mixtures using digital image processing," *presented at the Annual TRB meeting*, Washington, D.C, Jan. 2015.

[52] Florida Department of Transportation, "Florida Department of Transportation Specifications-Section 901 and 902," FDOT, 9 10 2013. [Online]. Available: http://www.dot.state.fl.us/specificationsoffice/implemented/specbooks/2010bk.shtm. [Accessed 4 15 2013].

[53] American Association of State Highway and Transportation Officials (AASHTO), "AASHTO Method T2: Sampling of Aggregates," [Online] Available at: ftp://ftp.odot.state.or.us/techserv/cons, 1991. [Accessed 4 15 2013].

[54] Florida Department of Transportation, "FM 1T-248: Florida Method test for reducing samples of aggregate to testing size," 1 September 2000. [Online]. Available: http://www2.dot.state.fl.us/procurement/ProfessionalServices/ advertise/pdf/14433.pdf. [Accessed 15 April 2013].

[55] Z. Zhang, "Camera Calibration," Photogrammetric, 1971. [Online]. Available: http://cronos.rutgers.edu/~meer/TEACHTOO/PAPERS/zhang.pdf. [Accessed 4 26 2014].

[56] The MathWorks Inc., Image Processing Toolbox User's Guide, Natick, MA: The MathWorks, Inc., 1997.

[57] H. M. Zelelew, Papagiannakis, A. T.; Masad, E., "Application of Digital image processing techniques for asphalt concrete mixture images," in *12th International Conference on Computer Methods and Advances in Geomechanics*, 2008.

[58] R.C. Gonzalez and Woods, R. E. "Some Basic Relationships Between Pixels," in *Digital Image Processing, Third Edition*, Saddle River, NJ, Pearson, 2007, pp. 68-71.

[59] J.-S. Chen, Shiah, M.-S., and Chen, H.-J. "Quantification of Coarse Aggregate Shape and Its Effect on Engineering Properties of Hot-Mix Asphalt Mixtures," *Journal of Testing and Evaluation, JTEVA, Vol. 29, No. 6,* pp. 513–519, 2001.

[60] FDOT Materials office collaborators consisting of the project managers, Personal *Communication.* State Materials FDOT, 2014-2015.

[61] L. Bessa, Castelo Branco, V., and Soares, J. "Evaluation of different digital images processing software for aggregates and hot mix asphalt characterizations," *Construction and building materials*, no. 37, pp. 370-378, 2012.

[62] N.A. Hassan, Airey, G.D., Khan R., and Collop, A.C. Nondestructive Characterization of the Effect of Asphalt Mixture Compaction on Aggregate Orientation and Segregation Using X-ray Computed Tomography," *International Journal of Pavement Research and Technology*, vol. 5, no. 2, pp. 84-92, 2012.

[63] M. Vadood, Johari, M.S. and Rahaei, A. R. "Introducing a simple method to determine aggregate gradation of hot mix asphalt using image processing," *International Journal of Pavement Engineering*, vol. 15, no. 2 DOI: 10.1080/10298436.2013.786076, 2014, pp. 142-150, 2014.

[64] E. Masad, "Review of imaging techniques for characterizing the shape of aggregates used in asphalt mixes," in *Symposium*, 2001.

[65] E. Masad, "The Development of a Computer Controlled lmage Analysis System for Measuring Aggregate Shape Properties," *Transportation research Board: Final Report for Highway-IDEA Project 77*, Vols. Washington State university, Pullman, WA., 2003.

[66] C.F. Mora, Kwan, A.K.H., and Chan, H.C. "Particle Size Distribution Analysis of Coarse Aggregate," *Cement and Concrete Research, Vol. 28, No. 6,* pp. 921–932, 1998.

[67] A.K.H. Kwan, Mora, C.F., and Chan, H. C. "Particle shape analysis of coarse aggregate using digital image processing," *Cement and Concrete research,* vol. Elsevier Science Ltd, PII: S0008-8846(99)00105-2, pp. 1403-1410, 1999.

[68] Z. Q. Yue, Bekking, W., and Morin, I, "Characterization of Aggregates and Quantitatively Study of Asphalt Concrete Microstructure," in *Transportation Research Record 1492*, Washington, D.C, National Research Council, 1995, pp. 53-60.

[69] A. R. Coenen, Kutay, M. E., Sefidmazgi, N. R., and Bahia, H. U. "Aggregate structure characterization of asphalt mixtures using two-dimensional image analysis," *Road Materials and Pavement Design,* pp. 13:3, 433-454, DOI: 10.1080/14680629.2012.711923, 2012.

[70] C. J. LaVassar, Mahoney, J. P., and Willoughby, K. A. "Statistical Assessment of Quality Assurance-Quality Control Data for Hot Mix Asphalt," Washington State Department of Transportation, Seattle, Washington, 2009.

[71] National Quality Forum, "Measure testing and Scientific Acceptability of Measure Properties," 2011. [Online]. Available: http://www.qualityforum. org/docs/measure_evaluation_criteria.aspx. [Accessed 6 22 2015].

APPENDIX A: TABLE OF EXPERIMENTAL TEST PLAN

Table A1 Experimental test plan.

	MIX TYPE		DESIGN #		MIX #	FM5-588 PIE PLATE SAMPLES			DETERMINATION OF OPTIMUM ASPHALT BINDER CONTENT														image/labview
									SECTION 5.4		SECTION 5.5		SECTION 5.6		SECTION 5.7		SECTION 5.8		SECTION 5.9		
									5.4 Prepare three 1200 g aggregate batches.		5.5 Heat the aggregate batches and the asphalt binder for a minimum of two hours		5.6 mix the aggregate batch and asphalt binder in the mixing bowl		5.7 transfer the mixture from the mixing bowl into a pie plate AND place in an oven for one hour		5.8 remove the pie plate from the oven and allow it to cool undisturbed until it reaches room		5.9 invert the pie plates and inspect the bottom surfaces.		
									START TIME	END TIME	START TIME	END TIME	START TIME	END TIME	START TIME	END TIME	START TIME	END TIME	START TIME	END TIME	END TIME
trial 1	GRANITIC	NS315	9165A	A	1	pie 1	5.3	1	8:00:00 AM	8:00:00 AM	8:00:00 AM	8:00:00 AM	8:00:00 AM	8:00:00 AM	8:00:00 AM	8:00:00 AM	8:00:00 AM	8:00:00 AM	8:00:00 AM	8:00:00 AM	8:00:00 AM	8:00:00 AM	8:00:00 AM
						pie 2	5.8	1					8:00:00 AM	8:00:00 AM	8:00:00 AM	8:00:00 AM	8:00:00 AM	8:00:00 AM	8:00:00 AM	8:00:00 AM	8:00:00 AM
						pie 3	6.3	1					8:00:00 AM	8:00:00 AM	8:00:00 AM	8:00:00 AM	8:00:00 AM	8:00:00 AM	8:00:00 AM	8:00:00 AM	8:00:00 AM
			9476A	B	2	pie 1	5.3	1	8:00:00 AM	8:00:00 AM	8:00:00 AM	8:00:00 AM	8:00:00 AM	8:00:00 AM	8:00:00 AM	8:00:00 AM	8:00:00 AM	8:00:00 AM	8:00:00 AM	8:00:00 AM	8:00:00 AM	8:00:00 AM	8:00:00 AM
						pie 2	5.8	1					8:00:00 AM	8:00:00 AM	8:00:00 AM	8:00:00 AM	8:00:00 AM	8:00:00 AM	8:00:00 AM	8:00:00 AM	8:00:00 AM
						pie 3	6.3	1					8:00:00 AM	8:00:00 AM	8:00:00 AM	8:00:00 AM	8:00:00 AM	8:00:00 AM	8:00:00 AM	8:00:00 AM	8:00:00 AM
			9642A	C	3	pie 1	5.3	1	8:00:00 AM	8:00:00 AM	8:00:00 AM	8:00:00 AM	8:00:00 AM	8:00:00 AM	8:00:00 AM	8:00:00 AM	8:00:00 AM	8:00:00 AM	8:00:00 AM	8:00:00 AM	8:00:00 AM	8:00:00 AM	8:00:00 AM
						pie 2	5.8	1					8:00:00 AM	8:00:00 AM	8:00:00 AM	8:00:00 AM	8:00:00 AM	8:00:00 AM	8:00:00 AM	8:00:00 AM	8:00:00 AM
						pie 3	6.3	1					8:00:00 AM	8:00:00 AM	8:00:00 AM	8:00:00 AM	8:00:00 AM	8:00:00 AM	8:00:00 AM	8:00:00 AM	8:00:00 AM
			9646A	D	4	pie 1	5.3	1	8:00:00 AM	8:00:00 AM	8:00:00 AM	8:00:00 AM	8:00:00 AM	8:00:00 AM	8:00:00 AM	8:00:00 AM	8:00:00 AM	8:00:00 AM	8:00:00 AM	8:00:00 AM	8:00:00 AM	8:00:00 AM	8:00:00 AM
						pie 2	5.8	1					8:00:00 AM	8:00:00 AM	8:00:00 AM	8:00:00 AM	8:00:00 AM	8:00:00 AM	8:00:00 AM	8:00:00 AM	8:00:00 AM
						pie 3	6.3	1					8:00:00 AM	8:00:00 AM	8:00:00 AM	8:00:00 AM	8:00:00 AM	8:00:00 AM	8:00:00 AM	8:00:00 AM	8:00:00 AM
			9657A	E	5	pie 1	5.3	1	8:00:00 AM	8:00:00 AM	8:00:00 AM	8:00:00 AM	8:00:00 AM	8:00:00 AM	8:00:00 AM	8:00:00 AM	8:00:00 AM	8:00:00 AM	8:00:00 AM	8:00:00 AM	8:00:00 AM	8:00:00 AM	8:00:00 AM
						pie 2	5.8	1					8:00:00 AM	8:00:00 AM	8:00:00 AM	8:00:00 AM	8:00:00 AM	8:00:00 AM	8:00:00 AM	8:00:00 AM	8:00:00 AM
						pie 3	6.3	1					8:00:00 AM	8:00:00 AM	8:00:00 AM	8:00:00 AM	8:00:00 AM	8:00:00 AM	8:00:00 AM	8:00:00 AM	8:00:00 AM
		GA553	9160A	F	6	pie 1	5.3	1	8:00:00 AM	8:00:00 AM	8:00:00 AM	8:00:00 AM	8:00:00 AM	8:00:00 AM	8:00:00 AM	8:00:00 AM	8:00:00 AM	8:00:00 AM	8:00:00 AM	8:00:00 AM	8:00:00 AM	8:00:00 AM	8:00:00 AM
						pie 2	5.8	1					8:00:00 AM	8:00:00 AM	8:00:00 AM	8:00:00 AM	8:00:00 AM	8:00:00 AM	8:00:00 AM	8:00:00 AM	8:00:00 AM
						pie 3	6.3	1					8:00:00 AM	8:00:00 AM	8:00:00 AM	8:00:00 AM	8:00:00 AM	8:00:00 AM	8:00:00 AM	8:00:00 AM	8:00:00 AM
			9184A	G	7	pie 1	5.3	1	8:00:00 AM	8:00:00 AM	8:00:00 AM	8:00:00 AM	8:00:00 AM	8:00:00 AM	8:00:00 AM	8:00:00 AM	8:00:00 AM	8:00:00 AM	8:00:00 AM	8:00:00 AM	8:00:00 AM	8:00:00 AM	8:00:00 AM
						pie 2	5.8	1					8:00:00 AM	8:00:00 AM	8:00:00 AM	8:00:00 AM	8:00:00 AM	8:00:00 AM	8:00:00 AM	8:00:00 AM	8:00:00 AM
						pie 3	6.3	1					8:00:00 AM	8:00:00 AM	8:00:00 AM	8:00:00 AM	8:00:00 AM	8:00:00 AM	8:00:00 AM	8:00:00 AM	8:00:00 AM
			9250A	H	8	pie 1	5.3	1	8:00:00 AM	8:00:00 AM	8:00:00 AM	8:00:00 AM	8:00:00 AM	8:00:00 AM	8:00:00 AM	8:00:00 AM	8:00:00 AM	8:00:00 AM	8:00:00 AM	8:00:00 AM	8:00:00 AM	8:00:00 AM	8:00:00 AM
						pie 2	5.8	1					8:00:00 AM	8:00:00 AM	8:00:00 AM	8:00:00 AM	8:00:00 AM	8:00:00 AM	8:00:00 AM	8:00:00 AM	8:00:00 AM
						pie 3	6.3	1					8:00:00 AM	8:00:00 AM	8:00:00 AM	8:00:00 AM	8:00:00 AM	8:00:00 AM	8:00:00 AM	8:00:00 AM	8:00:00 AM
			9824A	I	9	pie 1	5.3	1	8:00:00 AM	8:00:00 AM	8:00:00 AM	8:00:00 AM	8:00:00 AM	8:00:00 AM	8:00:00 AM	8:00:00 AM	8:00:00 AM	8:00:00 AM	8:00:00 AM	8:00:00 AM	8:00:00 AM	8:00:00 AM	8:00:00 AM
						pie 2	5.8	1					8:00:00 AM	8:00:00 AM	8:00:00 AM	8:00:00 AM	8:00:00 AM	8:00:00 AM	8:00:00 AM	8:00:00 AM	8:00:00 AM
						pie 3	6.3	1					8:00:00 AM	8:00:00 AM	8:00:00 AM	8:00:00 AM	8:00:00 AM	8:00:00 AM	8:00:00 AM	8:00:00 AM	8:00:00 AM
			9773A	J	10	pie 1	5.3	1	8:00:00 AM	8:00:00 AM	8:00:00 AM	8:00:00 AM	8:00:00 AM	8:00:00 AM	8:00:00 AM	8:00:00 AM	8:00:00 AM	8:00:00 AM	8:00:00 AM	8:00:00 AM	8:00:00 AM	8:00:00 AM	8:00:00 AM
						pie 2	5.8	1					8:00:00 AM	8:00:00 AM	8:00:00 AM	8:00:00 AM	8:00:00 AM	8:00:00 AM	8:00:00 AM	8:00:00 AM	8:00:00 AM
						pie 3	6.3	1					8:00:00 AM	8:00:00 AM	8:00:00 AM	8:00:00 AM	8:00:00 AM	8:00:00 AM	8:00:00 AM	8:00:00 AM	8:00:00 AM
	OOLITIC	87339	9126A	K	11	pie 1	5.8	1	8:00:00 AM	8:00:00 AM	8:00:00 AM	8:00:00 AM	8:00:00 AM	8:00:00 AM	8:00:00 AM	8:00:00 AM	8:00:00 AM	8:00:00 AM	8:00:00 AM	8:00:00 AM	8:00:00 AM	8:00:00 AM	8:00:00 AM
						pie 2	6.3	1					8:00:00 AM	8:00:00 AM	8:00:00 AM	8:00:00 AM	8:00:00 AM	8:00:00 AM	8:00:00 AM	8:00:00 AM	8:00:00 AM
						pie 3	6.8	1					8:00:00 AM	8:00:00 AM	8:00:00 AM	8:00:00 AM	8:00:00 AM	8:00:00 AM	8:00:00 AM	8:00:00 AM	8:00:00 AM
			9400A	L	12	pie 1	5.8	1	8:00:00 AM	8:00:00 AM	8:00:00 AM	8:00:00 AM	8:00:00 AM	8:00:00 AM	8:00:00 AM	8:00:00 AM	8:00:00 AM	8:00:00 AM	8:00:00 AM	8:00:00 AM	8:00:00 AM	8:00:00 AM	8:00:00 AM
						pie 2	6.3	1					8:00:00 AM	8:00:00 AM	8:00:00 AM	8:00:00 AM	8:00:00 AM	8:00:00 AM	8:00:00 AM	8:00:00 AM	8:00:00 AM
						pie 3	6.8	1					8:00:00 AM	8:00:00 AM	8:00:00 AM	8:00:00 AM	8:00:00 AM	8:00:00 AM	8:00:00 AM	8:00:00 AM	8:00:00 AM
			9138A	M	13	pie 1	5.8	1	8:00:00 AM	8:00:00 AM	8:00:00 AM	8:00:00 AM	8:00:00 AM	8:00:00 AM	8:00:00 AM	8:00:00 AM	8:00:00 AM	8:00:00 AM	8:00:00 AM	8:00:00 AM	8:00:00 AM	8:00:00 AM	8:00:00 AM
						pie 2	6.3	1					8:00:00 AM	8:00:00 AM	8:00:00 AM	8:00:00 AM	8:00:00 AM	8:00:00 AM	8:00:00 AM	8:00:00 AM	8:00:00 AM
						pie 3	6.8	1					8:00:00 AM	8:00:00 AM	8:00:00 AM	8:00:00 AM	8:00:00 AM	8:00:00 AM	8:00:00 AM	8:00:00 AM	8:00:00 AM
			9139A	N	14	pie 1	5.8	1	8:00:00 AM	8:00:00 AM	8:00:00 AM	8:00:00 AM	8:00:00 AM	8:00:00 AM	8:00:00 AM	8:00:00 AM	8:00:00 AM	8:00:00 AM	8:00:00 AM	8:00:00 AM	8:00:00 AM	8:00:00 AM	8:00:00 AM
						pie 2	6.3	1					8:00:00 AM	8:00:00 AM	8:00:00 AM	8:00:00 AM	8:00:00 AM	8:00:00 AM	8:00:00 AM	8:00:00 AM	8:00:00 AM
						pie 3	6.8	1					8:00:00 AM	8:00:00 AM	8:00:00 AM	8:00:00 AM	8:00:00 AM	8:00:00 AM	8:00:00 AM	8:00:00 AM	8:00:00 AM
			9469A	O	15	pie 1	5.8	1	8:00:00 AM	8:00:00 AM	8:00:00 AM	8:00:00 AM	8:00:00 AM	8:00:00 AM	8:00:00 AM	8:00:00 AM	8:00:00 AM	8:00:00 AM	8:00:00 AM	8:00:00 AM	8:00:00 AM	8:00:00 AM	8:00:00 AM
						pie 2	6.3	1					8:00:00 AM	8:00:00 AM	8:00:00 AM	8:00:00 AM	8:00:00 AM	8:00:00 AM	8:00:00 AM	8:00:00 AM	8:00:00 AM
						pie 3	6.8	1					8:00:00 AM	8:00:00 AM	8:00:00 AM	8:00:00 AM	8:00:00 AM	8:00:00 AM	8:00:00 AM	8:00:00 AM	8:00:00 AM
			10134A	P	16	pie 1	5.8	1	8:00:00 AM	8:00:00 AM	8:00:00 AM	8:00:00 AM	8:00:00 AM	8:00:00 AM	8:00:00 AM	8:00:00 AM	8:00:00 AM	8:00:00 AM	8:00:00 AM	8:00:00 AM	8:00:00 AM	8:00:00 AM	8:00:00 AM
						pie 2	6.3	1					8:00:00 AM	8:00:00 AM	8:00:00 AM	8:00:00 AM	8:00:00 AM	8:00:00 AM	8:00:00 AM	8:00:00 AM	8:00:00 AM
						pie 3	6.8	1					8:00:00 AM	8:00:00 AM	8:00:00 AM	8:00:00 AM	8:00:00 AM	8:00:00 AM	8:00:00 AM	8:00:00 AM	8:00:00 AM
		87145	6954A	Q	17	pie 1	5.8	1	8:00:00 AM	8:00:00 AM	8:00:00 AM	8:00:00 AM	8:00:00 AM	8:00:00 AM	8:00:00 AM	8:00:00 AM	8:00:00 AM	8:00:00 AM	8:00:00 AM	8:00:00 AM	8:00:00 AM	8:00:00 AM	8:00:00 AM
						pie 2	6.3	1					8:00:00 AM	8:00:00 AM	8:00:00 AM	8:00:00 AM	8:00:00 AM	8:00:00 AM	8:00:00 AM	8:00:00 AM	8:00:00 AM
						pie 3	6.8	1					8:00:00 AM	8:00:00 AM	8:00:00 AM	8:00:00 AM	8:00:00 AM	8:00:00 AM	8:00:00 AM	8:00:00 AM	8:00:00 AM
			7806A	R	18	pie 1	5.8	1	8:00:00 AM	8:00:00 AM	8:00:00 AM	8:00:00 AM	8:00:00 AM	8:00:00 AM	8:00:00 AM	8:00:00 AM	8:00:00 AM	8:00:00 AM	8:00:00 AM	8:00:00 AM	8:00:00 AM	8:00:00 AM	8:00:00 AM
						pie 2	6.3	1					8:00:00 AM	8:00:00 AM	8:00:00 AM	8:00:00 AM	8:00:00 AM	8:00:00 AM	8:00:00 AM	8:00:00 AM	8:00:00 AM
						pie 3	6.8	1					8:00:00 AM	8:00:00 AM	8:00:00 AM	8:00:00 AM	8:00:00 AM	8:00:00 AM	8:00:00 AM	8:00:00 AM	8:00:00 AM
			9932A	S	19	pie 1	5.8	1	8:00:00 AM	8:00:00 AM	8:00:00 AM	8:00:00 AM	8:00:00 AM	8:00:00 AM	8:00:00 AM	8:00:00 AM	8:00:00 AM	8:00:00 AM	8:00:00 AM	8:00:00 AM	8:00:00 AM	8:00:00 AM	8:00:00 AM
						pie 2	6.3	1					8:00:00 AM	8:00:00 AM	8:00:00 AM	8:00:00 AM	8:00:00 AM	8:00:00 AM	8:00:00 AM	8:00:00 AM	8:00:00 AM
						pie 3	6.8	1					8:00:00 AM	8:00:00 AM	8:00:00 AM	8:00:00 AM	8:00:00 AM	8:00:00 AM	8:00:00 AM	8:00:00 AM	8:00:00 AM

Table A1 (Continued)

A	B	C	D	E	F	G	H	I	P	Q	R	S	T	U	V	W	X	Y	Z	AA	AB			
									DETERMINATION OF OPTIMUM ASPHALT BINDER CONTENT																
	MIX TYPE		DESIGN #		MIX #	FMS-588 PIE PLATES AMPLES			SECTION 5.4		SECTION 5.5		SECTION 5.6		SECTION 5.7		SECTION 5.8		SECTION 5.9		image/labview				
									5.4 Prepare three 1200 g aggregate batches.		5.5 Heat the aggregate batches and the asphalt binder for a minimum of two hours		5.6 mix the aggregate batch and asphalt binder in the mixing bowl		5.7 transfer the mixture from the mixing bowl into a pie plate AND place in an oven for one hour		5.8 remove the pie plate from the oven and allow it to cool undisturbed until it reaches room		5.9 invert the pie plates and inspect the bottom surfaces.				
						pie 3	6.8	1					8:00:00 AM	8:00:00 AM	8:00:00 AM	8:00:00 AM	8:00:00 AM	8:00:00 AM	8:00:00 AM	8:00:00 AM	8:00:00 AM				
trial 2	GRANITIC	NS315	9165A	A	1	pie 1	5.3	1	8:00:00 AM	8:00:00 AM	8:00:00 AM	8:00:00 AM	8:00:00 AM	8:00:00 AM	8:00:00 AM	8:00:00 AM	8:00:00 AM	8:00:00 AM	8:00:00 AM	8:00:00 AM	8:00:00 AM	8:00:00 AM	8:00:00 AM			
						pie 2	5.8	1					8:00:00 AM	8:00:00 AM	8:00:00 AM	8:00:00 AM	8:00:00 AM	8:00:00 AM	8:00:00 AM	8:00:00 AM	8:00:00 AM				
						pie 3	6.3	1					8:00:00 AM	8:00:00 AM	8:00:00 AM	8:00:00 AM	8:00:00 AM	8:00:00 AM	8:00:00 AM	8:00:00 AM	8:00:00 AM				
			9476A	B	2	pie 1	5.3	1	7:00:00 AM	7:00:00 AM	7:00:00 AM	7:00:00 AM	8:00:00 AM	8:00:00 AM	8:00:00 AM	8:00:00 AM	8:00:00 AM	8:00:00 AM	8:00:00 AM	8:00:00 AM	8:00:00 AM				
						pie 2	5.8	1					8:00:00 AM	8:00:00 AM	8:00:00 AM	8:00:00 AM	8:00:00 AM	8:00:00 AM	8:00:00 AM	8:00:00 AM	8:00:00 AM				
						pie 3	6.3	1					8:00:00 AM	8:00:00 AM	8:00:00 AM	8:00:00 AM	8:00:00 AM	8:00:00 AM	8:00:00 AM	8:00:00 AM	8:00:00 AM				
			9642A	C	3	pie 1	5.3	1	8:00:00 AM	8:00:00 AM	8:00:00 AM	8:00:00 AM	8:00:00 AM	8:00:00 AM	8:00:00 AM	8:00:00 AM	8:00:00 AM	8:00:00 AM	8:00:00 AM	8:00:00 AM	8:00:00 AM				
						pie 2	5.8	1					8:00:00 AM	8:00:00 AM	8:00:00 AM	8:00:00 AM	8:00:00 AM	8:00:00 AM	8:00:00 AM	8:00:00 AM	8:00:00 AM				
						pie 3	6.3	1					8:00:00 AM	8:00:00 AM	8:00:00 AM	8:00:00 AM	8:00:00 AM	8:00:00 AM	8:00:00 AM	8:00:00 AM	8:00:00 AM				
			9646A	D	4	pie 1	5.3	1	7:00:00 AM	7:00:00 AM	7:00:00 AM	7:00:00 AM	8:00:00 AM	8:00:00 AM	8:00:00 AM	8:00:00 AM	8:00:00 AM	8:00:00 AM	8:00:00 AM	8:00:00 AM	8:00:00 AM				
						pie 2	5.8	1					8:00:00 AM	8:00:00 AM	8:00:00 AM	8:00:00 AM	8:00:00 AM	8:00:00 AM	8:00:00 AM	8:00:00 AM	8:00:00 AM				
						pie 3	6.3	1					8:00:00 AM	8:00:00 AM	8:00:00 AM	8:00:00 AM	8:00:00 AM	8:00:00 AM	8:00:00 AM	8:00:00 AM	8:00:00 AM				
			9657A	E	5	pie 1	5.3	1	8:00:00 AM	8:00:00 AM	8:00:00 AM	8:00:00 AM	8:00:00 AM	8:00:00 AM	8:00:00 AM	8:00:00 AM	8:00:00 AM	8:00:00 AM	8:00:00 AM	8:00:00 AM	8:00:00 AM				
						pie 2	5.8	1					8:00:00 AM	8:00:00 AM	8:00:00 AM	8:00:00 AM	8:00:00 AM	8:00:00 AM	8:00:00 AM	8:00:00 AM	8:00:00 AM				
						pie 3	6.3	1					8:00:00 AM	8:00:00 AM	8:00:00 AM	8:00:00 AM	8:00:00 AM	8:00:00 AM	8:00:00 AM	8:00:00 AM	8:00:00 AM				
		GA553	9160A	F	6	pie 1	5.3	1	7:00:00 AM	7:00:00 AM	7:00:00 AM	7:00:00 AM	8:00:00 AM	8:00:00 AM	8:00:00 AM	8:00:00 AM	8:00:00 AM	8:00:00 AM	8:00:00 AM	8:00:00 AM	8:00:00 AM				
						pie 2	5.8	1					8:00:00 AM	8:00:00 AM	8:00:00 AM	8:00:00 AM	8:00:00 AM	8:00:00 AM	8:00:00 AM	8:00:00 AM	8:00:00 AM				
						pie 3	6.3	1					8:00:00 AM	8:00:00 AM	8:00:00 AM	8:00:00 AM	8:00:00 AM	8:00:00 AM	8:00:00 AM	8:00:00 AM	8:00:00 AM				
			9184A	G	7	pie 1	5.3	1	8:00:00 AM	8:00:00 AM	8:00:00 AM	8:00:00 AM	8:00:00 AM	8:00:00 AM	8:00:00 AM	8:00:00 AM	8:00:00 AM	8:00:00 AM	8:00:00 AM	8:00:00 AM	8:00:00 AM				
						pie 2	5.8	1					8:00:00 AM	8:00:00 AM	8:00:00 AM	8:00:00 AM	8:00:00 AM	8:00:00 AM	8:00:00 AM	8:00:00 AM	8:00:00 AM				
						pie 3	6.3	1					8:00:00 AM	8:00:00 AM	8:00:00 AM	8:00:00 AM	8:00:00 AM	8:00:00 AM	8:00:00 AM	8:00:00 AM	8:00:00 AM				
			9250A	H	8	pie 1	5.3	1	7:00:00 AM	7:00:00 AM	7:00:00 AM	7:00:00 AM	8:00:00 AM	8:00:00 AM	8:00:00 AM	8:00:00 AM	8:00:00 AM	8:00:00 AM	8:00:00 AM	8:00:00 AM	8:00:00 AM				
						pie 2	5.8	1					8:00:00 AM	8:00:00 AM	8:00:00 AM	8:00:00 AM	8:00:00 AM	8:00:00 AM	8:00:00 AM	8:00:00 AM	8:00:00 AM				
						pie 3	6.3	1					8:00:00 AM	8:00:00 AM	8:00:00 AM	8:00:00 AM	8:00:00 AM	8:00:00 AM	8:00:00 AM	8:00:00 AM	8:00:00 AM				
			9824A	I	9	pie 1	5.3	1	8:00:00 AM	8:00:00 AM	8:00:00 AM	8:00:00 AM	8:00:00 AM	8:00:00 AM	8:00:00 AM	8:00:00 AM	8:00:00 AM	8:00:00 AM	8:00:00 AM	8:00:00 AM	8:00:00 AM				
						pie 2	5.8	1					8:00:00 AM	8:00:00 AM	8:00:00 AM	8:00:00 AM	8:00:00 AM	8:00:00 AM	8:00:00 AM	8:00:00 AM	8:00:00 AM				
						pie 3	6.3	1					8:00:00 AM	8:00:00 AM	8:00:00 AM	8:00:00 AM	8:00:00 AM	8:00:00 AM	8:00:00 AM	8:00:00 AM	8:00:00 AM				
			9773A	J	10	pie 1	5.3	1	7:00:00 AM	7:00:00 AM	7:00:00 AM	7:00:00 AM	8:00:00 AM	8:00:00 AM	8:00:00 AM	8:00:00 AM	8:00:00 AM	8:00:00 AM	8:00:00 AM	8:00:00 AM	8:00:00 AM				
						pie 2	5.8	1					8:00:00 AM	8:00:00 AM	8:00:00 AM	8:00:00 AM	8:00:00 AM	8:00:00 AM	8:00:00 AM	8:00:00 AM	8:00:00 AM				
						pie 3	6.3	1					8:00:00 AM	8:00:00 AM	8:00:00 AM	8:00:00 AM	8:00:00 AM	8:00:00 AM	8:00:00 AM	8:00:00 AM	8:00:00 AM				
	OOLITIC	87339	9126A	K	11	pie 1	5.8	1	8:00:00 AM	8:00:00 AM	8:00:00 AM	8:00:00 AM	8:00:00 AM	8:00:00 AM	8:00:00 AM	8:00:00 AM	8:00:00 AM	8:00:00 AM	8:00:00 AM	8:00:00 AM	8:00:00 AM				
						pie 2	6.3	1					8:00:00 AM	8:00:00 AM	8:00:00 AM	8:00:00 AM	8:00:00 AM	8:00:00 AM	8:00:00 AM	8:00:00 AM	8:00:00 AM				
						pie 3	6.8	1					8:00:00 AM	8:00:00 AM	8:00:00 AM	8:00:00 AM	8:00:00 AM	8:00:00 AM	8:00:00 AM	8:00:00 AM	8:00:00 AM				
			9400A	L	12	pie 1	5.8	1	7:00:00 AM	7:00:00 AM	7:00:00 AM	7:00:00 AM	8:00:00 AM	8:00:00 AM	8:00:00 AM	8:00:00 AM	8:00:00 AM	8:00:00 AM	8:00:00 AM	8:00:00 AM	8:00:00 AM				
						pie 2	6.3	1					8:00:00 AM	8:00:00 AM	8:00:00 AM	8:00:00 AM	8:00:00 AM	8:00:00 AM	8:00:00 AM	8:00:00 AM	8:00:00 AM				
						pie 3	6.8	1					8:00:00 AM	8:00:00 AM	8:00:00 AM	8:00:00 AM	8:00:00 AM	8:00:00 AM	8:00:00 AM	8:00:00 AM	8:00:00 AM				
			9138A	M	13	pie 1	5.8	1	8:00:00 AM	8:00:00 AM	8:00:00 AM	8:00:00 AM	8:00:00 AM	8:00:00 AM	8:00:00 AM	8:00:00 AM	8:00:00 AM	8:00:00 AM	8:00:00 AM	8:00:00 AM	8:00:00 AM				
						pie 2	6.3	1					8:00:00 AM	8:00:00 AM	8:00:00 AM	8:00:00 AM	8:00:00 AM	8:00:00 AM	8:00:00 AM	8:00:00 AM	8:00:00 AM				
						pie 3	6.8	1					8:00:00 AM	8:00:00 AM	8:00:00 AM	8:00:00 AM	8:00:00 AM	8:00:00 AM	8:00:00 AM	8:00:00 AM	8:00:00 AM				
			9139A	N	14	pie 1	5.8	1	7:00:00 AM	7:00:00 AM	7:00:00 AM	7:00:00 AM	8:00:00 AM	8:00:00 AM	8:00:00 AM	8:00:00 AM	8:00:00 AM	8:00:00 AM	8:00:00 AM	8:00:00 AM	8:00:00 AM				
						pie 2	6.3	1					8:00:00 AM	8:00:00 AM	8:00:00 AM	8:00:00 AM	8:00:00 AM	8:00:00 AM	8:00:00 AM	8:00:00 AM	8:00:00 AM				
						pie 3	6.8	1					8:00:00 AM	8:00:00 AM	8:00:00 AM	8:00:00 AM	8:00:00 AM	8:00:00 AM	8:00:00 AM	8:00:00 AM	8:00:00 AM				
			9469A	O	15	pie 1	5.8	1	8:00:00 AM	8:00:00 AM	8:00:00 AM	8:00:00 AM	8:00:00 AM	8:00:00 AM	8:00:00 AM	8:00:00 AM	8:00:00 AM	8:00:00 AM	8:00:00 AM	8:00:00 AM	8:00:00 AM				
						pie 2	6.3	1					8:00:00 AM	8:00:00 AM	8:00:00 AM	8:00:00 AM	8:00:00 AM	8:00:00 AM	8:00:00 AM	8:00:00 AM	8:00:00 AM				
						pie 3	6.8	1					8:00:00 AM	8:00:00 AM	8:00:00 AM	8:00:00 AM	8:00:00 AM	8:00:00 AM	8:00:00 AM	8:00:00 AM	8:00:00 AM				
			10134A	P	16	pie 1	5.8	1	7:00:00 AM	7:00:00 AM	7:00:00 AM	7:00:00 AM	8:00:00 AM	8:00:00 AM	8:00:00 AM	8:00:00 AM	8:00:00 AM	8:00:00 AM	8:00:00 AM	8:00:00 AM	8:00:00 AM				
						pie 2	6.3	1					8:00:00 AM	8:00:00 AM	8:00:00 AM	8:00:00 AM	8:00:00 AM	8:00:00 AM	8:00:00 AM	8:00:00 AM	8:00:00 AM				
						pie 3	6.8	1					8:00:00 AM	8:00:00 AM	8:00:00 AM	8:00:00 AM	8:00:00 AM	8:00:00 AM	8:00:00 AM	8:00:00 AM	8:00:00 AM				
		87145	6954A	Q	17	pie 1	5.8	1	8:00:00 AM	8:00:00 AM	8:00:00 AM	8:00:00 AM	8:00:00 AM	8:00:00 AM	8:00:00 AM	8:00:00 AM	8:00:00 AM	8:00:00 AM	8:00:00 AM	8:00:00 AM	8:00:00 AM				
						pie 2	6.3	1					8:00:00 AM	8:00:00 AM	8:00:00 AM	8:00:00 AM	8:00:00 AM	8:00:00 AM	8:00:00 AM	8:00:00 AM	8:00:00 AM				
						pie 3	6.8	1					8:00:00 AM	8:00:00 AM	8:00:00 AM	8:00:00 AM	8:00:00 AM	8:00:00 AM	8:00:00 AM	8:00:00 AM	8:00:00 AM				
			7806A	R	18	pie 1	5.8	1	7:00:00 AM	7:00:00 AM	7:00:00 AM	7:00:00 AM	8:00:00 AM	8:00:00 AM	8:00:00 AM	8:00:00 AM	8:00:00 AM	8:00:00 AM	8:00:00 AM	8:00:00 AM	8:00:00 AM				
						pie 2	6.3	1					8:00:00 AM	8:00:00 AM	8:00:00 AM	8:00:00 AM	8:00:00 AM	8:00:00 AM	8:00:00 AM	8:00:00 AM	8:00:00 AM				
						pie 3	6.8	1					8:00:00 AM	8:00:00 AM	8:00:00 AM	8:00:00 AM	8:00:00 AM	8:00:00 AM	8:00:00 AM	8:00:00 AM	8:00:00 AM				
			9932A	S	19	pie 1	5.8	1	8:00:00 AM	8:00:00 AM	8:00:00 AM	8:00:00 AM	8:00:00 AM	8:00:00 AM	8:00:00 AM	8:00:00 AM	8:00:00 AM	8:00:00 AM	8:00:00 AM	8:00:00 AM	8:00:00 AM				
						pie 2	6.3	1					8:00:00 AM	8:00:00 AM	8:00:00 AM	8:00:00 AM	8:00:00 AM	8:00:00 AM	8:00:00 AM	8:00:00 AM	8:00:00 AM				
						pie 3	6.8	1					8:00:00 AM	8:00:00 AM	8:00:00 AM	8:00:00 AM	8:00:00 AM	8:00:00 AM	8:00:00 AM	8:00:00 AM	8:00:00 AM				

Table A1 (Continued)

	MIX TYPE		DESIGN #		MIX #	FM5-588 PIE PLATES SAMPLES			DETERMINATION OF OPTIMUM ASPHALT BINDER CONTENT												
									SECTION 5.4		SECTION 5.5		SECTION 5.6		SECTION 5.7		SECTION 5.8		SECTION 5.9		image/labview
									5.4 Prepare three 1200 g aggregate batches.		5.5 Heat the aggregate batches and the asphalt binder for a minimum of two hours		5.6 mix the aggregate batch and asphalt binder in the mixing bowl		5.7 transfer the mixture from the mixing bowl into a pie plate AND place in an oven for one hour		5.8 remove the pie plate from the oven and allow it to cool undisturbed until it reaches room		5.9 invert the pie plates and inspect the bottom surfaces.		
trial 3	GRANITIC	NS315				pie 3	6.3	1					7:00:00 AM	7:00:00 AM	7:00:00 AM	7:00:00 AM	7:00:00 AM	7:00:00 AM	7:00:00 AM	7:00:00 AM	7:00:00 AM
			9476A	B	2	pie 1	5.3	1	7:00:00 AM	7:00:00 AM	7:00:00 AM	7:00:00 AM	7:00:00 AM	7:00:00 AM	7:00:00 AM	7:00:00 AM	7:00:00 AM	7:00:00 AM	7:00:00 AM	7:00:00 AM	7:00:00 AM
						pie 2	5.8	1					7:00:00 AM	7:00:00 AM	7:00:00 AM	7:00:00 AM	7:00:00 AM	7:00:00 AM	7:00:00 AM	7:00:00 AM	7:00:00 AM
						pie 3	6.3	1					7:00:00 AM	7:00:00 AM	7:00:00 AM	7:00:00 AM	7:00:00 AM	7:00:00 AM	7:00:00 AM	7:00:00 AM	7:00:00 AM
			9642A	C	3	pie 1	5.3	1	7:00:00 AM	7:00:00 AM	7:00:00 AM	7:00:00 AM	7:00:00 AM	7:00:00 AM	7:00:00 AM	7:00:00 AM	7:00:00 AM	7:00:00 AM	7:00:00 AM	7:00:00 AM	7:00:00 AM
						pie 2	5.8	1					7:00:00 AM	7:00:00 AM	7:00:00 AM	7:00:00 AM	7:00:00 AM	7:00:00 AM	7:00:00 AM	7:00:00 AM	7:00:00 AM
						pie 3	6.3	1					7:00:00 AM	7:00:00 AM	7:00:00 AM	7:00:00 AM	7:00:00 AM	7:00:00 AM	7:00:00 AM	7:00:00 AM	7:00:00 AM
			9646A	D	4	pie 1	5.3	1	7:00:00 AM	7:00:00 AM	7:00:00 AM	7:00:00 AM	7:00:00 AM	7:00:00 AM	7:00:00 AM	7:00:00 AM	7:00:00 AM	7:00:00 AM	7:00:00 AM	7:00:00 AM	7:00:00 AM
						pie 2	5.8	1					7:00:00 AM	7:00:00 AM	7:00:00 AM	7:00:00 AM	7:00:00 AM	7:00:00 AM	7:00:00 AM	7:00:00 AM	7:00:00 AM
						pie 3	6.3	1					7:00:00 AM	7:00:00 AM	7:00:00 AM	7:00:00 AM	7:00:00 AM	7:00:00 AM	7:00:00 AM	7:00:00 AM	7:00:00 AM
			9657A	E	5	pie 1	5.3	1	7:00:00 AM	7:00:00 AM	7:00:00 AM	7:00:00 AM	7:00:00 AM	7:00:00 AM	7:00:00 AM	7:00:00 AM	7:00:00 AM	7:00:00 AM	7:00:00 AM	7:00:00 AM	7:00:00 AM
						pie 2	5.8	1					7:00:00 AM	7:00:00 AM	7:00:00 AM	7:00:00 AM	7:00:00 AM	7:00:00 AM	7:00:00 AM	7:00:00 AM	7:00:00 AM
						pie 3	6.3	1					7:00:00 AM	7:00:00 AM	7:00:00 AM	7:00:00 AM	7:00:00 AM	7:00:00 AM	7:00:00 AM	7:00:00 AM	7:00:00 AM
		GA553	9160A	F	6	pie 1	5.3	1	7:00:00 AM	7:00:00 AM	7:00:00 AM	7:00:00 AM	7:00:00 AM	7:00:00 AM	7:00:00 AM	7:00:00 AM	7:00:00 AM	7:00:00 AM	7:00:00 AM	7:00:00 AM	7:00:00 AM
						pie 2	5.8	1					7:00:00 AM	7:00:00 AM	7:00:00 AM	7:00:00 AM	7:00:00 AM	7:00:00 AM	7:00:00 AM	7:00:00 AM	7:00:00 AM
						pie 3	6.3	1					7:00:00 AM	7:00:00 AM	7:00:00 AM	7:00:00 AM	7:00:00 AM	7:00:00 AM	7:00:00 AM	7:00:00 AM	7:00:00 AM
			9184A	G	7	pie 1	5.3	1	7:00:00 AM	7:00:00 AM	7:00:00 AM	7:00:00 AM	7:00:00 AM	7:00:00 AM	7:00:00 AM	7:00:00 AM	7:00:00 AM	7:00:00 AM	7:00:00 AM	7:00:00 AM	7:00:00 AM
						pie 2	5.8	1					7:00:00 AM	7:00:00 AM	7:00:00 AM	7:00:00 AM	7:00:00 AM	7:00:00 AM	7:00:00 AM	7:00:00 AM	7:00:00 AM
						pie 3	6.3	1					7:00:00 AM	7:00:00 AM	7:00:00 AM	7:00:00 AM	7:00:00 AM	7:00:00 AM	7:00:00 AM	7:00:00 AM	7:00:00 AM
			9250A	H	8	pie 1	5.3	1	7:00:00 AM	7:00:00 AM	7:00:00 AM	7:00:00 AM	7:00:00 AM	7:00:00 AM	7:00:00 AM	7:00:00 AM	7:00:00 AM	7:00:00 AM	7:00:00 AM	7:00:00 AM	7:00:00 AM
						pie 2	5.8	1					7:00:00 AM	7:00:00 AM	7:00:00 AM	7:00:00 AM	7:00:00 AM	7:00:00 AM	7:00:00 AM	7:00:00 AM	7:00:00 AM
						pie 3	6.3	1					7:00:00 AM	7:00:00 AM	7:00:00 AM	7:00:00 AM	7:00:00 AM	7:00:00 AM	7:00:00 AM	7:00:00 AM	7:00:00 AM
			9824A	I	9	pie 1	5.3	1	7:00:00 AM	7:00:00 AM	7:00:00 AM	7:00:00 AM	7:00:00 AM	7:00:00 AM	7:00:00 AM	7:00:00 AM	7:00:00 AM	7:00:00 AM	7:00:00 AM	7:00:00 AM	7:00:00 AM
						pie 2	5.8	1					7:00:00 AM	7:00:00 AM	7:00:00 AM	7:00:00 AM	7:00:00 AM	7:00:00 AM	7:00:00 AM	7:00:00 AM	7:00:00 AM
						pie 3	6.3	1					7:00:00 AM	7:00:00 AM	7:00:00 AM	7:00:00 AM	7:00:00 AM	7:00:00 AM	7:00:00 AM	7:00:00 AM	7:00:00 AM
			9773A	J	10	pie 1	5.3	1	7:00:00 AM	7:00:00 AM	7:00:00 AM	7:00:00 AM	7:00:00 AM	7:00:00 AM	7:00:00 AM	7:00:00 AM	7:00:00 AM	7:00:00 AM	7:00:00 AM	7:00:00 AM	7:00:00 AM
						pie 2	5.8	1					7:00:00 AM	7:00:00 AM	7:00:00 AM	7:00:00 AM	7:00:00 AM	7:00:00 AM	7:00:00 AM	7:00:00 AM	7:00:00 AM
						pie 3	6.3	1					7:00:00 AM	7:00:00 AM	7:00:00 AM	7:00:00 AM	7:00:00 AM	7:00:00 AM	7:00:00 AM	7:00:00 AM	7:00:00 AM
	OOLITIC	87339	9126A	K	11	pie 1	5.8	1	7:00:00 AM	7:00:00 AM	7:00:00 AM	7:00:00 AM	7:00:00 AM	7:00:00 AM	7:00:00 AM	7:00:00 AM	7:00:00 AM	7:00:00 AM	7:00:00 AM	7:00:00 AM	7:00:00 AM
						pie 2	6.3	1					7:00:00 AM	7:00:00 AM	7:00:00 AM	7:00:00 AM	7:00:00 AM	7:00:00 AM	7:00:00 AM	7:00:00 AM	7:00:00 AM
						pie 3	6.8	1					7:00:00 AM	7:00:00 AM	7:00:00 AM	7:00:00 AM	7:00:00 AM	7:00:00 AM	7:00:00 AM	7:00:00 AM	7:00:00 AM
			9400A	L	12	pie 1	5.8	1	7:00:00 AM	7:00:00 AM	7:00:00 AM	7:00:00 AM	7:00:00 AM	7:00:00 AM	7:00:00 AM	7:00:00 AM	7:00:00 AM	7:00:00 AM	7:00:00 AM	7:00:00 AM	7:00:00 AM
						pie 2	6.3	1					7:00:00 AM	7:00:00 AM	7:00:00 AM	7:00:00 AM	7:00:00 AM	7:00:00 AM	7:00:00 AM	7:00:00 AM	7:00:00 AM
						pie 3	6.8	1					7:00:00 AM	7:00:00 AM	7:00:00 AM	7:00:00 AM	7:00:00 AM	7:00:00 AM	7:00:00 AM	7:00:00 AM	7:00:00 AM
			9138A	M	13	pie 1	5.8	1	7:00:00 AM	7:00:00 AM	7:00:00 AM	7:00:00 AM	7:00:00 AM	7:00:00 AM	7:00:00 AM	7:00:00 AM	7:00:00 AM	7:00:00 AM	7:00:00 AM	7:00:00 AM	7:00:00 AM
						pie 2	6.3	1					7:00:00 AM	7:00:00 AM	7:00:00 AM	7:00:00 AM	7:00:00 AM	7:00:00 AM	7:00:00 AM	7:00:00 AM	7:00:00 AM
						pie 3	6.8	1					7:00:00 AM	7:00:00 AM	7:00:00 AM	7:00:00 AM	7:00:00 AM	7:00:00 AM	7:00:00 AM	7:00:00 AM	7:00:00 AM
			9139A	N	14	pie 1	5.8	1	7:00:00 AM	7:00:00 AM	7:00:00 AM	7:00:00 AM	7:00:00 AM	7:00:00 AM	7:00:00 AM	7:00:00 AM	7:00:00 AM	7:00:00 AM	7:00:00 AM	7:00:00 AM	7:00:00 AM
						pie 2	6.3	1					7:00:00 AM	7:00:00 AM	7:00:00 AM	7:00:00 AM	7:00:00 AM	7:00:00 AM	7:00:00 AM	7:00:00 AM	7:00:00 AM
						pie 3	6.8	1					7:00:00 AM	7:00:00 AM	7:00:00 AM	7:00:00 AM	7:00:00 AM	7:00:00 AM	7:00:00 AM	7:00:00 AM	7:00:00 AM
			9469A	O	15	pie 1	5.8	1	7:00:00 AM	7:00:00 AM	7:00:00 AM	7:00:00 AM	7:00:00 AM	7:00:00 AM	7:00:00 AM	7:00:00 AM	7:00:00 AM	7:00:00 AM	7:00:00 AM	7:00:00 AM	7:00:00 AM
						pie 2	6.3	1					7:00:00 AM	7:00:00 AM	7:00:00 AM	7:00:00 AM	7:00:00 AM	7:00:00 AM	7:00:00 AM	7:00:00 AM	7:00:00 AM
						pie 3	6.8	1					7:00:00 AM	7:00:00 AM	7:00:00 AM	7:00:00 AM	7:00:00 AM	7:00:00 AM	7:00:00 AM	7:00:00 AM	7:00:00 AM
			10134A	P	16	pie 1	5.8	1	7:00:00 AM	7:00:00 AM	7:00:00 AM	7:00:00 AM	7:00:00 AM	7:00:00 AM	7:00:00 AM	7:00:00 AM	7:00:00 AM	7:00:00 AM	7:00:00 AM	7:00:00 AM	7:00:00 AM
						pie 2	6.3	1					7:00:00 AM	7:00:00 AM	7:00:00 AM	7:00:00 AM	7:00:00 AM	7:00:00 AM	7:00:00 AM	7:00:00 AM	7:00:00 AM
						pie 3	6.8	1					7:00:00 AM	7:00:00 AM	7:00:00 AM	7:00:00 AM	7:00:00 AM	7:00:00 AM	7:00:00 AM	7:00:00 AM	7:00:00 AM
		87145	6954A	Q	17	pie 1	5.8	1	7:00:00 AM	7:00:00 AM	7:00:00 AM	7:00:00 AM	7:00:00 AM	7:00:00 AM	7:00:00 AM	7:00:00 AM	7:00:00 AM	7:00:00 AM	7:00:00 AM	7:00:00 AM	7:00:00 AM
						pie 2	6.3	1					7:00:00 AM	7:00:00 AM	7:00:00 AM	7:00:00 AM	7:00:00 AM	7:00:00 AM	7:00:00 AM	7:00:00 AM	7:00:00 AM
						pie 3	6.8	1					7:00:00 AM	7:00:00 AM	7:00:00 AM	7:00:00 AM	7:00:00 AM	7:00:00 AM	7:00:00 AM	7:00:00 AM	7:00:00 AM
			7806A	R	18	pie 1	5.8	1	7:00:00 AM	7:00:00 AM	7:00:00 AM	7:00:00 AM	7:00:00 AM	7:00:00 AM	7:00:00 AM	7:00:00 AM	7:00:00 AM	7:00:00 AM	7:00:00 AM	7:00:00 AM	7:00:00 AM
						pie 2	6.3	1					7:00:00 AM	7:00:00 AM	7:00:00 AM	7:00:00 AM	7:00:00 AM	7:00:00 AM	7:00:00 AM	7:00:00 AM	7:00:00 AM
						pie 3	6.8	1					7:00:00 AM	7:00:00 AM	7:00:00 AM	7:00:00 AM	7:00:00 AM	7:00:00 AM	7:00:00 AM	7:00:00 AM	7:00:00 AM
			9932A	S	19	pie 1	5.8	1	7:00:00 AM	7:00:00 AM	7:00:00 AM	7:00:00 AM	7:00:00 AM	7:00:00 AM	7:00:00 AM	7:00:00 AM	7:00:00 AM	7:00:00 AM	7:00:00 AM	7:00:00 AM	7:00:00 AM
						pie 2	6.3	1					7:00:00 AM	7:00:00 AM	7:00:00 AM	7:00:00 AM	7:00:00 AM	7:00:00 AM	7:00:00 AM	7:00:00 AM	7:00:00 AM
						pie 3	6.8	1					7:00:00 AM	7:00:00 AM	7:00:00 AM	7:00:00 AM	7:00:00 AM	7:00:00 AM	7:00:00 AM	7:00:00 AM	7:00:00 AM

Table A1 (Continued)

	MIX TYPE		DESIGN #		MIX #	FM5-588 PIE PLATES SAMPLES			DETERMINATION OF OPTIMUM ASPHALT BINDER CONTENT												
									SECTION 5.4		SECTION 5.5		SECTION 5.6		SECTION 5.7		SECTION 5.8		SECTION 5.9		image/labview
									5.4 Prepare three 1200 g aggregate batches.		5.5 Heat the aggregate batches and the asphalt binder for a minimum of two hours		5.6 mix the aggregate batch and asphalt binder in the mixing bowl		5.7 transfer the mixture from the mixing bowl into a pie plate AND place in an oven for one hour		5.8 remove the pie plate from the oven and allow it to cool undisturbed until it reaches room		5.9 invert the pie plates and inspect the bottom surfaces.		
trial 1 results	GRANITIC	NS315	9165A	A	1	OBC	VISUAL	1													
			9476A	B	2	OBC	VISUAL	1	7:00:00 AM	7:00:00 AM	7:00:00 AM	7:00:00 AM	7:00:00 AM	7:00:00 AM	7:00:00 AM	7:00:00 AM	7:00:00 AM	7:00:00 AM	7:00:00 AM	7:00:00 AM	7:00:00 AM
			9642A	C	3	OBC	VISUAL	1					7:00:00 AM	7:00:00 AM	7:00:00 AM	7:00:00 AM	7:00:00 AM	7:00:00 AM	7:00:00 AM	7:00:00 AM	7:00:00 AM
			9646A	D	4	OBC	VISUAL	1					7:00:00 AM	7:00:00 AM	7:00:00 AM	7:00:00 AM	7:00:00 AM	7:00:00 AM	7:00:00 AM	7:00:00 AM	7:00:00 AM
			9657A	E	5	OBC	VISUAL	1	7:00:00 AM	7:00:00 AM	7:00:00 AM	7:00:00 AM	7:00:00 AM	7:00:00 AM	7:00:00 AM	7:00:00 AM	7:00:00 AM	7:00:00 AM	7:00:00 AM	7:00:00 AM	7:00:00 AM
		GA553	9160A	F	6	OBC	VISUAL	1					7:00:00 AM	7:00:00 AM	7:00:00 AM	7:00:00 AM	7:00:00 AM	7:00:00 AM	7:00:00 AM	7:00:00 AM	7:00:00 AM
			9184A	G	7	OBC	VISUAL	1					7:00:00 AM	7:00:00 AM	7:00:00 AM	7:00:00 AM	7:00:00 AM	7:00:00 AM	7:00:00 AM	7:00:00 AM	7:00:00 AM
			9250A	H	8	OBC	VISUAL	1	7:00:00 AM	7:00:00 AM	7:00:00 AM	7:00:00 AM	7:00:00 AM	7:00:00 AM	7:00:00 AM	7:00:00 AM	7:00:00 AM	7:00:00 AM	7:00:00 AM	7:00:00 AM	7:00:00 AM
			9824A	I	9	OBC	VISUAL	1					7:00:00 AM	7:00:00 AM	7:00:00 AM	7:00:00 AM	7:00:00 AM	7:00:00 AM	7:00:00 AM	7:00:00 AM	7:00:00 AM
			9773A	J	10	OBC	VISUAL	1					7:00:00 AM	7:00:00 AM	7:00:00 AM	7:00:00 AM	7:00:00 AM	7:00:00 AM	7:00:00 AM	7:00:00 AM	7:00:00 AM
	OOLITIC	87339	9126A	K	11	OBC	VISUAL	1	7:00:00 AM	7:00:00 AM	7:00:00 AM	7:00:00 AM	7:00:00 AM	7:00:00 AM	7:00:00 AM	7:00:00 AM	7:00:00 AM	7:00:00 AM	7:00:00 AM	7:00:00 AM	7:00:00 AM
			9400A	L	12	OBC	VISUAL	1					7:00:00 AM	7:00:00 AM	7:00:00 AM	7:00:00 AM	7:00:00 AM	7:00:00 AM	7:00:00 AM	7:00:00 AM	7:00:00 AM
			9138A	M	13	OBC	VISUAL	1					7:00:00 AM	7:00:00 AM	7:00:00 AM	7:00:00 AM	7:00:00 AM	7:00:00 AM	7:00:00 AM	7:00:00 AM	7:00:00 AM
			9139A	N	14	OBC	VISUAL	1	7:00:00 AM	7:00:00 AM	7:00:00 AM	7:00:00 AM	7:00:00 AM	7:00:00 AM	7:00:00 AM	7:00:00 AM	7:00:00 AM	7:00:00 AM	7:00:00 AM	7:00:00 AM	7:00:00 AM
			9469A	O	15	OBC	VISUAL	1					7:00:00 AM	7:00:00 AM	7:00:00 AM	7:00:00 AM	7:00:00 AM	7:00:00 AM	7:00:00 AM	7:00:00 AM	7:00:00 AM
			10134A	P	16	OBC	VISUAL	1					7:00:00 AM	7:00:00 AM	7:00:00 AM	7:00:00 AM	7:00:00 AM	7:00:00 AM	7:00:00 AM	7:00:00 AM	7:00:00 AM
		87145	6954A	Q	17	OBC	VISUAL	1	7:00:00 AM	7:00:00 AM	7:00:00 AM	7:00:00 AM	7:00:00 AM	7:00:00 AM	7:00:00 AM	7:00:00 AM	7:00:00 AM	7:00:00 AM	7:00:00 AM	7:00:00 AM	7:00:00 AM
			7806A	R	18	OBC	VISUAL	1					7:00:00 AM	7:00:00 AM	7:00:00 AM	7:00:00 AM	7:00:00 AM	7:00:00 AM	7:00:00 AM	7:00:00 AM	7:00:00 AM
			9932A	S	19	OBC	VISUAL	1					7:00:00 AM	7:00:00 AM	7:00:00 AM	7:00:00 AM	7:00:00 AM	7:00:00 AM	7:00:00 AM	7:00:00 AM	7:00:00 AM
trial 2 results	GRANITIC	NS315	9165A	A	1	OBC	VISUAL	1	7:00:00 AM	7:00:00 AM	7:00:00 AM	7:00:00 AM	7:00:00 AM	7:00:00 AM	7:00:00 AM	7:00:00 AM	7:00:00 AM	7:00:00 AM	7:00:00 AM	7:00:00 AM	7:00:00 AM
			9476A	B	2	OBC	VISUAL	1					7:00:00 AM	7:00:00 AM	7:00:00 AM	7:00:00 AM	7:00:00 AM	7:00:00 AM	7:00:00 AM	7:00:00 AM	7:00:00 AM
			9642A	C	3	OBC	VISUAL	1					7:00:00 AM	7:00:00 AM	7:00:00 AM	7:00:00 AM	7:00:00 AM	7:00:00 AM	7:00:00 AM	7:00:00 AM	7:00:00 AM
			9646A	D	4	OBC	VISUAL	1					7:00:00 AM	7:00:00 AM	7:00:00 AM	7:00:00 AM	7:00:00 AM	7:00:00 AM	7:00:00 AM	7:00:00 AM	7:00:00 AM
			9657A	E	5	OBC	VISUAL	1					7:00:00 AM	7:00:00 AM	7:00:00 AM	7:00:00 AM	7:00:00 AM	7:00:00 AM	7:00:00 AM	7:00:00 AM	7:00:00 AM
		GA553	9160A	F	6	OBC	VISUAL	1	7:00:00 AM	7:00:00 AM	7:00:00 AM	7:00:00 AM	7:00:00 AM	7:00:00 AM	7:00:00 AM	7:00:00 AM	7:00:00 AM	7:00:00 AM	7:00:00 AM	7:00:00 AM	7:00:00 AM
			9184A	G	7	OBC	VISUAL	1					7:00:00 AM	7:00:00 AM	7:00:00 AM	7:00:00 AM	7:00:00 AM	7:00:00 AM	7:00:00 AM	7:00:00 AM	7:00:00 AM
			9250A	H	8	OBC	VISUAL	1					7:00:00 AM	7:00:00 AM	7:00:00 AM	7:00:00 AM	7:00:00 AM	7:00:00 AM	7:00:00 AM	7:00:00 AM	7:00:00 AM
			9824A	I	9	OBC	VISUAL	1					7:00:00 AM	7:00:00 AM	7:00:00 AM	7:00:00 AM	7:00:00 AM	7:00:00 AM	7:00:00 AM	7:00:00 AM	7:00:00 AM
			9773A	J	10	OBC	VISUAL	1	7:00:00 AM	7:00:00 AM	7:00:00 AM	7:00:00 AM	7:00:00 AM	7:00:00 AM	7:00:00 AM	7:00:00 AM	7:00:00 AM	7:00:00 AM	7:00:00 AM	7:00:00 AM	7:00:00 AM
	OOLITIC		9126A	K	11	OBC	VISUAL	1					7:00:00 AM	7:00:00 AM	7:00:00 AM	7:00:00 AM	7:00:00 AM	7:00:00 AM	7:00:00 AM	7:00:00 AM	7:00:00 AM
			9400A	L	12	OBC	VISUAL	1					7:00:00 AM	7:00:00 AM	7:00:00 AM	7:00:00 AM	7:00:00 AM	7:00:00 AM	7:00:00 AM	7:00:00 AM	7:00:00 AM
		87339	9138A	M	13	OBC	VISUAL	1	7:00:00 AM	7:00:00 AM	7:00:00 AM	7:00:00 AM	7:00:00 AM	7:00:00 AM	7:00:00 AM	7:00:00 AM	7:00:00 AM	7:00:00 AM	7:00:00 AM	7:00:00 AM	7:00:00 AM
			9139A	N	14	OBC	VISUAL	1					7:00:00 AM	7:00:00 AM	7:00:00 AM	7:00:00 AM	7:00:00 AM	7:00:00 AM	7:00:00 AM	7:00:00 AM	7:00:00 AM
			9469A	O	15	OBC	VISUAL	1					7:00:00 AM	7:00:00 AM	7:00:00 AM	7:00:00 AM	7:00:00 AM	7:00:00 AM	7:00:00 AM	7:00:00 AM	7:00:00 AM
			10134A	P	16	OBC	VISUAL	1	7:00:00 AM	7:00:00 AM	7:00:00 AM	7:00:00 AM	7:00:00 AM	7:00:00 AM	7:00:00 AM	7:00:00 AM	7:00:00 AM	7:00:00 AM	7:00:00 AM	7:00:00 AM	7:00:00 AM
		87145	6954A	Q	17	OBC	VISUAL	1					7:00:00 AM	7:00:00 AM	7:00:00 AM	7:00:00 AM	7:00:00 AM	7:00:00 AM	7:00:00 AM	7:00:00 AM	7:00:00 AM
			7806A	R	18	OBC	VISUAL	1					7:00:00 AM	7:00:00 AM	7:00:00 AM	7:00:00 AM	7:00:00 AM	7:00:00 AM	7:00:00 AM	7:00:00 AM	7:00:00 AM
			9932A	S	19	OBC	VISUAL	1					7:00:00 AM	7:00:00 AM	7:00:00 AM	7:00:00 AM	7:00:00 AM	7:00:00 AM	7:00:00 AM	7:00:00 AM	7:00:00 AM
trial 3 results	GRANITIC	NS315	9165A	A	1	OBC	VISUAL	1													
			9476A	B	2	OBC	VISUAL	1					7:00:00 AM	7:00:00 AM	7:00:00 AM	7:00:00 AM	7:00:00 AM	7:00:00 AM	7:00:00 AM	7:00:00 AM	7:00:00 AM
			9642A	C	3	OBC	VISUAL	1	7:00:00 AM	7:00:00 AM	7:00:00 AM	7:00:00 AM	7:00:00 AM	7:00:00 AM	7:00:00 AM	7:00:00 AM	7:00:00 AM	7:00:00 AM	7:00:00 AM	7:00:00 AM	7:00:00 AM
			9646A	D	4	OBC	VISUAL	1					7:00:00 AM	7:00:00 AM	7:00:00 AM	7:00:00 AM	7:00:00 AM	7:00:00 AM	7:00:00 AM	7:00:00 AM	7:00:00 AM
			9657A	E	5	OBC	VISUAL	1					7:00:00 AM	7:00:00 AM	7:00:00 AM	7:00:00 AM	7:00:00 AM	7:00:00 AM	7:00:00 AM	7:00:00 AM	7:00:00 AM
		GA553	9160A	F	6	OBC	VISUAL	1	7:00:00 AM	7:00:00 AM	7:00:00 AM	7:00:00 AM	7:00:00 AM	7:00:00 AM	7:00:00 AM	7:00:00 AM	7:00:00 AM	7:00:00 AM	7:00:00 AM	7:00:00 AM	7:00:00 AM
			9184A	G	7	OBC	VISUAL	1					7:00:00 AM	7:00:00 AM	7:00:00 AM	7:00:00 AM	7:00:00 AM	7:00:00 AM	7:00:00 AM	7:00:00 AM	7:00:00 AM
			9250A	H	8	OBC	VISUAL	1					7:00:00 AM	7:00:00 AM	7:00:00 AM	7:00:00 AM	7:00:00 AM	7:00:00 AM	7:00:00 AM	7:00:00 AM	7:00:00 AM
			9824A	I	9	OBC	VISUAL	1					7:00:00 AM	7:00:00 AM	7:00:00 AM	7:00:00 AM	7:00:00 AM	7:00:00 AM	7:00:00 AM	7:00:00 AM	7:00:00 AM
			9773A	J	10	OBC	VISUAL	1					7:00:00 AM	7:00:00 AM	7:00:00 AM	7:00:00 AM	7:00:00 AM	7:00:00 AM	7:00:00 AM	7:00:00 AM	7:00:00 AM
	OOLITIC	87339	9126A	K	11	OBC	VISUAL	1	7:00:00 AM	7:00:00 AM	7:00:00 AM	7:00:00 AM	7:00:00 AM	7:00:00 AM	7:00:00 AM	7:00:00 AM	7:00:00 AM	7:00:00 AM	7:00:00 AM	7:00:00 AM	7:00:00 AM
			9400A	L	12	OBC	VISUAL	1					7:00:00 AM	7:00:00 AM	7:00:00 AM	7:00:00 AM	7:00:00 AM	7:00:00 AM	7:00:00 AM	7:00:00 AM	7:00:00 AM
			9138A	M	13	OBC	VISUAL	1					7:00:00 AM	7:00:00 AM	7:00:00 AM	7:00:00 AM	7:00:00 AM	7:00:00 AM	7:00:00 AM	7:00:00 AM	7:00:00 AM
			9139A	N	14	OBC	VISUAL	1	7:00:00 AM	7:00:00 AM	7:00:00 AM	7:00:00 AM	7:00:00 AM	7:00:00 AM	7:00:00 AM	7:00:00 AM	7:00:00 AM	7:00:00 AM	7:00:00 AM	7:00:00 AM	7:00:00 AM
			9469A	O	15	OBC	VISUAL	1					7:00:00 AM	7:00:00 AM	7:00:00 AM	7:00:00 AM	7:00:00 AM	7:00:00 AM	7:00:00 AM	7:00:00 AM	7:00:00 AM
			10134A	P	16	OBC	VISUAL	1					7:00:00 AM	7:00:00 AM	7:00:00 AM	7:00:00 AM	7:00:00 AM	7:00:00 AM	7:00:00 AM	7:00:00 AM	7:00:00 AM
		87145	6954A	Q	17	OBC	VISUAL	1					7:00:00 AM	7:00:00 AM	7:00:00 AM	7:00:00 AM	7:00:00 AM	7:00:00 AM	7:00:00 AM	7:00:00 AM	7:00:00 AM
			7806A	R	18	OBC	VISUAL	1	7:00:00 AM	7:00:00 AM	7:00:00 AM	7:00:00 AM	7:00:00 AM	7:00:00 AM	7:00:00 AM	7:00:00 AM	7:00:00 AM	7:00:00 AM	7:00:00 AM	7:00:00 AM	7:00:00 AM
			9932A	S	19	OBC	VISUAL	1					7:00:00 AM	7:00:00 AM	7:00:00 AM	7:00:00 AM	7:00:00 AM	7:00:00 AM	7:00:00 AM	7:00:00 AM	7:00:00 AM

APPENDIX B: TRACKING OF THE EXPERIMENTAL PROCESS

Table B1 Tracking of experimental process for granite NS315 mix designs.

(a)

Batch													
		TRIAL 1			TRIAL 2			TRIAL 3			OPT GRADE		
MIX # /NAME		5.3%	5.8%	6.3%	5.3%	5.8%	6.3%	5.3%	5.8%	6.3%	TRIAL 1	TRIAL 2	TRIAL 3
9165A	A	x	x	x	x	x	x	x	x	x	x	x	x
9476A	B	x	x	x	x	x	x	x	x	x	x	x	x
9642A	C	x	x	x	x	x	x	x	x	x	x	x	x
9646A	D	x	x	x	x	x	x	x	x	x	x	x	x
9657A	E	x	x	x	x	x	x	x	x	x	x	x	x

(b)

Pie													
		TRIAL 1			TRIAL 2			TRIAL 3			OPT GRADE		
MIX NAME		5.3%	5.8%	6.3%	5.3%	5.8%	6.3%	5.3%	5.8%	6.3%	TRIAL 1	TRIAL 2	TRIAL 3
9165A	A	x	x	x	x	x	x	x	x	x	x	x	x
9476A	B	x	x	x	x	x	x	x	x	x	x	x	x
9642A	C	x	x	x	x	x	x	x	x	x	x	x	x
9646A	D	x	x	x	x	x	x	x	x	x	x	x	x
9657A	E	x	x	x	x	x	x	x	x	x	x	x	x

(c)

Image without plaster													
		TRIAL 1			TRIAL 2			TRIAL 3			OPT GRADE		
MIX NAME		5.3%	5.8%	6.3%	5.3%	5.8%	6.3%	5.3%	5.8%	6.3%	TRIAL 1	TRIAL 2	TRIAL 3
9165A	A	x	x	x	x	x	x	x	x	x	x	x	x
9476A	B	x	x	x	x	x	x	x	x	x	x	x	x
9642A	C	x	x	x	x	x	x	x	x	x	x	x	x
9646A	D	x	x	x	x	x	x	x	x	x	x	x	x
9657A	E	x	x	x	x	x	x	x	x	x	x	x	x

(d)

Plaster													
		TRIAL 1			TRIAL 2			TRIAL 3			OPT GRADE		
MIX NAME		5.3%	5.8%	6.3%	5.3%	5.8%	6.3%	5.3%	5.8%	6.3%	TRIAL 1	TRIAL 2	TRIAL 3
9165A	A	x	x	x	x	x	x	x	x	x	x	x	x
9476A	B	x	x	x	x	x	x	x	x	x	x	x	x
9642A	C	x	x	x	x	x	x	x	x	x	x	x	x
9646A	D	x	x	x	x	x	x	x	x	x	x	x	x
9657A	E	x	x	x	x	x	x	x	x	x	x	x	x

(e)

Image with plaster													
		TRIAL 1			TRIAL 2			TRIAL 3			OPT GRADE		
MIX NAME		5.3%	5.8%	6.3%	5.3%	5.8%	6.3%	5.3%	5.8%	6.3%	TRIAL 1	TRIAL 2	TRIAL 3
9165A	A	x	x	x	x	x	x	x	x	x	x	x	x
9476A	B	x	x	x	x	x	x	x	x	x	x	x	x
9642A	C	x	x	x	x	x	x	x	x	x	x	x	x
9646A	D	x	x	x	x	x	x	x	x	x	x	x	x
9657A	E	x	x	x	x	x	x	x	x	x	x	x	x

Table B2 Tracking of experimental process for granite GA553 mix designs.

(a)

	Batch												
		TRIAL 1			TRIAL 2			TRIAL 3			OPT GRADE		
MIX # /NAME		5.3%	5.8%	6.3%	5.3%	5.8%	6.3%	5.3%	5.8%	6.3%	TRIAL 1	TRIAL 2	TRIAL 3
9160A	F	x	x	x	x	x	x	x	x	x	x	x	x
9184A	G	x	x	x	x	x	x	x	x	x	x	x	x
9250A	H	x	x	x	x	x	x	x	x	x	x	x	x
9773A	J	x	x	x	x	x	x	x	x	x	x	x	x
9824A	I	x	x	x	x	x	x	x	x	x	x	x	x

(b)

	Pie												
		TRIAL 1			TRIAL 2			TRIAL 3			OPT GRADE		
	MIX NAME	5.3%	5.8%	6.3%	5.3%	5.8%	6.3%	5.3%	5.8%	6.3%	TRIAL 1	TRIAL 2	TRIAL 3
9160A	F	x	x	x	x	x	x	x	x	x	x	x	x
9184A	G	x	x	x	x	x	x	x	x	x	x	x	x
9250A	H	x	x	x	x	x	x	x	x	x	x	x	x
9824A	I	x	x	x	x	x	x	x	x	x	x	x	x
9773A	J	x	x	x	x	x	x	x	x	x	x	x	x

(c)

	Image without plaster												
	MIX	TRIAL 1			TRIAL 2			TRIAL 3			OPT GRADE		
	NA	5.3%	5.8%	6.3%	5.3%	5.8%	6.3%	5.3%	5.8%	6.3%	TRIAL 1	TRIAL 2	TRIAL 3
9160A	F	x	x	x	x	x	x	x	x	x	x	x	x
9184A	G	x	x	x	x	x	x	x	x	x	x	x	x
9250A	H	x	x	x	x	x	x	x	x	x	x	x	x
9824A	I	x	x	x	x	x	x	x	x	x	x	x	x
9773A	J	x	x	x	x	x	x	x	x	x	x	x	x

(d)

	Plaster												
	MIX	TRIAL 1			TRIAL 2			TRIAL 3			OPT GRADE		
	NA	5.3%	5.8%	6.3%	5.3%	5.8%	6.3%	5.3%	5.8%	6.3%	TRIAL 1	TRIAL 2	TRIAL 3
9160A	F	x	x	x	x	x	x	x	x	x	x	x	x
9184A	G	x	x	x	x	x	x	x	x	x	x	x	x
9250A	H	x	x	x	x	x	x	x	x	x	x	x	x
9824A	I	x	x	x	x	x	x	x	x	x	x	x	x
9773A	J	x	x	x	x	x	x	x	x	x	x	x	x

(e)

	Image with plaster												
	MIX	TRIAL 1			TRIAL 2			TRIAL 3			OPT GRADE		
	NA	5.3%	5.8%	6.3%	5.3%	5.8%	6.3%	5.3%	5.8%	6.3%	TRIAL 1	TRIAL 2	TRIAL 3
9160A	F	x	x	x	x	x	x	x	x	x	x	x	x
9184A	G	x	x	x	x	x	x	x	x	x	x	x	x
9250A	H	x	x	x	x	x	x	x	x	x	x	x	x
9824A	I	x	x	x	x	x	x	x	x	x	x	x	x
9773A	J	x	x	x	x	x	x	x	x	x	x	x	x

Table B3 Tracking of experimental process for oolitic 87339 mix designs.

(a)

	Batch												
		TRIAL 1			TRIAL 2			TRIAL 3			OPT GRADE		
MIX # /NAME		5.8%	6.3%	6.8%	5.8%	6.3%	6.8%	5.8%	6.3%	6.8%	TRIAL 1	TRIAL 2	TRIAL 3
9138A	M	x	x	x	x	x	x	x	x	x	x	x	x
9139A	N	x	x	x	x	x	x	x	x	x	x	x	x
9400A	L	x	x	x	x	x	x	x	x	x	x	x	x
9469A	O	x	x	x	x	x	x	x	x	x	x	x	x
10134A	P	x	x	x	x	x	x	x	x	x	x	x	x
9126A	K	x	x	x	x	x	x	x	x	x	x	x	x

(b) Pie

	MIX	TRIAL 1			TRIAL 2			TRIAL 3			OPT GRADE pies		
	NAME	5.8%	6.3%	6.8%	5.8%	6.3%	6.8%	5.8%	6.3%	6.8%	TRIAL 1	TRIAL 2	TRIAL 3
9138A	M	x	x	x	x	x	x	x	x	x	x	x	x
9139A	N	x	x	x	x	x	x	x	x	x	x	x	x
9400A	L	x	x	x	x	x	x	x	x	x	x	x	x
9469A	O	x	x	x	x	x	x	x	x	x	x	x	x
10134A	P	x	x	x	x	x	x	x	x	x	x	x	x
9126A	K	x	x	x	x	x	x	x	x	x	x	x	x

(c) Plaster

	MIX	TRIAL 1			TRIAL 2			TRIAL 3			OPT GRADE		
	NAME	5.8%	6.3%	6.8%	5.8%	6.3%	6.8%	5.8%	6.3%	6.8%	TRIAL 1	TRIAL 2	TRIAL 3
9138A	M	x	x	x	x	x	x	x	x	x	x	x	x
9139A	N	x	x	x	x	x	x	x	x	x	x	x	x
9400A	L	x	x	x	x	x	x	x	x	x	x	x	x
9469A	O	x	x	x	x	x	x	x	x	x	X	x	x
10134A	P	x	x	x	x	x	x	x	x	x	x	x	x
9126A	K	x	x	x	x	x	x	x	x	x	x	x	x

(d) Image before plaster

	MIX	TRIAL 1			TRIAL 2			TRIAL 3			OPT GRADE		
	NAME	5.8%	6.3%	6.8%	5.8%	6.3%	6.8%	5.8%	6.3%	6.8%	TRIAL 1	TRIAL 2	TRIAL 3
9138A	M										x	x	x
9139A	N										x	x	x
9400A	L												
9469A	O							x	x	x	X	x	x
10134A	P										x	x	x
9126A	K										x	x	x

(e) Image with plaster

	MIX	TRIAL 1			TRIAL 2			TRIAL 3			OPT GRADE		
	NAME	5.8%	6.3%	6.8%	5.8%	6.3%	6.8%	5.8%	6.3%	6.8%	TRIAL 1	TRIAL 2	TRIAL 3
9138A	M	x	x	x	x	x	x	x	x	x	x	x	x
9139A	N	x	x	x	x	x	x	x	x	x	x	x	x
9400A	L	x	x	x	x	x	x	x	x	x	x	x	x
9469A	O	x	x	x	x	x	x	x	x	x	x	x	x
10134A	P	x	x	x	x	x	x	x	x	x	x	x	x
9126A	K	x	x	x	x	x	x	x	x	x	x	x	x

Table B4 Tracking of experimental process for oolitic 87145 mix designs.

(a)

	Batch											
MIX # /NAME		TRIAL 1			TRIAL 2			TRIAL 3			OPT GRADE		
		5.8%	6.3%	6.8%	5.8%	6.3%	6.8%	5.8%	6.3%	6.8%	TRIAL 1	TRIAL 2	TRIAL 3
6954A	Q	x	x	x	x	x	x	x	x	x	x	x	x
7806A	R	x	x	x	x	x	x	x	x	x	x	x	x
9932A	S	x	x	x	x	x	x	x	x	x	x	x	x

(b)

	Pie											
	MIX NAME	TRIAL 1			TRIAL 2			TRIAL 3			OPT GRADE		
		5.8%	6.3%	6.8%	5.8%	6.3%	6.8%	5.8%	6.3%	6.8%	TRIAL 1	TRIAL 2	TRIAL 3
6954A	Q	x	x	x	x	x	x	x	x	x	x	x	x
7806A	R	x	x	x	x	x	x	x	x	x	x	x	x
9932A	S	x	x	x	x	x	x	x	x	x	x	x	x

(c)

Image without plaster												
	MIX	TRIAL 1			TRIAL 2			TRIAL 3			OPT GRADE		
	NAME	5.3%	5.8%	6.3%	5.3%	5.8%	6.3%	5.3%	5.8%	6.3%	TRIAL 1	TRIAL 2	TRIAL 3
6954A	Q	x	x	x	x	x	x	x	x	x	x	x	x
7806A	R	x	x	x	x	x	x	x	x	x	x	x	x
9932A	S	x	x	x	x	x	x	x	x	x	x	x	x

(d)

	Plaster											
	MIX	TRIAL 1			TRIAL 2			TRIAL 3			OPT GRADE		
	NAME	5.8%	6.3%	6.8%	5.8%	6.3%	6.8%	5.8%	6.3%	6.8%	TRIAL 1	TRIAL 2	TRIAL 3
6954A	Q	x	x	x	x	x	x	x	x	x	x	x	x
7806A	R	x	x	x	x	x	x	x	x	x	x	x	x
9932A	S	x	x	x	x	x	x	x	x	x	x	x	x

(e)

Image with plaster												
	MIX	TRIAL 1			TRIAL 2			TRIAL 3			OPT GRADE		
	NAME	5.3%	5.8%	6.3%	5.3%	5.8%	6.3%	5.3%	5.8%	6.3%	TRIAL 1	TRIAL 2	TRIAL 3
6954A	Q	x	x	x	x	x	x	x	x	x	x	x	x
7806A	R	x	x	x	x	x	x	x	x	x	x	x	x
9932A	S	x	x	x	x	x	x	x	x	x	x	x	x

APPENDIX C: DETERMINATION OF OBC TEST FOR OGFC MIXTURES

Florida Method of Test
for
DETERMINING THE OPTIMUM ASPHALT BINDER CONTENT OF AN OPEN–GRADED FRICTION COURSE MIXTURE USING THE PIE PLATE METHOD

Designation: FM 5-588

1. SCOPE

1.1 This method covers the determination of the optimum asphalt binder content in open-graded friction course mixtures using the pie plate method.

2. REFERENCED DOCUMENTS

2.1 Florida Department of Transportation Specifications:

Section 901
Section 902
Section 916

2.2 AASHTO Specification:

M 231, Weighing Devices Used in the Testing of Materials

2.3 Florida Methods of Test:

FM 5-563, Quantitative Determination of Asphalt Content from Asphalt Paving Mixtures by the Ignition Method

3. APPARATUS

3.1 Oven – An oven of sufficient size capable of maintaining the required temperature up to 320 ± 5°F (160 ± 3°C).

3.2 Balance – A balance conforming to the requirements of AASHTO M 231, Class G2. Balances with a greater degree of accuracy may be used.

3.3 No. 4 Sieve – An 8 or 12 in. diameter sieve used to break up fiber conglomerates.

3.4 Mixing Bowl – A "buttered" metal bowl of sufficient capacity to allow hand mixing the aggregate, asphalt binder, and fibers.

3.5 Spatula – A clean spatula capable of hand mixing the aggregate, asphalt binder, and fibers.

3.6 Pie Plate – A clear, 9 in., flat-bottomed heat resistant pie plate, in which the mixture will be placed, to determine optimum asphalt binder content. Pyrex brand pie plates have been found to meet these requirements.

3.7 Digital Camera – A camera with suitable resolution to photograph the bottom of the pie plate after the mixture has cooled. The photographs will be used to record the appearance of the bottom of the pie plate at each asphalt binder content.

4. MATERIALS

4.1 Aggregates, Hydrated Lime, and Fiber Stabilizing Additive – As defined in Section 337 of the Department's Specifications.

4.2 Asphalt Binder – Use PG 67-22 asphalt binder as defined in Section 916 of the Department's Specifications to determine the optimum asphalt binder content. Use the asphalt binder type specified on the mix design to determine the asphalt binder calibration factor in accordance with FM 5-563.

5. DETERMINATION OF OPTIMUM ASPHALT BINDER CONTENT

5.1 Develop an aggregate blend meeting the gradation and component requirements of Section 337 of the Department's Specifications.

5.2 Determine the amount of fiber material using the following calculations:

Percent Mineral Fibers = (A ÷ 0.996) - A

Percent Cellulose Fibers = (A ÷ 0.997) - A

Where:

A = Total weight of aggregate and binder

5.3 Break up any large conglomerates of fibers using the No. 4 sieve.

5.4 Prepare three 1200 g aggregate batches. Add the hydrated lime additive (if required) and the fiber material into the aggregate batches. Ensure that the fiber material is distributed evenly throughout the aggregate batch. Place each batch in a mixing bowl.

5.5 Heat the aggregate batches and the asphalt binder for a minimum of two hours in an oven at 320 ± 5°F (160 ± 3°C).

5.6 Using the spatula, gently mix the aggregate batch and asphalt binder in the mixing bowl at the following three prescribed asphalt binder contents (by weight of total mix): 5.3%, 5.8%, and 6.3% for granite aggregate or 5.8%, 6.3%, and 6.8% for limestone aggregate. Continue mixing until all of the aggregate particles are thoroughly coated, ensuring that there are no large conglomerates of fine particles.

5.7 Immediately after mixing, carefully transfer the mixture from the mixing bowl into a pie plate using a method that will evenly distribute the mixture over the entire bottom surface of the pie plate without causing segregation. Care should be taken to ensure that the mixture is not disturbed once it has contacted the pie plate. After placing the mixture in the pie plate, place the pie plate on a level surface in an oven and heat for one hour at 320 ± 5°F (160 ± 3°C). Repeat this step for each of the remaining samples.

5.8 After the one hour heating period, carefully remove the pie plate from the oven, place it on a heat resistant surface and allow it to cool undisturbed until it reaches room temperature.

5.9 After all of the mixtures have cooled to room temperature, invert the pie plates and inspect the bottom surfaces. Determine the optimum asphalt binder content based on the sample which displays sufficient bonding between the mixture and the bottom of the pie plate without evidence of excessive asphalt binder drainage (see Figures 1, 2, and 3). The optimum asphalt binder content may be one of the three trial asphalt binder contents or may be estimated to be higher or lower than one of the three trial asphalt binder contents. Additional samples may be prepared, at different asphalt binder contents, if necessary.

NOTE: The optimum asphalt binder content should exhibit slight drainage of

asphalt binder at points of contact between the coated aggregate particles and the glass plate.

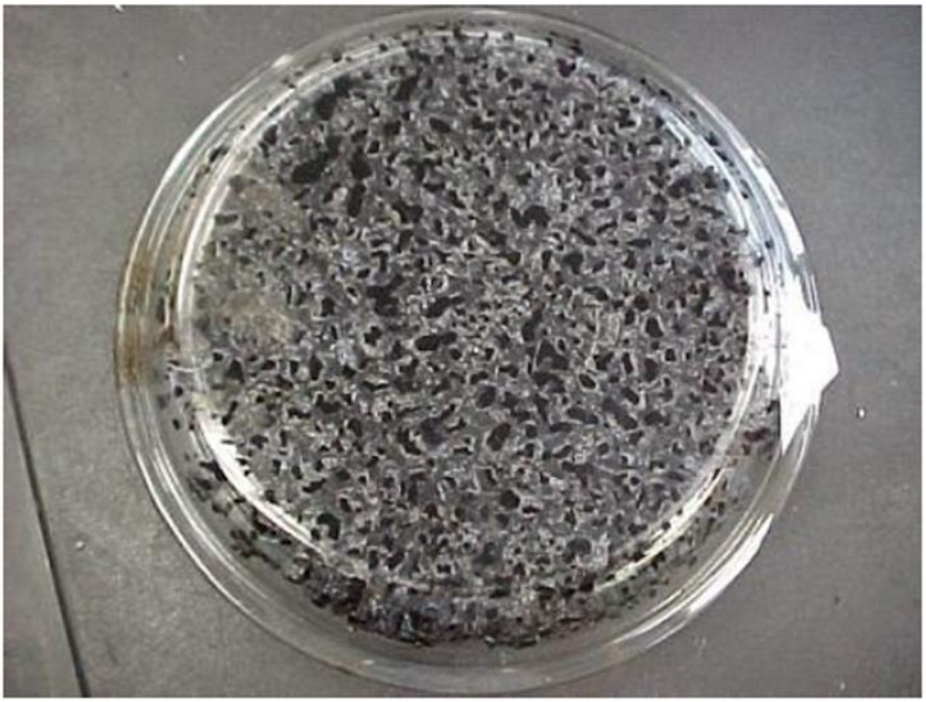

FIGURE 1
FC-5 @ 5.3% asphalt binder
Insufficient bonding/drainage – asphalt binder content too low

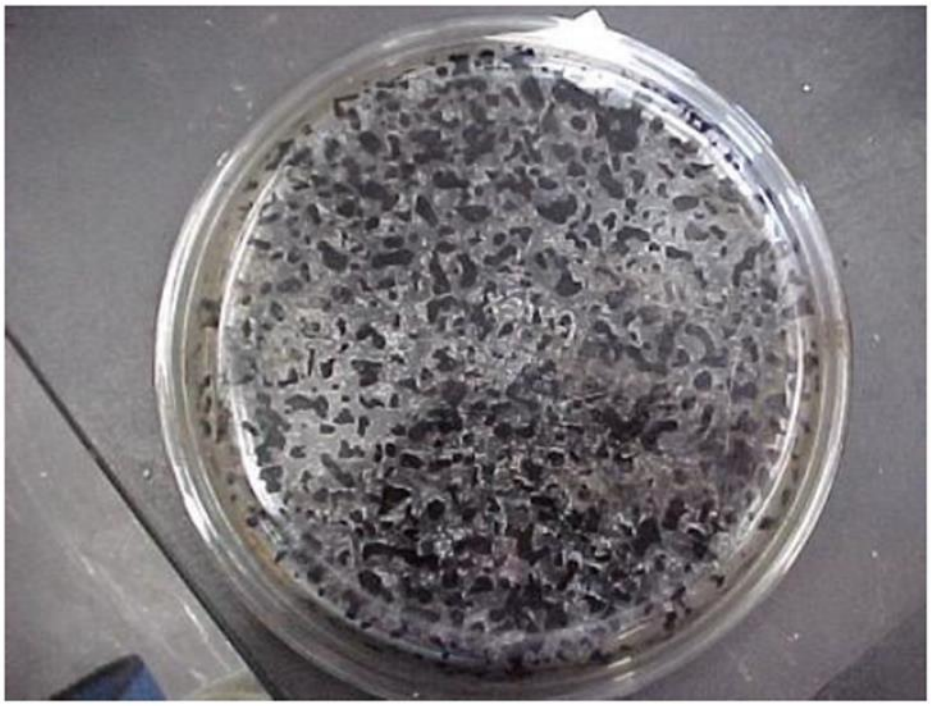

FIGURE 2
FC-5 @ 5.8% asphalt binder
Sufficient bonding/drainage – optimum asphalt binder content

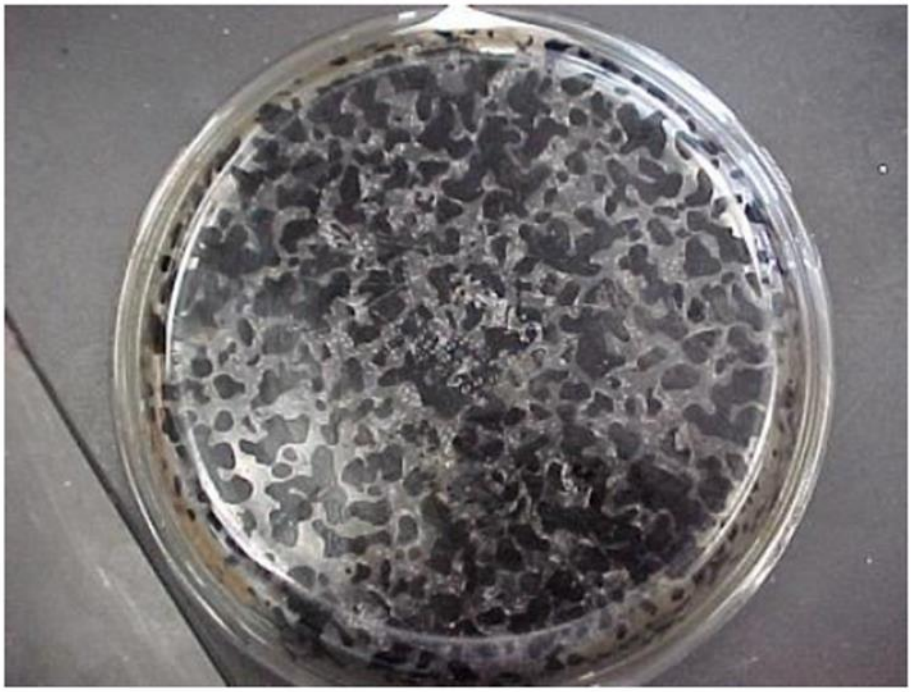

FIGURE 3
FC-5 @ 6.3% asphalt binder
Excessive bonding/drainage – asphalt binder content too high

5.10 Photograph the bottom of each pie plate for documentation.

NOTE: If PG 76-22 asphalt binder is required, the total asphalt binder content will be the same as the original asphalt binder content determined using PG 67-22 asphalt binder. If ARB-12 asphalt rubber binder is required, the total asphalt binder content must be increased to include the percent of rubber by weight of optimum asphalt binder using the following calculation:

Total ARB-12 content = PG 67-22 optimum asphalt binder content x 1.12

6. DETERMINATION OF ASPHALT BINDER CALIBRATION FACTOR

6.1 Prepare two 1500 g aggregate batches. Include the hydrated lime additive (if required) and the fiber material into the aggregate batches. Place each batch in a mixing bowl.

6.2 Heat the aggregate batches and the required asphalt binder (PG 76-22 or ARB-12) for a minimum of two hours in an oven at 320 ± 5°F (160 ± 3°C).

6.3 Using a spatula, gently mix the aggregate batch and asphalt binder in the mixing bowl. Continue mixing until all of the aggregate particles are thoroughly coated.

6.4 Determine the asphalt binder calibration factor in accordance with FM 5-563.

APPENDIX D: GENERAL INFORMATION BY MIX

D.1 General Information of Mix A

Table D1 Aggregate and binder type for mix A.

Mix ID	Mix A
Aggregate Type	Granite
Quarry Location	Nova Scotia
Supplier	Martin Marietta
FDOT designation No.	9165A
FDOT code	NS315
Binder Grade	PG 67-22

Table D2 FDOT OGFC gradation specifications for mix A.

Sieve Size	GRANITIC NS315 FDOT mix design number 9165A Percent Pasing (%) MIX A	CONTROL POINTS		
3/4" 19.0mm	100		100	
1/2" 12.5mm	95	85	_	100
3/8" 9.5mm	74	55	_	75
No. 4 4.75mm	20	15	_	25
No. 8 2.36mm	8	5	_	10
No. 16 1.18mm	6			
No. 30 600µm	4			
No. 50 300µm	4			
No. 100 150µm	4			
No. 200 75µm	3.40	2	_	4
GSB	2.624			

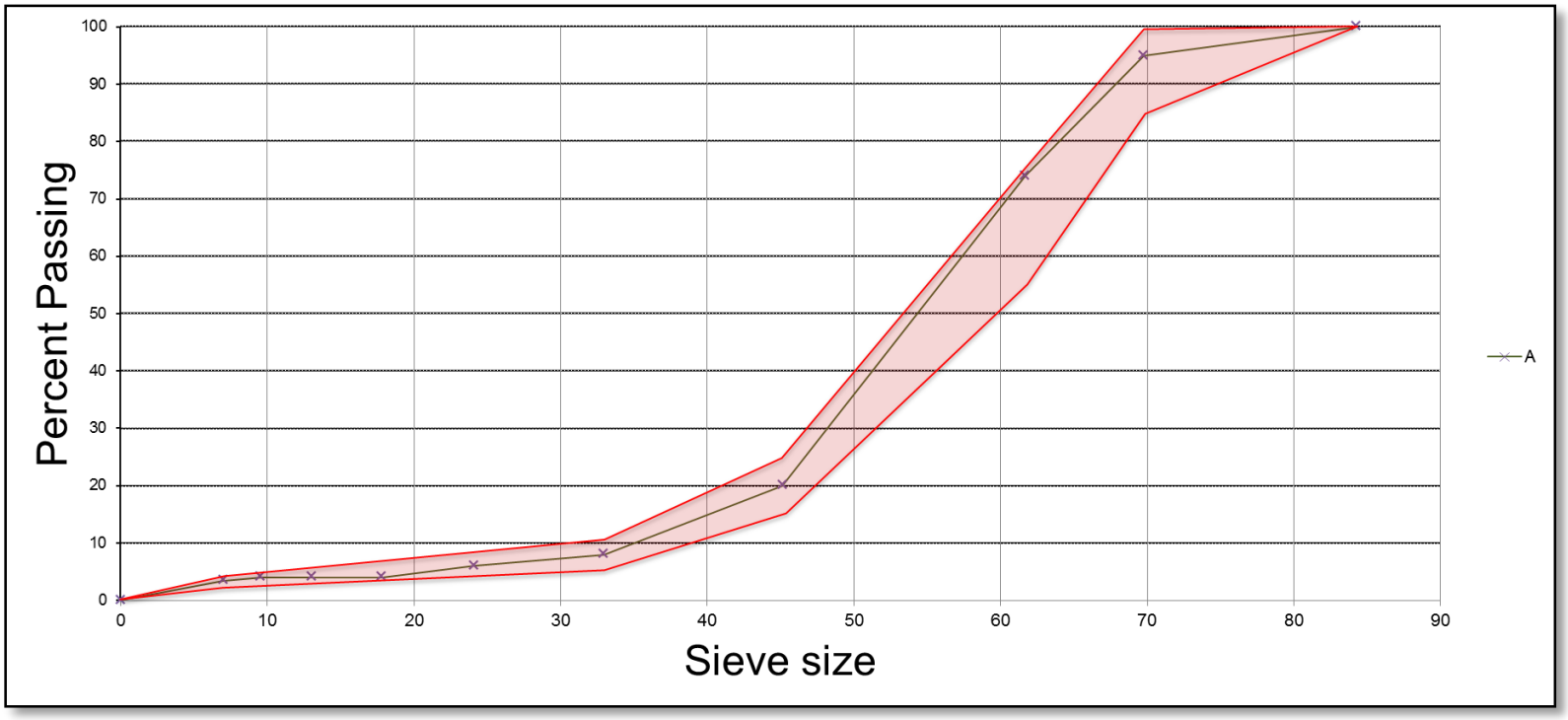

Figure D1 Gradation curves for mix A.

D.2 General Information of Mix B

Table D3 Aggregate and binder type for mix B.

Mix ID	Mix B
Aggregate Type	Granite
Quarry Location	Nova Scotia
Supplier	Martin Marietta
FDOT designation No.	9476A
FDOT code	NS315
Binder Grade	PG 67-22

Table D4 FDOT OGFC gradation specifications for mix B.

Sieve Size	GRANITIC NS315 FDOT mix design number 9476A Percent Pasing (%) MIX B	CONTROL POINTS		
3/4" 19.0mm	100		100	
1/2" 12.5mm	96	85	_	100
3/8" 9.5mm	70	55	_	75
No. 4 4.75mm	23	15	_	25
No. 8 2.36mm	10	5	_	10
No. 16 1.18mm	5			
No. 30 600µm	4			
No. 50 300µm	3			
No. 100 150µm	3			
No. 200 75µm	2.50	2	_	4
GSB	2.677			

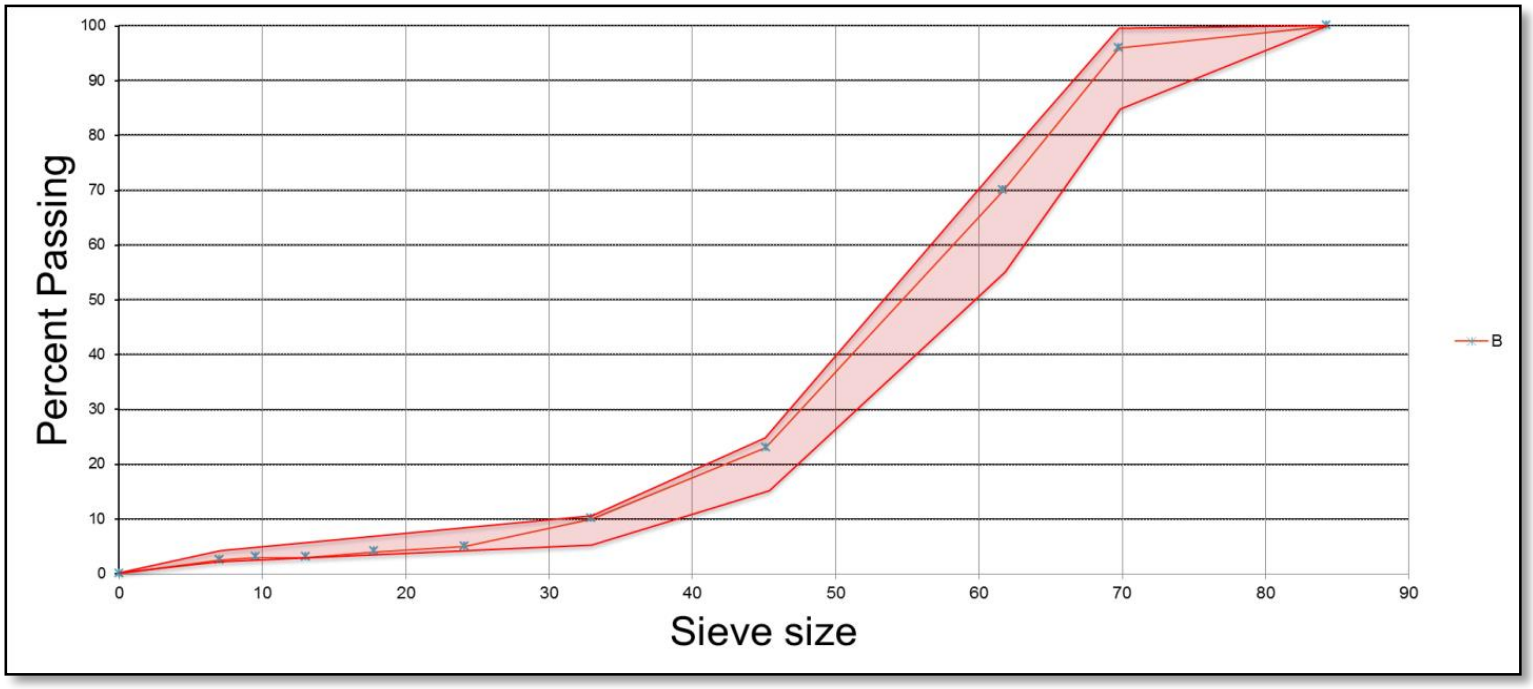

Figure D2 Gradation curves for mix B.

D.3 General Information of Mix C

Table D5 Aggregate and binder type for mix C.

Mix ID	Mix C
Aggregate Type	Granite
Quarry Location	Nova Scotia
Supplier	Martin Marietta
FDOT designation No.	9642A
FDOT code	NS315
Binder Grade	PG 67-22

Table D6 FDOT OGFC gradation specifications for mix C.

Sieve Size	GRANITIC NS315 FDOT mix design number 9642A Percent Pasing (%) MIX C	CONTROL POINTS		
3/4" 19.0mm	100		100	
1/2" 12.5mm	96	85	_	100
3/8" 9.5mm	71	55	_	75
No. 4 4.75mm	15	15	_	25
No. 8 2.36mm	8	5	_	10
No. 16 1.18mm	6			
No. 30 600µm	5			
No. 50 300µm	4			
No. 100 150µm	3			
No. 200 75µm	2.30	2	_	4
GSB	2.626			

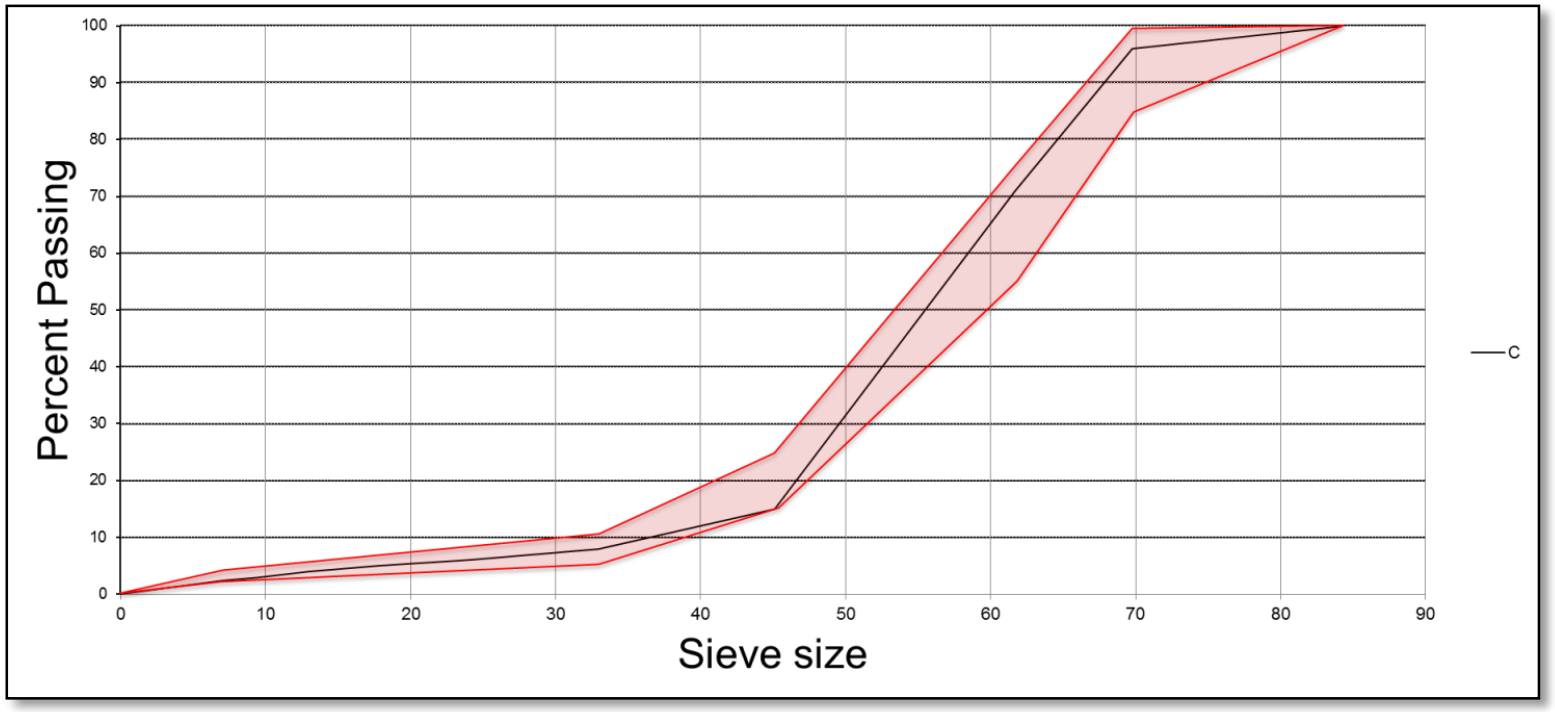

Figure D3 Gradation curves for mix C.

D.4 General Information of Mix D

Table D7 Aggregate and binder type for mix D.

Mix ID	Mix D
Aggregate Type	Granite
Quarry Location	Nova Scotia
Supplier	Martin Marietta
FDOT designation No.	9646A
FDOT code	NS315
Binder Grade	PG 67-22

Table D8 FDOT OGFC gradation specifications for mix D.

Sieve Size	GRANITIC NS315 FDOT mix design number 9646A Percent Pasing (%) MIX D	CONTROL POINTS		
3/4" 19.0mm	100		100	
1/2" 12.5mm	96	85	_	100
3/8" 9.5mm	71	55	_	75
No. 4 4.75mm	15	15	_	25
No. 8 2.36mm	8	5	_	10
No. 16 1.18mm	6			
No. 30 600µm	5			
No. 50 300µm	4			
No. 100 150µm	3			
No. 200 75µm	2.30	2	_	4
GSB	2.627			

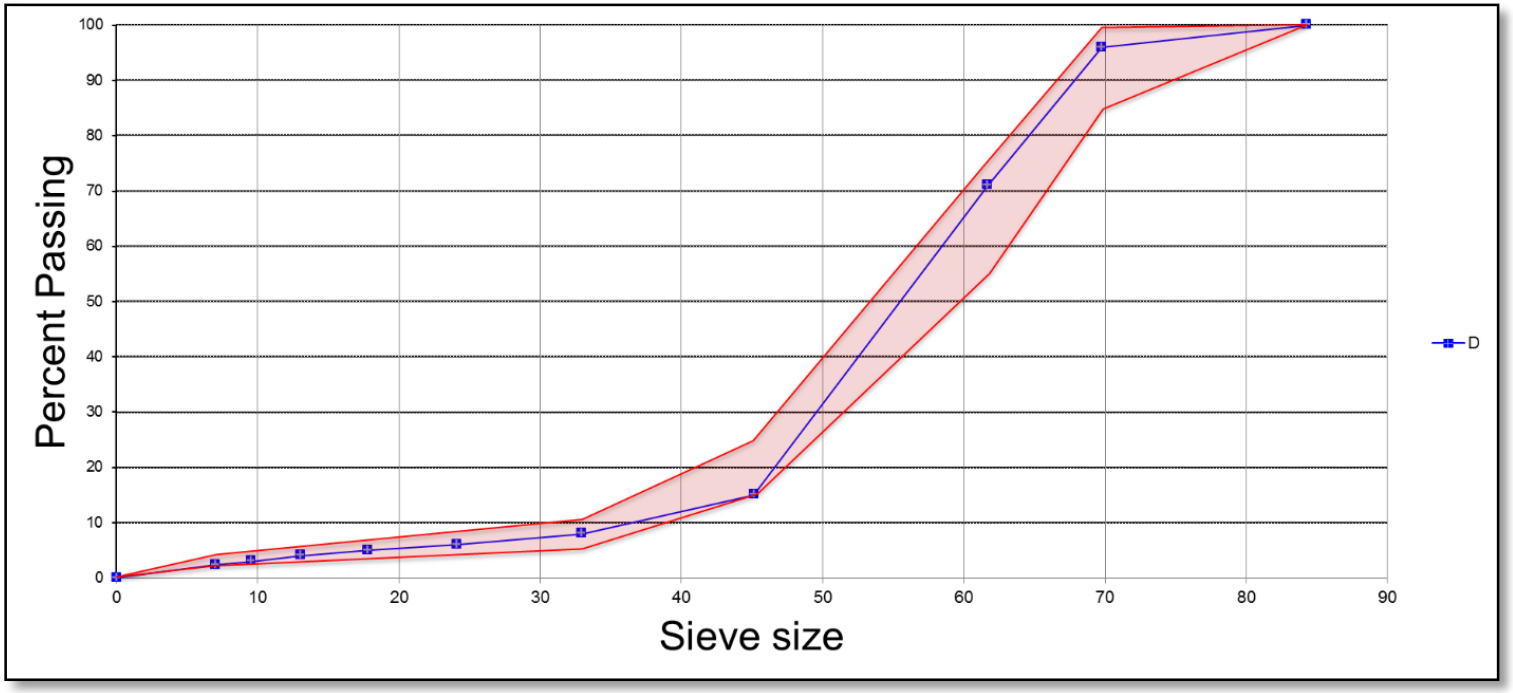

Figure D4 Gradation curves for mix D.

D.5 General Information of Mix E

Table D9 Aggregate and binder type for mix E.

Mix ID	Mix E
Aggregate Type	Granite
Quarry Location	Nova Scotia
Supplier	Martin Marietta
FDOT designation No.	9657A
FDOT code	NS315
Binder Grade	PG 67-22

Table D10 FDOT OGFC gradation specifications for mix E.

Sieve Size	GRANITIC NS315 FDOT mix design number 9657A Percent Pasing (%) MIX E	CONTROL POINTS		
3/4" 19.0mm	100		100	
1/2" 12.5mm	85	85	_	100
3/8" 9.5mm	67	55	_	75
No. 4 4.75mm	23	15	_	25
No. 8 2.36mm	10	5	_	10
No. 16 1.18mm	6			
No. 30 600µm	4			
No. 50 300µm	3			
No. 100 150µm	3			
No. 200 75µm	2.50	2	_	4
GSB	2.630			

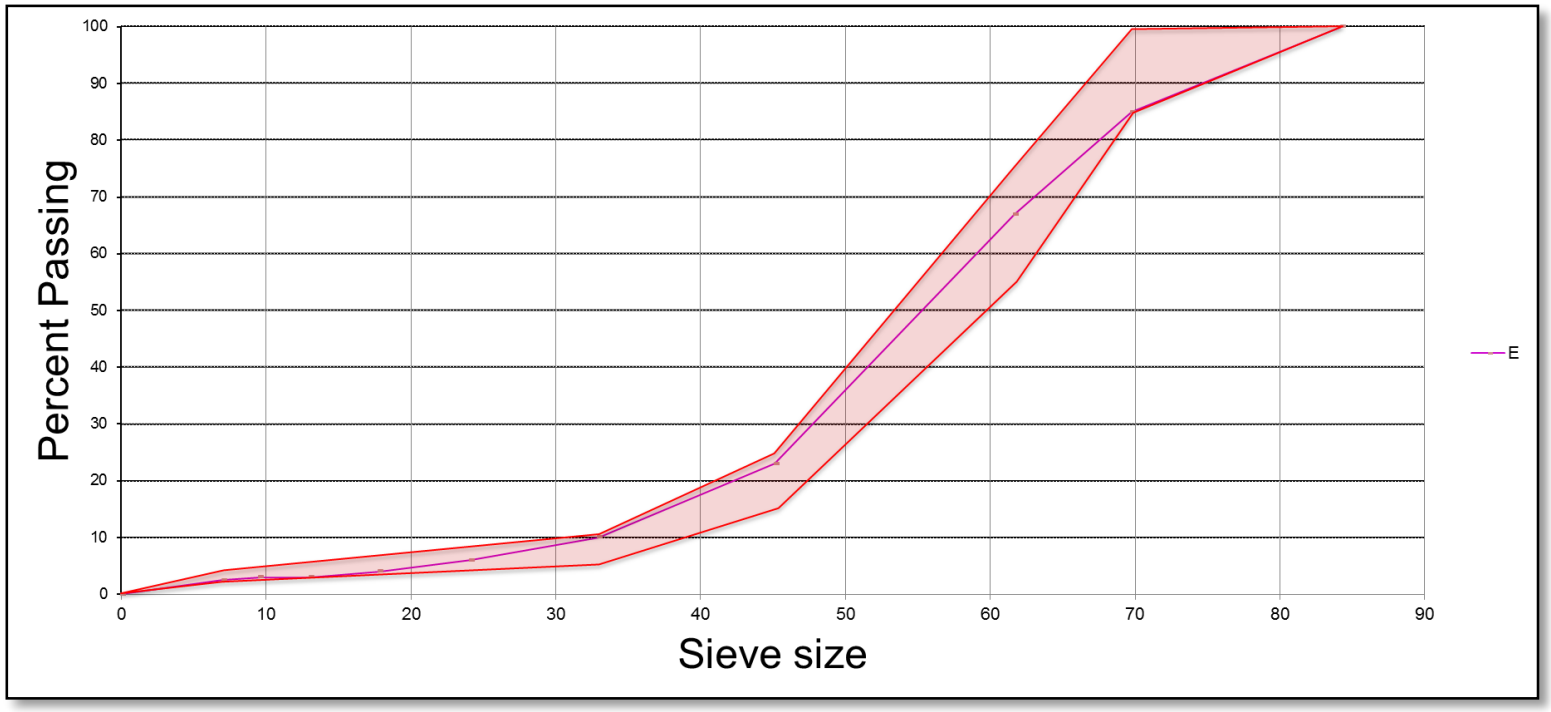

Figure D5 Gradation curves for mix E.

D.6 General Information of Mix F

Table D11 Aggregate and binder type for mix F.

Mix ID	Mix F
Aggregate Type	Granite
Quarry Location	Georgia
Supplier	Junction City
FDOT designation No.	9160A
FDOT code	GA553
Binder Grade	PG 67-22

Table D12 FDOT OGFC gradation specifications for mix F.

Sieve Size	GRANITIC GA553 FDOT mix design number 9160A Percent Pasing (%) MIX F	CONTROL POINTS		
3/4" 19.0mm	100		100	
1/2" 12.5mm	100	85	_	100
3/8" 9.5mm	74	55	_	75
No. 4 4.75mm	23	15	_	25
No. 8 2.36mm	9	5	_	10
No. 16 1.18mm	6			
No. 30 600µm	4			
No. 50 300µm	3			
No. 100 150µm	3			
No. 200 75µm	2.70	2	_	4
GSB	2.767			

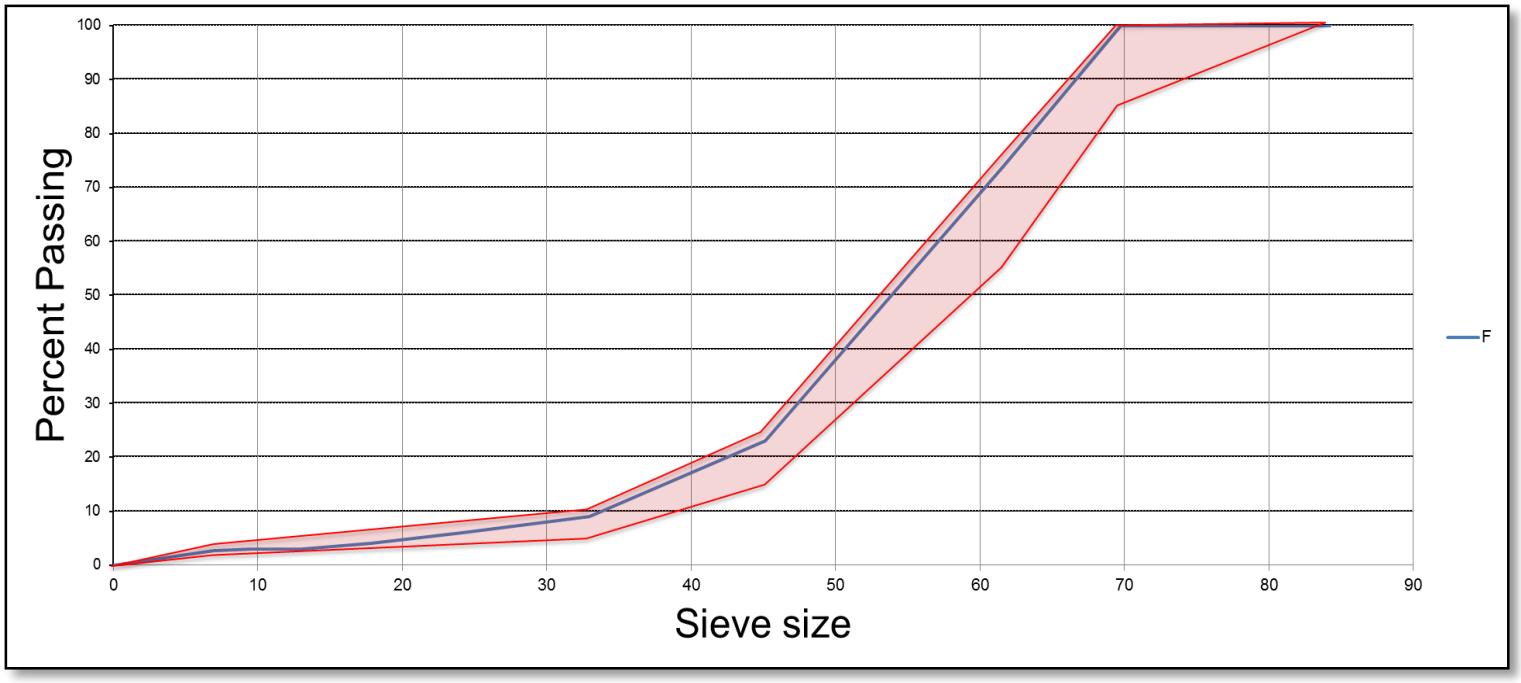

Figure D6 Gradation curves for mix F.

D.7 General Information of Mix G

Table D13 Aggregate and binder type for mix G.

Mix ID	Mix G
Aggregate Type	Granite
Quarry Location	Georgia
Supplier	Junction City
FDOT designation No.	9184A
FDOT code	GA553
Binder Grade	PG 67-22

Table D14 FDOT OGFC gradation specifications for mix G.

Sieve Size	GRANITIC GA553 FDOT mix design number 9184A Percent Pasing (%) MIX G	CONTROL POINTS		
3/4" 19.0mm	100		100	
1/2" 12.5mm	97	85	_	100
3/8" 9.5mm	75	55	_	75
No. 4 4.75mm	23	15	_	25
No. 8 2.36mm	9	5	_	10
No. 16 1.18mm	6			
No. 30 600µm	5			
No. 50 300µm	5			
No. 100 150µm	4			
No. 200 75µm	2.50	2	_	4
GSB	2.769			

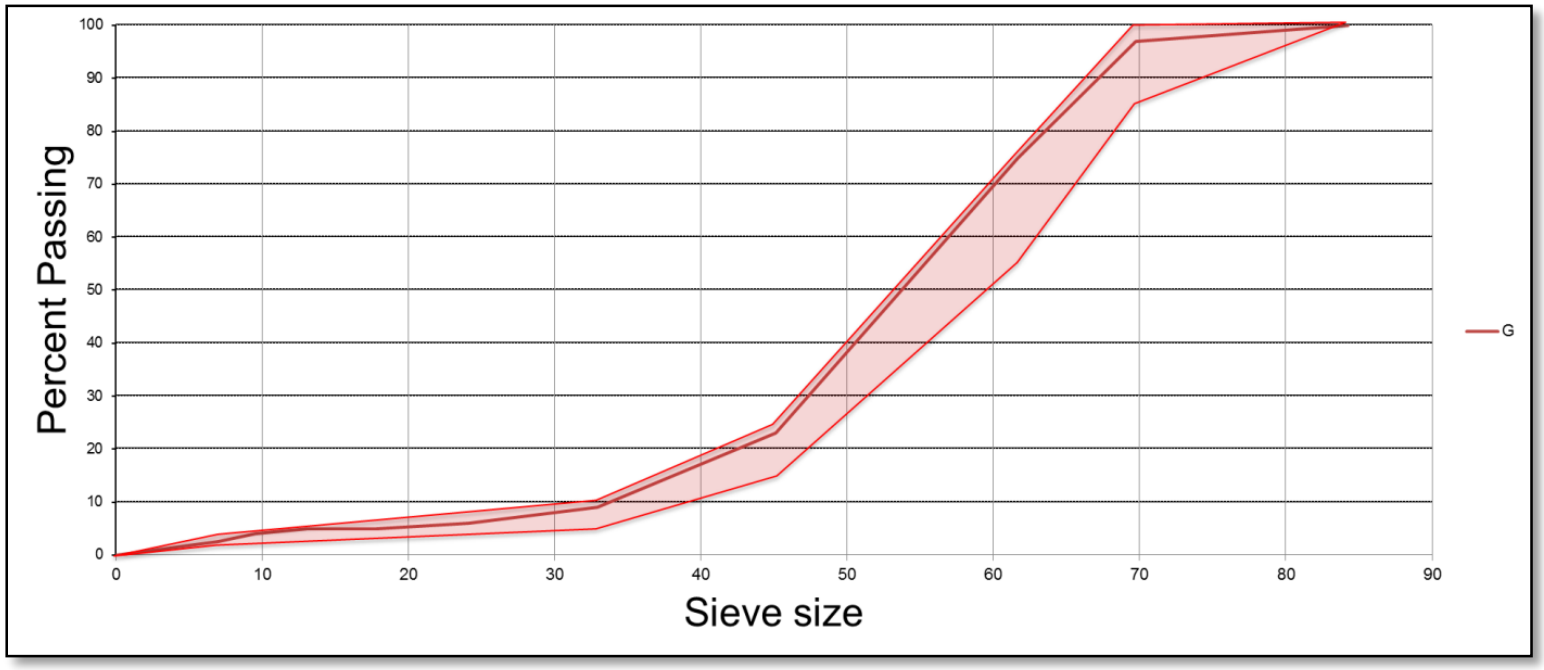

Figure D7 Gradation curves for mix G.

D.8 General Information of Mix H

Table D15 Aggregate and binder type for mix H.

Mix ID	Mix H
Aggregate Type	Granite
Quarry Location	Georgia
Supplier	Junction City
FDOT designation No.	9250A
FDOT code	GA553
Binder Grade	PG 67-22

Table D16 FDOT OGFC gradation specifications for mix H.

Sieve Size	GRANITIC GA553 FDOT mix design number 9250A Percent Pasing (%) MIX H	CONTROL POINTS		
3/4" 19.0mm	100		100	
1/2" 12.5mm	94	85	_	100
3/8" 9.5mm	68	55	_	75
No. 4 4.75mm	19	15	_	25
No. 8 2.36mm	8	5	_	10
No. 16 1.18mm	6			
No. 30 600µm	4			
No. 50 300µm	3			
No. 100 150µm	3			
No. 200 75µm	2.40	2	_	4
GSB	2.766			

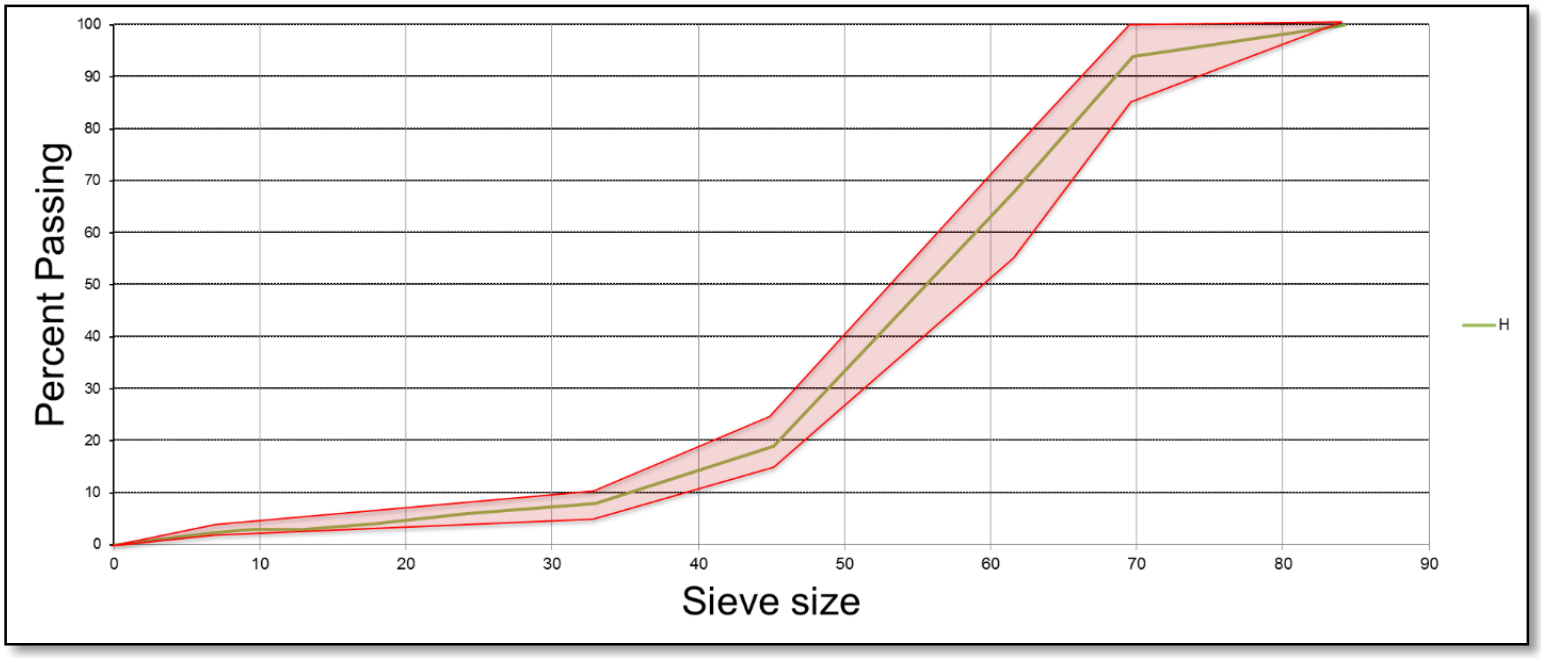

Figure D8 Gradation curves for mix H.

D.9 General Information of Mix I

Table D17 Aggregate and binder type for mix I.

Mix ID	Mix I
Aggregate Type	Granite
Quarry Location	Georgia
Supplier	Junction City
FDOT designation No.	9824A
FDOT code	GA553
Binder Grade	PG 67-22

Table D18 FDOT OGFC gradation specifications for mix I.

Sieve Size	GRANITIC GA553 FDOT mix design number 9824A Percent Pasing (%) MIX I	CONTROL POINTS		
3/4" 19.0mm	100		100	
1/2" 12.5mm	97	85	_	100
3/8" 9.5mm	66	55	_	75
No. 4 4.75mm	20	15	_	25
No. 8 2.36mm	9	5	_	10
No. 16 1.18mm	7			
No. 30 600µm	4			
No. 50 300µm	3			
No. 100 150µm	3			
No. 200 75µm	2.90	2	_	4
GSB	2.768			

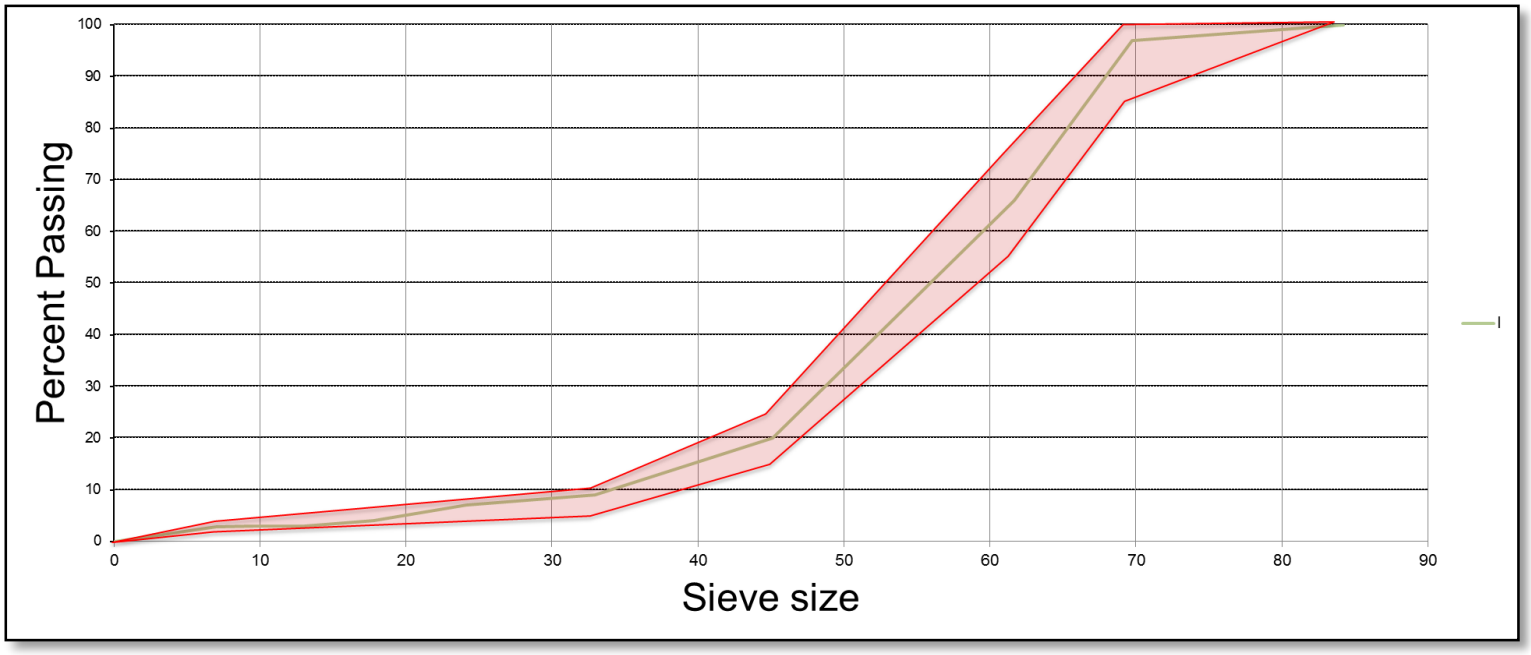

Figure D9 Gradation curves for mix I.

D.10 General Information of Mix J

Table D19 Aggregate and binder type for mix J.

Mix ID	Mix J
Aggregate Type	Granite
Quarry Location	Georgia
Supplier	Junction City
FDOT designation No.	9773A
FDOT code	GA553
Binder Grade	PG 67-22

Table D20 FDOT OGFC gradation specifications for mix J.

Sieve Size	GRANITIC GA553 FDOT mix design number 9773A Percent Pasing (%) MIX J	CONTROL POINTS		
3/4" 19.0mm	100		100	
1/2" 12.5mm	96	85	_	100
3/8" 9.5mm	67	55	_	75
No. 4 4.75mm	23	15	_	25
No. 8 2.36mm	9	5	_	10
No. 16 1.18mm	5			
No. 30 600µm	4			
No. 50 300µm	3			
No. 100 150µm	3			
No. 200 75µm	2.60	2	_	4
GSB	2.769			

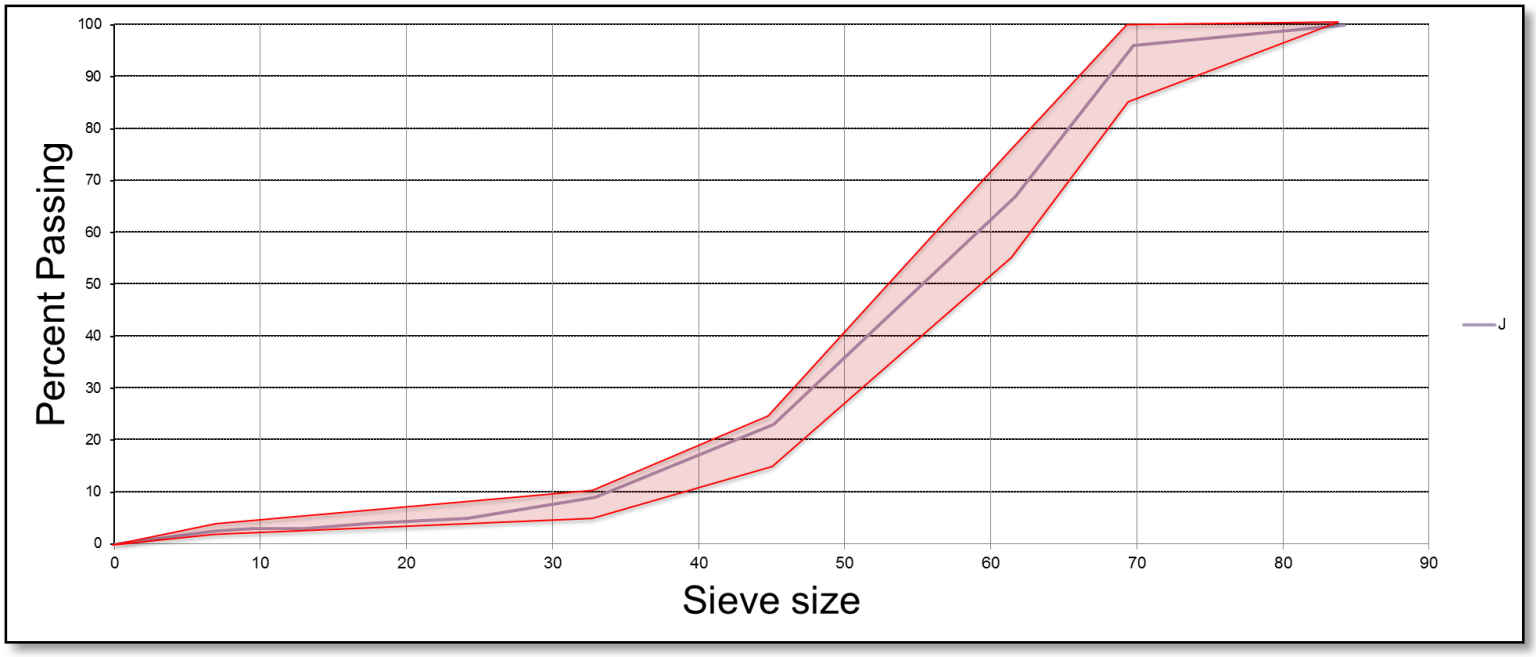

Figure D10 Gradation curves for mix J.

D.11 General Information of Mix K

Table D21 Aggregate and binder type for mix K.

Mix ID	Mix K
Aggregate Type	Oolite
Quarry Location	Miami/Dade
Supplier	White Rock
FDOT designation No.	9126A
FDOT code	87339
Binder Grade	PG 67-22

Table D22 FDOT OGFC gradation specifications for mix K.

Sieve Size	OOLITIC 87339 FDOT mix design number 9126A Percent Pasing (%) MIX K	CONTROL POINTS		
3/4" 19.0mm	100		100	
1/2" 12.5mm	88	85	_	100
3/8" 9.5mm	64	55	_	75
No. 4 4.75mm	20	15	_	25
No. 8 2.36mm	6	5	_	10
No. 16 1.18mm	3			
No. 30 600µm	2			
No. 50 300µm	2			
No. 100 150µm	2			
No. 200 75µm	2.00	2	_	4
GSB	2.415			

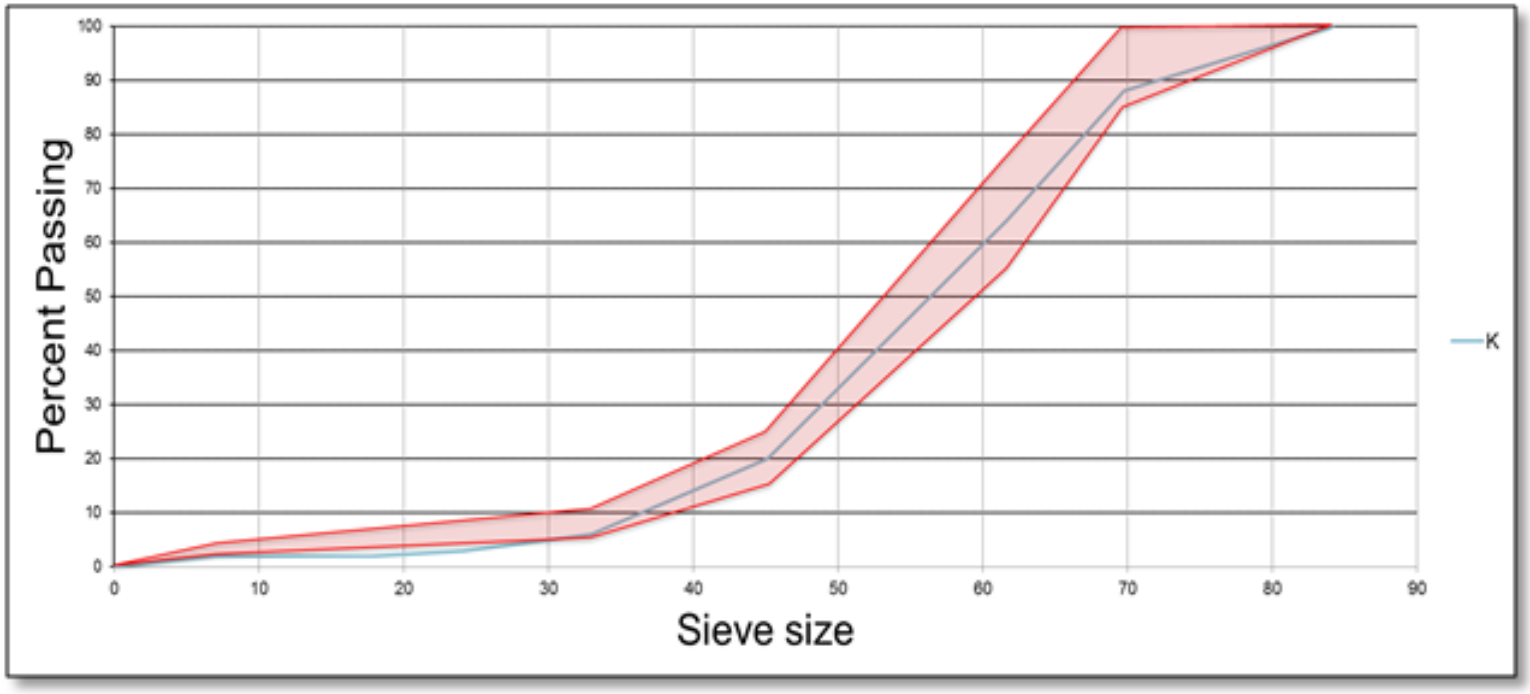

Figure D11 Gradation curves for mix K.

D.12 General Information of Mix L

Table D23 Aggregate and binder type for mix L.

Mix ID	Mix L
Aggregate Type	Oolite
Quarry Location	Miami/Dade
Supplier	White Rock
FDOT designation No.	9400A
FDOT code	87339
Binder Grade	PG 67-22

Table D24 FDOT OGFC gradation specifications for mix L.

Sieve Size	OOLITIC 87339 FDOT mix design number 9400A Percent Pasing (%) MIX L	CONTROL POINTS		
3/4" 19.0mm	100		100	
1/2" 12.5mm	92	85	_	100
3/8" 9.5mm	69	55	_	75
No. 4 4.75mm	24	15	_	25
No. 8 2.36mm	8	5	_	10
No. 16 1.18mm	6			
No. 30 600µm	5			
No. 50 300µm	4			
No. 100 150µm	3			
No. 200 75µm	2.60	2	_	4
GSB	2.415			

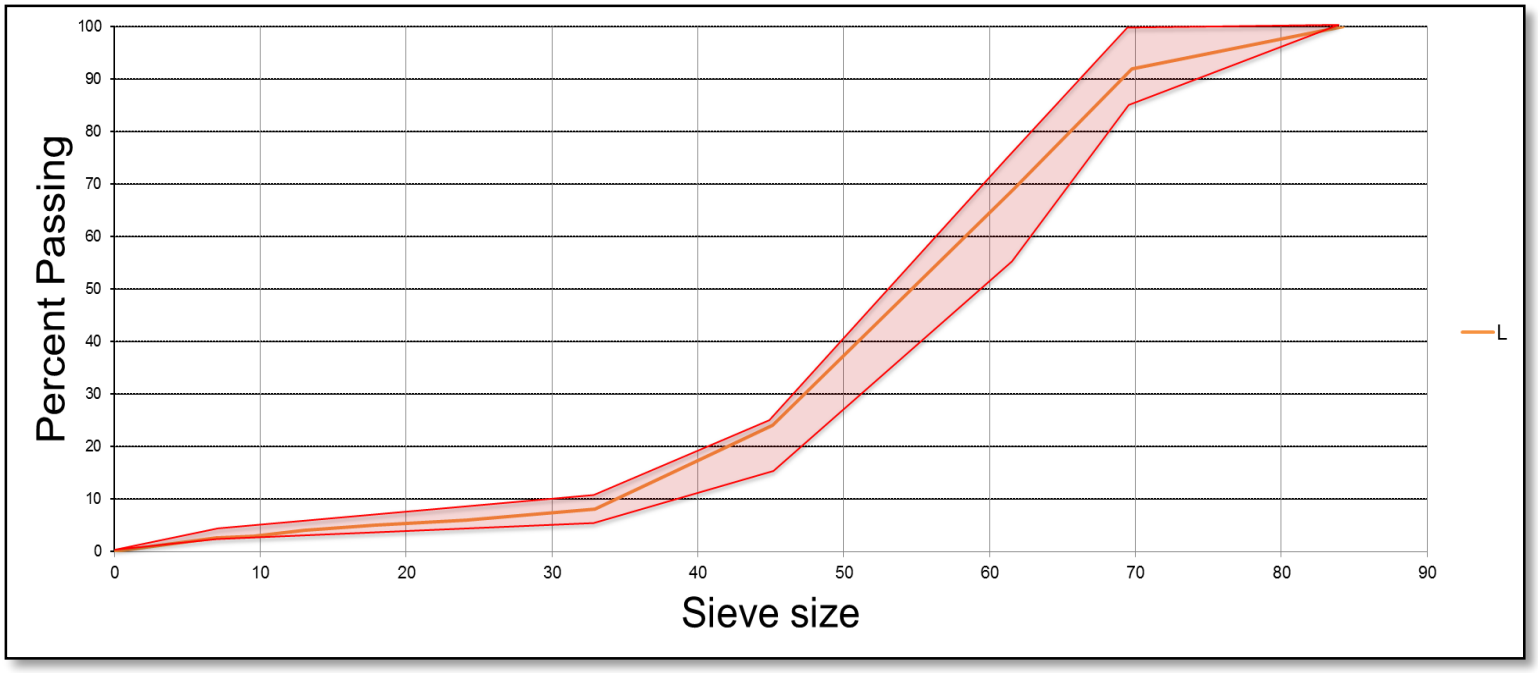

Figure D12 Gradation curves for mix L.

D.13 General Information of Mix M

Table D25 Aggregate and binder type for mix M.

Mix ID	Mix M
Aggregate Type	Oolite
Quarry Location	Miami/Dade
Supplier	White Rock
FDOT designation No.	9138A
FDOT code	87339
Binder Grade	PG 67-22

Table D26 FDOT OGFC gradation specifications for mix M.

Sieve Size	OOLITIC 87339 FDOT mix design number 9138A Percent Pasing (%) MIX M	CONTROL POINTS		
3/4" 19.0mm	100		100	
1/2" 12.5mm	86	85	_	100
3/8" 9.5mm	68	55	_	75
No. 4 4.75mm	24	15	_	25
No. 8 2.36mm	10	5	_	10
No. 16 1.18mm	7			
No. 30 600µm	6			
No. 50 300µm	5			
No. 100 150µm	4			
No. 200 75µm	2.50	2	_	4
GSB	2.409			

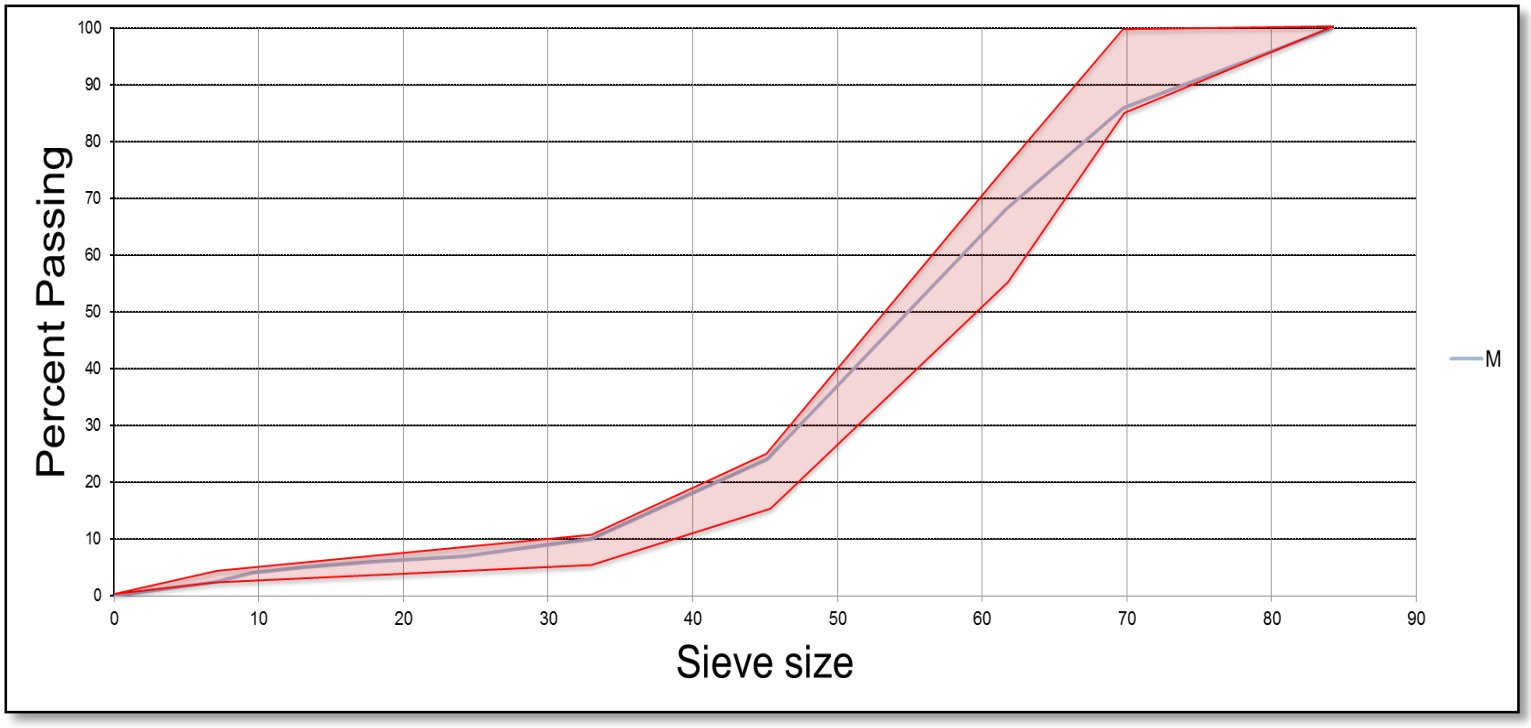

Figure D13 Gradation curves for mix M.

D.14 General Information of Mix N

Table D27 Aggregate and binder type for mix N.

Mix ID	Mix N
Aggregate Type	Oolite
Quarry Location	Miami/Dade
Supplier	White Rock
FDOT designation No.	9139A
FDOT code	87339
Binder Grade	PG 67-22

Table D28 FDOT OGFC gradation specifications for mix N.

Sieve Size	OOLITIC 87339 FDOT mix design number 9139A Percent Pasing (%) MIX N	CONTROL POINTS		
3/4" 19.0mm	100		100	
1/2" 12.5mm	87	85	_	100
3/8" 9.5mm	66	55	_	75
No. 4 4.75mm	25	15	_	25
No. 8 2.36mm	10	5	_	10
No. 16 1.18mm	7			
No. 30 600µm	5			
No. 50 300µm	4			
No. 100 150µm	3			
No. 200 75µm	3.00	2	_	4
GSB	2.410			

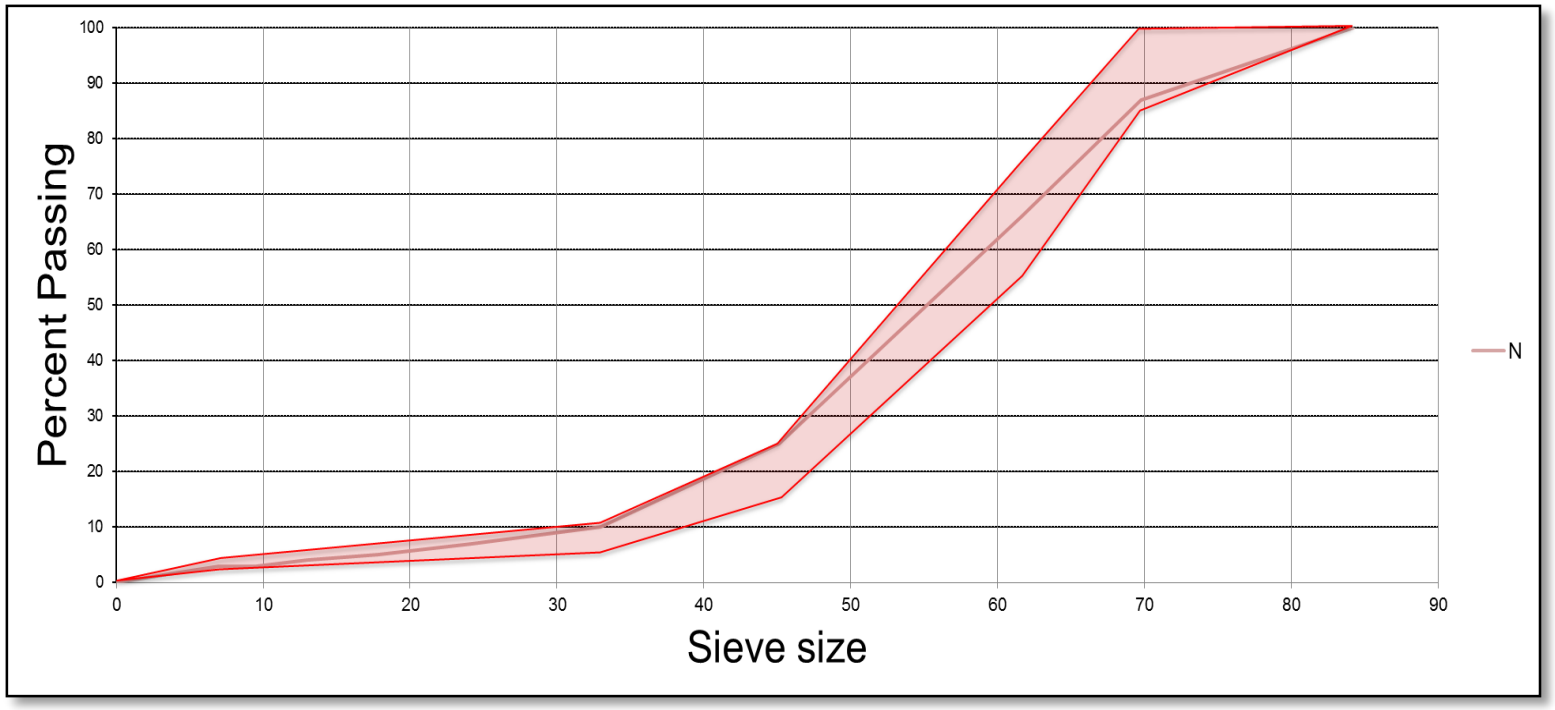

Figure D14 Gradation curves for mix N.

D.15 General Information of Mix O

Table D29 Aggregate and binder type for mix O.

Mix ID	Mix O
Aggregate Type	Oolite
Quarry Location	Miami/Dade
Supplier	White Rock
FDOT designation No.	9469A
FDOT code	87339
Binder Grade	PG 67-22

Table D30 FDOT OGFC gradation specifications for mix O.

Sieve Size	OOLITIC 87339 FDOT mix design number 9469A Percent Pasing (%) MIX O	CONTROL POINTS		
3/4" 19.0mm	100		100	
1/2" 12.5mm	92	85	_	100
3/8" 9.5mm	71	55	_	75
No. 4 4.75mm	25	15	_	25
No. 8 2.36mm	10	5	_	10
No. 16 1.18mm	8			
No. 30 600µm	6			
No. 50 300µm	5			
No. 100 150µm	3			
No. 200 75µm	2.30	2	_	4
GSB	2.416			

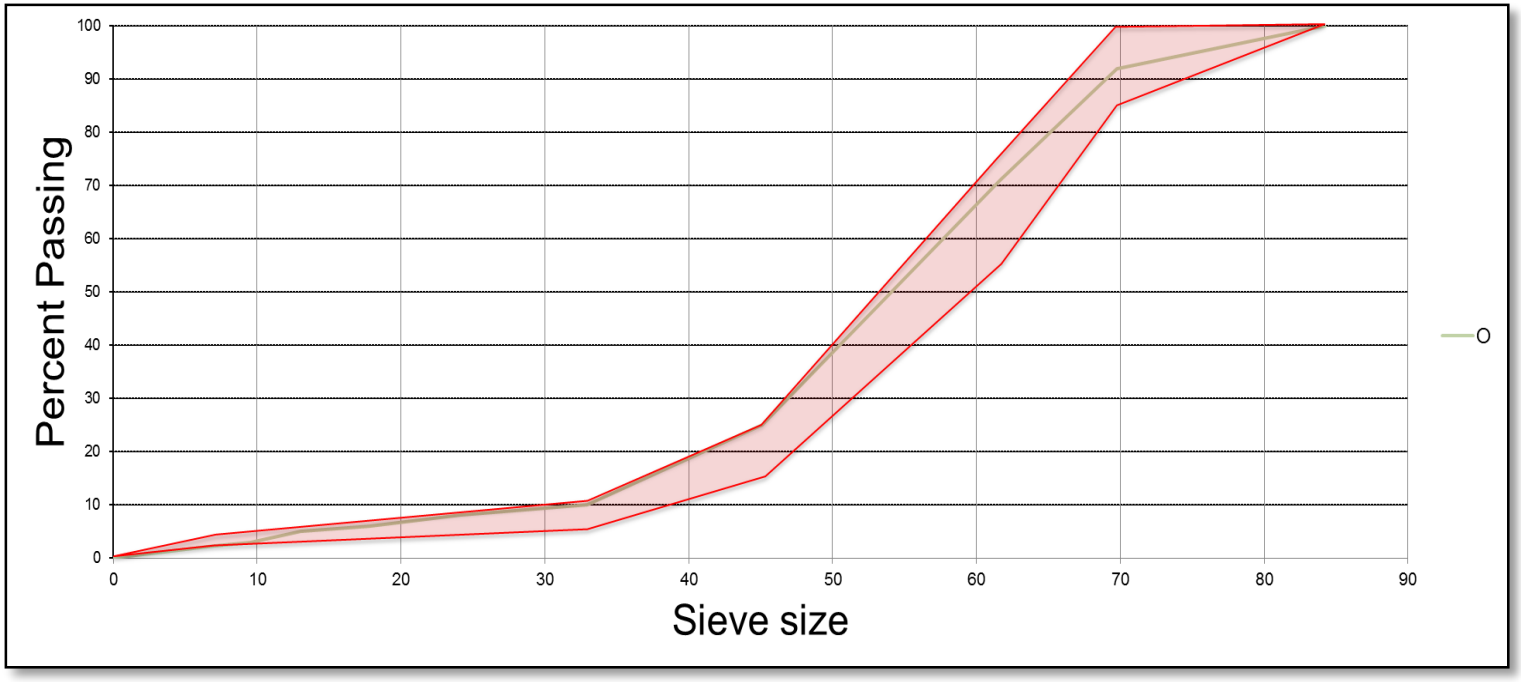

Figure D15 Gradation curves for mix O.

D.16 General Information of Mix P

Table D31 Aggregate and binder type for mix P.

Mix ID	Mix P
Aggregate Type	Oolite
Quarry Location	Miami/Dade
Supplier	White Rock
FDOT designation No.	10134A
FDOT code	87339
Binder Grade	PG 67-22

Table D32 FDOT OGFC gradation specifications for mix P.

Sieve Size	OOLITIC 87339 FDOT mix design number 10134A Percent Pasing (%) MIX P	CONTROL POINTS		
3/4" 19.0mm	100		100	
1/2" 12.5mm	90	85	_	100
3/8" 9.5mm	70	55	_	75
No. 4 4.75mm	23	15	_	25
No. 8 2.36mm	7	5	_	10
No. 16 1.18mm	3			
No. 30 600µm	3			
No. 50 300µm	2			
No. 100 150µm	2			
No. 200 75µm	2.00	2	_	4
GSB	2.409			

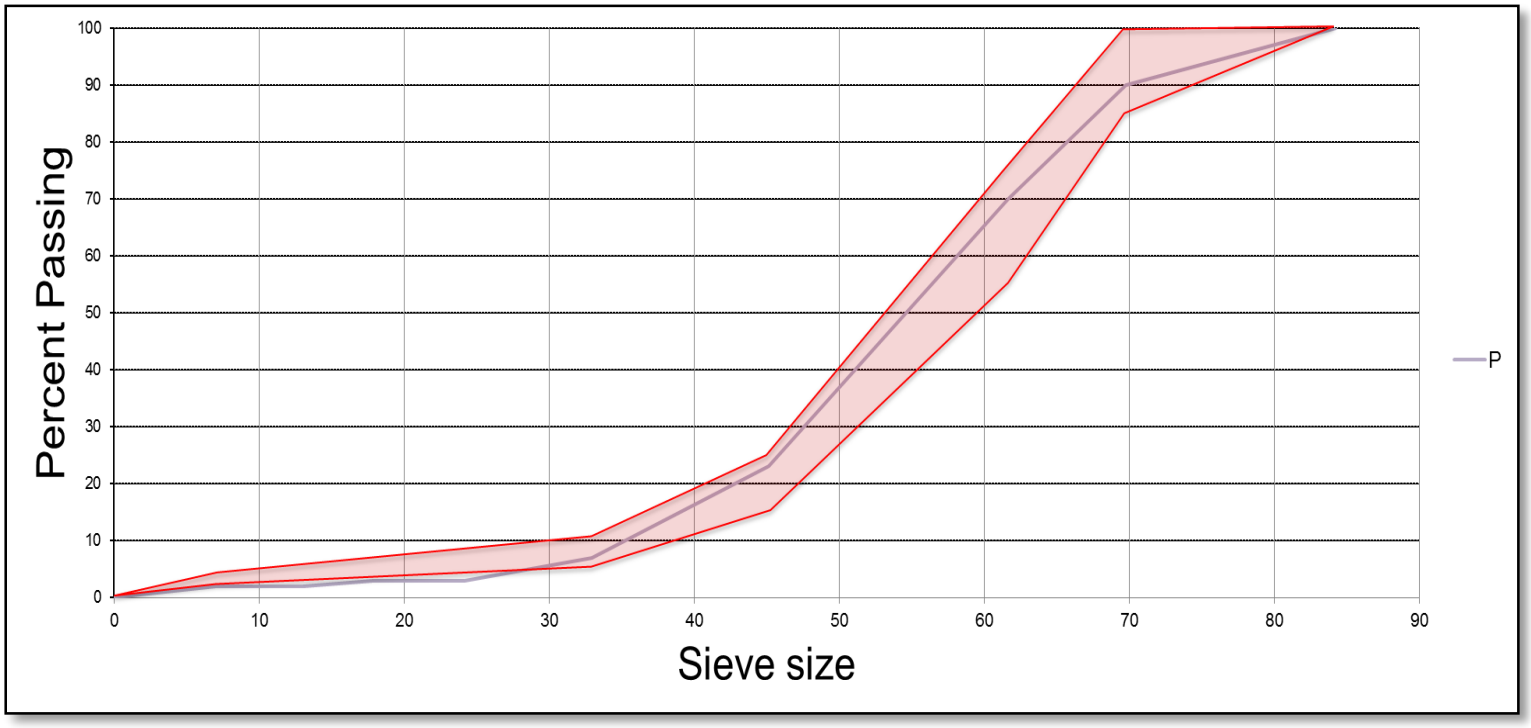

Figure D16 Gradation curves for mix P.

D.17 General Information of Mix Q

Table D33 Aggregate and binder type for mix Q.

Mix ID	Mix Q
Aggregate Type	Oolite
Quarry Location	Miami/Dade
Supplier	Titan America
FDOT designation No.	6954A
FDOT code	87145
Binder Grade	PG 67-22

Table D34 FDOT OGFC gradation specifications for mix Q.

Sieve Size	OOLITIC 87145 FDOT mix design number 6954A Percent Pasing (%) MIX Q	CONTROL POINTS		
3/4" 19.0mm	100		100	
1/2" 12.5mm	86	85	_	100
3/8" 9.5mm	64	55	_	75
No. 4 4.75mm	18	15	_	25
No. 8 2.36mm	7	5	_	10
No. 16 1.18mm	5			
No. 30 600µm	4			
No. 50 300µm	3			
No. 100 150µm	2			
No. 200 75µm	2.00	2	_	4
GSB	2.388			

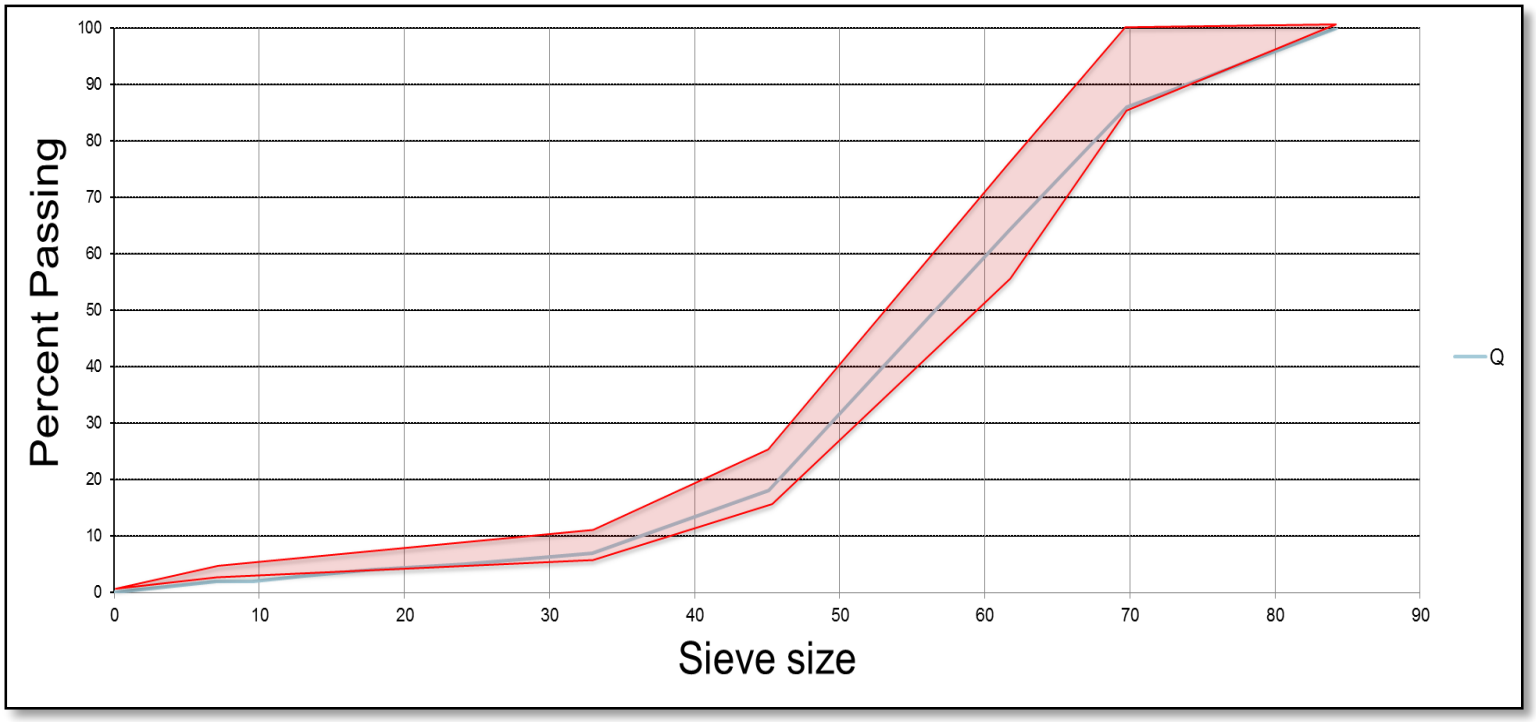

Figure D17 Gradation curves for mix Q.

D.18 General Information of Mix R

Table D35 Aggregate and binder type for mix R.

Mix ID	Mix R
Aggregate Type	Oolite
Quarry Location	Miami/Dade
Supplier	Titan America
FDOT designation No.	7806A
FDOT code	87145
Binder Grade	PG 67-22

Table D36 FDOT OGFC gradation specifications for mix R.

Sieve Size	OOLITIC 87145 FDOT mix design number 7806A Percent Pasing (%) MIX R	CONTROL POINTS		
3/4" 19.0mm	100		100	
1/2" 12.5mm	91	85	_	100
3/8" 9.5mm	68	55	_	75
No. 4 4.75mm	20	15	_	25
No. 8 2.36mm	8	5	_	10
No. 16 1.18mm	6			
No. 30 600µm	5			
No. 50 300µm	4			
No. 100 150µm	3			
No. 200 75µm	2.60	2	_	4
GSB	2.354			

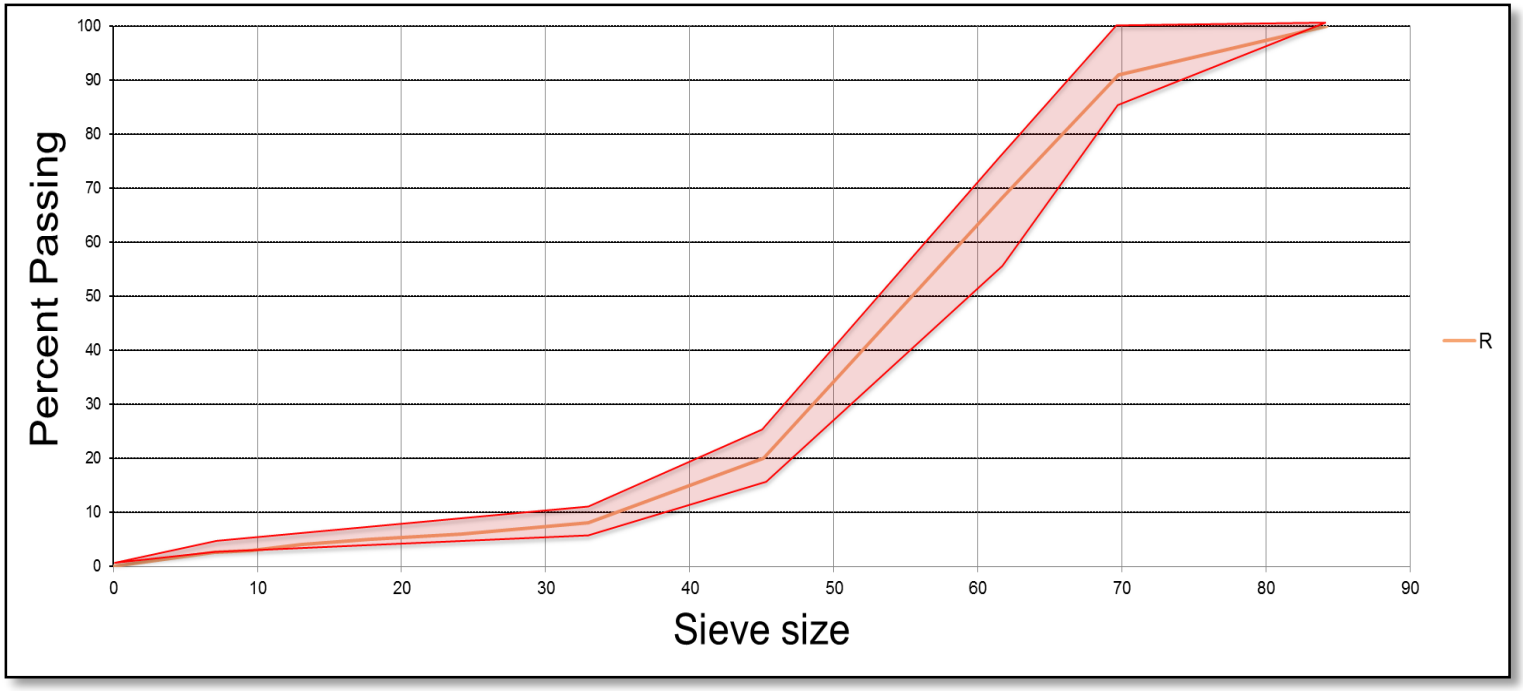

Figure D18 Gradation curves for mix R.

D.19 General Information of Mix S

Table D37 Aggregate and binder type for mix S.

Mix ID	Mix S
Aggregate Type	Oolite
Quarry Location	Miami/Dade
Supplier	Titan America
FDOT designation No.	9932A
FDOT code	87145
Binder Grade	PG 67-22

Table D38 FDOT OGFC gradation specifications for mix S.

Sieve Size	OOLITIC 87145 FDOT mix design number 9932A Percent Pasing (%) MIX S	CONTROL POINTS		
3/4" 19.0mm	100		100	
1/2" 12.5mm	89	85	_	100
3/8" 9.5mm	66	55	_	75
No. 4 4.75mm	25	15	_	25
No. 8 2.36mm	10	5	_	10
No. 16 1.18mm	7			
No. 30 600µm	5			
No. 50 300µm	4			
No. 100 150µm	2			
No. 200 75µm	2.00	2	_	4
GSB	2.355			

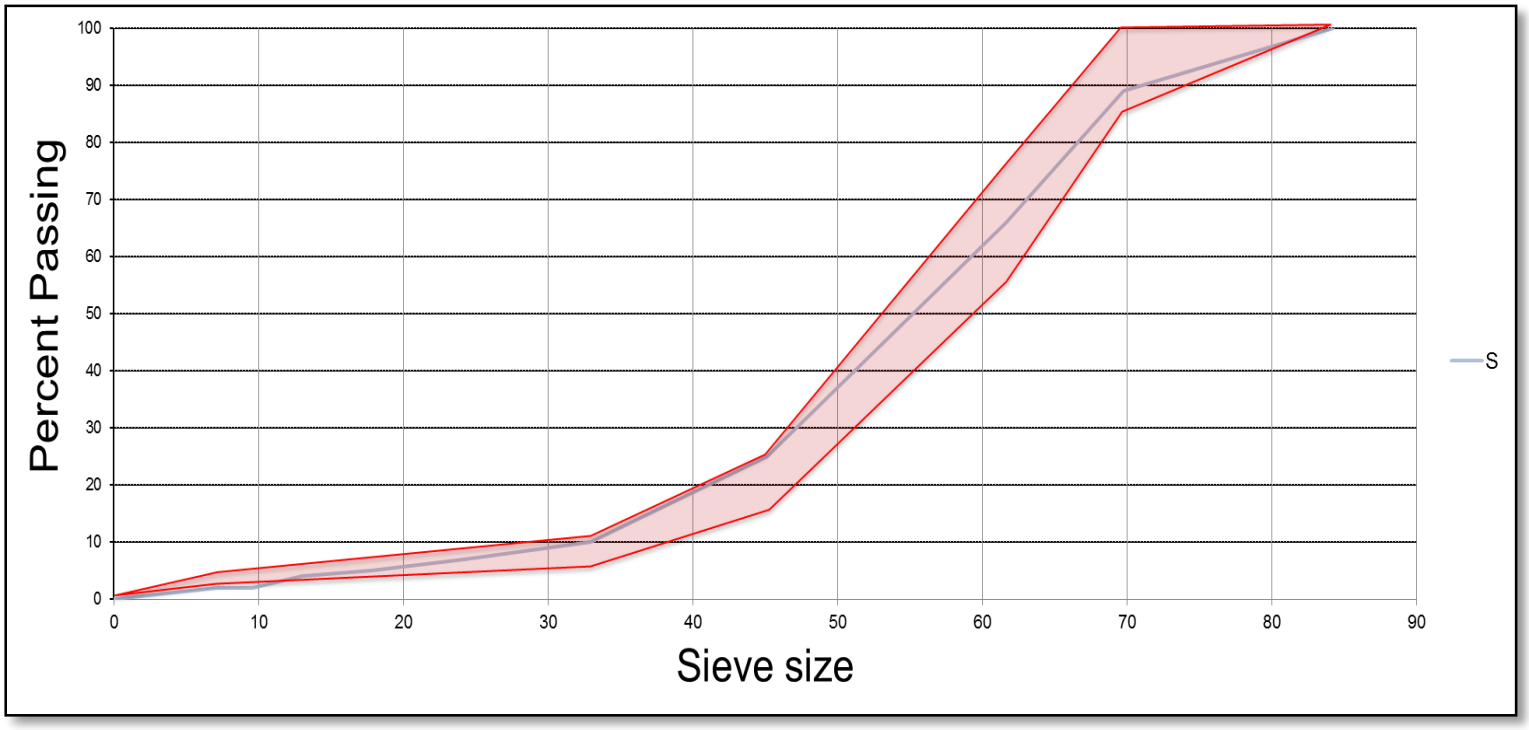

Figure D19 Gradation curves for mix S.

APPENDIX E: COMPARISON OF LABVIEW AND MATLAB RESULTS

GRANITE N315: MIX A (9165A)			Pie AC (%)	PBA (%)
			LABVIEW	MATLAB
MIX A OPT.1			MIX A OPT.1	MIX A OPT.1
5.5	291.48	143.07	49.083	48.9505
5.4	291.48	137.43	47.148	47.848
5.7	291.48	139.87	47.986	47.0232
			LABVIEW	MATLAB
MIX A OPT.2			MIX A OPT.2	MIX A OPT.2
5.7	291.48	137.32	47.111	46.985
5.4	291.48	142.82	48.996	48.0236
5.5	291.48	140.39	48.163	48.8617
			LABVIEW	MATLAB
MIX A TRIAL 1.1			MIX A TRIAL 1.	MIX A TRIAL 1.1
5.3	291.48	92.638	31.782	31.6537
5.8	291.48	128.76	44.175	44.036
6.3	291.48	179.06	61.431	61.3103
			LABVIEW	MATLAB
MIX A TRIAL 1.2			MIX A TRIAL 1.	MIX A TRIAL 1.2
5.3	291.48	92.916	31.877	31.75411
5.8	291.48	129.06	44.277	44.1432
6.3	291.48	178.96	61.397	61.2701
			LABVIEW	MATLAB
MIX A TRIAL 2.1			MIX A TRIAL 2.	MIX A TRIAL 2.1
5.3	291.48	101.64	34.868	34.7398
5.8	291.48	131.5	45.113	44.9811
6.3	291.48	179.72	61.659	61.5391
			LABVIEW	MATLAB
MIX A TRIAL 2.2			MIX A TRIAL 2.	MIX A TRIAL 2.2
5.3	291.48	101.46	34.808	34.685
5.8	291.48	131.46	45.099	44.9703
6.3	291.48	179.66	61.635	61.5167
			LABVIEW	MATLAB
MIX A TRIAL 3.1			MIX A TRIAL 3.	MIX A TRIAL 3.1
5.3	291.48	114.45	39.266	39.1411
5.8	291.48	164.58	56.461	56.3448
6.3	291.48	204.89	70.291	70.1769
			LABVIEW	MATLAB
MIX A TRIAL 3.2			MIX A TRIAL 3.	MIX A TRIAL 3.2
5.3	291.48	114.39	39.245	39.1212
5.8	291.48	164.33	56.376	56.2611
6.3	291.48	204.59	70.19	70.0726

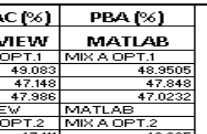

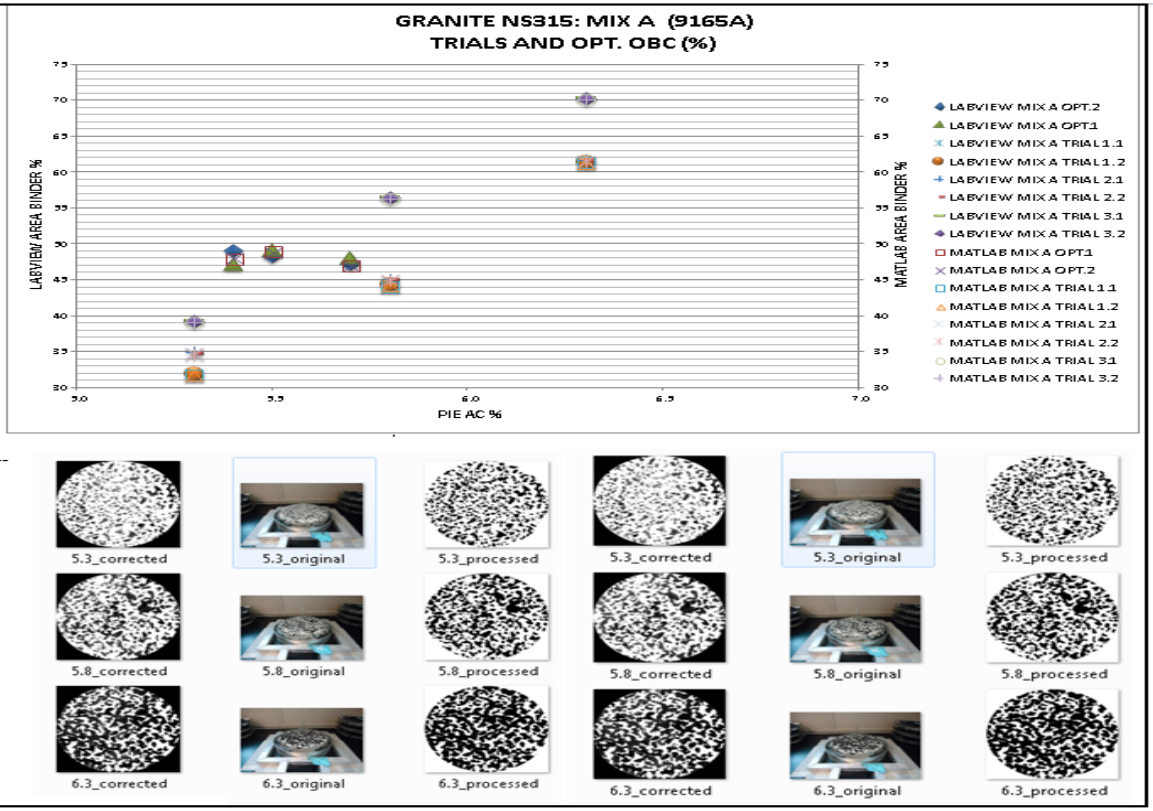

Figure E1 Labview versus Matlab digital image results -mix A.

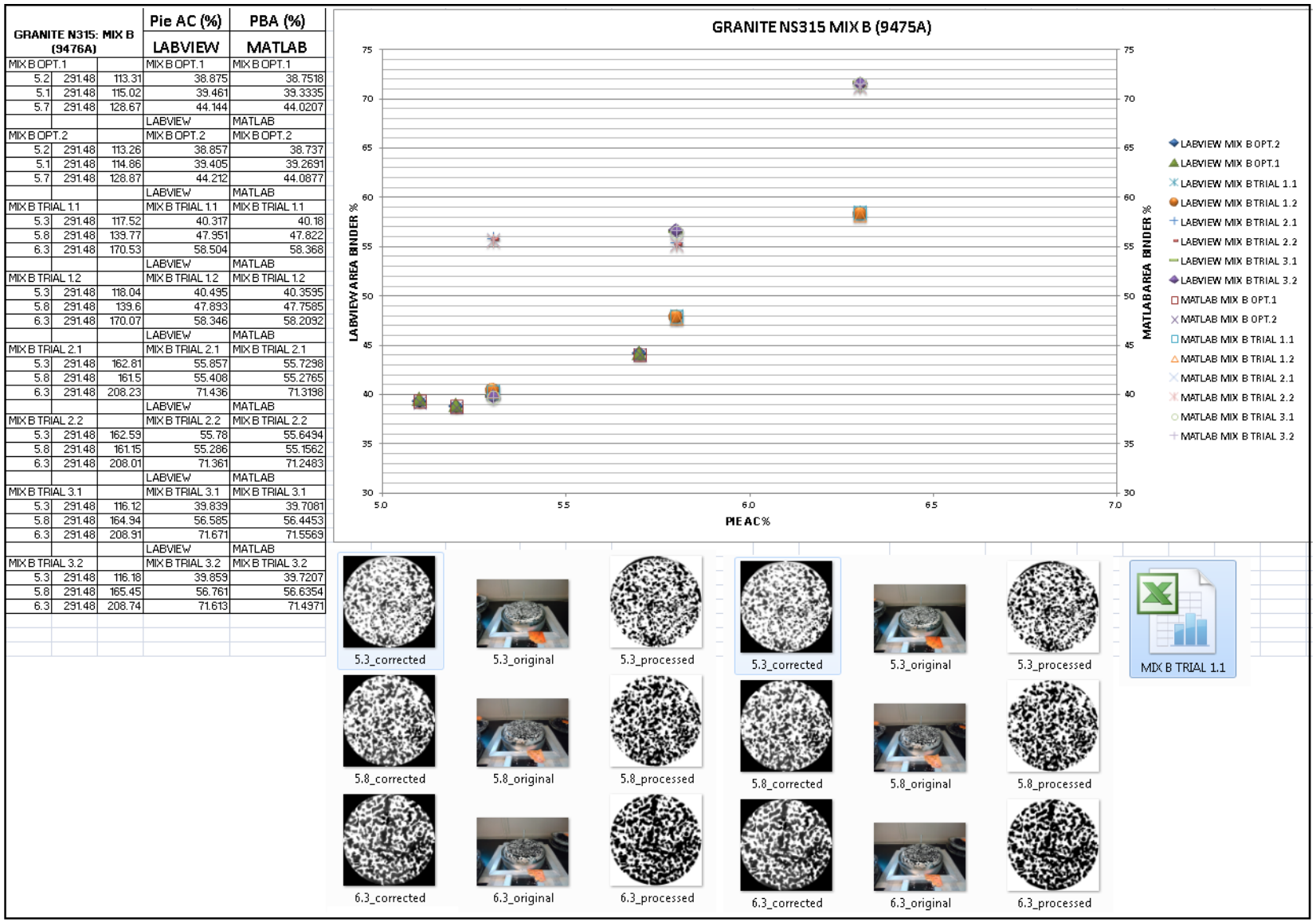

Figure E2 Labview versus Matlab digital image results -mix B.

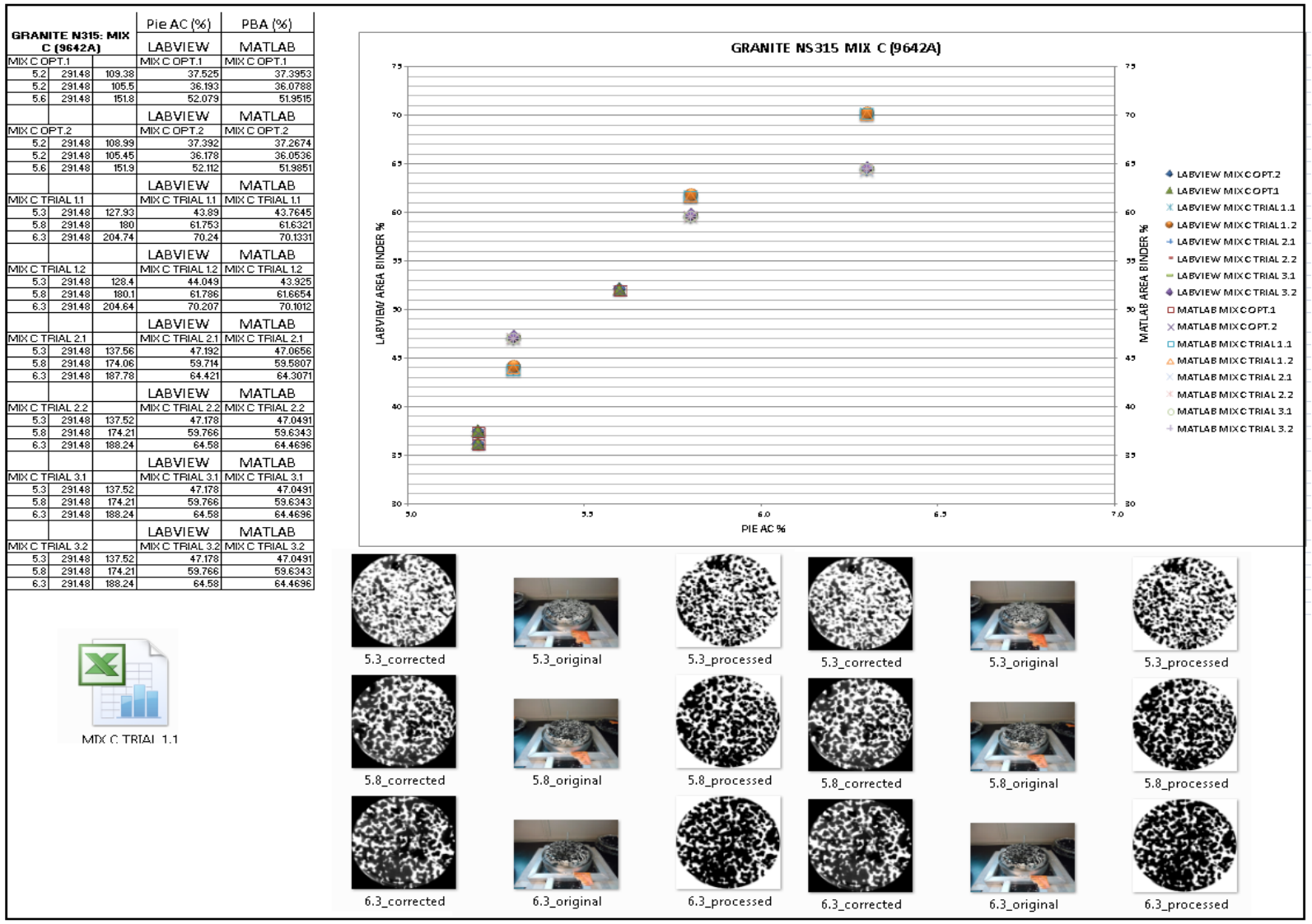

Figure E3 Labview versus Matlab digital image results -mix C.

GRANITE N315: MIX D (9646A)			Pie AC (%)	PBA (%)
			LABVIEW	MATLAB
MIX D OPT.1			MIX D OPT.1	MIX D OPT.1
5.2	291.48	147.01	50.435	50.3065
5.3	291.48	123.9	42.507	42.3861
5.4	291.48	147.86	50.727	50.5878
			LABVIEW	MATLAB
MIX D OPT.2			MIX D OPT.2	MIX D OPT.2
5.2	291.48	147.21	50.505	50.3723
5.3	291.48	123.82	42.48	42.3628
5.4	291.48	147.91	50.745	50.6073
			LABVIEW	MATLAB
MIX D TRIAL 1.1			MIX D TRIAL 1.1	MIX D TRIAL 1.1
5.3	291.48	129.38	44.388	44.2611
5.8	291.48	163.25	56.008	55.89
6.3	291.48	198.42	68.072	67.9683
			LABVIEW	MATLAB
MIX D TRIAL 1.2			MIX D TRIAL 1.2	MIX D TRIAL 1.2
5.3	291.48	129.64	44.476	44.3543
5.8	291.48	163.68	56.152	56.0301
6.3	291.48	198.32	68.039	67.9345
			LABVIEW	MATLAB
MIX D TRIAL 2.1			MIX D TRIAL 2.1	MIX D TRIAL 2.1
5.3	291.48	128.72	44.162	44.0367
5.8	291.48	181.84	62.385	62.2607
6.3	291.48	216.97	74.436	74.3406
			LABVIEW	MATLAB
MIX D TRIAL 2.2			MIX D TRIAL 2.2	MIX D TRIAL 2.2
5.3	291.48	129.22	44.333	44.2137
5.8	291.48	181.58	62.296	62.1704
6.3	291.48	217.11	74.483	74.3827
			LABVIEW	MATLAB
MIX D TRIAL 3.1			MIX D TRIAL 3.1	MIX D TRIAL 3.1
5.3	291.48	119.07	40.849	40.7215
5.8	291.48	158.95	54.531	54.4036
6.3	291.48	199.43	68.417	68.3124
			LABVIEW	MATLAB
MIX D TRIAL 3.2			MIX D TRIAL 3.2	MIX D TRIAL 3.2
5.3	291.48	119.81	41.102	40.9718
5.8	291.48	158.95	54.531	54.4031
6.3	291.48	199.35	68.391	68.278

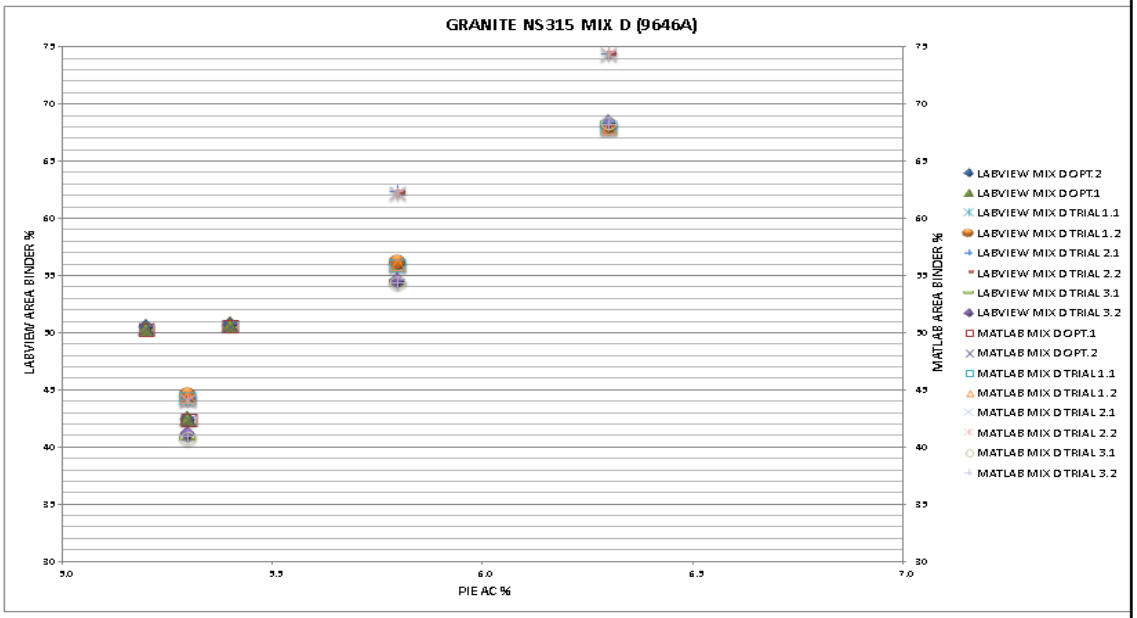

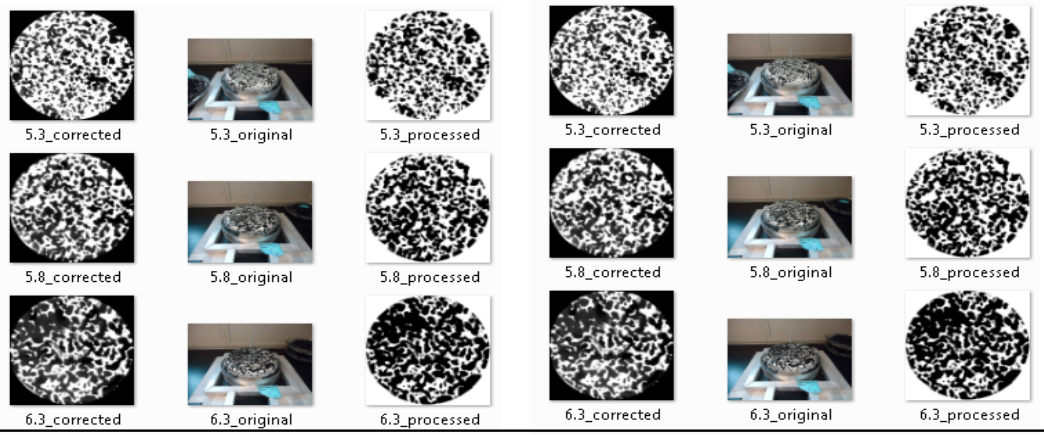

Figure E4 Labview versus Matlab digital image results -mix D.

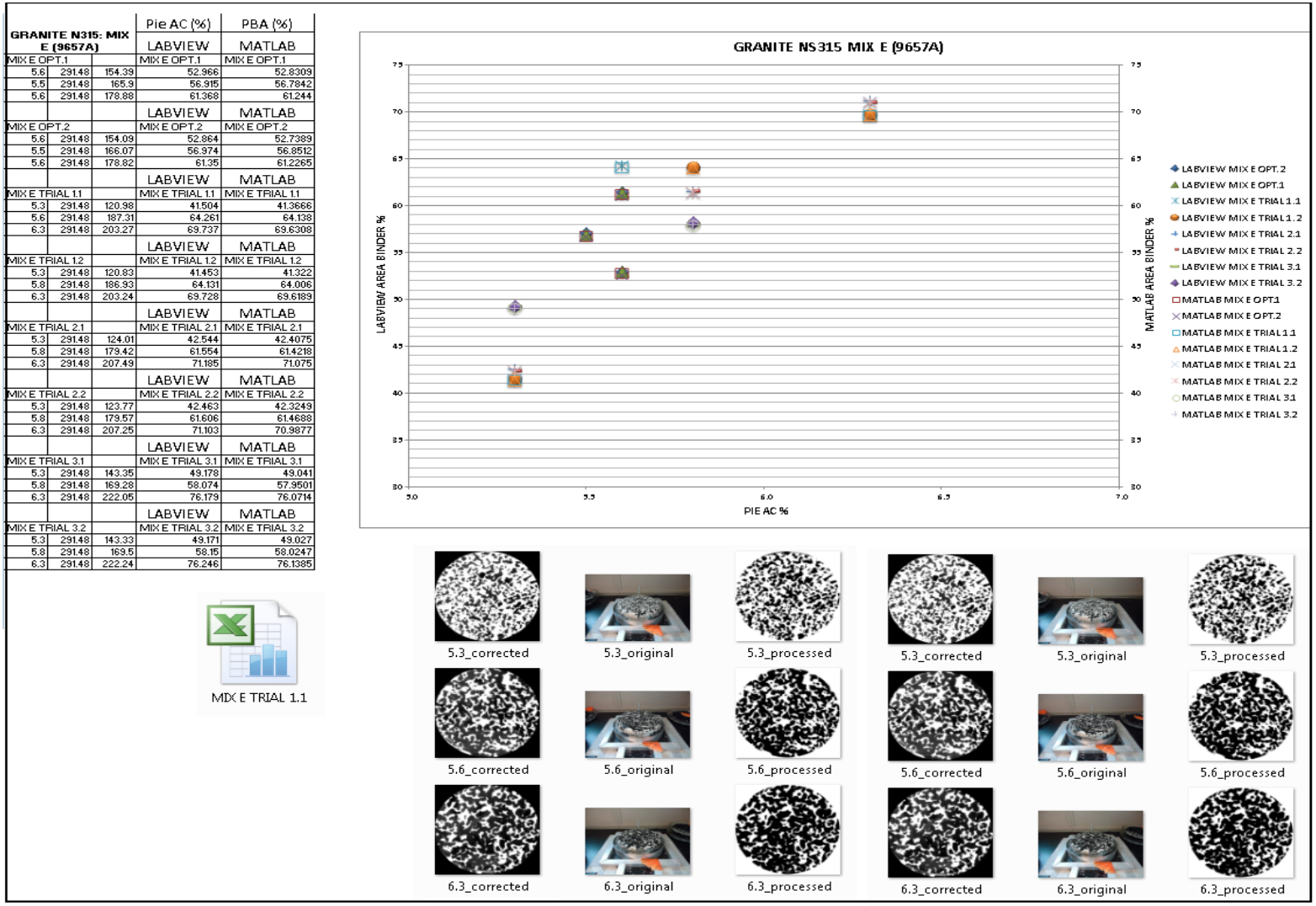

GRANITE N315: MIX E (9657A)			Pie AC (%)	PBA (%)
			LABVIEW	MATLAB
MIX E OPT.1			MIX E OPT.1	MIX E OPT.1
5.6	291.48	154.39	52.966	52.8309
5.5	291.48	165.9	56.915	56.7842
5.6	291.48	178.88	61.368	61.244
			LABVIEW	MATLAB
MIX E OPT.2			MIX E OPT.2	MIX E OPT.2
5.6	291.48	154.09	52.864	52.7389
5.5	291.48	166.07	56.974	56.8512
5.6	291.48	178.82	61.35	61.2265
			LABVIEW	MATLAB
MIX E TRIAL 1.1			MIX E TRIAL 1.1	MIX E TRIAL 1.1
5.3	291.48	120.98	41.504	41.3666
5.6	291.48	187.31	64.261	64.138
6.3	291.48	203.27	69.737	69.6308
			LABVIEW	MATLAB
MIX E TRIAL 1.2			MIX E TRIAL 1.2	MIX E TRIAL 1.2
5.3	291.48	120.83	41.453	41.322
5.8	291.48	186.93	64.131	64.006
6.3	291.48	203.24	69.728	69.6189
			LABVIEW	MATLAB
MIX E TRIAL 2.1			MIX E TRIAL 2.1	MIX E TRIAL 2.1
5.3	291.48	124.01	42.544	42.4075
5.8	291.48	179.42	61.554	61.4218
6.3	291.48	207.49	71.185	71.075
			LABVIEW	MATLAB
MIX E TRIAL 2.2			MIX E TRIAL 2.2	MIX E TRIAL 2.2
5.3	291.48	123.77	42.463	42.3249
5.8	291.48	179.57	61.606	61.4688
6.3	291.48	207.25	71.103	70.9877
			LABVIEW	MATLAB
MIX E TRIAL 3.1			MIX E TRIAL 3.1	MIX E TRIAL 3.1
5.3	291.48	143.35	49.178	49.041
5.8	291.48	169.28	58.074	57.9501
6.3	291.48	222.05	76.179	76.0714
			LABVIEW	MATLAB
MIX E TRIAL 3.2			MIX E TRIAL 3.2	MIX E TRIAL 3.2
5.3	291.48	143.33	49.171	49.027
5.8	291.48	169.5	58.15	58.0247
6.3	291.48	222.24	76.246	76.1385

Figure E5 Labview versus Matlab digital image results -mix E.

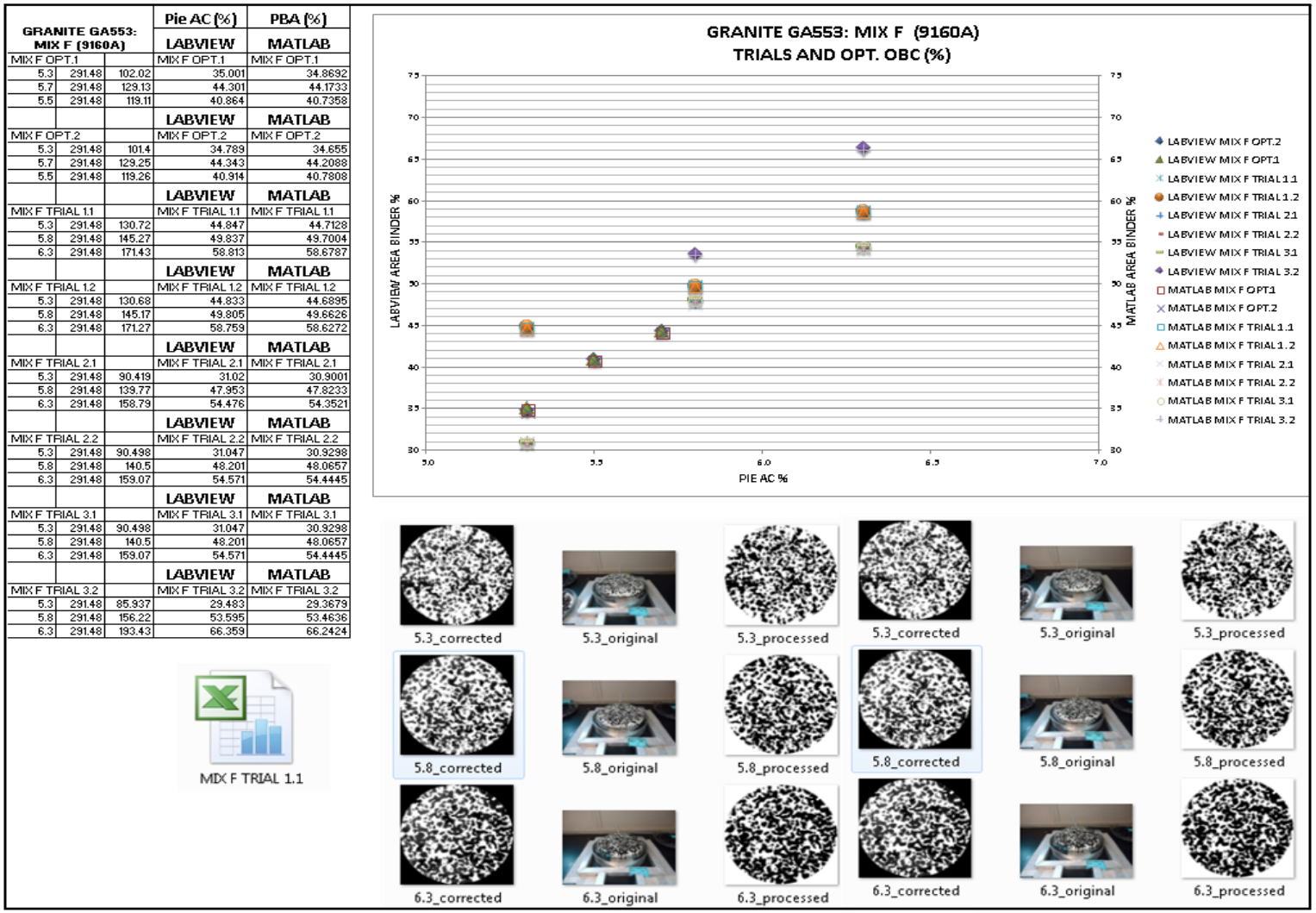

GRANITE GA553: MIX F (9160A)			Pie AC (%)	PBA (%)
			LABVIEW	MATLAB
MIX F OPT.1			MIX F OPT.1	MIX F OPT.1
5.3	291.48	102.02	35.001	34.8692
5.7	291.48	129.13	44.301	44.1733
5.5	291.48	119.11	40.864	40.7358
			LABVIEW	MATLAB
MIX F OPT.2			MIX F OPT.2	MIX F OPT.2
5.3	291.48	101.4	34.789	34.655
5.7	291.48	129.25	44.343	44.2088
5.5	291.48	119.26	40.914	40.7808
			LABVIEW	MATLAB
MIX F TRIAL 1.1			MIX F TRIAL 1.1	MIX F TRIAL 1.1
5.3	291.48	130.72	44.847	44.7128
5.8	291.48	145.27	49.837	49.7004
6.3	291.48	171.43	58.813	58.6787
			LABVIEW	MATLAB
MIX F TRIAL 1.2			MIX F TRIAL 1.2	MIX F TRIAL 1.2
5.3	291.48	130.68	44.833	44.6895
5.8	291.48	145.17	49.805	49.6626
6.3	291.48	171.27	58.759	58.6272
			LABVIEW	MATLAB
MIX F TRIAL 2.1			MIX F TRIAL 2.1	MIX F TRIAL 2.1
5.3	291.48	90.419	31.02	30.9001
5.8	291.48	139.77	47.953	47.8233
6.3	291.48	158.79	54.476	54.3521
			LABVIEW	MATLAB
MIX F TRIAL 2.2			MIX F TRIAL 2.2	MIX F TRIAL 2.2
5.3	291.48	90.498	31.047	30.9298
5.8	291.48	140.5	48.201	48.0657
6.3	291.48	159.07	54.571	54.4445
			LABVIEW	MATLAB
MIX F TRIAL 3.1			MIX F TRIAL 3.1	MIX F TRIAL 3.1
5.3	291.48	90.498	31.047	30.9298
5.8	291.48	140.5	48.201	48.0657
6.3	291.48	159.07	54.571	54.4445
			LABVIEW	MATLAB
MIX F TRIAL 3.2			MIX F TRIAL 3.2	MIX F TRIAL 3.2
5.3	291.48	85.937	29.483	29.3679
5.8	291.48	156.22	53.595	53.4636
6.3	291.48	193.43	66.359	66.2424

Figure E6 Labview versus Matlab digital image results -mix F.

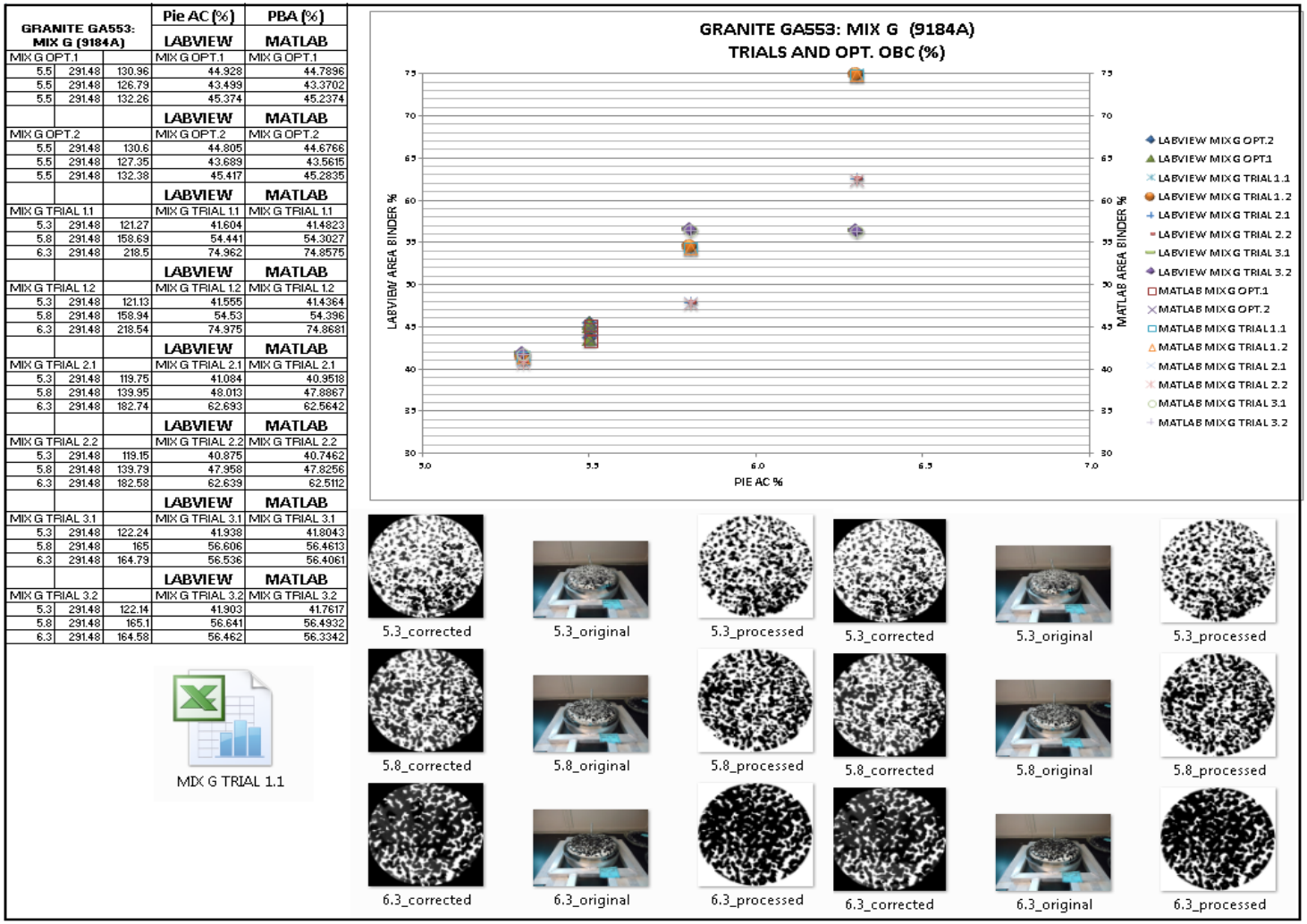

GRANITE GA553: MIX G (9184A)			Pie AC (%)	PBA (%)
			LABVIEW	MATLAB
MIX G OPT.1			MIX G OPT.1	MIX G OPT.1
5.5	291.48	130.96	44.928	44.7896
5.5	291.48	126.79	43.499	43.3702
5.5	291.48	132.26	45.374	45.2374
			LABVIEW	MATLAB
MIX G OPT.2			MIX G OPT.2	MIX G OPT.2
5.5	291.48	130.6	44.805	44.6766
5.5	291.48	127.35	43.689	43.5615
5.5	291.48	132.38	45.417	45.2835
			LABVIEW	MATLAB
MIX G TRIAL 1.1			MIX G TRIAL 1.1	MIX G TRIAL 1.1
5.3	291.48	121.27	41.604	41.4823
5.8	291.48	158.69	54.441	54.3027
6.3	291.48	218.5	74.962	74.8575
			LABVIEW	MATLAB
MIX G TRIAL 1.2			MIX G TRIAL 1.2	MIX G TRIAL 1.2
5.3	291.48	121.13	41.555	41.4364
5.8	291.48	158.94	54.53	54.396
6.3	291.48	218.54	74.975	74.8681
			LABVIEW	MATLAB
MIX G TRIAL 2.1			MIX G TRIAL 2.1	MIX G TRIAL 2.1
5.3	291.48	119.75	41.084	40.9518
5.8	291.48	139.95	48.013	47.8867
6.3	291.48	182.74	62.693	62.5642
			LABVIEW	MATLAB
MIX G TRIAL 2.2			MIX G TRIAL 2.2	MIX G TRIAL 2.2
5.3	291.48	119.15	40.875	40.7462
5.8	291.48	139.79	47.958	47.8256
6.3	291.48	182.58	62.639	62.5112
			LABVIEW	MATLAB
MIX G TRIAL 3.1			MIX G TRIAL 3.1	MIX G TRIAL 3.1
5.3	291.48	122.24	41.938	41.8043
5.8	291.48	165	56.606	56.4613
6.3	291.48	164.79	56.536	56.4061
			LABVIEW	MATLAB
MIX G TRIAL 3.2			MIX G TRIAL 3.2	MIX G TRIAL 3.2
5.3	291.48	122.14	41.903	41.7617
5.8	291.48	165.1	56.641	56.4932
6.3	291.48	164.58	56.462	56.3342

Figure E7 Labview versus Matlab digital image results -mix G.

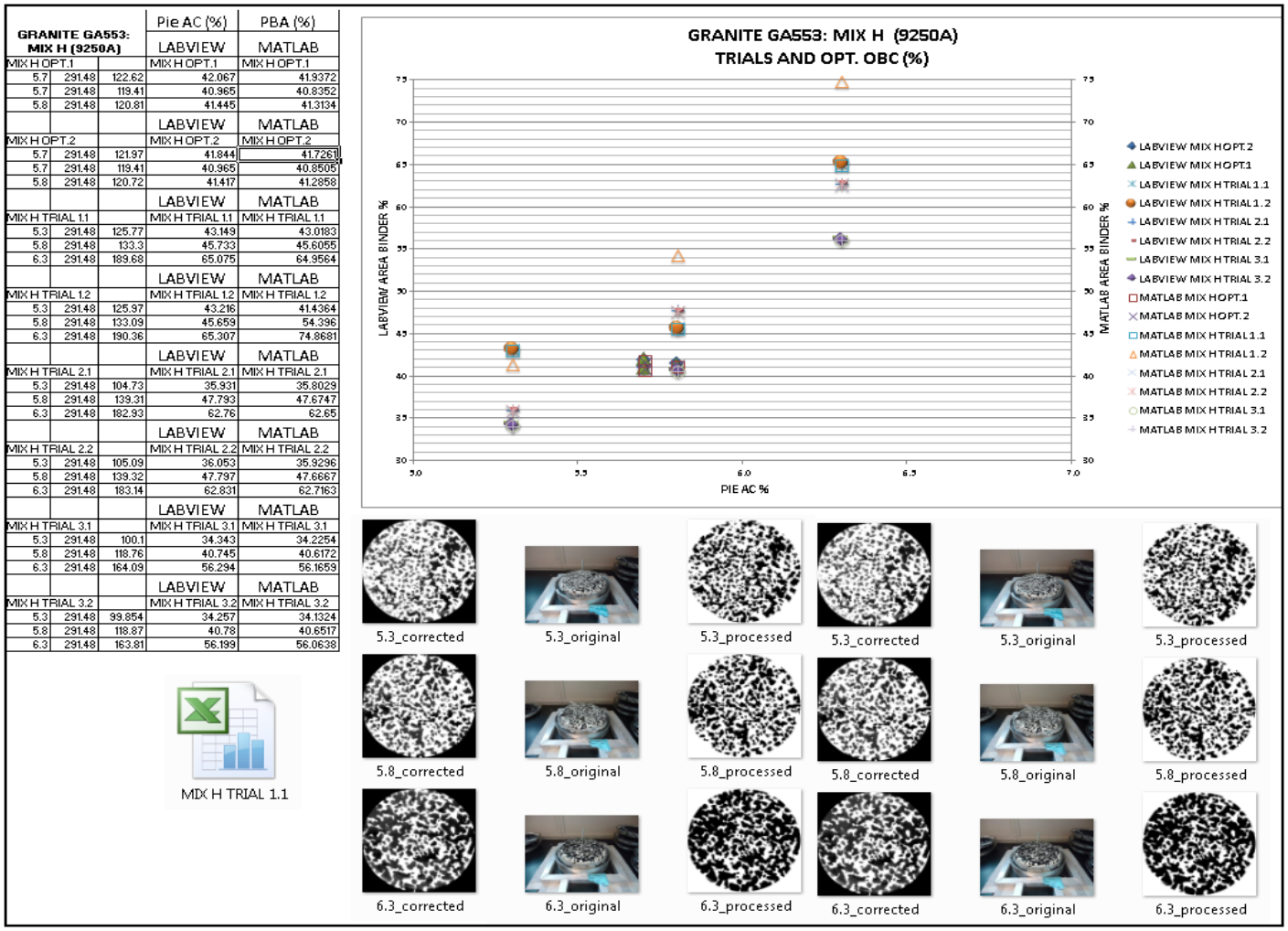

GRANITE GA553: MIX H (9250A)			Pie AC (%)	PBA (%)
			LABVIEW	MATLAB
MIX H OPT.1			MIX H OPT.1	MIX H OPT.1
5.7	291.48	122.62	42.067	41.9372
5.7	291.48	119.41	40.965	40.8352
5.8	291.48	120.81	41.445	41.3134
			LABVIEW	MATLAB
MIX H OPT.2			MIX H OPT.2	MIX H OPT.2
5.7	291.48	121.97	41.844	41.7261
5.7	291.48	119.41	40.965	40.8505
5.8	291.48	120.72	41.417	41.2858
			LABVIEW	MATLAB
MIX H TRIAL 1.1			MIX H TRIAL 1.1	MIX H TRIAL 1.1
5.3	291.48	125.77	43.149	43.0183
5.8	291.48	133.3	45.733	45.6055
6.3	291.48	189.68	65.075	64.9564
			LABVIEW	MATLAB
MIX H TRIAL 1.2			MIX H TRIAL 1.2	MIX H TRIAL 1.2
5.3	291.48	125.97	43.216	41.4364
5.8	291.48	133.09	45.659	54.396
6.3	291.48	190.36	65.307	74.8681
			LABVIEW	MATLAB
MIX H TRIAL 2.1			MIX H TRIAL 2.1	MIX H TRIAL 2.1
5.3	291.48	104.73	35.931	35.8029
5.8	291.48	139.31	47.793	47.6747
6.3	291.48	182.93	62.76	62.65
			LABVIEW	MATLAB
MIX H TRIAL 2.2			MIX H TRIAL 2.2	MIX H TRIAL 2.2
5.3	291.48	105.09	36.053	35.9296
5.8	291.48	139.32	47.797	47.6667
6.3	291.48	183.14	62.831	62.7163
			LABVIEW	MATLAB
MIX H TRIAL 3.1			MIX H TRIAL 3.1	MIX H TRIAL 3.1
5.3	291.48	100.1	34.343	34.2254
5.8	291.48	118.76	40.745	40.6172
6.3	291.48	164.09	56.294	56.1659
			LABVIEW	MATLAB
MIX H TRIAL 3.2			MIX H TRIAL 3.2	MIX H TRIAL 3.2
5.3	291.48	99.854	34.257	34.1324
5.8	291.48	118.87	40.78	40.6517
6.3	291.48	163.81	56.199	56.0638

Figure E8 Labview versus Matlab digital image results -mix H.

GRANITE GA553: MIX I (9824A)			Pie AC (%)	PBA (%)
			LABVIEW	MATLAB
MIX I OPT.1			MIX I OPT.1	MIX I OPT.1
5.3	291.48	97.344	33.396	33.2741
5.4	291.48	90.497	31.047	30.9256
5.6	291.48	114.38	39.241	39.112
			LABVIEW	MATLAB
MIX I OPT.2			MIX I OPT.2	MIX I OPT.2
5.3	291.48	97.873	33.578	33.4551
5.4	291.48	90.451	31.031	30.9174
5.6	291.48	113.81	39.043	38.9197
			LABVIEW	MATLAB
MIX I TRIAL 1.1			MIX I TRIAL 1.1	MIX I TRIAL 1.1
5.3	291.48	119.78	41.095	40.9652
5.8	291.48	178.11	61.105	60.9722
6.3	291.48	197.62	67.799	67.6905
			LABVIEW	MATLAB
MIX I TRIAL 1.2			MIX I TRIAL 1.2	MIX I TRIAL 1.2
5.3	291.48	119.54	41.012	40.8749
5.8	291.48	177.61	60.933	60.8077
6.3	291.48	197.1	67.62	67.5036
			LABVIEW	MATLAB
MIX I TRIAL 2.1			MIX I TRIAL 2.1	MIX I TRIAL 2.1
5.3	291.48	137.42	47.146	47.0079
5.8	291.48	160.99	55.231	55.1069
6.3	291.48	191.43	65.673	65.5613
			LABVIEW	MATLAB
MIX I TRIAL 2.2			MIX I TRIAL 2.2	MIX I TRIAL 2.2
5.3	291.48	136.86	46.953	46.8185
5.8	291.48	160.49	55.058	54.9338
6.3	291.48	191.04	65.54	65.4328
			LABVIEW	MATLAB
MIX I TRIAL 3.1			MIX I TRIAL 3.1	MIX I TRIAL 3.1
5.3	291.48	123.43	42.346	42.2043
5.8	291.48	160.13	54.937	54.8097
6.3	291.48	177.24	60.804	60.6845
			LABVIEW	MATLAB
MIX I TRIAL 3.2			MIX I TRIAL 3.2	MIX I TRIAL 3.2
5.3	291.48	123.4	42.336	42.1996
5.8	291.48	160.14	54.939	54.8112
6.3	291.48	176.96	60.71	60.5814

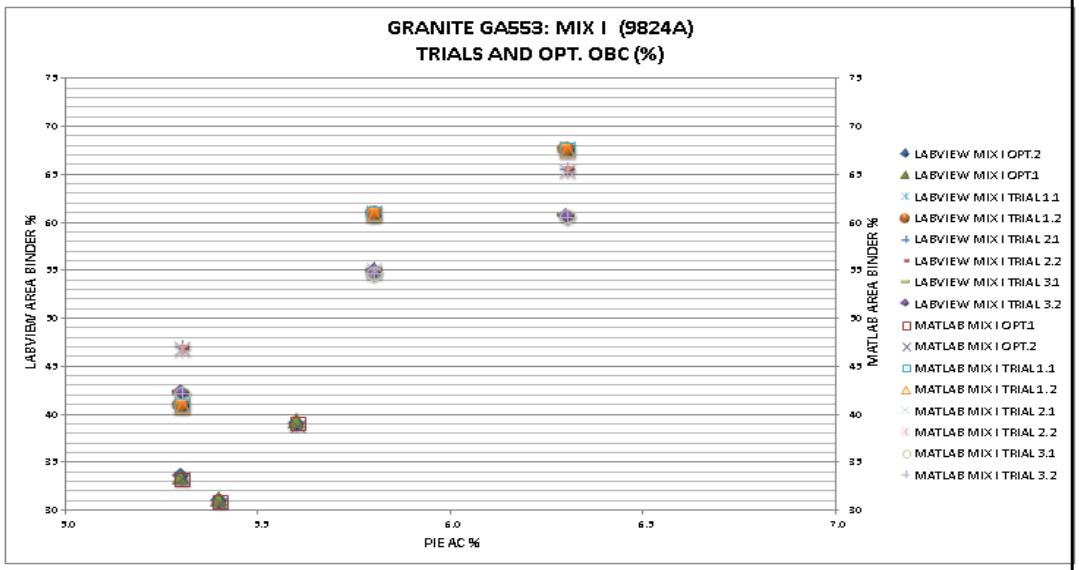

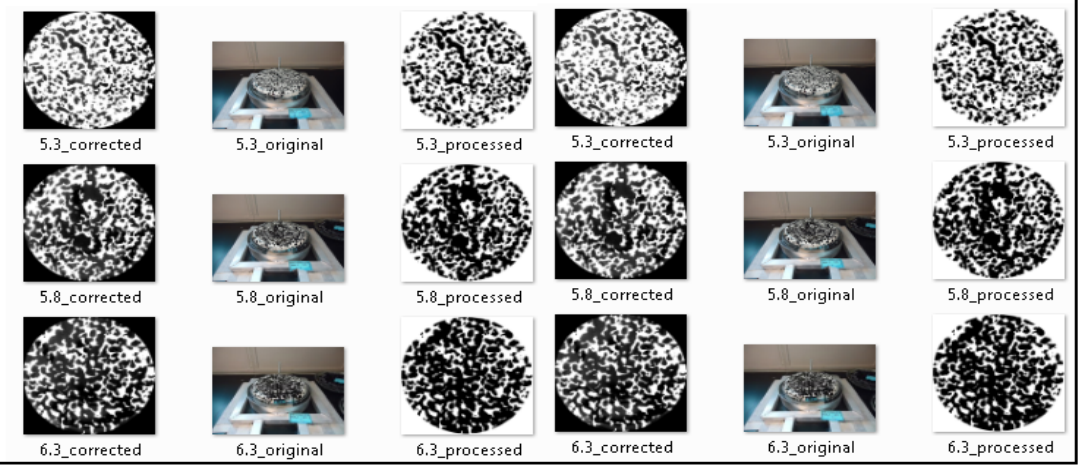

Figure E9 Labview versus Matlab digital image results -mix I.

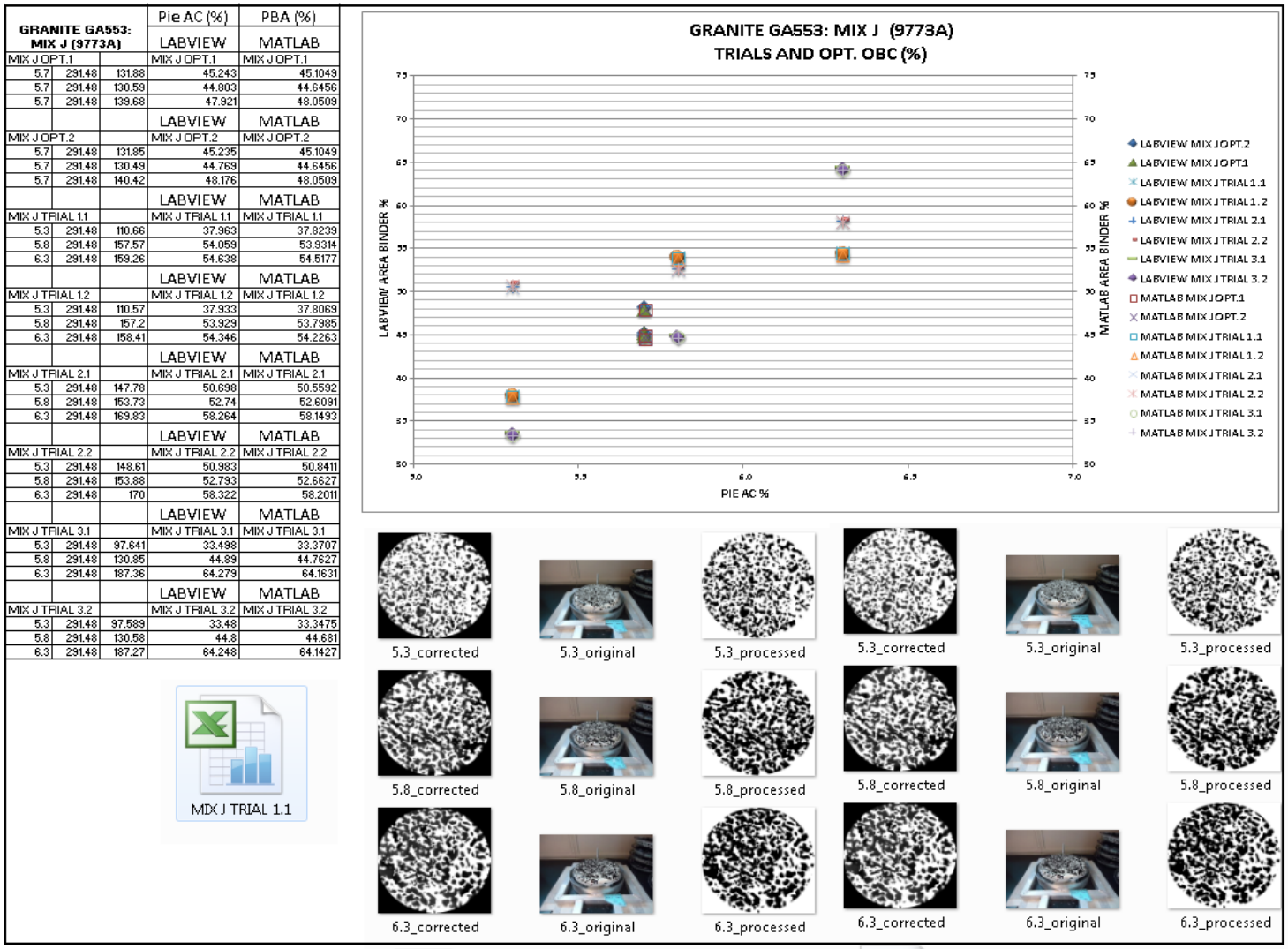

GRANITE GA553: MIX J (9773A)			Pie AC (%)	PBA (%)
			LABVIEW	MATLAB
MIX J OPT.1			MIX J OPT.1	MIX J OPT.1
5.7	291.48	131.88	45.243	45.1049
5.7	291.48	130.59	44.803	44.6456
5.7	291.48	139.68	47.921	48.0509
			LABVIEW	MATLAB
MIX J OPT.2			MIX J OPT.2	MIX J OPT.2
5.7	291.48	131.85	45.235	45.1049
5.7	291.48	130.49	44.769	44.6456
5.7	291.48	140.42	48.176	48.0509
			LABVIEW	MATLAB
MIX J TRIAL 1.1			MIX J TRIAL 1.1	MIX J TRIAL 1.1
5.3	291.48	110.66	37.963	37.8239
5.8	291.48	157.57	54.059	53.9314
6.3	291.48	159.26	54.638	54.5177
			LABVIEW	MATLAB
MIX J TRIAL 1.2			MIX J TRIAL 1.2	MIX J TRIAL 1.2
5.3	291.48	110.57	37.933	37.8069
5.8	291.48	157.2	53.929	53.7985
6.3	291.48	158.41	54.346	54.2263
			LABVIEW	MATLAB
MIX J TRIAL 2.1			MIX J TRIAL 2.1	MIX J TRIAL 2.1
5.3	291.48	147.78	50.698	50.5592
5.8	291.48	153.73	52.74	52.6091
6.3	291.48	169.83	58.264	58.1493
			LABVIEW	MATLAB
MIX J TRIAL 2.2			MIX J TRIAL 2.2	MIX J TRIAL 2.2
5.3	291.48	148.61	50.983	50.8411
5.8	291.48	153.88	52.793	52.6627
6.3	291.48	170	58.322	58.2011
			LABVIEW	MATLAB
MIX J TRIAL 3.1			MIX J TRIAL 3.1	MIX J TRIAL 3.1
5.3	291.48	97.641	33.498	33.3707
5.8	291.48	130.85	44.89	44.7627
6.3	291.48	187.36	64.279	64.1631
			LABVIEW	MATLAB
MIX J TRIAL 3.2			MIX J TRIAL 3.2	MIX J TRIAL 3.2
5.3	291.48	97.589	33.48	33.3475
5.8	291.48	130.58	44.8	44.681
6.3	291.48	187.27	64.248	64.1427

Figure E10 Labview versus Matlab digital image results -mix J.

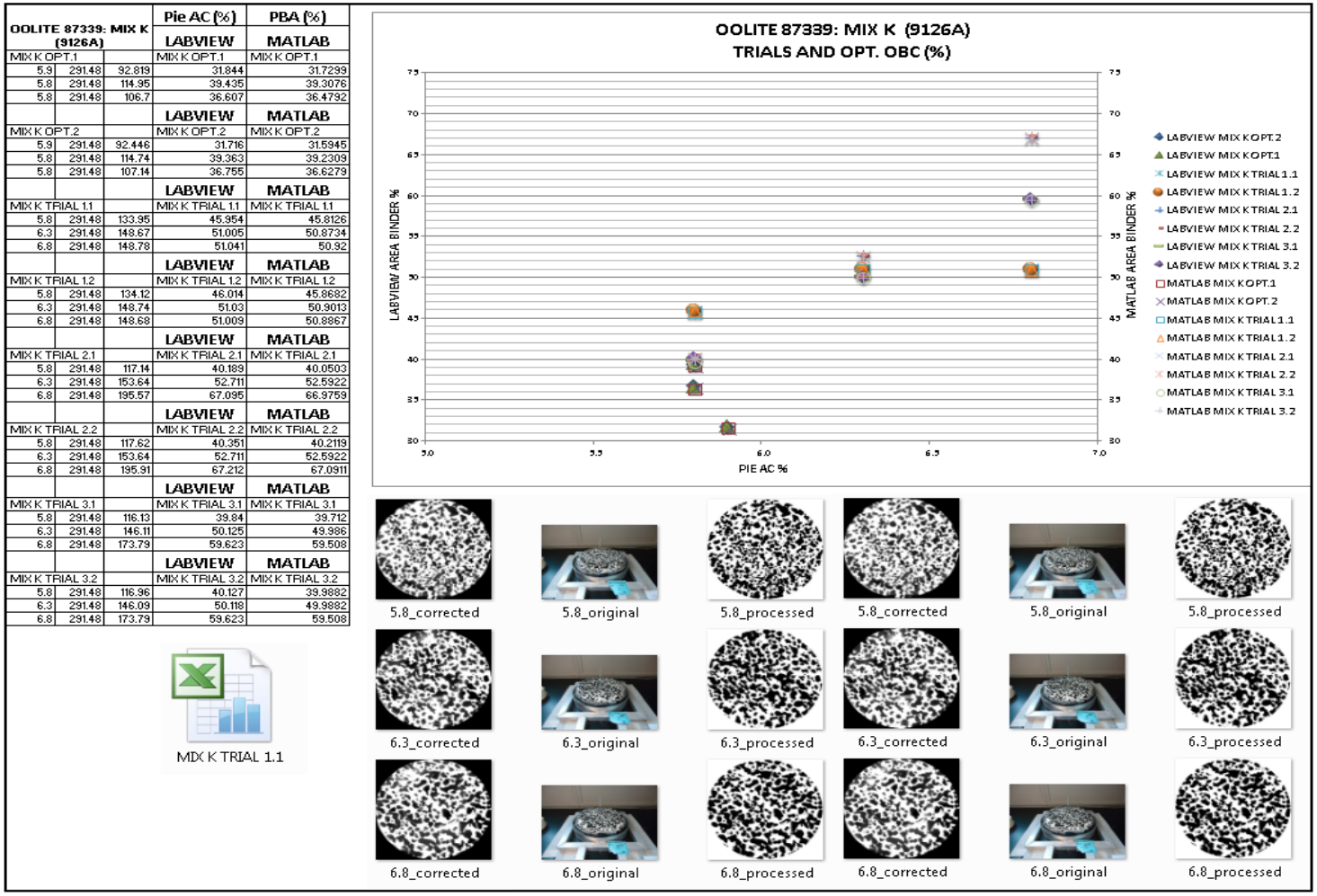

OOLITE 87339: MIX K (9126A)			Pie AC (%)	PBA (%)
			LABVIEW	MATLAB
MIX K OPT.1			MIX K OPT.1	MIX K OPT.1
5.9	291.48	92.819	31.844	31.7299
5.8	291.48	114.95	39.435	39.3076
5.8	291.48	106.7	36.607	36.4792
			LABVIEW	MATLAB
MIX K OPT.2			MIX K OPT.2	MIX K OPT.2
5.9	291.48	92.446	31.716	31.5945
5.8	291.48	114.74	39.363	39.2309
5.8	291.48	107.14	36.755	36.6279
			LABVIEW	MATLAB
MIX K TRIAL 1.1			MIX K TRIAL 1.1	MIX K TRIAL 1.1
5.8	291.48	133.95	45.954	45.8126
6.3	291.48	148.67	51.005	50.8734
6.8	291.48	148.78	51.041	50.92
			LABVIEW	MATLAB
MIX K TRIAL 1.2			MIX K TRIAL 1.2	MIX K TRIAL 1.2
5.8	291.48	134.12	46.014	45.8682
6.3	291.48	148.74	51.03	50.9013
6.8	291.48	148.68	51.009	50.8867
			LABVIEW	MATLAB
MIX K TRIAL 2.1			MIX K TRIAL 2.1	MIX K TRIAL 2.1
5.8	291.48	117.14	40.189	40.0503
6.3	291.48	153.64	52.711	52.5922
6.8	291.48	195.57	67.095	66.9759
			LABVIEW	MATLAB
MIX K TRIAL 2.2			MIX K TRIAL 2.2	MIX K TRIAL 2.2
5.8	291.48	117.62	40.351	40.2119
6.3	291.48	153.64	52.711	52.5922
6.8	291.48	195.91	67.212	67.0911
			LABVIEW	MATLAB
MIX K TRIAL 3.1			MIX K TRIAL 3.1	MIX K TRIAL 3.1
5.8	291.48	116.13	39.84	39.712
6.3	291.48	146.11	50.125	49.986
6.8	291.48	173.79	59.623	59.508
			LABVIEW	MATLAB
MIX K TRIAL 3.2			MIX K TRIAL 3.2	MIX K TRIAL 3.2
5.8	291.48	116.96	40.127	39.9882
6.3	291.48	146.09	50.118	49.9882
6.8	291.48	173.79	59.623	59.508

Figure E11 Labview versus Matlab digital image results -mix K.

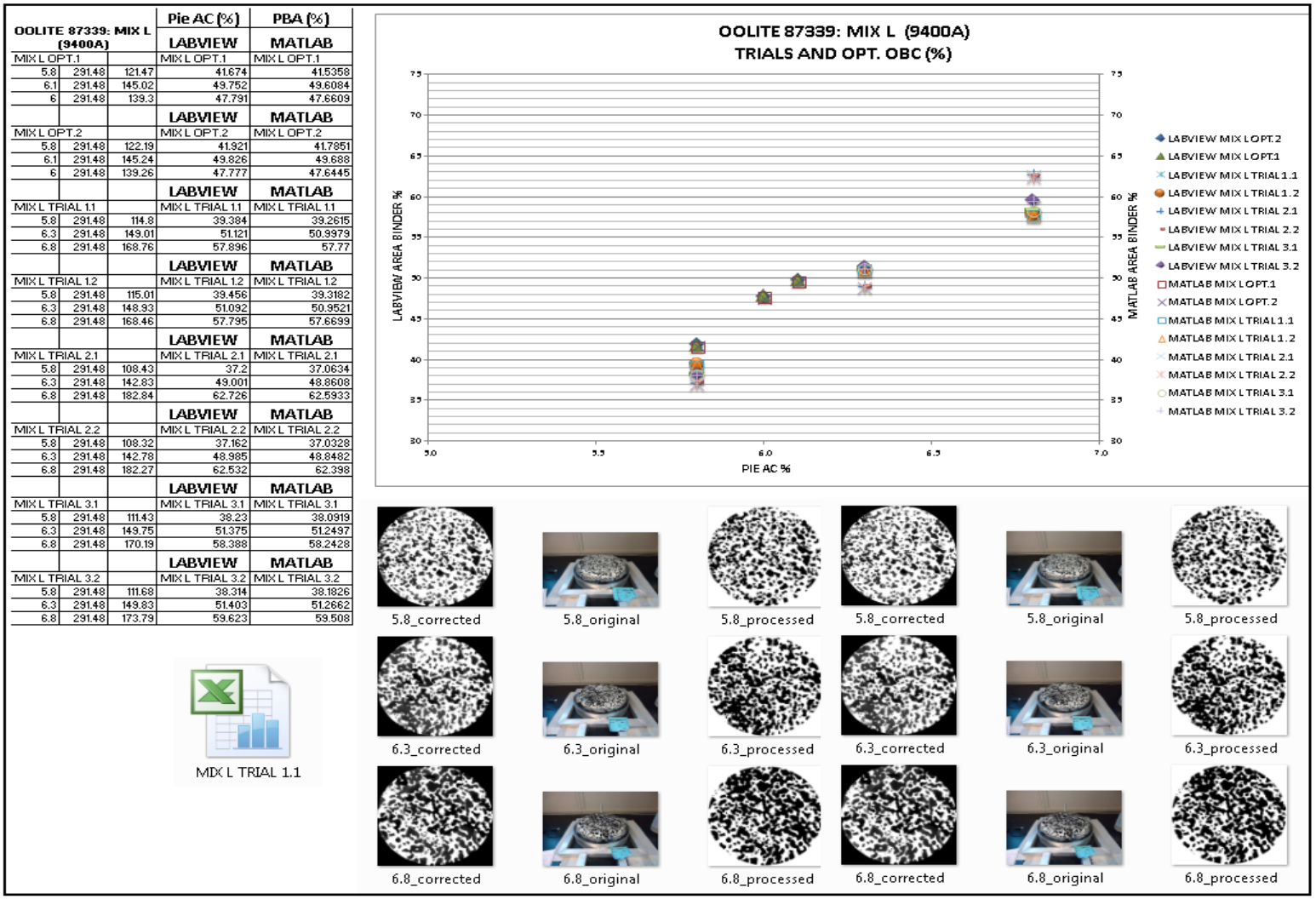

OOLITE 87339: MIX L (9400A)			Pie AC (%)	PBA (%)
			LABVIEW	MATLAB
MIX L OPT.1			MIX L OPT.1	MIX L OPT.1
5.8	291.48	121.47	41.674	41.5358
6.1	291.48	145.02	49.752	49.6084
6	291.48	139.3	47.791	47.6609
			LABVIEW	MATLAB
MIX L OPT.2			MIX L OPT.2	MIX L OPT.2
5.8	291.48	122.19	41.921	41.7851
6.1	291.48	145.24	49.826	49.688
6	291.48	139.26	47.777	47.6445
			LABVIEW	MATLAB
MIX L TRIAL 1.1			MIX L TRIAL 1.1	MIX L TRIAL 1.1
5.8	291.48	114.8	39.384	39.2615
6.3	291.48	149.01	51.121	50.9979
6.8	291.48	168.76	57.896	57.77
			LABVIEW	MATLAB
MIX L TRIAL 1.2			MIX L TRIAL 1.2	MIX L TRIAL 1.2
5.8	291.48	115.01	39.456	39.3182
6.3	291.48	148.93	51.092	50.9521
6.8	291.48	168.46	57.795	57.6699
			LABVIEW	MATLAB
MIX L TRIAL 2.1			MIX L TRIAL 2.1	MIX L TRIAL 2.1
5.8	291.48	108.43	37.2	37.0634
6.3	291.48	142.83	49.001	48.8608
6.8	291.48	182.84	62.726	62.5933
			LABVIEW	MATLAB
MIX L TRIAL 2.2			MIX L TRIAL 2.2	MIX L TRIAL 2.2
5.8	291.48	108.32	37.162	37.0328
6.3	291.48	142.78	48.985	48.8482
6.8	291.48	182.27	62.532	62.398
			LABVIEW	MATLAB
MIX L TRIAL 3.1			MIX L TRIAL 3.1	MIX L TRIAL 3.1
5.8	291.48	111.43	38.23	38.0919
6.3	291.48	149.75	51.375	51.2497
6.8	291.48	170.19	58.388	58.2428
			LABVIEW	MATLAB
MIX L TRIAL 3.2			MIX L TRIAL 3.2	MIX L TRIAL 3.2
5.8	291.48	111.68	38.314	38.1826
6.3	291.48	149.83	51.403	51.2662
6.8	291.48	173.79	59.623	59.508

Figure E12 Labview versus Matlab digital image results -mix L.

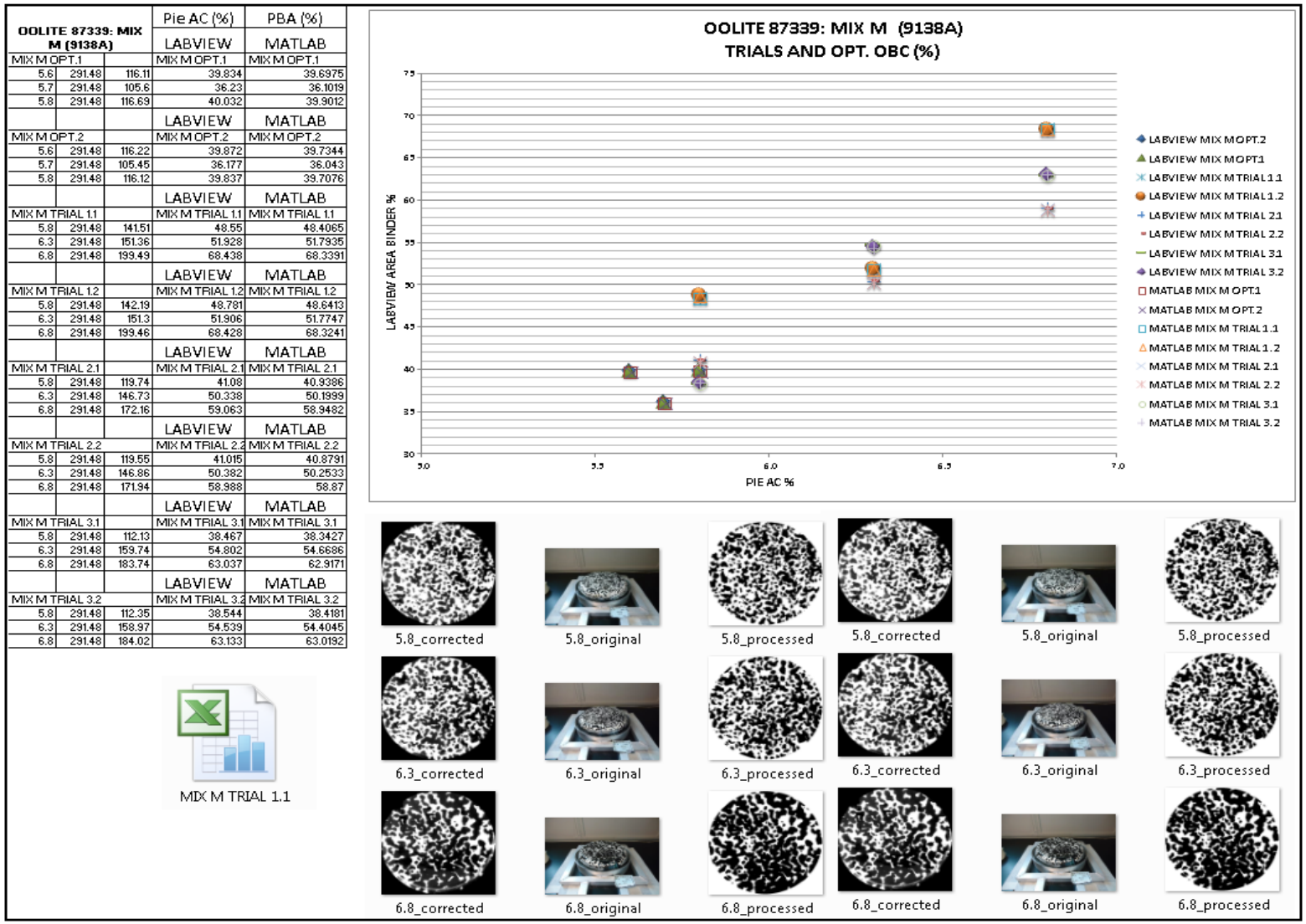

OOLITE 87339: MIX M (9138A)			Pie AC (%)	PBA (%)
			LABVIEW	MATLAB
MIX M OPT.1			MIX M OPT.1	MIX M OPT.1
5.6	291.48	116.11	39.834	39.6975
5.7	291.48	105.6	36.23	36.1019
5.8	291.48	116.69	40.032	39.9012
			LABVIEW	MATLAB
MIX M OPT.2			MIX M OPT.2	MIX M OPT.2
5.6	291.48	116.22	39.872	39.7344
5.7	291.48	105.45	36.177	36.043
5.8	291.48	116.12	39.837	39.7076
			LABVIEW	MATLAB
MIX M TRIAL 1.1			MIX M TRIAL 1.1	MIX M TRIAL 1.1
5.8	291.48	141.51	48.55	48.4065
6.3	291.48	151.36	51.928	51.7935
6.8	291.48	199.49	68.438	68.3391
			LABVIEW	MATLAB
MIX M TRIAL 1.2			MIX M TRIAL 1.2	MIX M TRIAL 1.2
5.8	291.48	142.19	48.781	48.6413
6.3	291.48	151.3	51.906	51.7747
6.8	291.48	199.46	68.428	68.3241
			LABVIEW	MATLAB
MIX M TRIAL 2.1			MIX M TRIAL 2.1	MIX M TRIAL 2.1
5.8	291.48	119.74	41.08	40.9386
6.3	291.48	146.73	50.338	50.1999
6.8	291.48	172.16	59.063	58.9482
			LABVIEW	MATLAB
MIX M TRIAL 2.2			MIX M TRIAL 2.2	MIX M TRIAL 2.2
5.8	291.48	119.55	41.015	40.8791
6.3	291.48	146.86	50.382	50.2533
6.8	291.48	171.94	58.988	58.87
			LABVIEW	MATLAB
MIX M TRIAL 3.1			MIX M TRIAL 3.1	MIX M TRIAL 3.1
5.8	291.48	112.13	38.467	38.3427
6.3	291.48	159.74	54.802	54.6686
6.8	291.48	183.74	63.037	62.9171
			LABVIEW	MATLAB
MIX M TRIAL 3.2			MIX M TRIAL 3.2	MIX M TRIAL 3.2
5.8	291.48	112.35	38.544	38.4181
6.3	291.48	158.97	54.539	54.4045
6.8	291.48	184.02	63.133	63.0192

Figure E13 Labview versus Matlab digital image results -mix M.

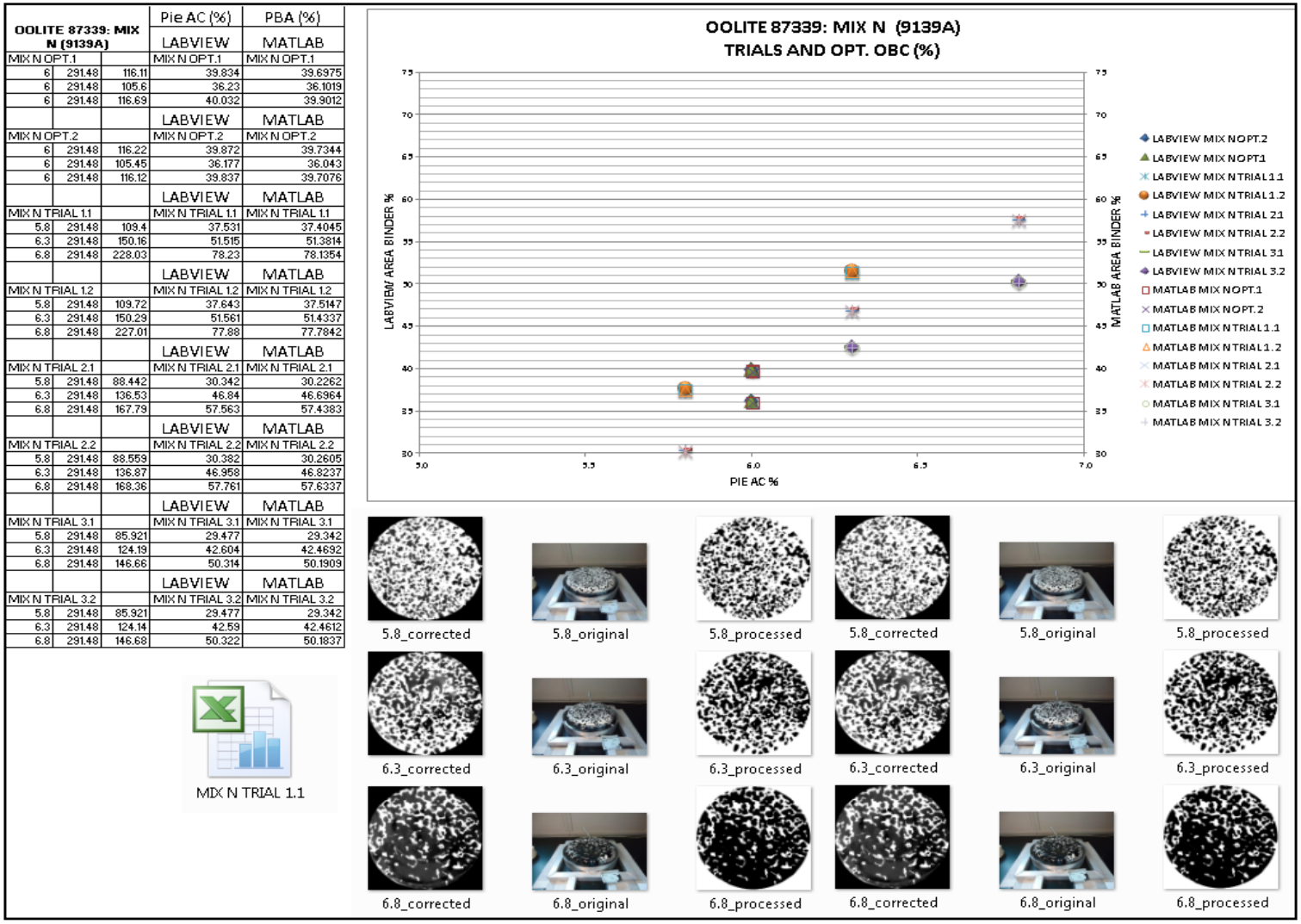

OOLITE 87339: MIX N (9139A)			Pie AC (%)	PBA (%)
			LABVIEW	MATLAB
MIX N OPT.1			MIX N OPT.1	MIX N OPT.1
6	291.48	116.11	39.834	39.6975
6	291.48	105.6	36.23	36.1019
6	291.48	116.69	40.032	39.9012
			LABVIEW	MATLAB
MIX N OPT.2			MIX N OPT.2	MIX N OPT.2
6	291.48	116.22	39.872	39.7344
6	291.48	105.45	36.177	36.043
6	291.48	116.12	39.837	39.7076
			LABVIEW	MATLAB
MIX N TRIAL 1.1			MIX N TRIAL 1.1	MIX N TRIAL 1.1
5.8	291.48	109.4	37.531	37.4045
6.3	291.48	150.16	51.515	51.3814
6.8	291.48	228.03	78.23	78.1354
			LABVIEW	MATLAB
MIX N TRIAL 1.2			MIX N TRIAL 1.2	MIX N TRIAL 1.2
5.8	291.48	109.72	37.643	37.5147
6.3	291.48	150.29	51.561	51.4337
6.8	291.48	227.01	77.88	77.7842
			LABVIEW	MATLAB
MIX N TRIAL 2.1			MIX N TRIAL 2.1	MIX N TRIAL 2.1
5.8	291.48	88.442	30.342	30.2262
6.3	291.48	136.53	46.84	46.6964
6.8	291.48	167.79	57.563	57.4383
			LABVIEW	MATLAB
MIX N TRIAL 2.2			MIX N TRIAL 2.2	MIX N TRIAL 2.2
5.8	291.48	88.559	30.382	30.2605
6.3	291.48	136.87	46.958	46.8237
6.8	291.48	168.36	57.761	57.6337
			LABVIEW	MATLAB
MIX N TRIAL 3.1			MIX N TRIAL 3.1	MIX N TRIAL 3.1
5.8	291.48	85.921	29.477	29.342
6.3	291.48	124.19	42.604	42.4692
6.8	291.48	146.66	50.314	50.1909
			LABVIEW	MATLAB
MIX N TRIAL 3.2			MIX N TRIAL 3.2	MIX N TRIAL 3.2
5.8	291.48	85.921	29.477	29.342
6.3	291.48	124.14	42.59	42.4612
6.8	291.48	146.68	50.322	50.1837

Figure E14 Labview versus Matlab digital image results -mix N.

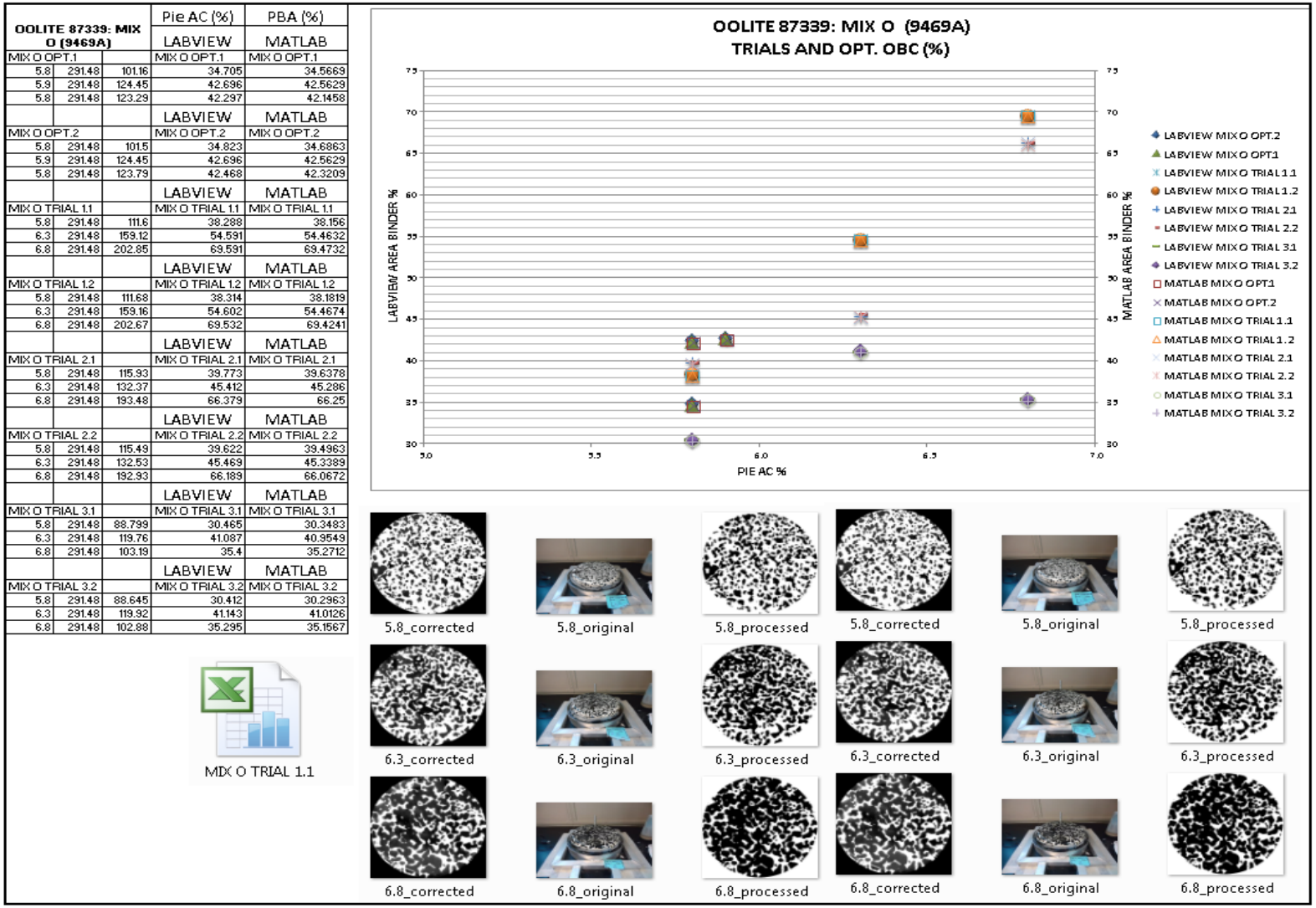

OOLITE 87339: MIX O (9469A)			Pie AC (%)	PBA (%)
			LABVIEW	MATLAB
MIX O OPT.1			MIX O OPT.1	MIX O OPT.1
5.8	291.48	101.16	34.705	34.5669
5.9	291.48	124.45	42.696	42.5629
5.8	291.48	123.29	42.297	42.1458
			LABVIEW	MATLAB
MIX O OPT.2			MIX O OPT.2	MIX O OPT.2
5.8	291.48	101.5	34.823	34.6863
5.9	291.48	124.45	42.696	42.5629
5.8	291.48	123.79	42.468	42.3209
			LABVIEW	MATLAB
MIX O TRIAL 1.1			MIX O TRIAL 1.1	MIX O TRIAL 1.1
5.8	291.48	111.6	38.288	38.156
6.3	291.48	159.12	54.591	54.4632
6.8	291.48	202.85	69.591	69.4732
			LABVIEW	MATLAB
MIX O TRIAL 1.2			MIX O TRIAL 1.2	MIX O TRIAL 1.2
5.8	291.48	111.68	38.314	38.1819
6.3	291.48	159.16	54.602	54.4674
6.8	291.48	202.67	69.532	69.4241
			LABVIEW	MATLAB
MIX O TRIAL 2.1			MIX O TRIAL 2.1	MIX O TRIAL 2.1
5.8	291.48	115.93	39.773	39.6378
6.3	291.48	132.37	45.412	45.286
6.8	291.48	193.48	66.379	66.25
			LABVIEW	MATLAB
MIX O TRIAL 2.2			MIX O TRIAL 2.2	MIX O TRIAL 2.2
5.8	291.48	115.49	39.622	39.4963
6.3	291.48	132.53	45.469	45.3389
6.8	291.48	192.93	66.189	66.0672
			LABVIEW	MATLAB
MIX O TRIAL 3.1			MIX O TRIAL 3.1	MIX O TRIAL 3.1
5.8	291.48	88.799	30.465	30.3483
6.3	291.48	119.76	41.087	40.9549
6.8	291.48	103.19	35.4	35.2712
			LABVIEW	MATLAB
MIX O TRIAL 3.2			MIX O TRIAL 3.2	MIX O TRIAL 3.2
5.8	291.48	88.645	30.412	30.2963
6.3	291.48	119.92	41.143	41.0126
6.8	291.48	102.88	35.295	35.1567

Figure E15 Labview versus Matlab digital image results -mix O.

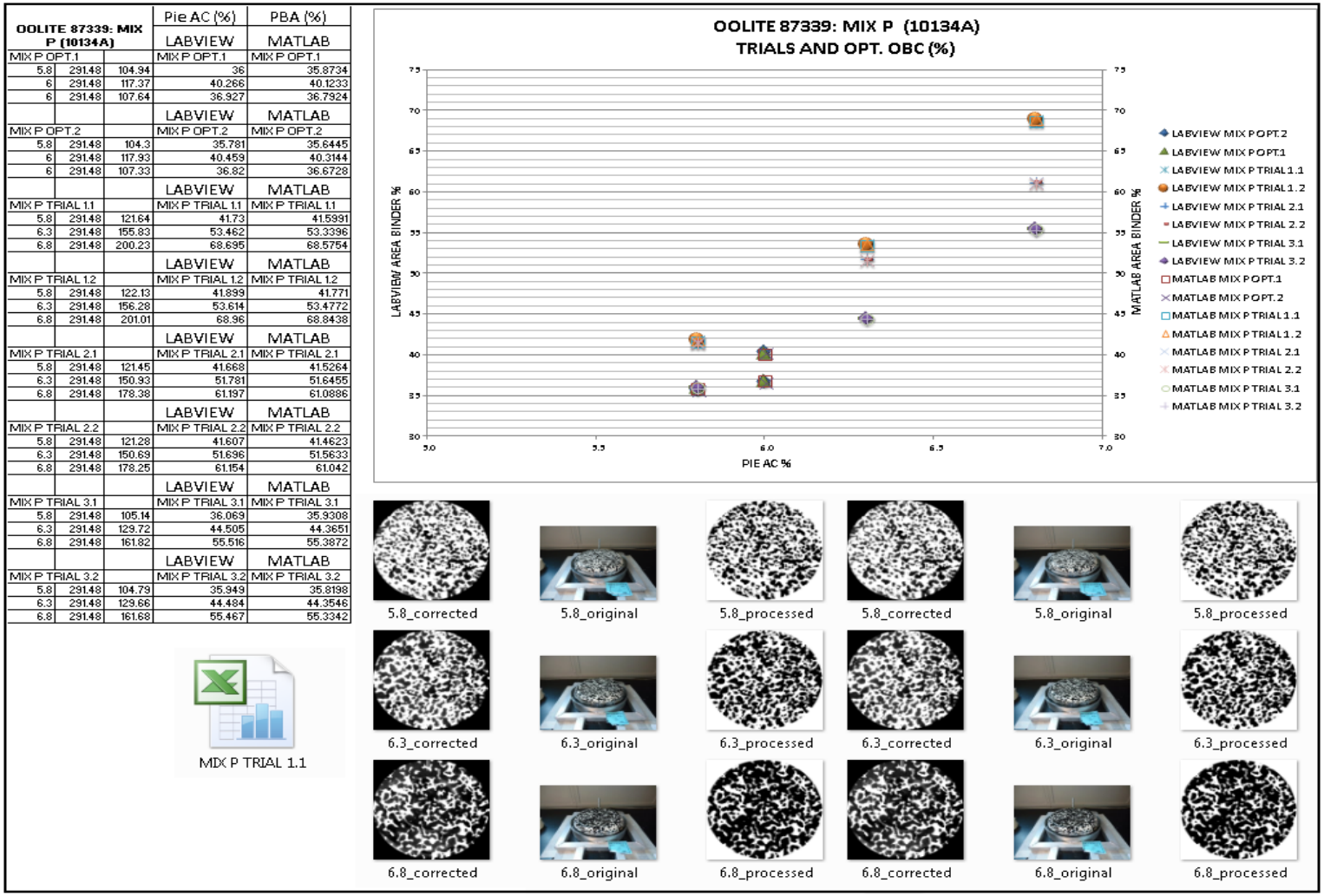

OOLITE 87339: MIX P (10134A)			Pie AC (%)	PBA (%)
			LABVIEW	MATLAB
MIX P OPT.1			MIX P OPT.1	MIX P OPT.1
5.8	291.48	104.94	36	35.8734
6	291.48	117.37	40.266	40.1233
6	291.48	107.64	36.927	36.7924
			LABVIEW	MATLAB
MIX P OPT.2			MIX P OPT.2	MIX P OPT.2
5.8	291.48	104.3	35.781	35.6445
6	291.48	117.93	40.459	40.3144
6	291.48	107.33	36.82	36.6728
			LABVIEW	MATLAB
MIX P TRIAL 1.1			MIX P TRIAL 1.1	MIX P TRIAL 1.1
5.8	291.48	121.64	41.73	41.5991
6.3	291.48	155.83	53.462	53.3396
6.8	291.48	200.23	68.695	68.5754
			LABVIEW	MATLAB
MIX P TRIAL 1.2			MIX P TRIAL 1.2	MIX P TRIAL 1.2
5.8	291.48	122.13	41.899	41.771
6.3	291.48	156.28	53.614	53.4772
6.8	291.48	201.01	68.96	68.8438
			LABVIEW	MATLAB
MIX P TRIAL 2.1			MIX P TRIAL 2.1	MIX P TRIAL 2.1
5.8	291.48	121.45	41.668	41.5264
6.3	291.48	150.93	51.781	51.6455
6.8	291.48	178.38	61.197	61.0886
			LABVIEW	MATLAB
MIX P TRIAL 2.2			MIX P TRIAL 2.2	MIX P TRIAL 2.2
5.8	291.48	121.28	41.607	41.4623
6.3	291.48	150.69	51.696	51.5633
6.8	291.48	178.25	61.154	61.042
			LABVIEW	MATLAB
MIX P TRIAL 3.1			MIX P TRIAL 3.1	MIX P TRIAL 3.1
5.8	291.48	105.14	36.069	35.9308
6.3	291.48	129.72	44.505	44.3651
6.8	291.48	161.82	55.516	55.3872
			LABVIEW	MATLAB
MIX P TRIAL 3.2			MIX P TRIAL 3.2	MIX P TRIAL 3.2
5.8	291.48	104.79	35.949	35.8198
6.3	291.48	129.66	44.484	44.3546
6.8	291.48	161.68	55.467	55.3342

Figure E16 Labview versus Matlab digital image results -mix P.

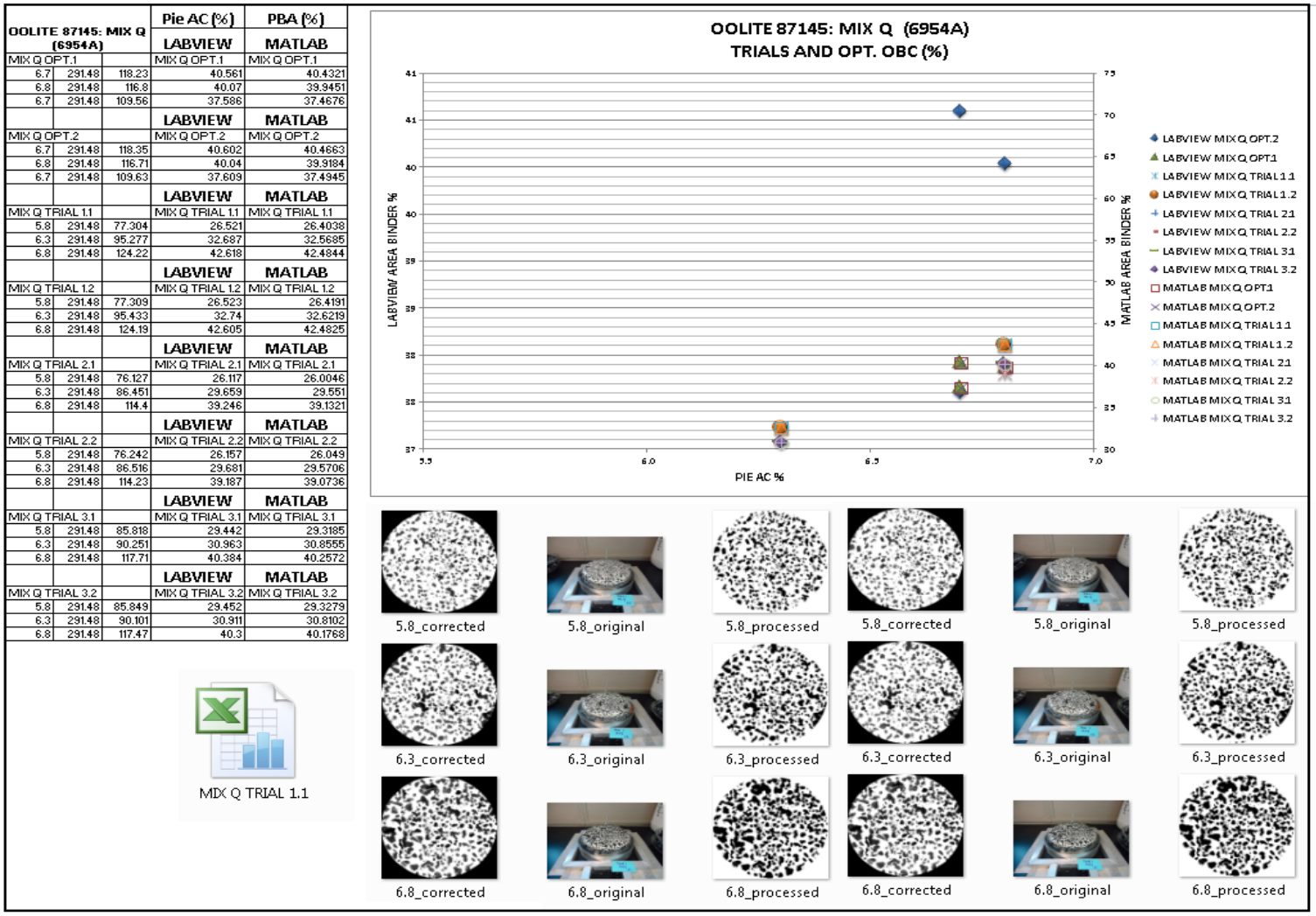

Figure E17 Labview versus Matlab digital image results -mix Q.

OOLITE 87145: MIX R (7806A)			Pie AC (%)	PBA (%)
			LABVIEW	MATLAB
MIX R OPT.1			MIX R OPT.1	MIX R OPT.1
7	291.48	139.99	48.026	47.884
6.7	291.48	105.32	36.134	36.0109
6.9	291.48	117.53	40.321	40.2007
			LABVIEW	MATLAB
MIX R OPT.2			MIX R OPT.2	MIX R OPT.2
7	291.48	140	48.029	47.8916
6.7	291.48	104.81	35.957	35.8374
6.9	291.48	117.33	40.251	40.1251
			LABVIEW	MATLAB
MIX R TRIAL 1.1			MIX R TRIAL 1.1	MIX R TRIAL 1.1
5.8	291.48	65.21	22.372	22.2663
6.3	291.48	83.427	28.622	28.5102
6.8	291.48	104.72	35.925	35.7991
			LABVIEW	MATLAB
MIX R TRIAL 1.2			MIX R TRIAL 1.2	MIX R TRIAL 1.2
5.8	291.48	65.635	22.518	22.4231
6.3	291.48	83.248	28.56	28.4545
6.8	291.48	104.68	35.913	35.7897
			LABVIEW	MATLAB
MIX R TRIAL 2.1			MIX R TRIAL 2.1	MIX R TRIAL 2.1
5.8	291.48	75.732	25.982	25.8694
6.3	291.48	105.42	36.165	36.025
6.8	291.48	134.57	46.166	46.0434
			LABVIEW	MATLAB
MIX R TRIAL 2.2			MIX R TRIAL 2.2	MIX R TRIAL 2.2
5.8	291.48	76.443	26.225	26.1168
6.3	291.48	105.05	36.039	35.9066
6.8	291.48	134.41	46.113	45.9778
			LABVIEW	MATLAB
MIX R TRIAL 3.1			MIX R TRIAL 3.1	MIX R TRIAL 3.1
5.8	291.48	60.942	20.908	20.803
6.3	291.48	88.732	30.442	30.3219
6.8	291.48	102.88	35.295	35.1679
			LABVIEW	MATLAB
MIX R TRIAL 3.2			MIX R TRIAL 3.2	MIX R TRIAL 3.2
5.8	291.48	61.003	20.928	20.8311
6.3	291.48	88.846	30.481	30.3688
6.8	291.48	102.65	35.216	35.0857

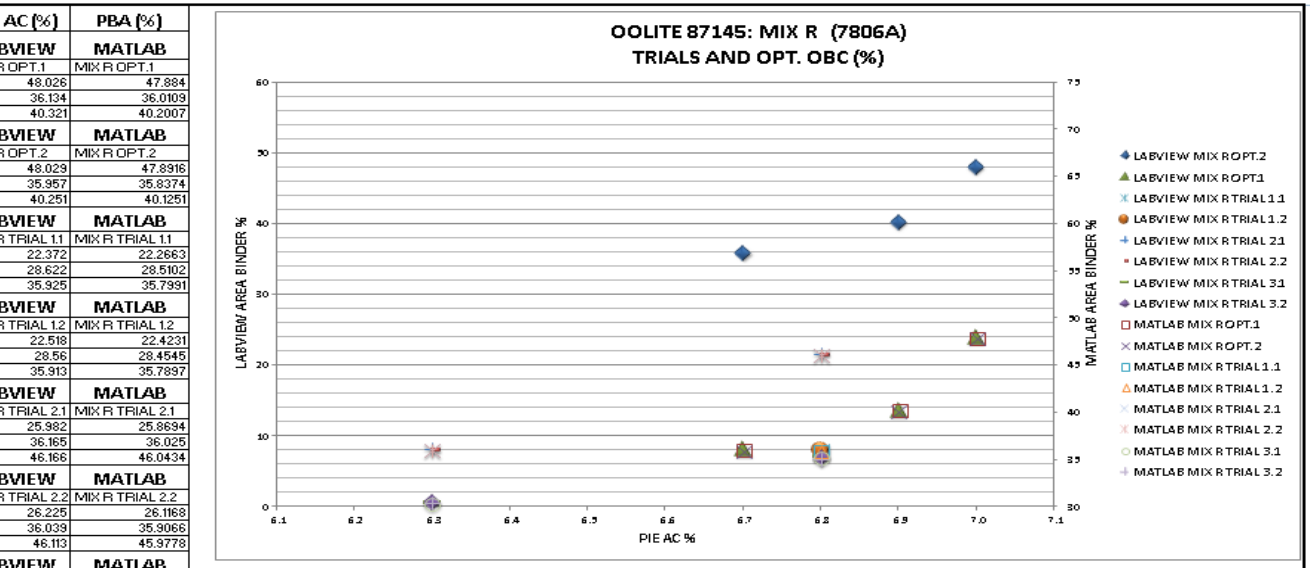

Figure E18 Labview versus Matlab digital image results -mix R.

OOLITE 87145: MIX S (9932A)	Pie AC (%)	PBA (%)
	LABVIEW	MATLAB
MIX S OPT.1	MIX S OPT.1	MIX S OPT.1
7	38.782	38.6549
6.8	40.065	39.929
6.7	33.611	33.4871
	LABVIEW	MATLAB
MIX S OPT.2	MIX S OPT.2	MIX S OPT.2
7	38.937	38.813
6.8	40.016	39.8797
6.7	33.602	33.4839
	LABVIEW	MATLAB
MIX S TRIAL 1.1	MIX S TRIAL 1.1	MIX S TRIAL 1.1
5.8	20.295	20.2023
6.3	27.322	27.2082
6.8	29.941	29.8208
	LABVIEW	MATLAB
MIX S TRIAL 1.2	MIX S TRIAL 1.2	MIX S TRIAL 1.2
5.8	20.324	20.2288
6.3	27.459	27.3497
6.8	29.87	29.7587
	LABVIEW	MATLAB
MIX S TRIAL 2.1	MIX S TRIAL 2.1	MIX S TRIAL 2.1
5.8	28.639	28.5147
6.3	33.756	33.6304
6.8	43.131	43.0015
	LABVIEW	MATLAB
MIX S TRIAL 2.2	MIX S TRIAL 2.2	MIX S TRIAL 2.2
5.8	28.658	28.5378
6.3	33.712	33.5813
6.8	43.09	42.9604
	LABVIEW	MATLAB
MIX S TRIAL 3.1	MIX S TRIAL 3.1	MIX S TRIAL 3.1
5.8	25.911	25.8011
6.3	37.142	37.002
6.8	42.366	42.2405
	LABVIEW	MATLAB
MIX S TRIAL 3.2	MIX S TRIAL 3.2	MIX S TRIAL 3.2
5.8	26.076	25.9646
6.3	36.626	36.4913
6.8	42.349	42.231

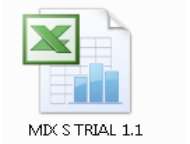

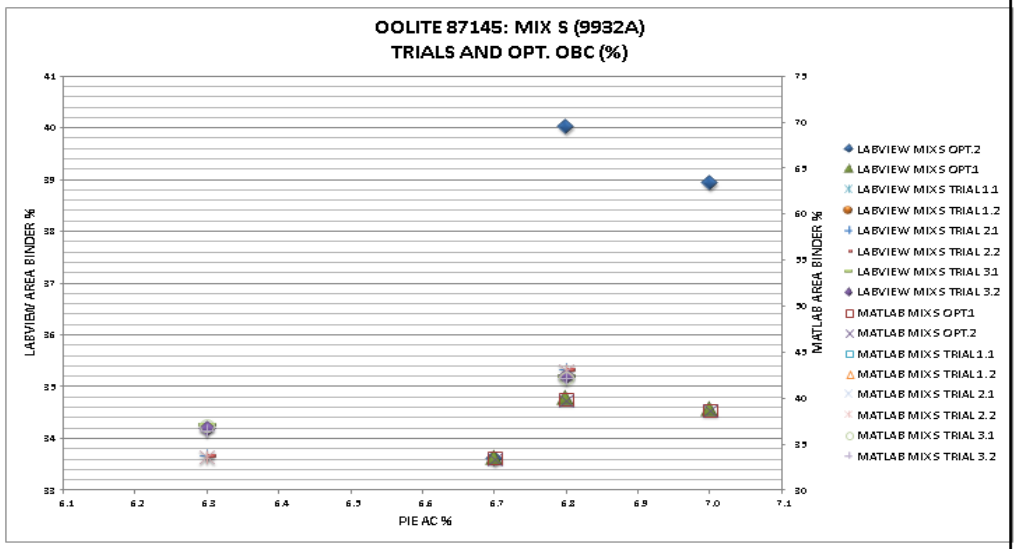

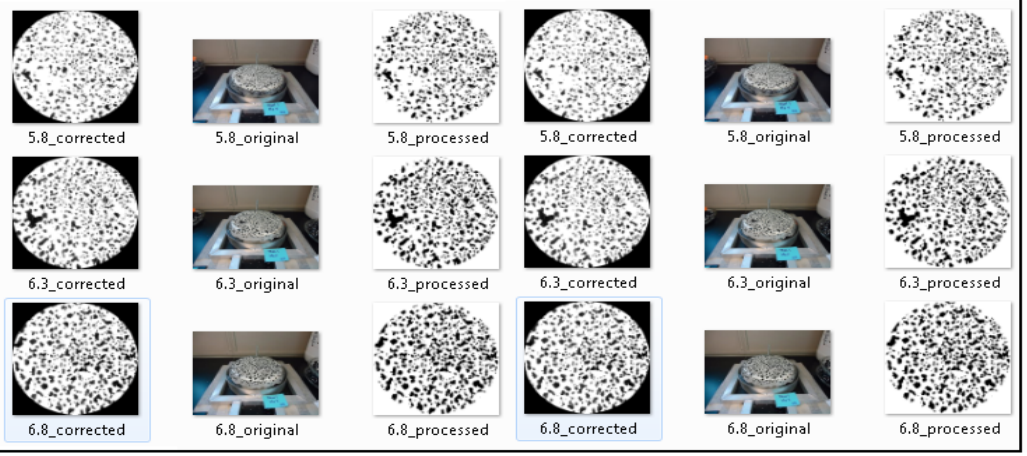

Figure E19 Labview versus Matlab digital image results -mix S.

APPENDIX F: RESULTS OF ASPHALT CONTENT CORRELATIONS

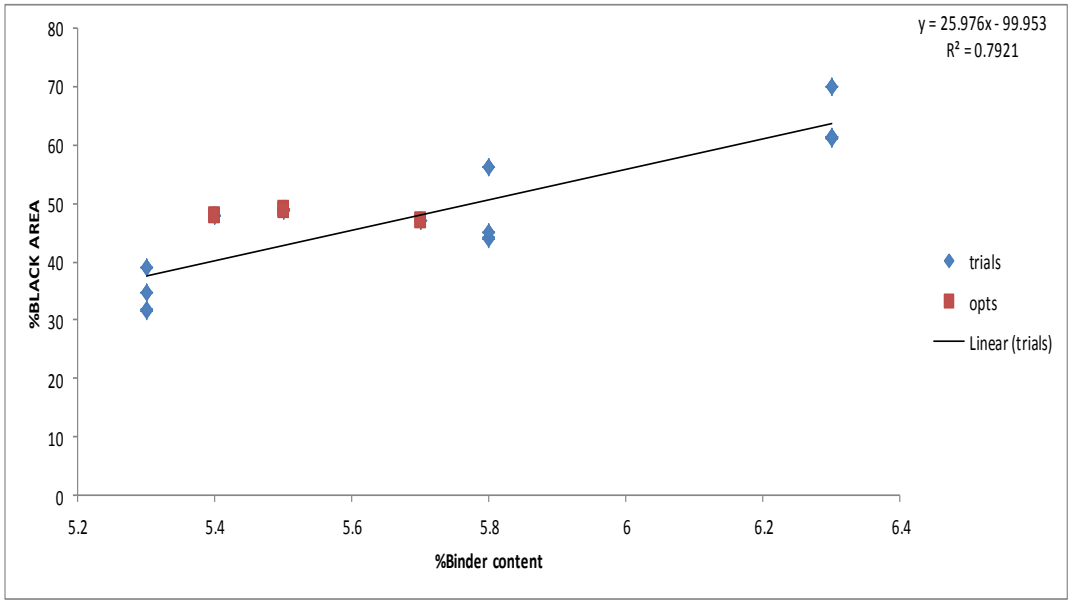

Figure F1 Mix A %black area versus %binder contents.

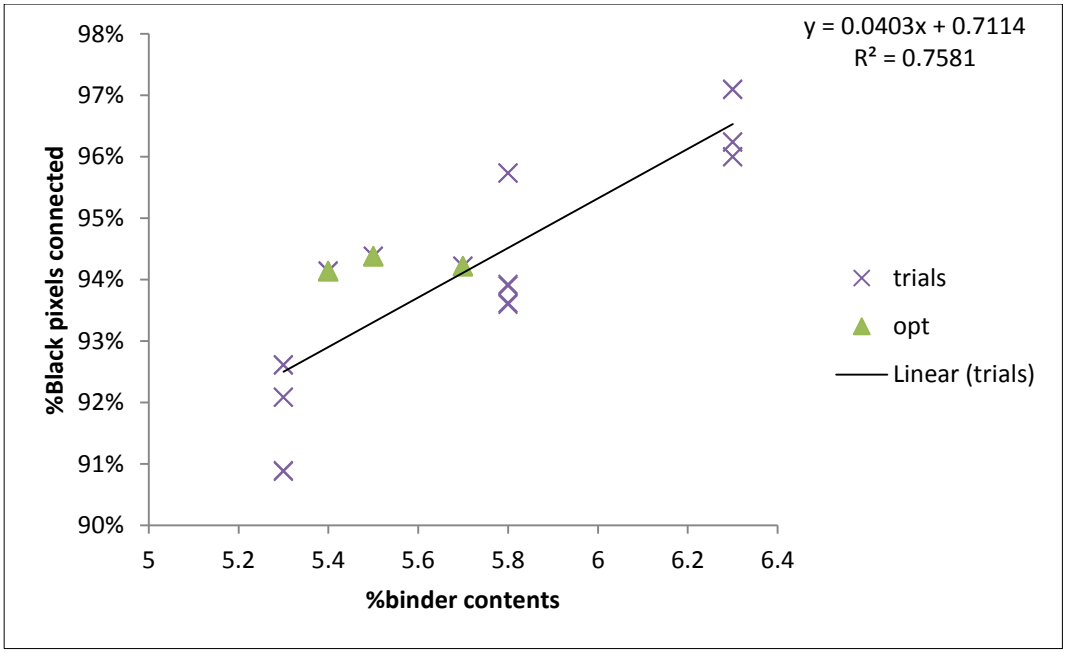

Figure F2 Mix A %connected black area versus %binder contents.

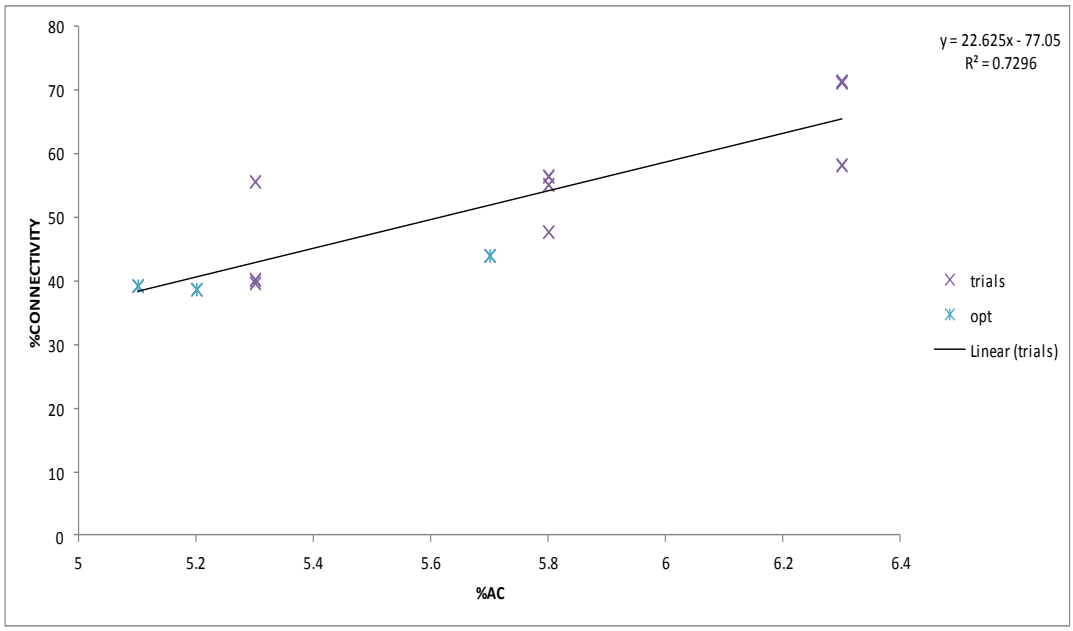

Figure F3 Mix B %black area versus %binder contents.

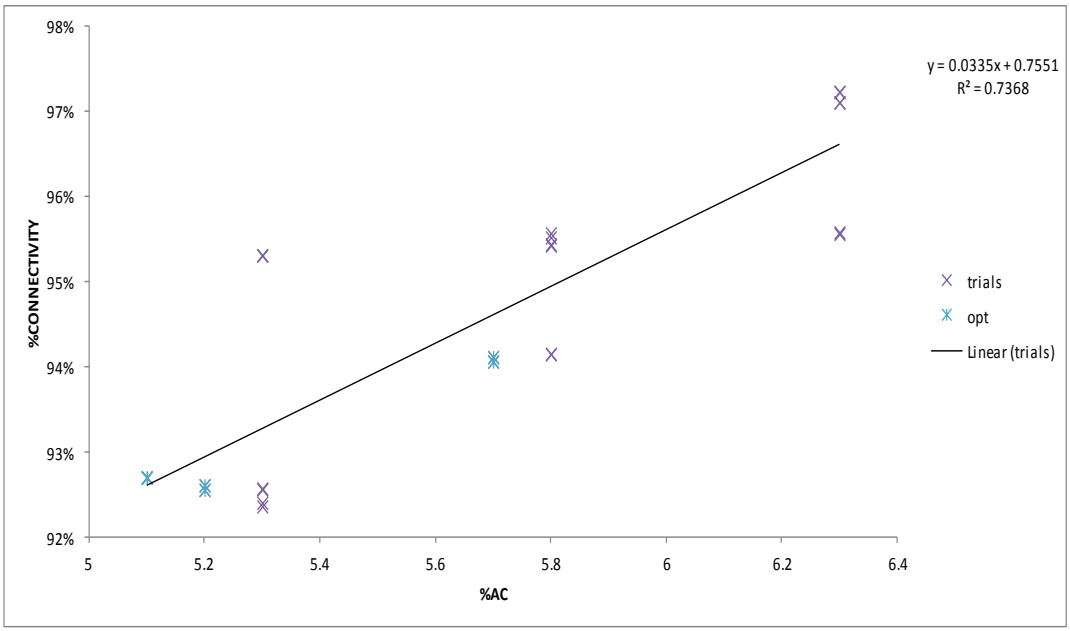

Figure F4 Mix B %connected black area versus %binder contents.

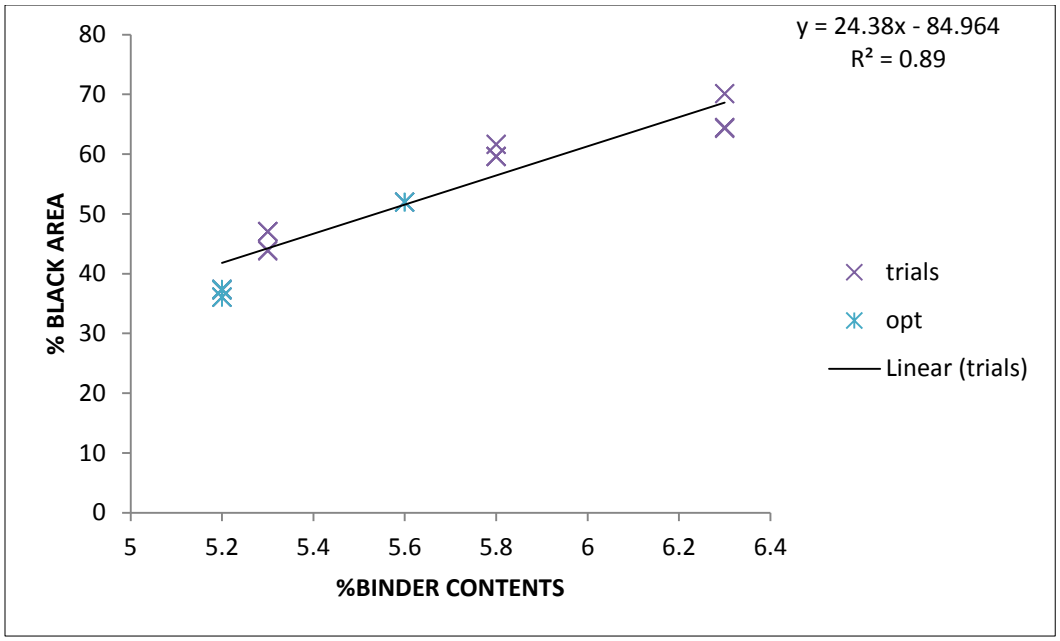

Figure F5 Mix C %black area versus %binder contents.

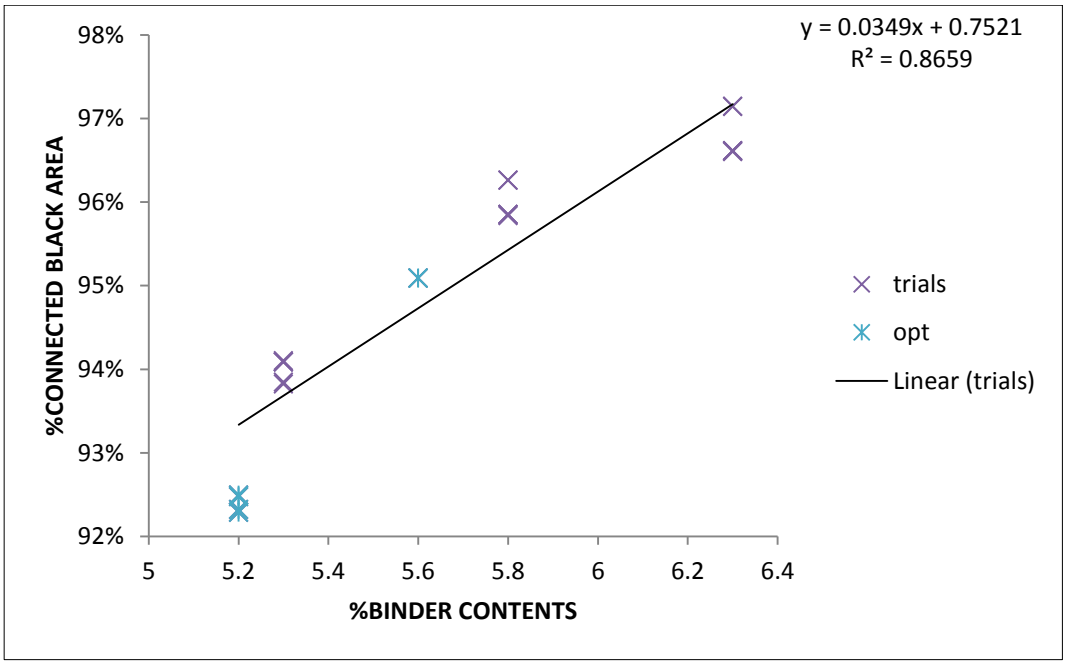

Figure F6 Mix C %connected black area versus %binder contents.

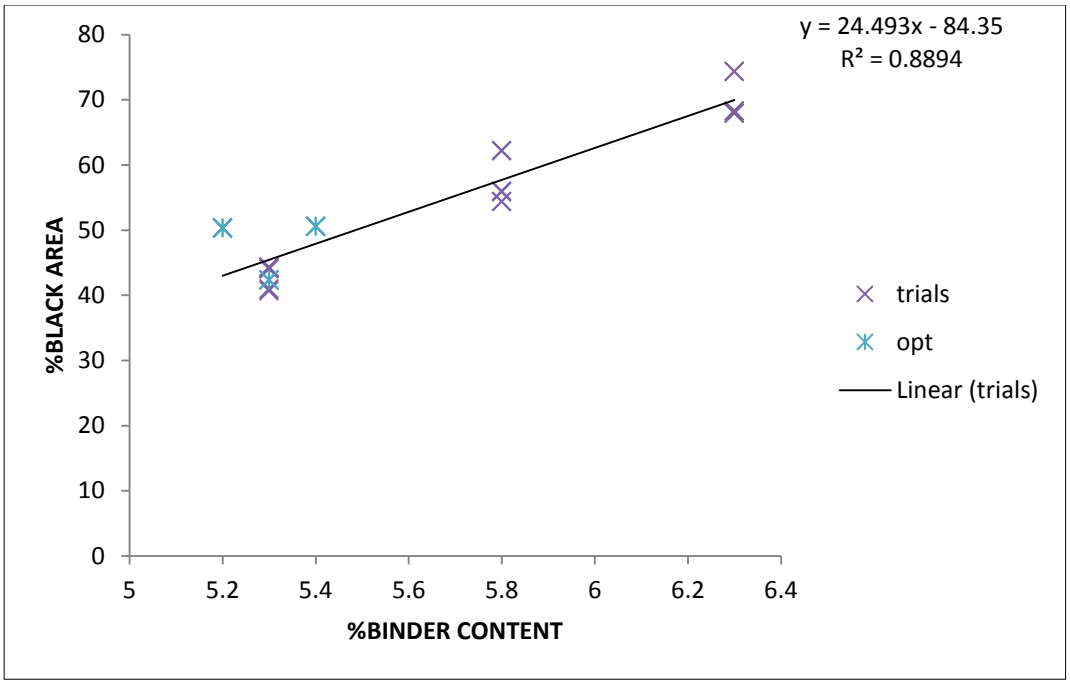

Figure F7 Mix D %black area versus %binder contents.

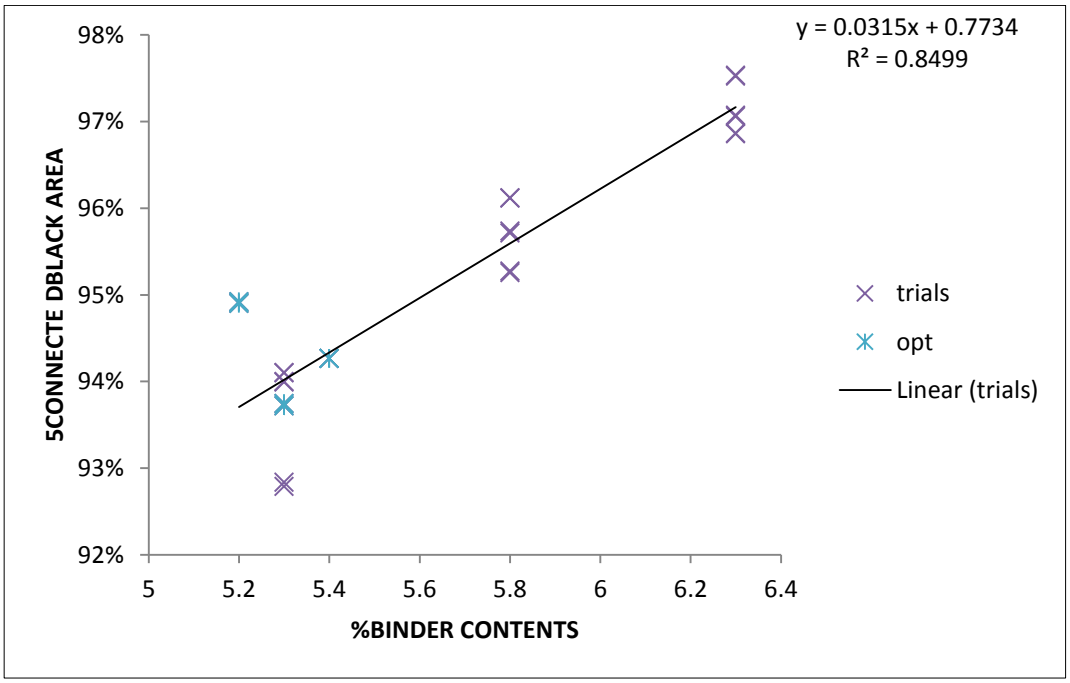

Figure F8 Mix D %connected black area versus %binder contents.

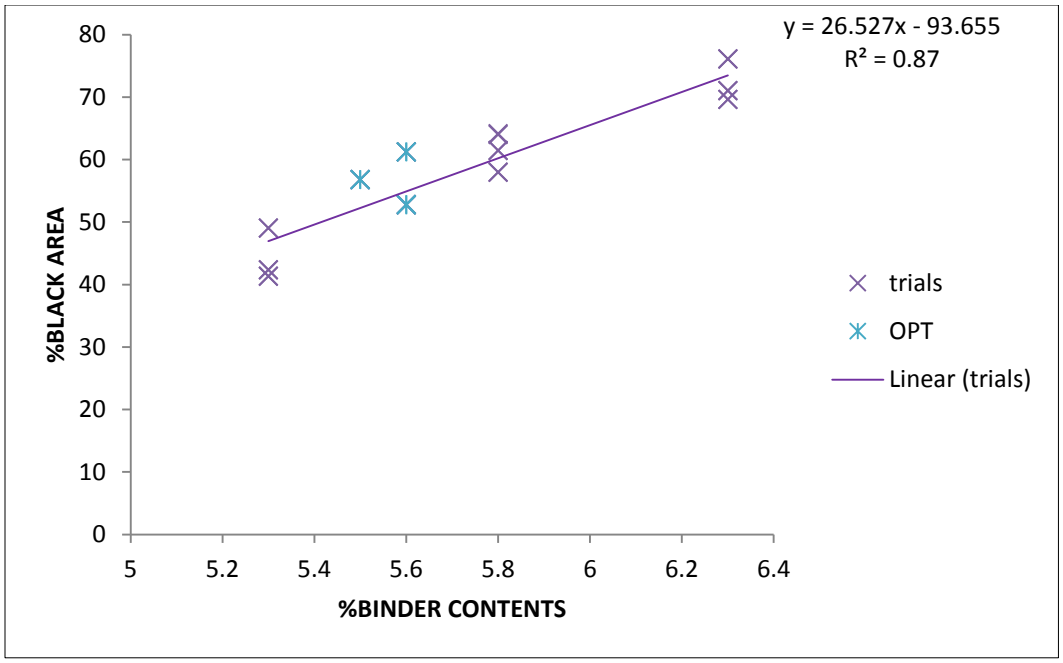

Figure F9 Mix E %black area versus %binder contents.

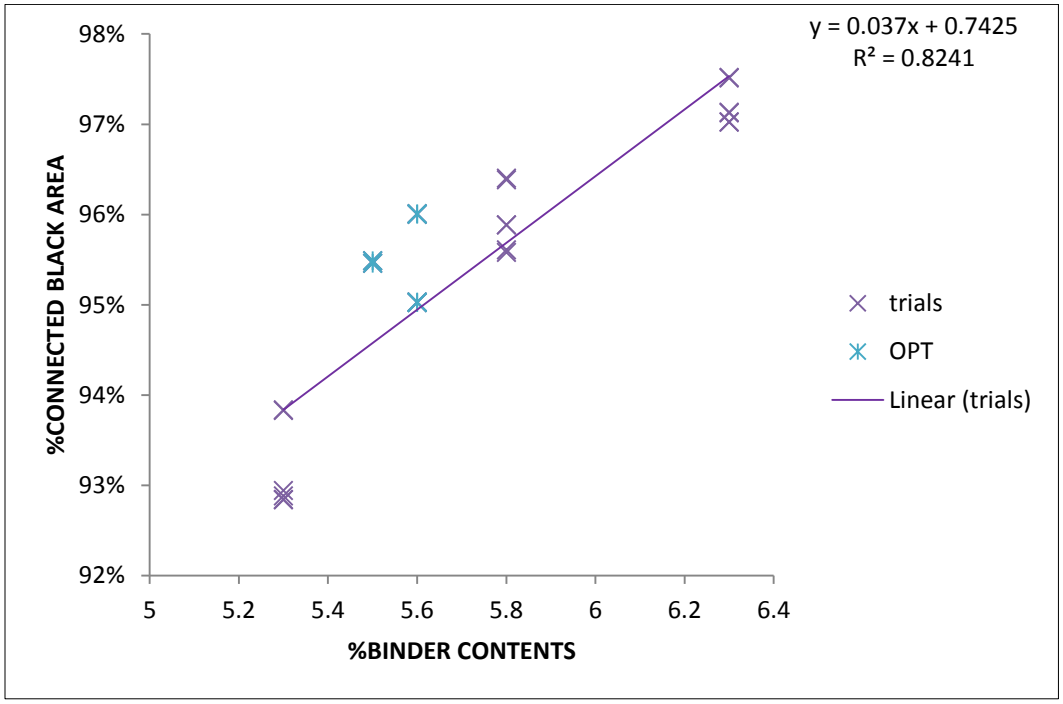

Figure F10 Mix E %connected black area versus %binder contents.

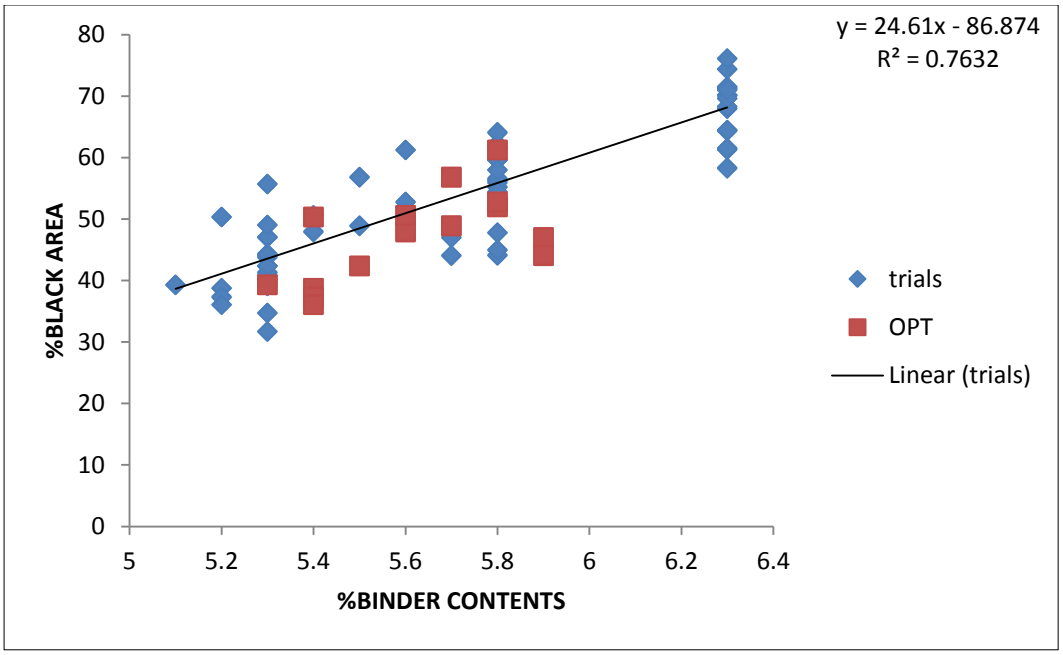

Figure F11 Mixtures NS315 %black area versus %binder contents.

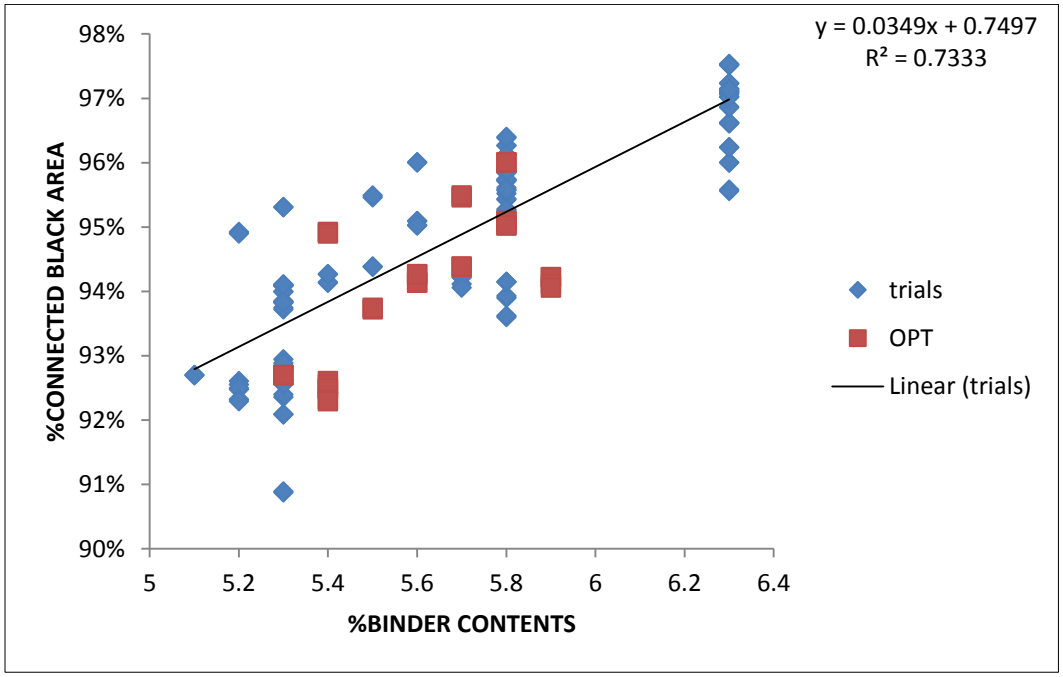

Figure F12 Mixtures NS315 %connected black area versus %binder contents.

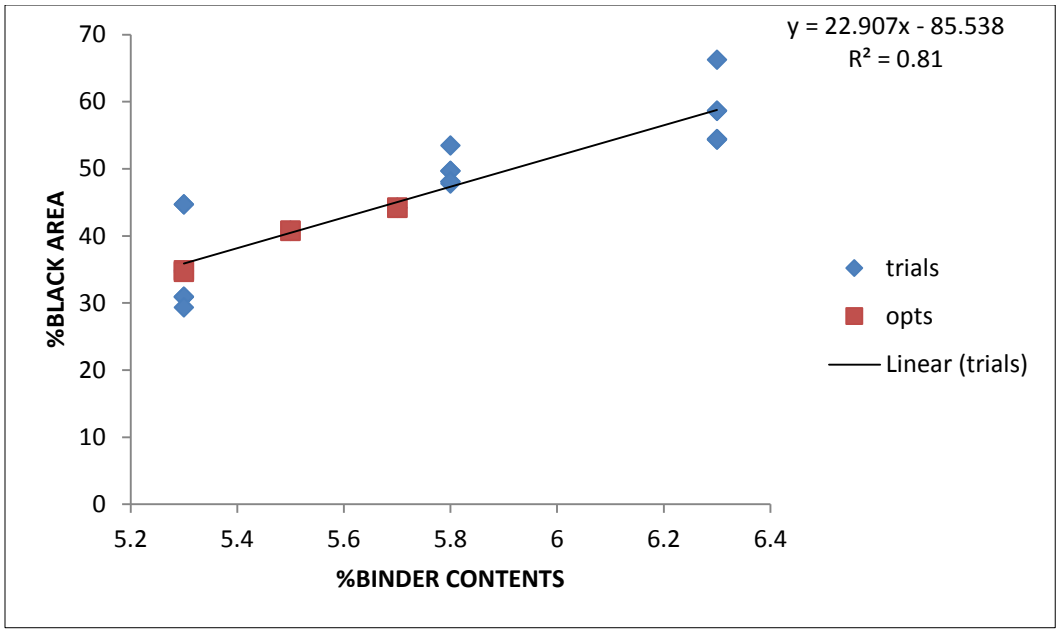

Figure F13 Mix F %black area versus %binder contents.

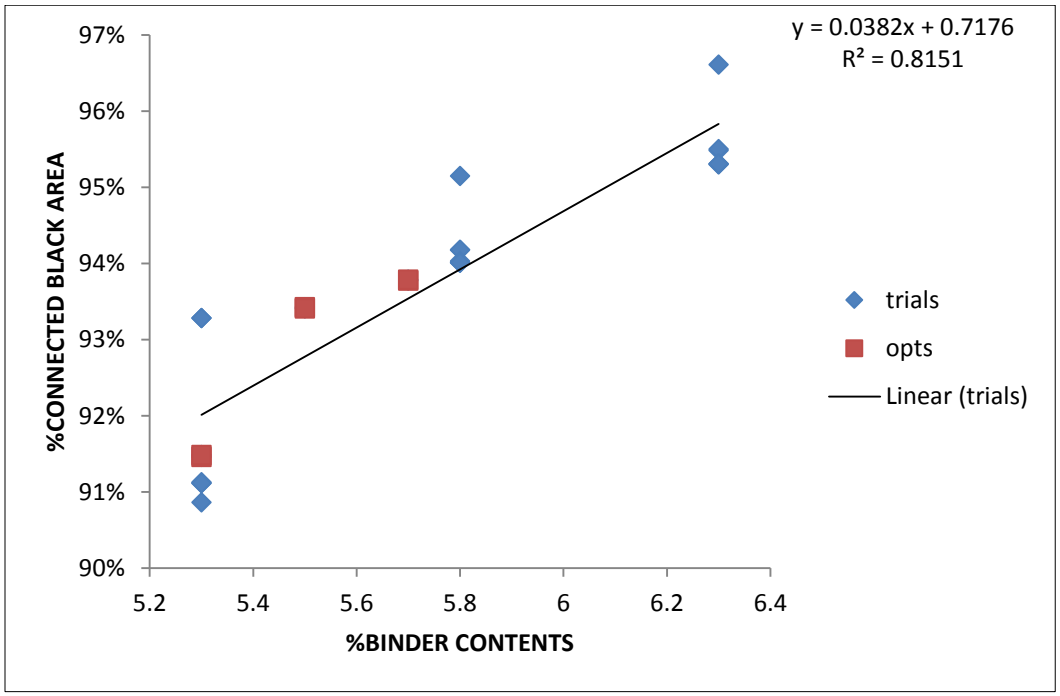

Figure F14 Mix F %connected black area versus %binder contents.

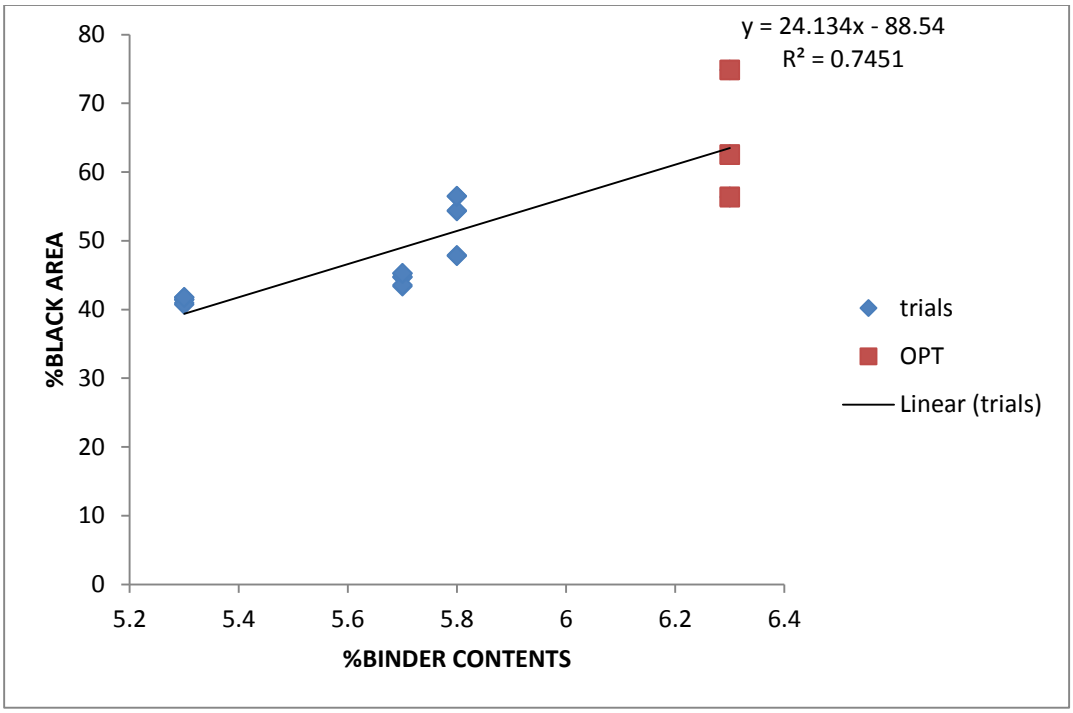

Figure F15 Mix G %black area versus %binder contents.

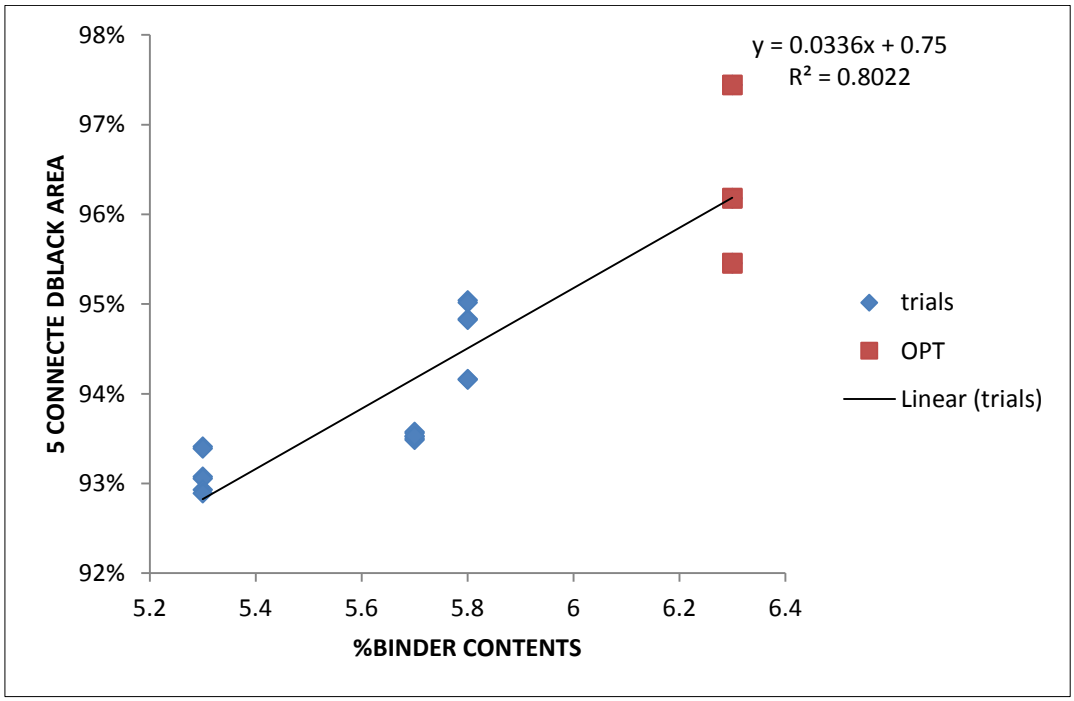

Figure F16 Mix G %connected black area versus %binder contents.

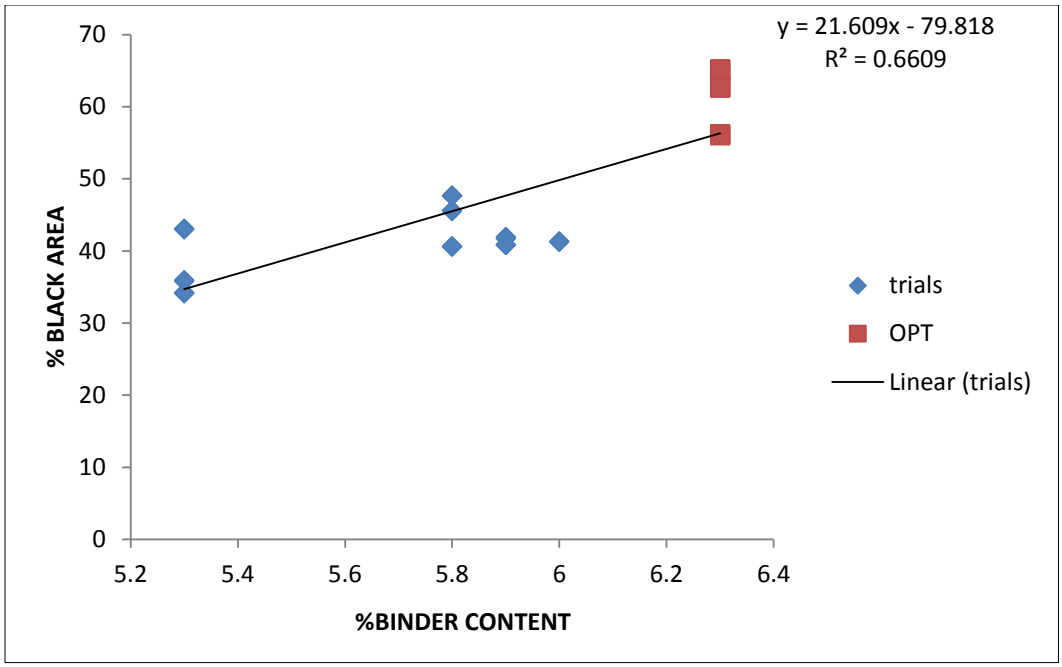

Figure F17 Mix H %black area versus %binder contents.

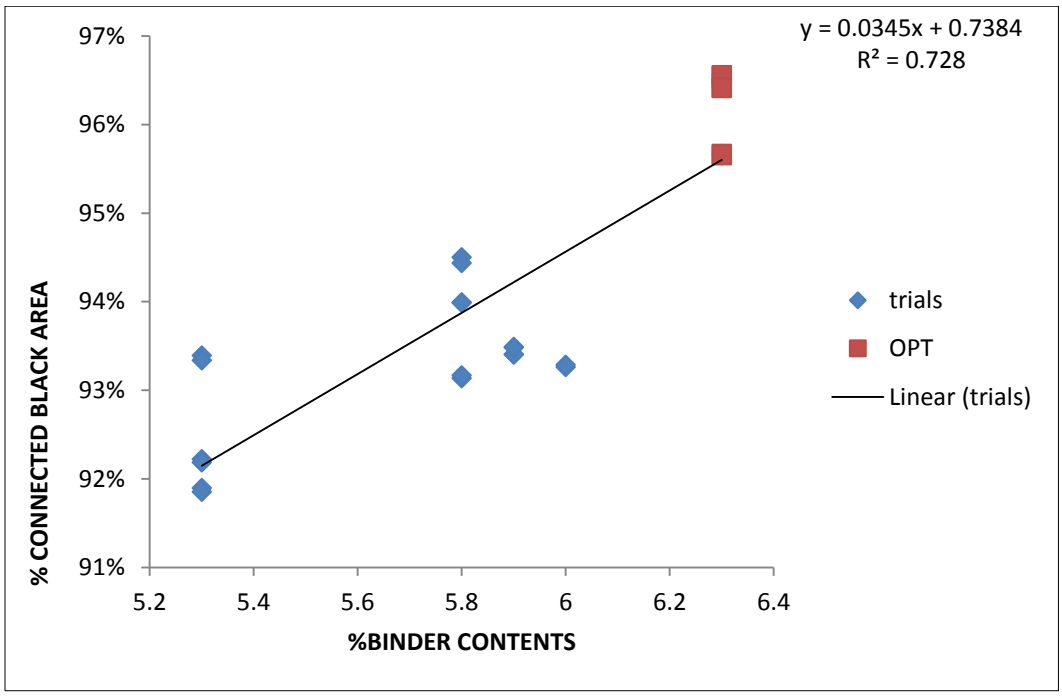

Figure F18 Mix H %connected black area versus %binder contents.

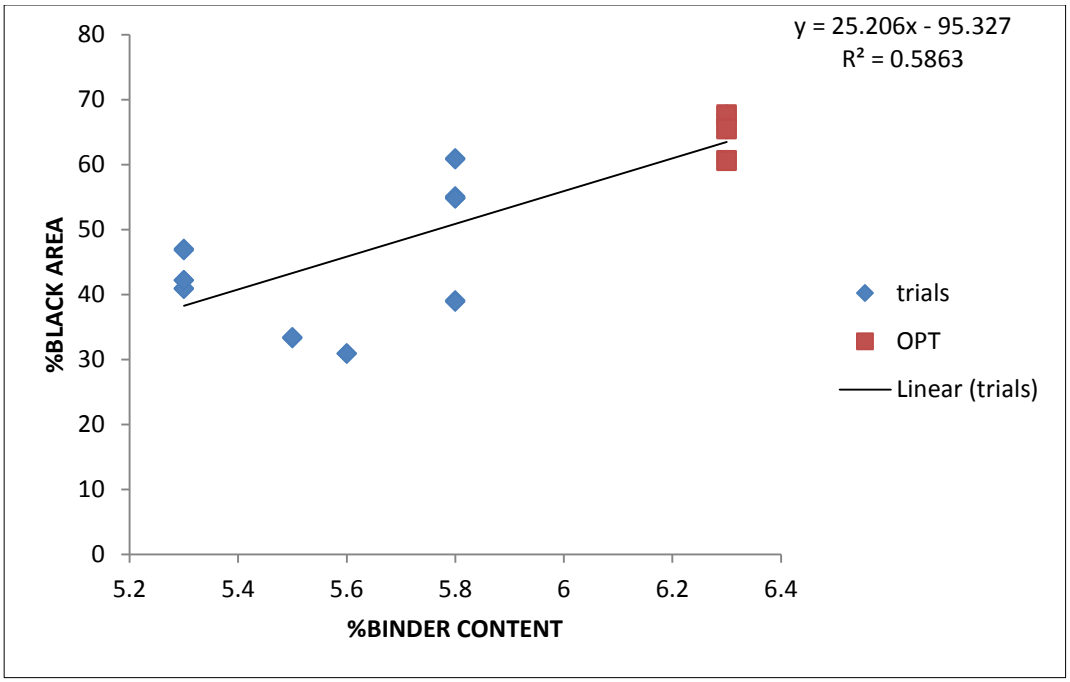

Figure F19 Mix I %black area versus %binder contents.

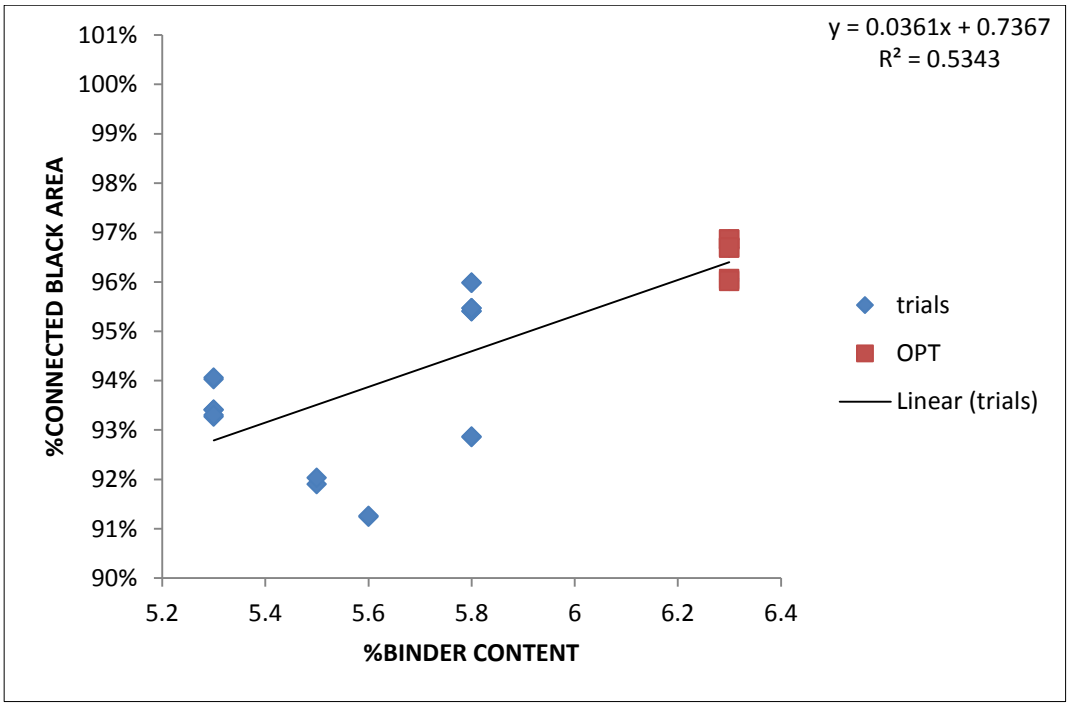

Figure F20 Mix I %connected black area versus %binder contents.

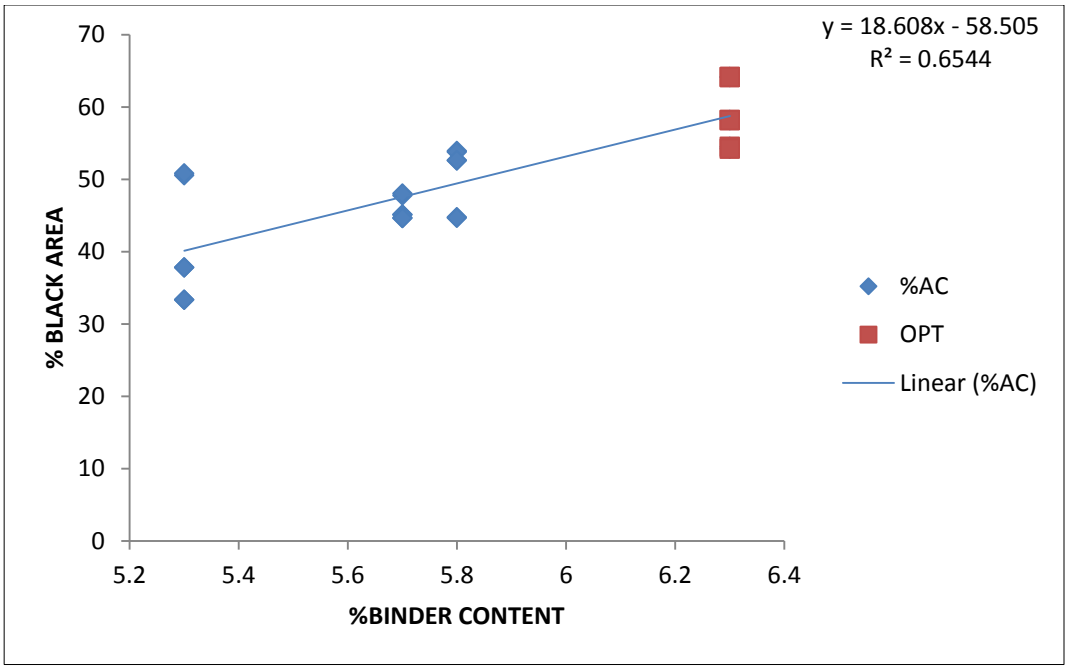

Figure F21 Mix J %black area versus %binder contents.

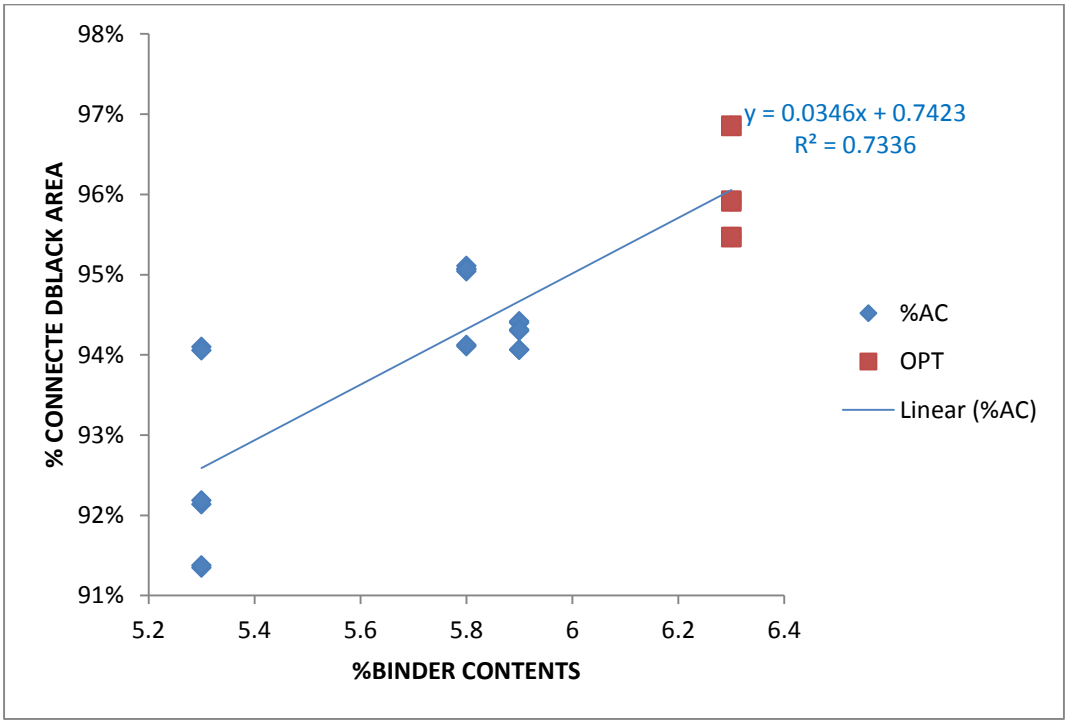

Figure F22 Mix J %connected black area versus %binder contents.

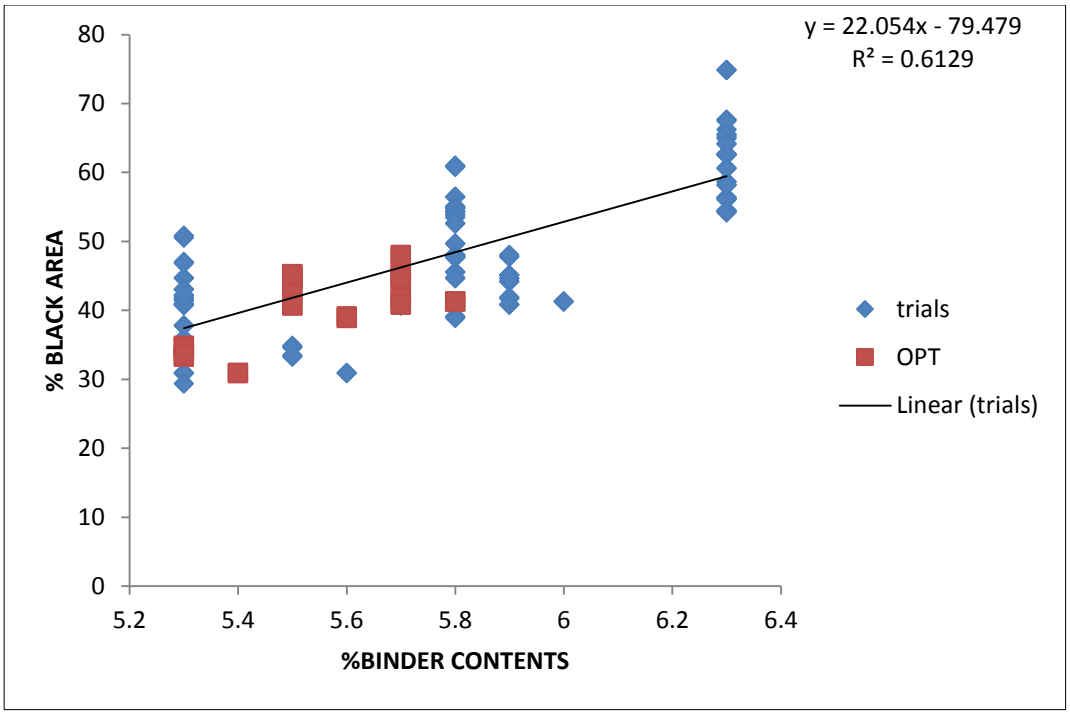

Figure F23 Mixtures GA553 %black area versus %binder contents.

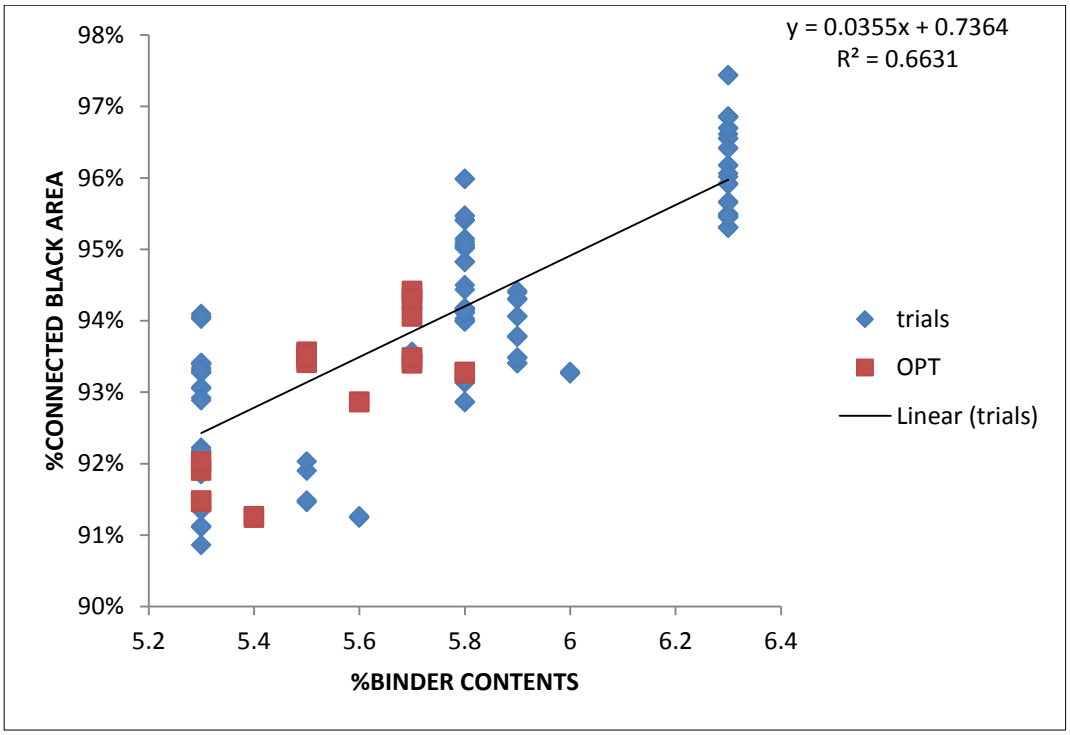

Figure F24 Mixtures GA553 %connected black area versus %binder contents.

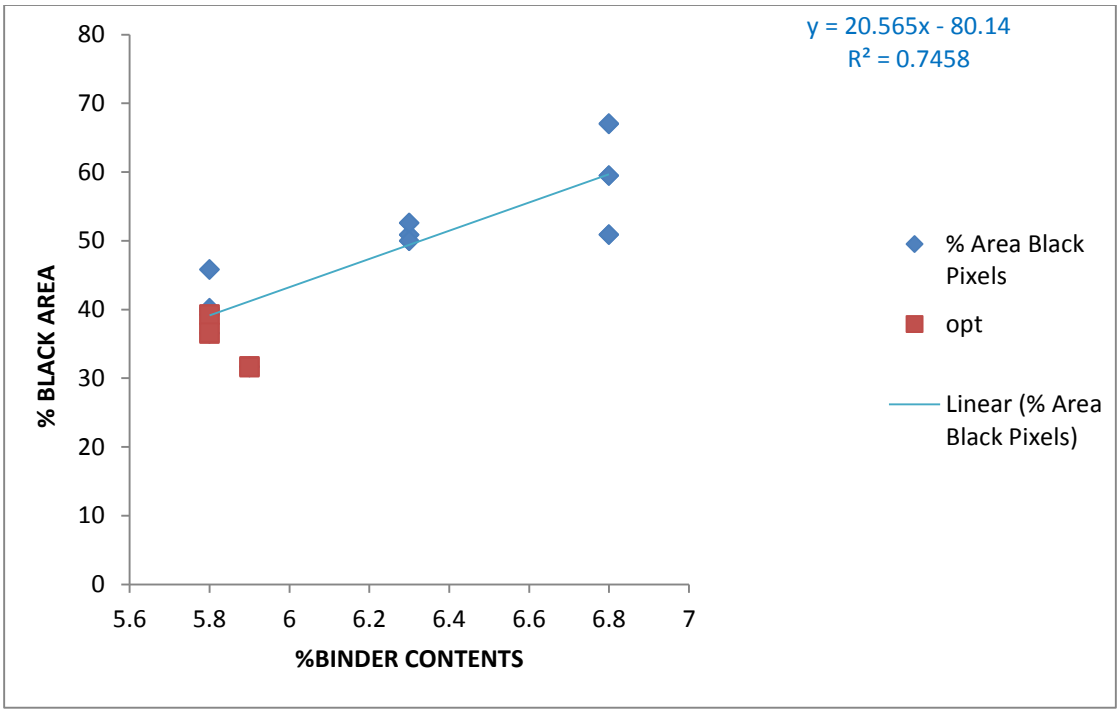

Figure F25 Mix K %black area versus %binder contents.

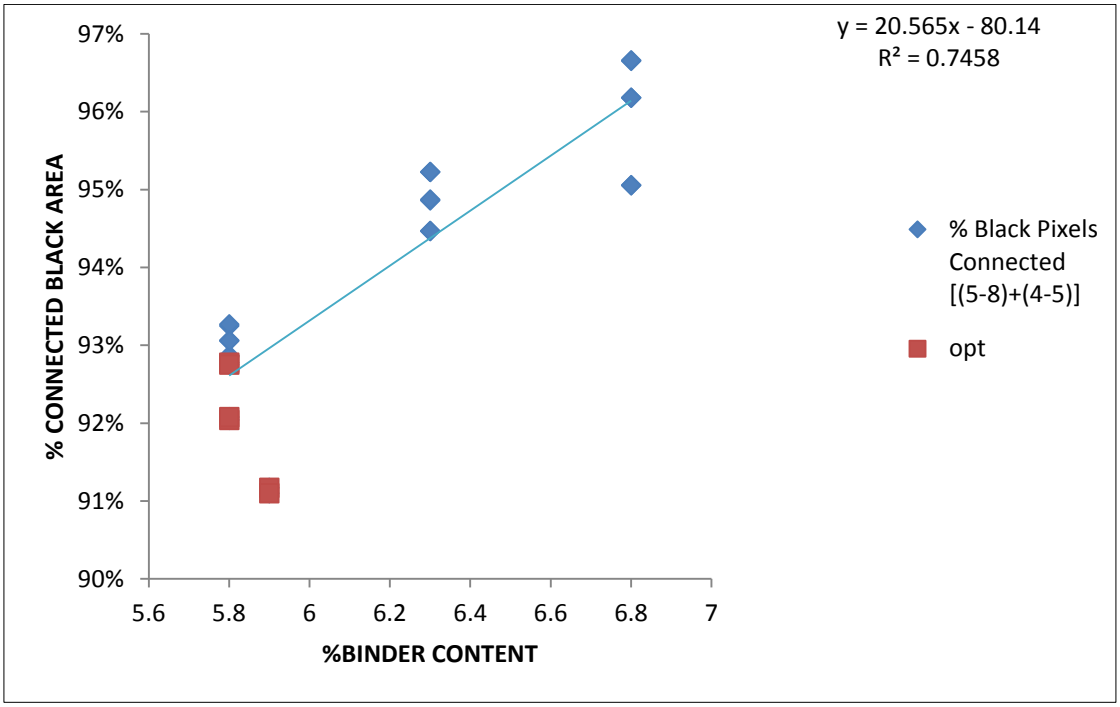

Figure F26 Mix K %connected black area versus %binder contents.

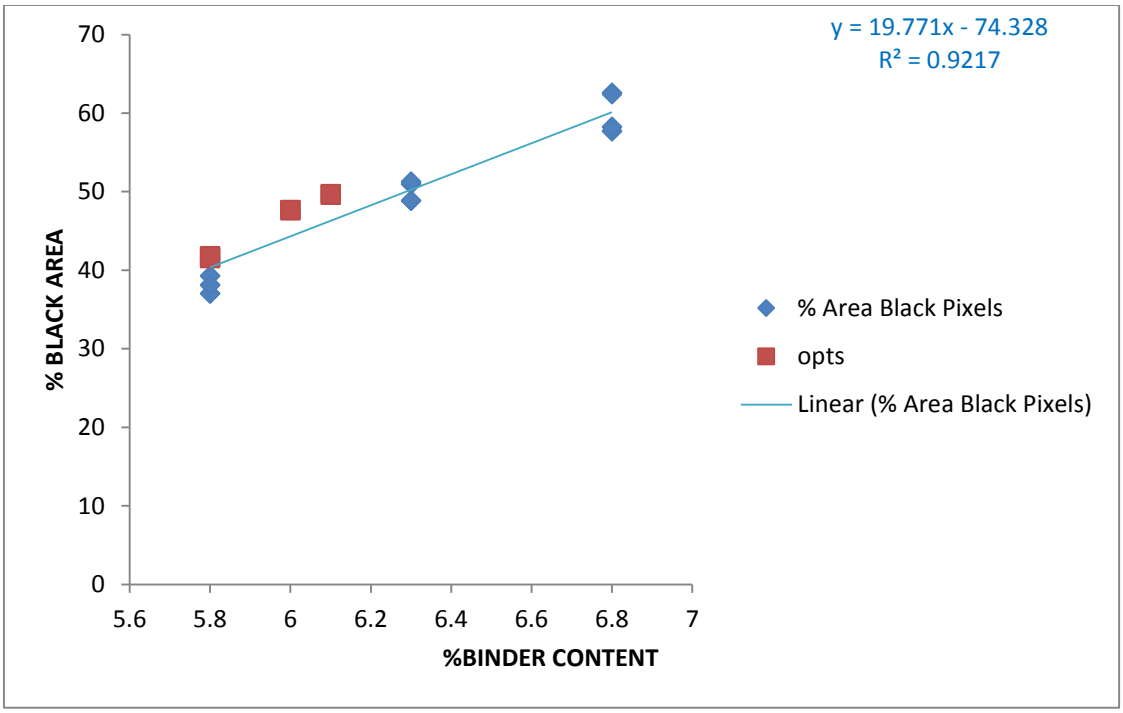

Figure F27 Mix L %black area versus %binder contents.

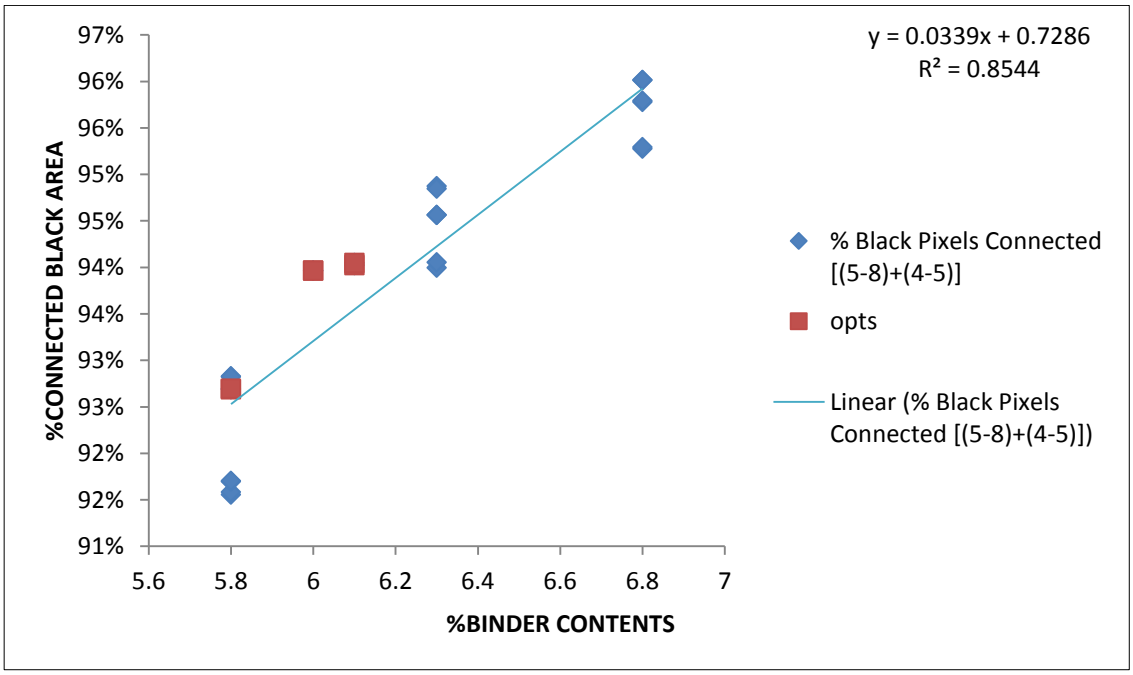

Figure F28 Mix L %connected black area versus %binder contents.

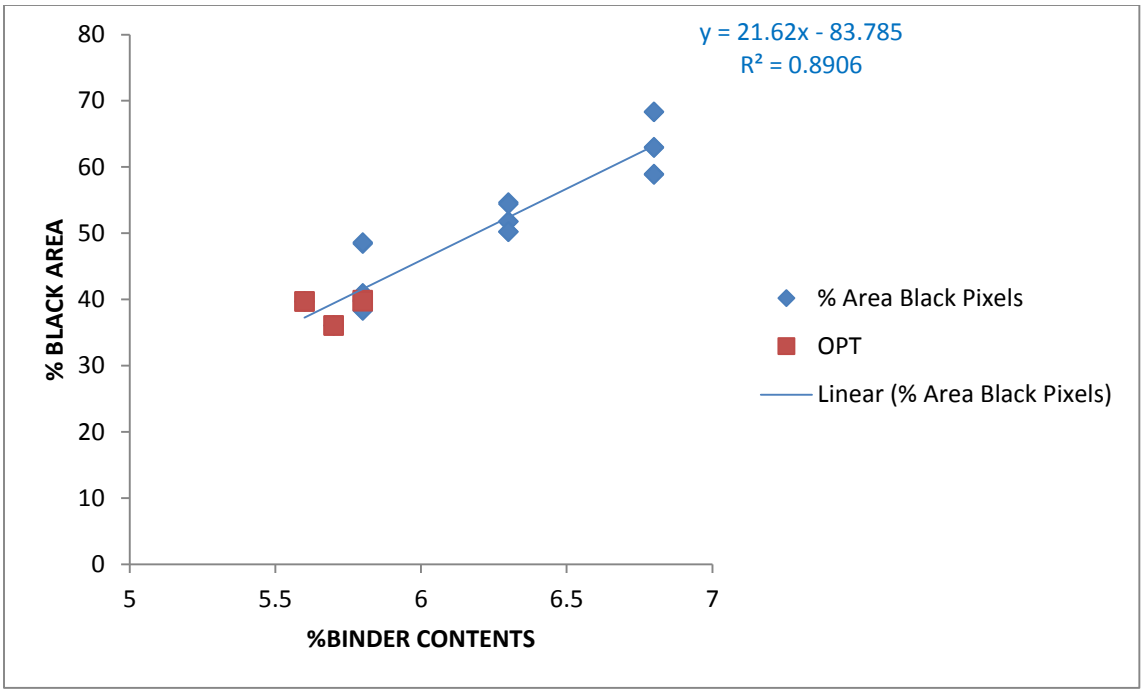

Figure F29 Mix M %black area versus %binder contents.

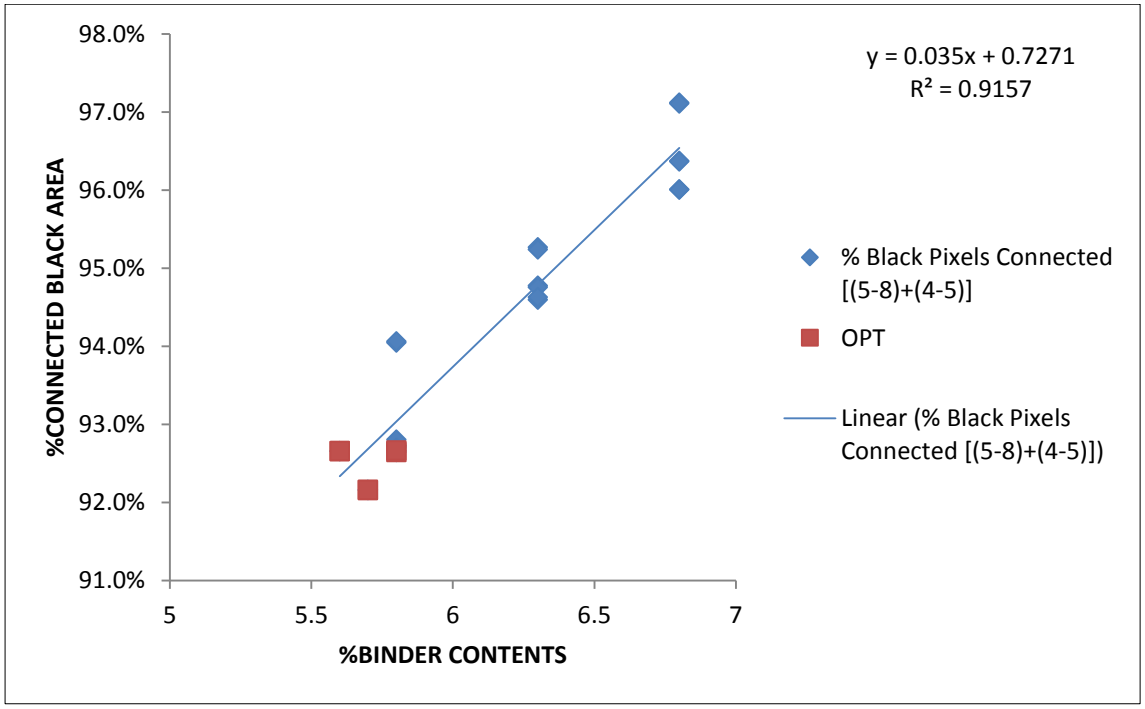

Figure F30 Mix M %connected black area versus %binder contents.

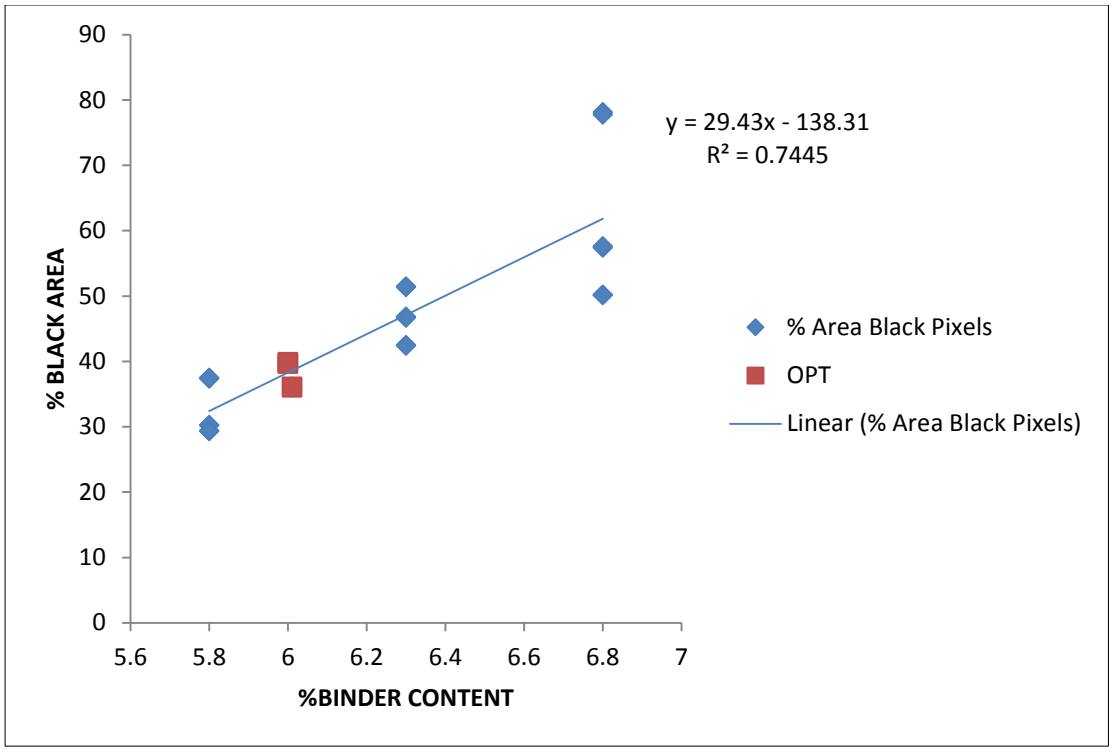

Figure F31 Mix N %black area versus %binder contents.

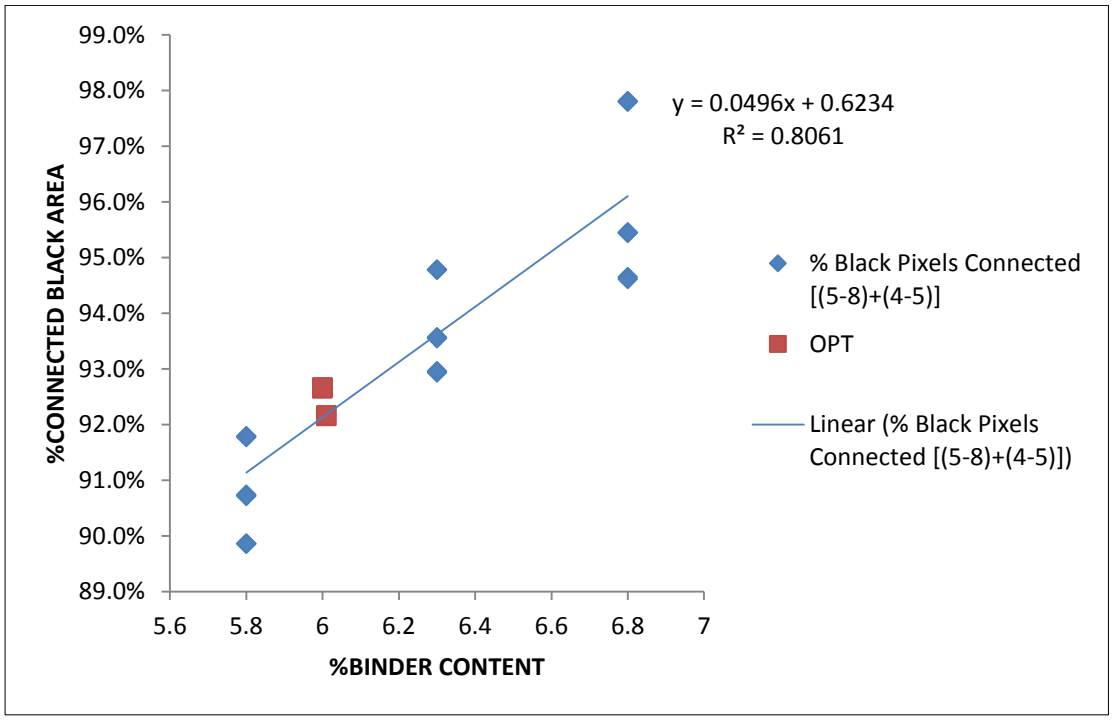

Figure F32 Mix N %connected black area versus %binder contents.

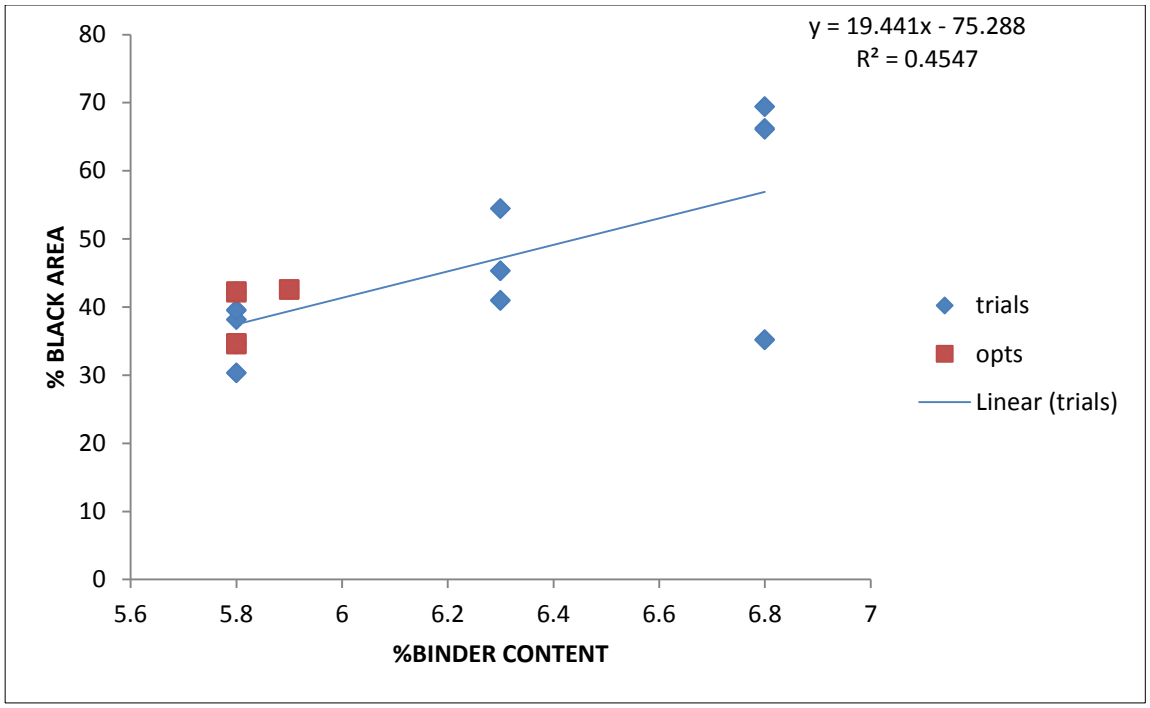

Figure F33 Mix O %black area versus %binder contents.

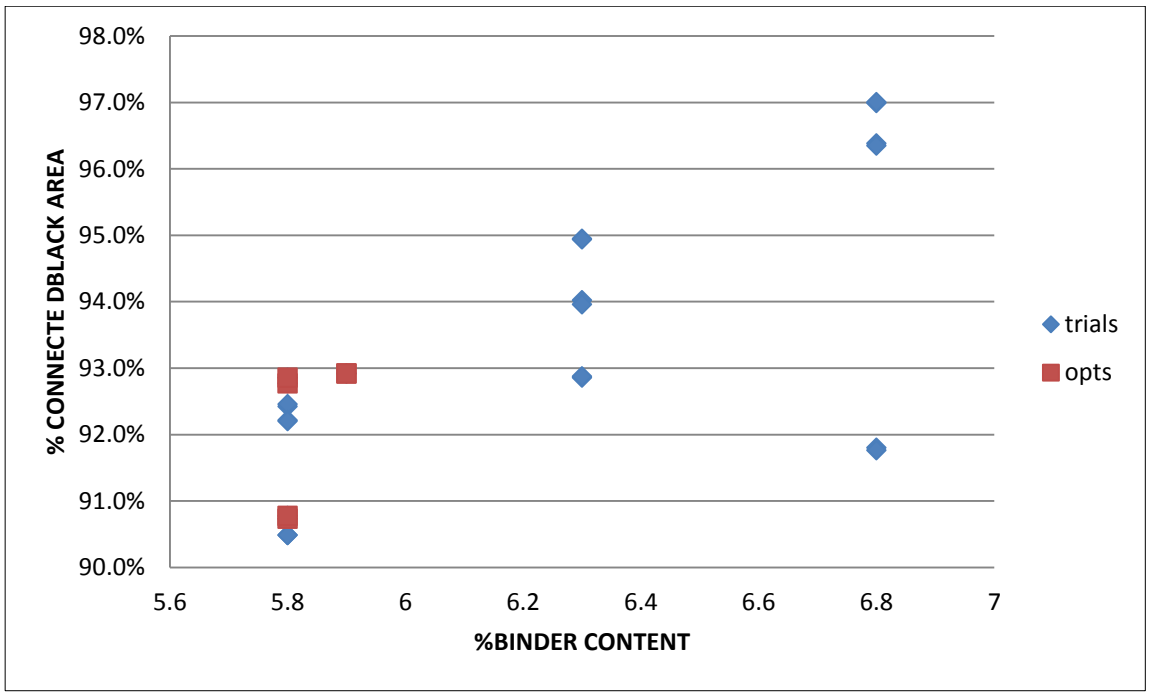

Figure F34 Mix O %connected black area versus %binder contents.

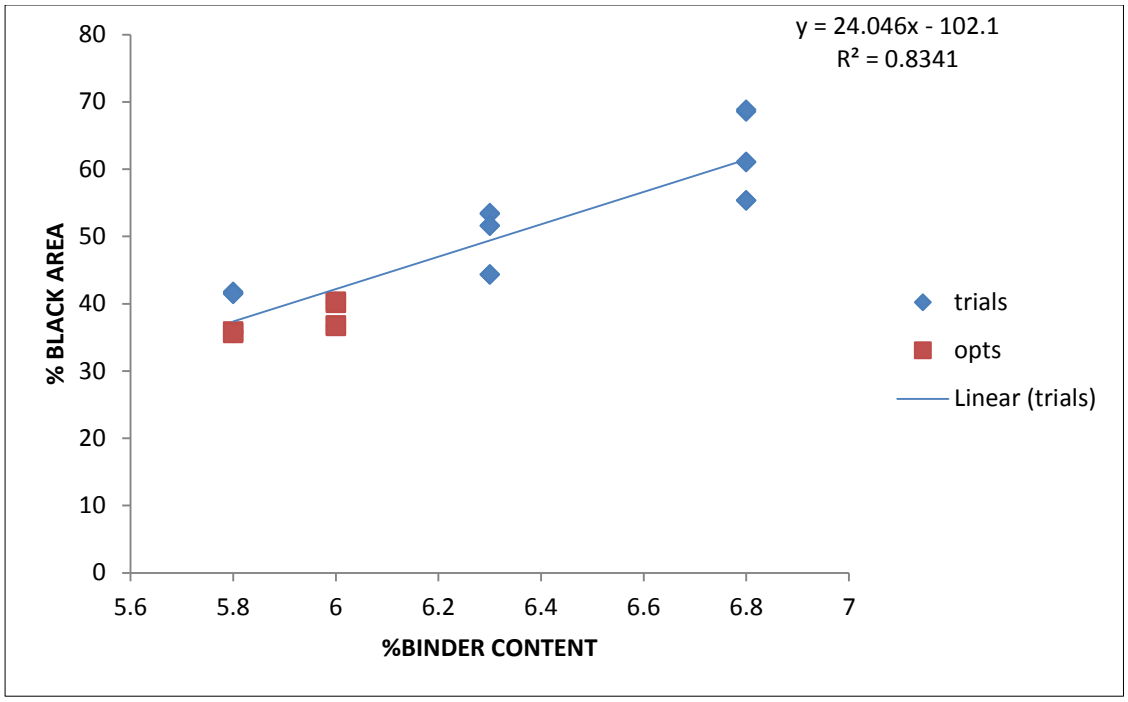

Figure F35 Mix P %black area versus %binder contents.

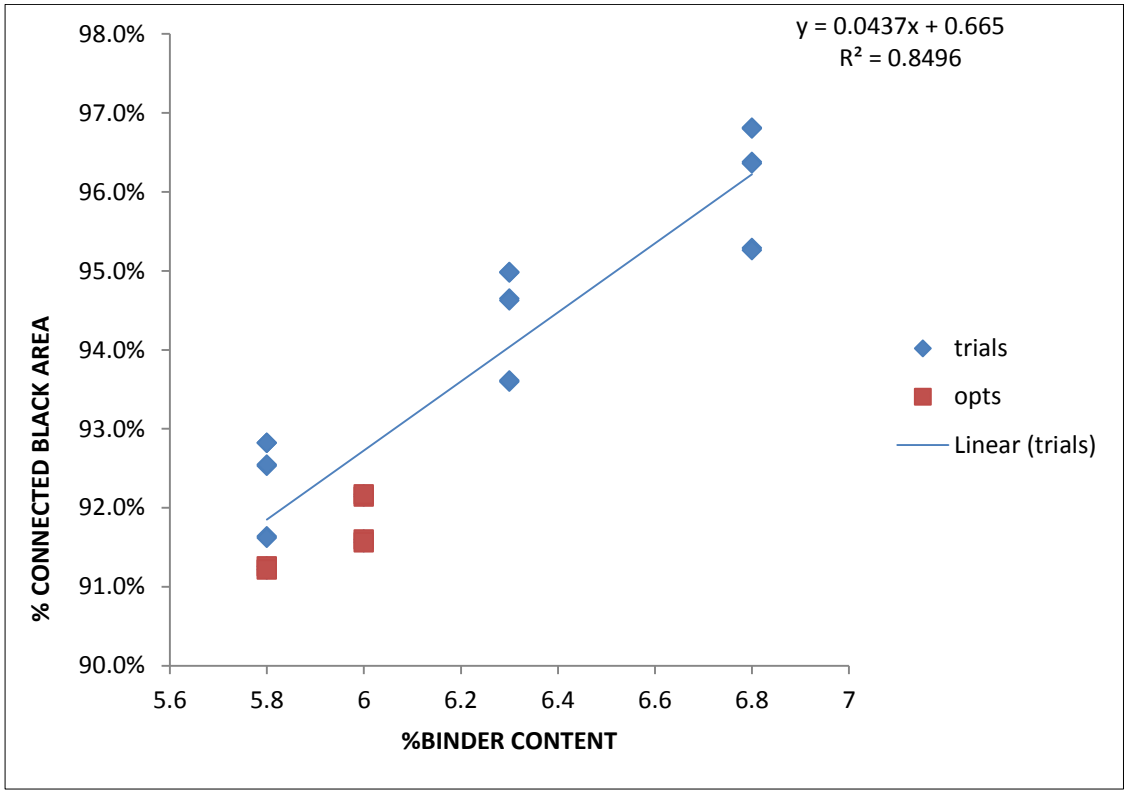

Figure F36 Mix P %connected black area versus %binder contents.

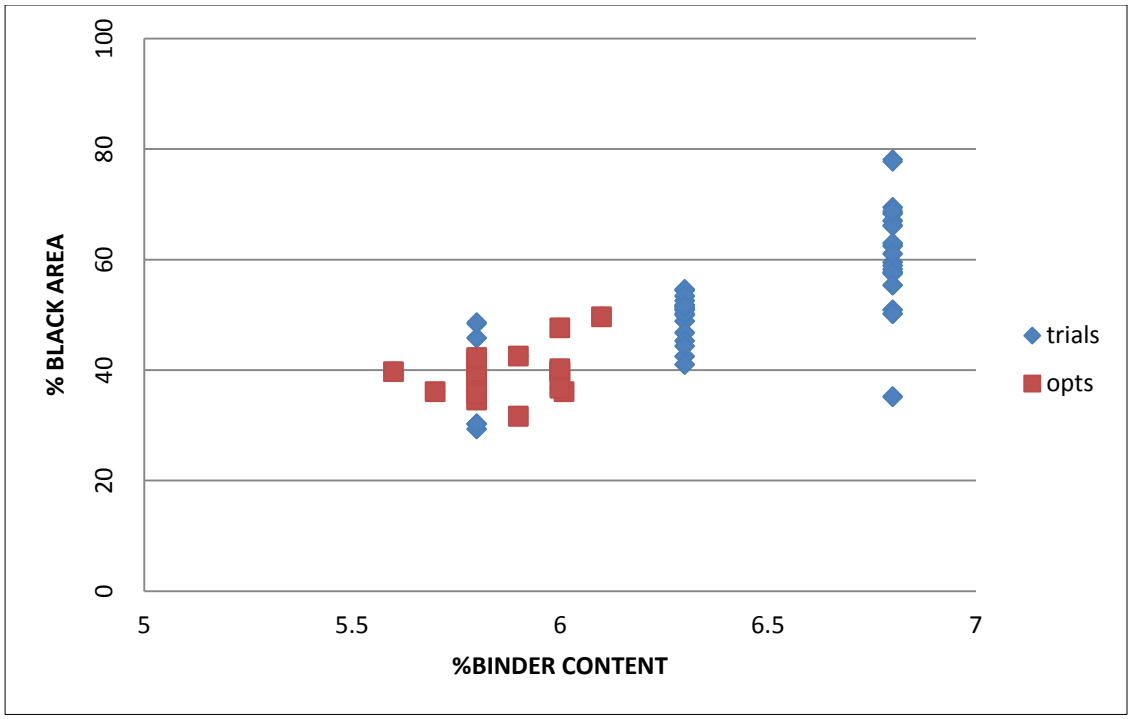

Figure F37 Mixtures 87339 %black area versus %binder contents.

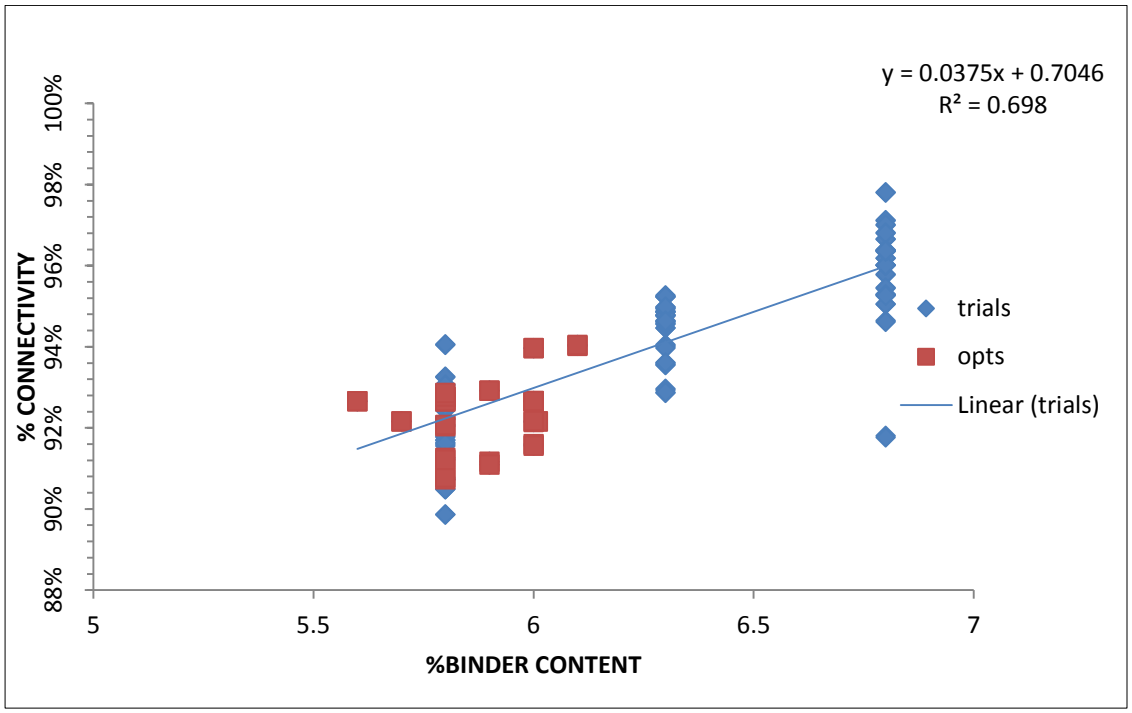

Figure F38 Mixtures 87399 %connected black area versus %binder contents.

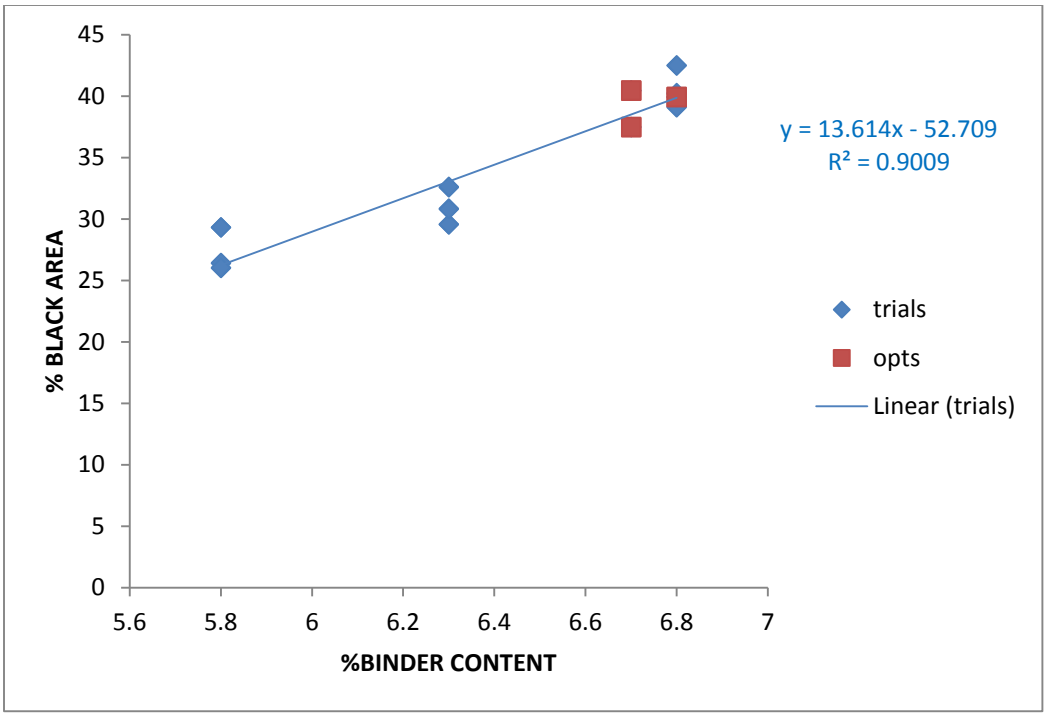

Figure F39 Mix Q %black area versus %binder contents.

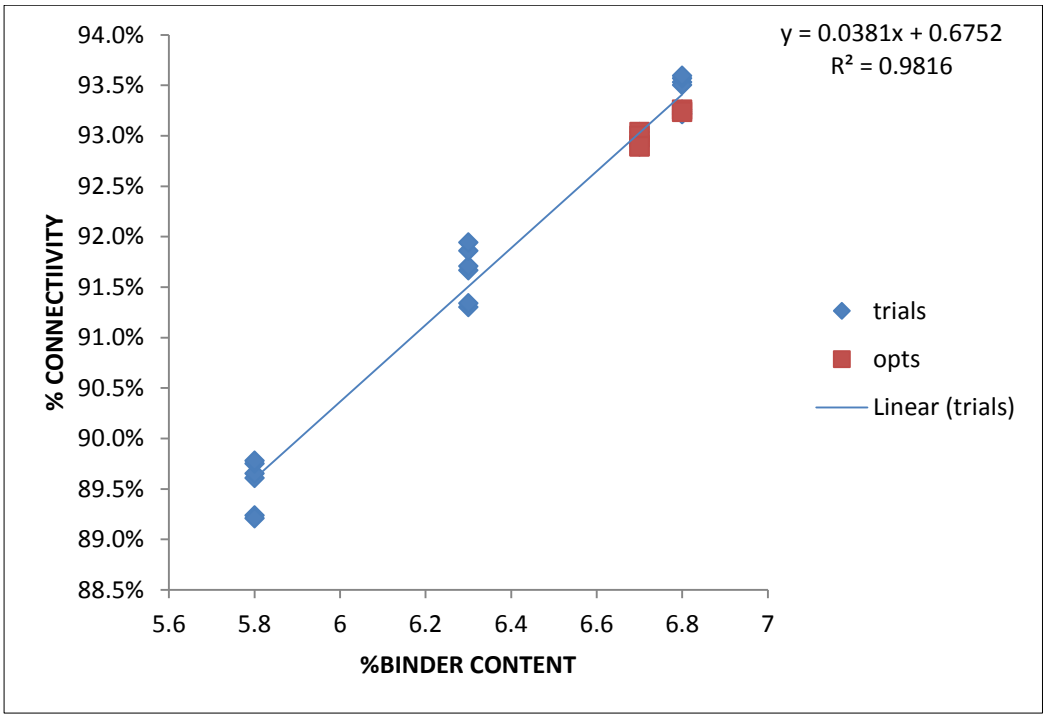

Figure F40 Mix Q %connected black area versus %binder contents.

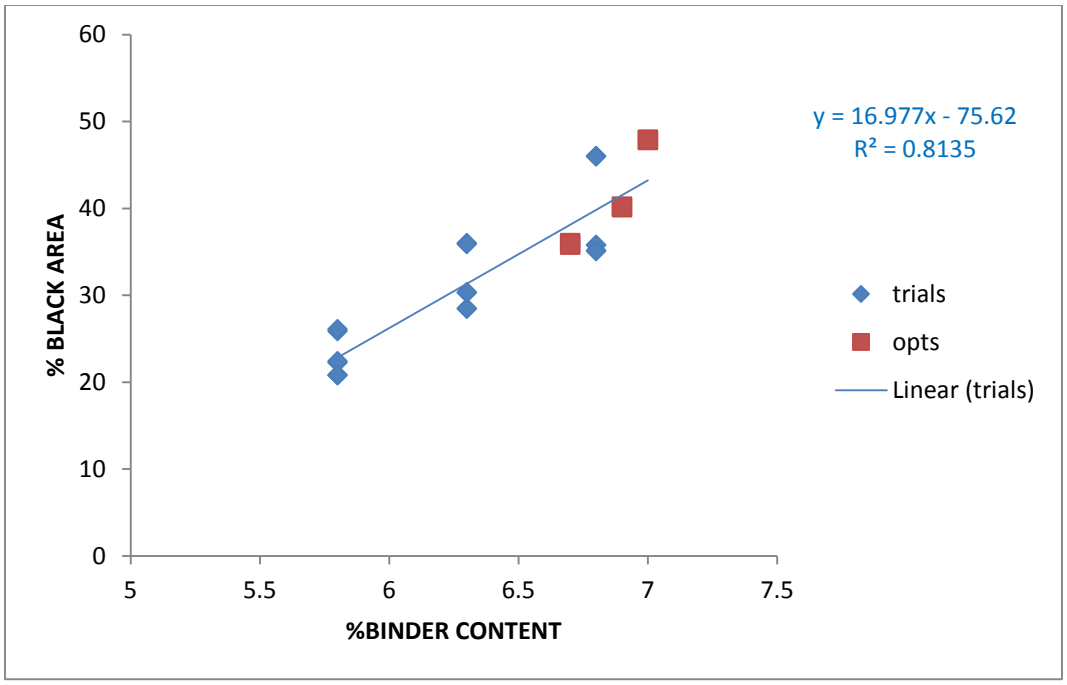

Figure F41 Mix R %black area versus %binder contents.

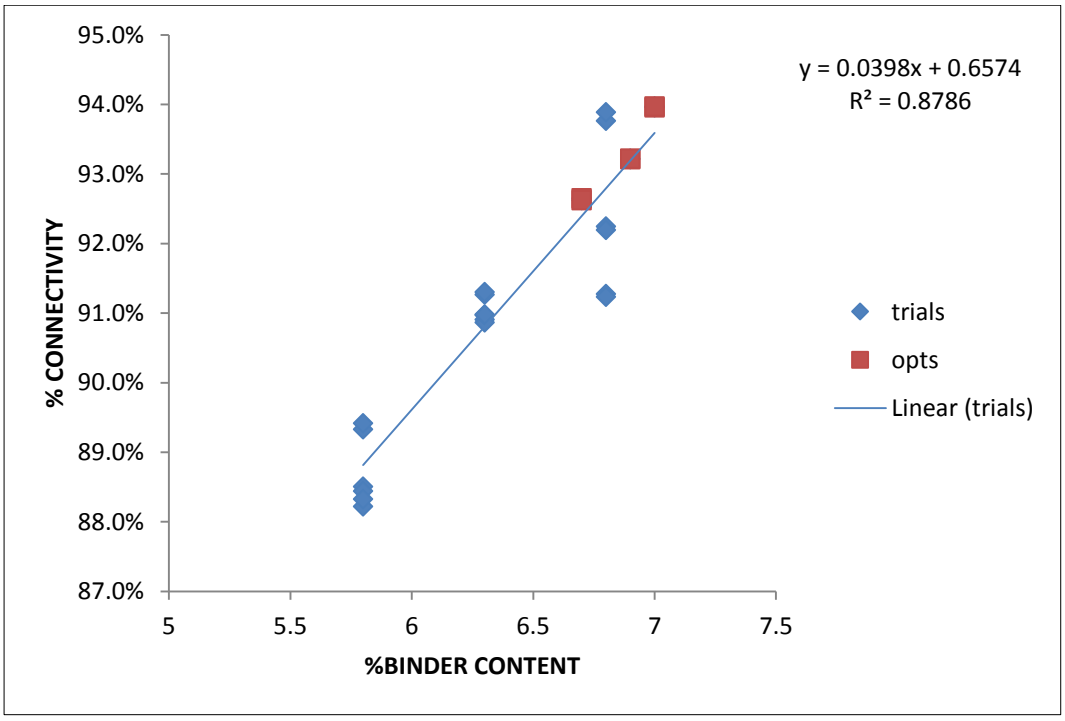

Figure F42 Mix R %connected black area versus %binder contents.

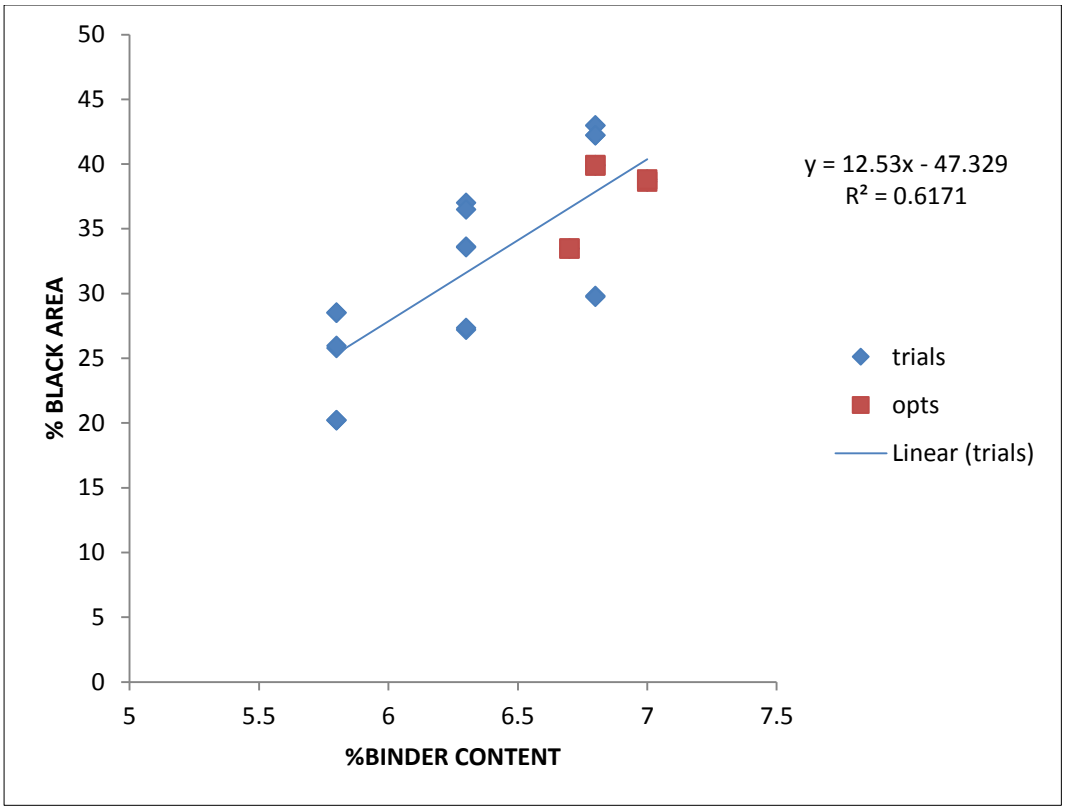

Figure F43 Mix S %black area versus %binder contents.

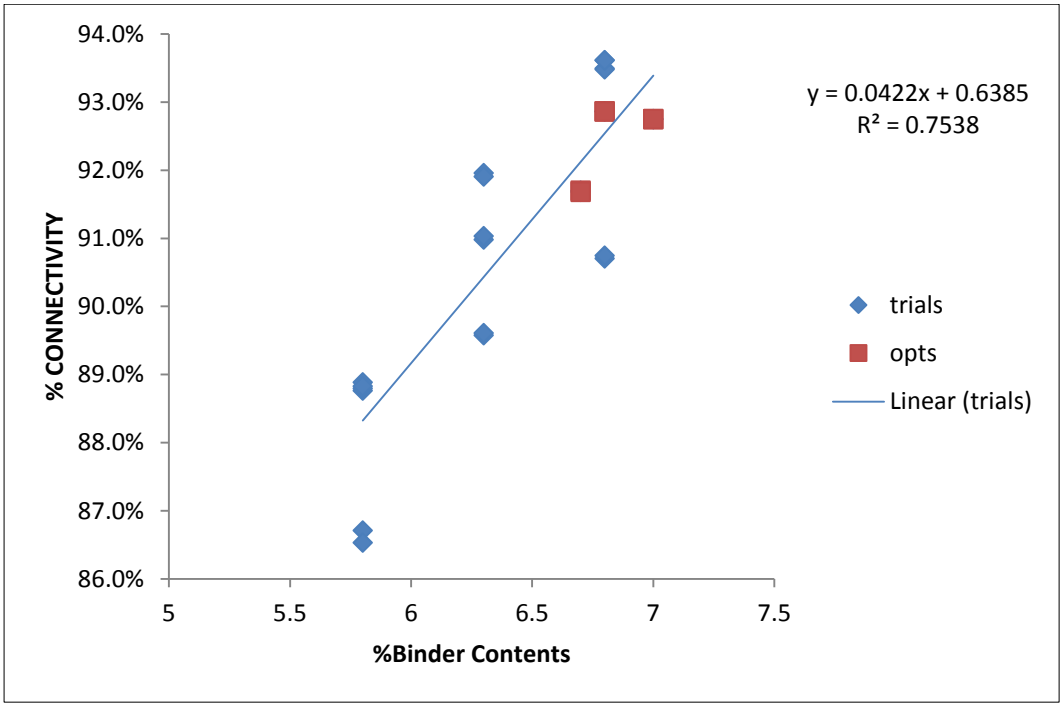

Figure F44 Mix S %connected black area versus %binder contents.

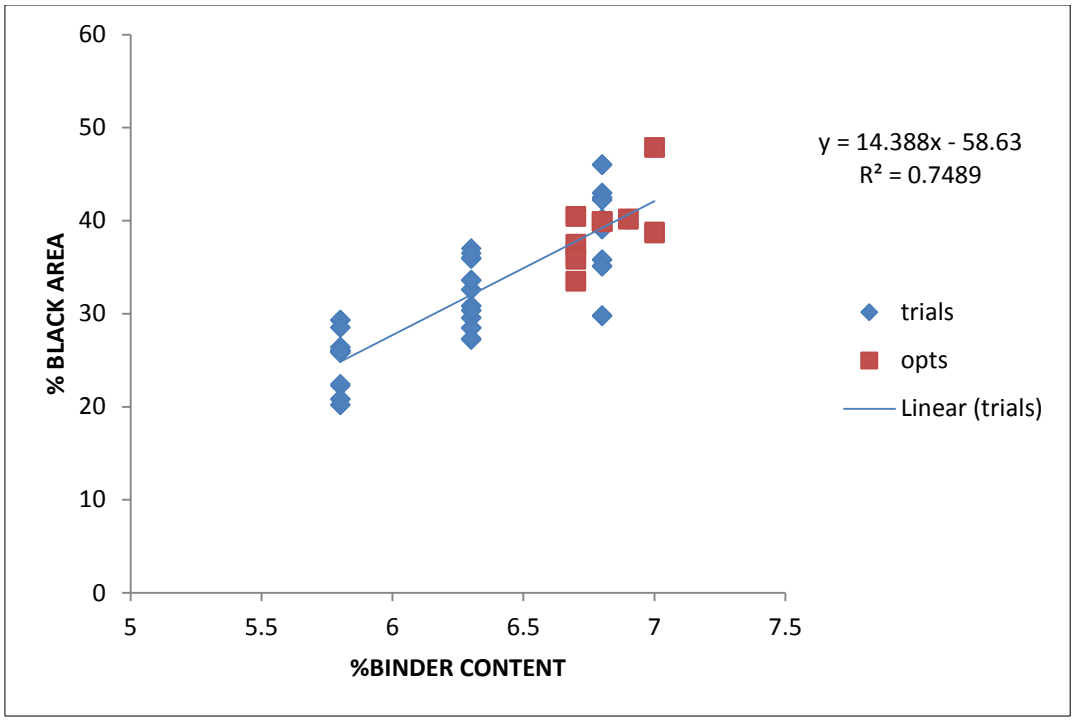

Figure F45 Mixtures 87145 %black area versus %binder contents.

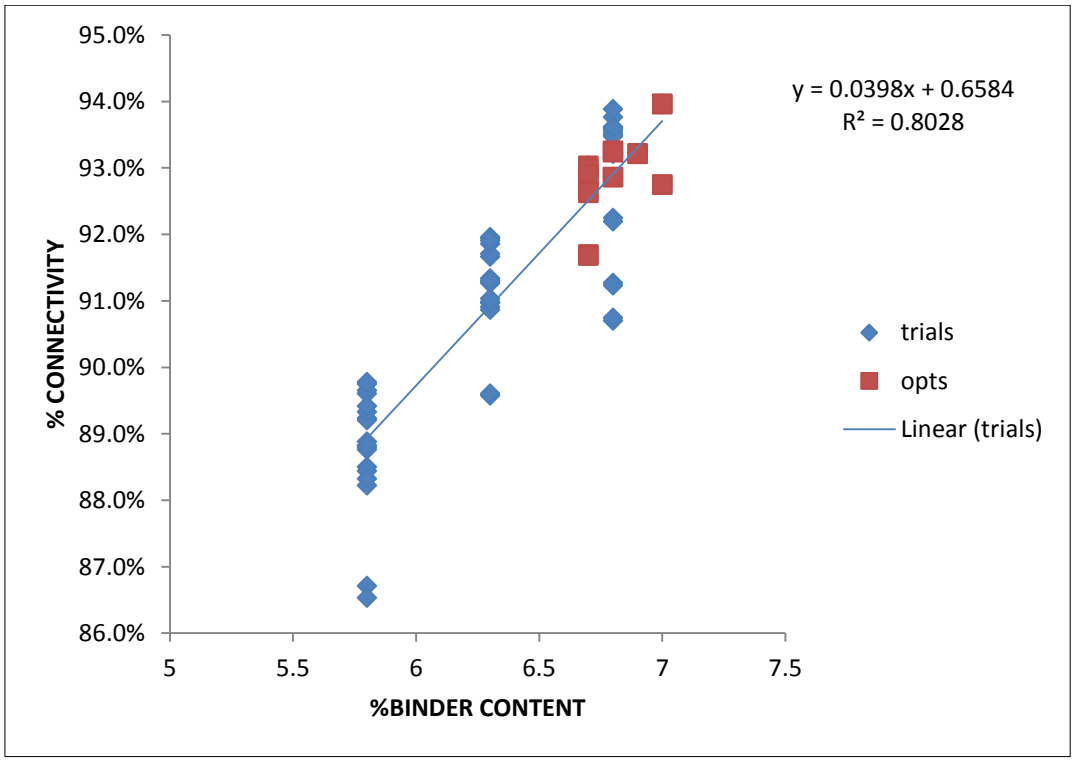

Figure F46 Mixtures 87145 %connected black area versus %binder contents.

APPENDIX G: GRNN PREDICTION MODEL TABLES

Table G1 Data base for the granitic and oolitic materials using GRNN model.

		Contrast	Visibility			Contrast Sensitivity				Frequency and Orientation Selectivity			Information Processing in the HVS				Contrast	Visibility			Contra	
IMAGE	PERCENT BINDER CONTENT	PERCENT AREA OF BLACK PIXELS	CONNECTIVITY OF BLACK PIXELS	NUMBER OF REGIONS	ORIENTATION	AREA OF REGIONS	AVERAGE PERIMETER PER REGION	UNIFORMITY RADIAL	UNIFORMITY ANGULAR	INCONSISTENCY COEFFICIENT	AVERAGE CENTROIDS DISTANCES	FORM FACTOR	AVERAGE COMPACTENESS PER REGION	SOLIDITY	ECCENTRICITY	PERCENT BINDER CONTENT	PERCENT AREA OF BLACK PIXELS	CONNECTIVITY OF BLACK PIXELS	NUMBER OF REGIONS	ORIENTATION	AREA OF REGIONS	AVERAGE PERIMETER PER REGION
MIX A TRIAL 1.1	5.3	31.68	94.11	421.00	49.72	447.36	82.55	3.98	9.40	1.78	858.27	0.86	18.15	0.90	5.56	5.80	44.14	98.34	257.00	48.77	1021.00	134.25
MIX A TRIAL 1.2	5.3	31.77	94.10	422.00	49.24	447.58	82.58	3.74	9.32	1.78	863.87	0.86	18.17	0.90	5.55	5.80	44.25	98.33	257.00	48.92	1023.49	134.09
MIX A TRIAL 2.1	5.3	34.78	94.13	370.00	51.77	558.80	89.90	6.52	15.81	1.70	836.99	0.90	18.30	0.91	6.32	5.80	45.08	98.38	237.00	58.31	1130.65	143.94
MIX A TRIAL 2.2	5.3	34.72	94.14	366.00	52.94	563.91	90.93	6.75	15.63	1.71	832.68	0.87	18.59	0.90	6.39	5.80	45.06	98.42	234.00	52.43	1144.74	144.45
MIX A TRIAL 3.1	5.3	39.19	93.66	351.00	49.84	663.69	100.04	5.68	14.73	1.99	902.66	0.92	19.33	0.90	6.67	5.80	56.45	98.19	137.00	56.34	2448.46	216.62
MIX A TRIAL 3.2	5.3	39.16	93.65	362.00	49.45	643.09	97.08	5.86	14.77	1.88	887.32	0.92	18.93	0.90	6.46	5.80	56.37	98.24	137.00	55.90	2445.92	215.68
MIX B TRIAL 1.1	5.3	40.23	93.19	355.00	45.19	673.74	105.30	0.52	8.88	2.10	891.07	0.94	20.38	0.90	6.59	5.80	47.91	98.05	241.00	52.34	1181.73	142.21
MIX B TRIAL 1.2	5.3	40.43	93.19	351.00	46.68	684.64	105.55	0.52	8.84	2.09	897.89	0.92	20.13	0.90	6.67	5.80	47.85	98.06	237.00	52.62	1200.32	144.58
MIX B TRIAL 2.1	5.3	55.86	92.76	167.00	54.12	1988.26	185.86	2.15	13.05	1.88	915.81	0.94	23.65	0.90	14.01	5.80	55.39	98.01	169.00	48.72	1948.21	184.66
MIX B TRIAL 2.2	5.3	55.78	92.79	167.00	54.47	1985.46	185.05	1.86	13.21	1.88	901.44	0.94	23.56	0.90	14.01	5.80	55.26	98.04	164.00	48.20	2008.20	190.02
MIX B TRIAL 3.1	5.3	39.77	93.43	334.00	49.20	707.79	108.30	4.08	13.83	1.89	880.19	0.88	20.23	0.89	7.01	5.80	56.58	92.89	145.00	55.05	2319.59	207.71
MIX B TRIAL 3.2	5.3	39.80	93.44	327.00	49.47	723.50	110.42	3.98	14.00	1.91	889.92	0.87	20.43	0.89	7.16	5.80	56.76	92.89	139.00	58.49	2427.65	213.21
MIX D TRIAL 1.1	5.3	44.34	93.69	253.00	51.80	1041.94	129.08	2.16	12.02	1.78	907.48	0.89	20.59	0.90	9.25	5.80	56.00	98.29	128.00	51.49	2600.91	230.94
MIX D TRIAL 1.2	5.3	44.43	93.65	254.00	51.90	1089.86	129.22	1.52	11.83	1.78	905.92	0.87	20.83	0.90	9.21	5.80	56.15	98.30	131.00	52.52	2548.23	222.29
MIX D TRIAL 2.1	5.3	44.12	93.88	239.00	49.95	1097.44	134.72	3.62	14.31	1.83	830.18	0.84	21.40	0.89	9.79	5.80	62.40	92.63	118.00	47.03	3148.69	231.48
MIX D TRIAL 2.2	5.3	44.29	93.84	245.00	50.27	1074.60	131.71	3.55	13.98	1.85	832.08	0.84	21.02	0.90	9.55	5.80	62.31	92.65	114.00	48.14	3249.15	231.62
MIX D TRIAL 3.1	5.3	40.77	93.41	335.00	46.65	723.55	107.13	6.58	13.70	1.89	850.12	0.89	19.77	0.90	6.99	5.80	54.54	98.06	148.00	52.54	2267.43	223.00
MIX D TRIAL 3.2	5.3	41.03	93.38	332.00	47.71	734.66	108.34	6.36	13.54	1.83	846.40	0.89	19.84	0.90	7.05	5.80	54.55	98.10	135.00	55.86	2402.14	236.40
MIX E TRIAL 1.1	5.3	41.43	93.27	318.00	50.45	774.51	114.60	11.54	11.47	1.82	888.67	0.90	21.04	0.89	7.36	5.80	64.27	92.62	92.00	56.98	4152.68	258.57
MIX E TRIAL 1.2	5.3	41.38	93.29	318.00	49.43	773.59	114.33	11.49	11.15	1.73	891.85	0.89	21.04	0.89	7.36	5.80	64.14	92.65	87.00	55.95	4382.82	273.11
MIX E TRIAL 2.1	5.3	42.49	93.17	305.00	56.33	828.06	119.71	4.88	16.14	1.79	850.98	0.93	21.63	0.90	7.67	5.80	61.62	92.37	83.00	58.11	4412.99	307.99
MIX E TRIAL 2.2	5.3	42.40	93.16	313.00	55.48	805.33	116.73	4.71	16.29	1.75	855.94	0.94	21.28	0.90	7.48	5.80	61.67	92.35	87.00	58.45	4213.51	294.44
MIX E TRIAL 3.1	5.3	48.14	92.37	246.00	50.43	1187.35	151.59	1.72	11.19	1.76	899.86	0.90	23.74	0.89	9.51	5.80	58.10	92.73	118.00	48.95	2927.13	245.19
MIX E TRIAL 3.2	5.3	48.15	92.39	242.00	51.20	1207.23	153.58	1.64	11.22	1.76	897.94	0.87	23.94	0.88	9.67	5.80	58.17	92.68	124.00	46.74	2788.67	236.27
MIX F TRIAL 1.1	5.3	44.78	92.84	317.00	52.53	839.68	116.47	0.16	11.55	1.87	881.36	0.90	20.78	0.89	7.38	5.80	49.80	92.74	227.00	46.57	1304.25	153.50
MIX F TRIAL 1.2	5.3	44.76	92.85	320.00	52.57	831.41	115.31	0.29	11.45	1.86	885.96	0.91	20.43	0.90	7.31	5.80	49.77	92.73	220.00	48.71	1344.83	160.48
MIX F TRIAL 2.1	5.3	30.92	94.42	393.00	52.03	467.66	84.22	1.80	13.57	1.77	866.37	0.87	18.38	0.90	5.95	5.80	47.92	92.87	252.00	48.38	1130.31	140.88
MIX F TRIAL 2.2	5.3	30.94	94.40	398.00	51.73	462.20	83.41	1.65	13.74	1.78	867.92	0.89	18.22	0.90	5.88	5.80	48.17	92.81	252.00	48.24	1136.21	141.14
MIX F TRIAL 3.1	5.3	30.94	94.40	398.00	51.73	462.20	83.41	1.65	13.74	1.78	867.92	0.89	18.22	0.90	5.88	5.80	48.17	92.81	252.00	48.24	1136.21	141.14
MIX F TRIAL 3.2	5.3	29.37	94.65	421.00	54.94	414.78	75.86	4.18	13.06	1.78	877.81	0.94	17.21	0.91	5.56	5.80	53.59	98.02	151.00	50.34	2109.89	207.98
MIX G TRIAL 1.1	5.3	41.54	93.76	300.00	49.46	823.22	112.88	4.41	22.71	1.81	846.71	0.88	19.97	0.89	7.80	5.80	54.42	92.44	205.00	48.41	1578.02	167.20
MIX G TRIAL 1.2	5.3	41.49	93.77	309.00	50.22	798.17	109.42	4.32	22.77	1.82	843.13	0.89	19.51	0.90	7.57	5.80	54.50	92.38	209.00	48.60	1550.24	165.74
MIX G TRIAL 2.1	5.3	41.01	93.48	322.00	48.01	757.07	108.34	0.68	13.94	1.72	825.39	0.87	19.57	0.90	7.27	5.80	47.98	92.99	222.00	52.72	1284.86	157.99
MIX G TRIAL 2.2	5.3	40.81	93.51	324.00	51.74	748.68	107.45	0.68	14.10	1.73	827.24	0.88	19.42	0.90	7.22	5.80	47.98	98.00	221.00	51.29	1289.34	158.90
MIX G TRIAL 3.1	5.3	41.88	93.29	322.00	43.82	773.08	112.01	4.68	12.27	1.85	890.29	0.90	20.18	0.90	7.27	5.80	56.61	92.23	171.00	48.54	1968.12	185.35
MIX G TRIAL 3.2	5.3	41.84	93.28	332.00	43.72	749.13	108.76	4.95	12.46	1.88	891.14	0.91	19.78	0.90	7.05	5.80	56.66	92.22	175.00	45.70	1924.64	181.27
MIX H TRIAL 1.1	5.3	48.11	93.41	287.00	49.30	892.98	121.51	0.51	13.30	1.87	845.81	0.85	20.97	0.89	8.15	5.80	45.70	98.39	256.00	50.44	1061.18	132.38
MIX H TRIAL 1.2	5.3	48.19	93.37	290.00	47.31	885.24	120.77	0.41	13.24	1.79	845.58	0.87	20.99	0.89	8.07	5.80	45.68	98.41	250.00	51.28	1084.90	135.29
MIX H TRIAL 2.1	5.3	35.84	93.80	391.00	49.63	544.91	89.74	1.23	8.01	1.91	873.26	0.88	18.31	0.90	5.98	5.80	47.76	98.44	222.00	51.96	1278.95	144.01
MIX H TRIAL 2.2	5.3	35.97	93.71	377.00	49.06	567.21	94.32	0.96	8.55	1.92	874.59	0.85	19.31	0.89	6.21	5.80	47.77	98.39	228.00	50.64	1245.47	141.80
MIX H TRIAL 3.1	5.3	34.27	94.41	342.00	51.72	595.73	94.99	8.81	11.74	1.78	866.09	0.86	18.54	0.90	6.84	5.80	40.67	98.71	315.00	46.69	767.56	108.49
MIX H TRIAL 3.2	5.3	34.18	94.40	350.00	51.30	580.52	92.95	8.79	11.86	1.81	869.84	0.87	18.34	0.90	6.69	5.80	40.70	98.75	311.00	47.02	777.92	109.35
MIX I TRIAL 1.1	5.3	41.04	93.93	281.00	55.33	868.18	118.60	9.16	10.68	1.98	900.08	0.86	19.90	0.90	8.33	5.80	61.11	92.68	122.00	52.48	2977.55	229.39
MIX I TRIAL 1.2	5.3	40.96	93.96	271.00	54.71	898.56	122.69	8.88	10.80	1.98	893.48	0.83	20.45	0.89	8.63	5.80	60.98	92.73	122.00	54.94	2989.13	229.10
MIX I TRIAL 2.1	5.3	47.12	93.12	251.00	50.80	1116.04	138.49	2.02	12.85	1.62	947.87	0.90	21.56	0.90	9.32	5.80	55.22	98.01	155.00	45.00	2117.95	197.30
MIX I TRIAL 2.2	5.3	46.93	93.17	247.00	49.38	1129.37	139.93	1.92	12.92	1.62	937.48	0.90	21.77	0.90	9.47	5.80	55.05	98.04	145.00	44.73	2257.03	210.70
MIX I TRIAL 3.1	5.3	42.29	93.38	283.00	50.10	888.31	125.13	2.52	8.85	1.76	888.60	0.84	21.07	0.89	8.27	5.80	54.98	98.20	170.00	52.96	1920.85	179.17
MIX I TRIAL 3.2	5.3	42.29	93.41	273.00	51.02	920.79	129.33	2.30	8.75	1.68	896.06	0.82	21.46	0.89	8.57	5.80	54.98	98.21	168.00	54.15	1948.81	177.89
MIX J TRIAL 1.1	5.3	37.89	93.47	356.00	49.56	632.72	101.57	0.41	15.53	1.79	858.99	0.87	20.02	0.89	6.57	5.80	54.06	92.88	164.00	42.64	1959.45	198.67
MIX J TRIAL 1.2	5.3	37.86	93.49	352.00	50.97	639.33	102.70	1.09	15.48	1.77	852.64	0.87	20.20	0.89	6.65	5.80	53.98	92.88	169.00	44.19	1896.87	194.08
MIX J TRIAL 2.1	5.3	50.70	92.18	212.00	46.48	1421.56	171.08	1.85	16.05	1.80	959.05	0.86	26.21	0.88	11.04	5.80	52.75	98.12	148.00	47.64	2118.97	218.10
MIX J TRIAL 2.2	5.3	50.98	92.06	220.00	47.17	1377.57	165.79	1.62	15.95	1.80	953.56	0.88	25.66	0.88	10.64	5.80	52.80	98.13	151.00	46.35	2078.68	213.16
MIX J TRIAL 3.1	5.3	33.41	94.03	404.00	52.93	491.54	85.81	7.45	12.94	1.78	873.37	0.87	18.47	0.90	5.79	5.80	44.85	98.68	237.00	47.66	1124.89	137.24
MIX J TRIAL 3.2	5.3	33.38	94.05	401.00	54.14	494.87	86.03	6.84	13.23	1.78	872.41	0.88	18.46	0.90	5.84	5.80	44.75	98.69	235.00	48.05	1132.00	138.80
MIX K TRIAL 1.1	5.8	45.89	92.65	339.00	50.35	804.70	111.60	8.83	9.03	1.72	894.24	0.92	19.25	0.91	6.90	6.30	50.98	98.10	202.00	51.34	1500.20	162.10
MIX K TRIAL 1.2	5.8	45.97	92.65	327.00	50.98	835.62	115.77	8.85	9.04	1.65	900.12	0.91	19.80	0.91	7.16	6.30	51.01	98.11	205.00	50.61	1479.05	159.87
MIX K TRIAL 2.1	5.8	40.12	93.64	329.00	49.11	724.84	106.40	6.04	18.53	1.82	861.60	0.88	19.33	0.90	7.11	6.30	52.67	98.32	196.00	58.39	1597.37	160.07
MIX K TRIAL 2.2	5.8	40.28	93.59	326.00	47.89	734.52	108.05	5.96	18.15	1.81	855.04	0.88	19.64	0.90	7.18	6.30	52.67	98.32	196.00	58.39	1597.37	160.07
MIX K TRIAL 3.1	5.8	39.79	93.77	320.00	52.84	739.15	105.14	3.57	12.53	1.74	841.79	0.90	18.53	0.91	7.31	6.30	50.12	92.98	230.00	46.30	1295.33	146.23
MIX K TRIAL 3.2	5.8	40.08	93.72	314.00	53.96	758.77	107.83	3.56	12.91	1.73	836.74	0.88	18.89	0.90	7.45	6.30	50.09	92.97	233.00	46.39	1278.04	144.77
MIX L TRIAL 1.1	5.8	39.31	93.67	335.00	48.59	697.59	108.04	4.72	13.72	1.92	857.92	0.88	18.86	0.90	6.99	6.30	51.08	98.25	215.00	56.86	1412.43	148.82
MIX L TRIAL 1.2	5.8	39.38	93.66	332.00	48.59	705.18	108.99	4.68	13.59	1.94	856.66	0.87	18.97	0.90	7.05	6.30	51.06	98.24	215.00	56.84	1411.68	148.37
MIX L TRIAL 2.1	5.8	37.10	93.25	445.00	49.06	495.65	84.46	2.12	9.02	1.71	844.72	0.92	17.83	0.91	5.26	6.30	48.96	92.64	288.00	49.50	1028.39	128.02
MIX L TRIAL 2.2	5.8	37.06	93.27	450.00	49.83	489.58	83.15	1.95	8.97	1.71	846.41	0.92	17.61	0.91	5.20	6.30	48.94	92.71	277.00	51.80	1050.23	129.41
MIX L TRIAL 3.1	5.8	38.13	93.09	428.00	45.26	529.62	88.87	1.37	9.66	1.73	811.27	0.89	17.98	0.91	5.47	6.30	51.35	92.80	227.00	51.75	1344.67	151.99
MIX L TRIAL 3.2	5.8	38.21	93.05	432.00	45.40	525.80	88.44	1.51	9.30	1.72	810.98	0.89	17.98	0.91	5.42	6.30	51.37	92.81	227.00	52.30	1345.39	150.48
MIX M TRIAL 1.1	5.8	48.52	92.80	257.00	50.40	1122.31	139.12	1.22	11.33	1.75	874.08	0.86	21.56	0.90	9.11	6.30	51.89	92.89	225.00	48.78	1370.84	149.82
MIX M TRIAL 1.2	5.8	48.75	92.78	258.00	49.22	1123.33	138.34	1.77	11.23	1.75	877.46	0.89	21.38	0.90	9.07	6.30	51.86	92.87	234.00	47.38	1317.56	144.55
MIX M TRIAL 2.1	5.8	41.02	93.24	329.00	50.12	741.19	111.79	3.24	8.48	1.81	882.84	0.83	19.95	0.90	7.11	6.30	50.28	98.03	246.00	52.21	1215.08	137.54
MIX M TRIAL 2.2	5.8	40.94	93.28	330.00	51.08	737.55	110.92	3.46	8.60	1.79	885.31	0.85	19.77	0.90	7.09	6.30	50.34	98.06	236.00	52.34	1267.90	142.61
MIX M TRIAL 3.1	5.8	38.40	93.94	322.00	48.68	708.86	105.18	9.07	8.51	1.80	890.50	0.85	19.24	0.89	7.27	6.30	54.80	92.88	152.00	50.21	2148.16	214.19
MIX M TRIAL 3.2	5.8	38.47	93.86	339.00	48.21	674.64	101.25	10.74	8.66	1.78	898.47	0.88	18.75	0.90	6.90	6.30	54.58	92.93	158.00	52.13	2118.51	212.97
MIX N TRIAL 1.1	5.8	37.44	93.31	400.00	49.06	556.48	93.04	3.47	14.29	1.77	862.58	0.88	19.23	0.90	5.85	6.30	51.50	98.05	209.00	47.80	1464.73	159.48
MIX N TRIAL 1.2	5.8	37.56	93.26	406.00	47.56	549.92	92.15	3.46	14.07	1.74	860.08	0.89	19.02	0.90	5.76	6.30	51.54	98.02	212.00	46.53	1445.16	157.19
MIX N TRIAL 2.1	5.8	30.20	94.46	470.00	47.10	381.98	70.69	0.29	16.56	1.77	875.21	0.97	16.44	0.92	4.98	6.30	46.77	92.63	299.00	48.69	929.96	124.85
MIX N TRIAL 2.2	5.8	30.25	94.45	465.00	47.38	386.73	71.60	0.11	16.82	1.77	876.09	0.96	16.59	0.92	5.03	6.30	46.89	92.60	298.00	50.90	935.41	125.47
MIX N TRIAL 3.1	5.8	29.35	94.10	504.00	50.42	346.17	69.84	1.37	13.58	1.81	857.83	0.92	16.90	0.92	4.64	6.30	42.58	98.06	365.00	48.52	692.66	99.79
MIX N TRIAL 3.2	5.8	29.35	94.10	504.00	50.42	346.17	69.84	1.37	13.58	1.81	857.83	0.92	16.90	0.92	4.64	6.30	42.51	98.09	365.00	47.55	692.41	99.35
MIX O TRIAL 1.1	5.8	38.21	93.63	361.00	56.44	629.15	96.99	0.02	15.49	1.78	877.32	0.91	18.81	0.90	6.48	6.30	54.57	92.44	199.00	52.25	1630.26	164.24
MIX O TRIAL 1.2	5.8	38.24	93.65	353.00	55.16	643.89	99.01	0.01	15.45	1.81	886.06	0.89	18.93	0.90	6.63	6.30	54.57	92.43	196.00	50.82	1655.19	167.33
MIX O TRIAL 2.1	5.8	39.69	93.25	379.00	44.97	622.58	98.86	5.37	16.00	1.77	890.25	0.91	19.16	0.90	6.17	6.30	45.36	98.54	276.00	51.20	977.07	120.36
MIX O TRIAL 2.2	5.8	39.53	93.25	382.00	44.67	615.16	98.08	5.47	15.76	1.80	886.47	0.90	19.03	0.91	6.13	6.30	45.42	98.48	277.00	50.56	974.75	121.04
MIX O TRIAL 3.1	5.8	30.35	94.24	471.00	51.09	383.02	73.01	7.64	16.09	1.73	858.41	0.93	17.00	0.92	4.97	6.30	41.02	98.41	323.00	50.95	755.03	111.38
MIX O TRIAL 3.2	5.8	30.29	94.24	465.00	51.66	387.29	73.90	7.40	15.96	1.76	861.81	0.92	17.21	0.92	5.03	6.30	41.08	98.41	318.00	52.78	768.02	113.10
MIX P TRIAL 1.1	5.8	41.64	93.11	363.00	46.76	681.88	101.02	2.18	14.40	1.86	847.79	0.91	18.88	0.91	6.45	6.30	53.44	92.80	191.00	46.33	1663.31	175.19
MIX P TRIAL 1.2	5.8	41.82	93.07	363.00	46.53	684.82	101.39	2.30	14.36	1.86	847.38	0.91	18.92	0.91	6.45	6.30	53.61	92.81	184.00	46.67	1731.89	181.73
MIX P TRIAL 2.1	5.8	41.59	92.94	369.00	60.66	670.08	102.54	1.85	15.53	1.73	852.28	0.87	19.16	0.90	6.34	6.30	51.74	92.67	228.00	52.52	1348.99	152.08
MIX P TRIAL 2.2	5.8	41.53	92.98	355.00	59.75	695.49	105.49	1.87	15.66	1.75	856.74	0.85	19.47	0.90	6.59	6.30	51.65	92.66	236.00	58.04	1300.98	146.37
MIX P TRIAL 3.1	5.8	35.96	93.62	426.00	50.77	501.77	84.82	5.33	14.47	1.85	864.58	0.90	17.74	0.91	5.49	6.30	44.44	98.31	327.00	51.93	807.90	104.74
MIX P TRIAL 3.2	5.8	35.84	93.65	429.00	49.93	496.67	83.98	5.41	14.45	1.86	872.58	0.91	17.64	0.91	5.45	6.30	44.42	98.31	321.00	54.65	822.55	106.80
MIX Q TRIAL 1.1	5.8	26.37	94.77	510.00	54.52	307.34	62.79	6.31	8.71	1.69	869.85	0.98	15.84	0.92	4.59	6.30	32.59	94.51	409.00	51.09	473.64	79.11
MIX Q TRIAL 1.2	5.8	26.36	94.78	505.00	53.49	310.32	63.47	6.65	8.68	1.68	871.83	0.98	15.96	0.93	4.63	6.30	32.64	94.52	407.00	52.33	476.75	79.40
MIX Q TRIAL 2.1	5.8	25.93	94.78	558.00	52.77	276.28	57.87	10.01	15.11	1.64	898.50	1.01	15.40	0.93	4.19	6.30	29.55	94.93	412.00	53.62	426.39	74.10
MIX Q TRIAL 2.2	5.8	25.99	94.76	559.00	52.03	276.34	58.02	10.17	15.29	1.65	906.53	1.00	15.42	0.93	4.19	6.30	29.57	94.94	418.00	52.50	420.46	72.87
MIX Q TRIAL 3.1	5.8	29.27	94.10	537.00	55.79	324.05	65.43	10.01	13.31	1.75	888.44	1.00	16.52	0.92	4.36	6.30	30.85	95.01	406.00	49.41	451.70	73.28
MIX Q TRIAL 3.2	5.8	29.28	94.11	539.00	55.26	322.96	64.96	10.07	13.29	1.74	884.74	1.01	16.36	0.92	4.34	6.30	30.80	95.04	408.00	49.16	454.29	73.28
MIX R TRIAL 1.1	5.8	22.22	95.31	505.00	51.97	261.56	58.90	1.17	12.45	1.72	876.37	0.97	15.67	0.92	4.63	6.30	28.51	94.90	420.00	52.26	403.56	73.45
MIX R TRIAL 1.2	5.8	22.36	95.25	518.00	51.95	256.62	57.97	0.66	12.67	1.71	873.68	0.99	15.54	0.93	4.52	6.30	28.45	94.89	425.00	51.68	397.92	72.75
MIX R TRIAL 2.1	5.8	25.83	94.76	518.00	49.05	296.40	62.24	1.32	15.93	1.63	884.63	0.95	15.78	0.93	4.52	6.30	36.07	98.34	463.00	49.21	463.09	80.14
MIX R TRIAL 2.2	5.8	26.07	94.73	525.00	48.89	295.23	61.58	0.96	15.84	1.64	888.97	0.97	15.60	0.93	4.46	6.30	35.94	98.37	467.00	48.72	457.45	79.18
MIX R TRIAL 3.1	5.8	20.75	95.62	496.00	53.23	248.71	56.80	7.96	14.41	1.76	871.25	0.99	15.55	0.93	4.72	6.30	30.32	94.56	459.00	54.83	392.68	70.32
MIX R TRIAL 3.2	5.8	20.78	95.64	485.00	54.02	254.73	57.96	7.47	14.36	1.76	869.40	0.98	15.73	0.92	4.82	6.30	30.36	94.54	468.00	55.77	389.74	69.80
MIX S TRIAL 1.1	5.8	20.10	95.27	623.00	53.54	191.79	48.83	1.46	14.93	1.73	879.67	0.98	15.02	0.93	3.76	6.30	27.17	94.60	521.00	52.73	309.96	63.52
MIX S TRIAL 1.2	5.8	20.12	95.20	637.00	52.72	187.79	48.39	3.44	14.36	1.72	879.40	0.98	15.02	0.93	3.67	6.30	27.31	94.58	515.00	52.78	315.18	64.48
MIX S TRIAL 2.1	5.8	28.47	93.70	566.00	50.68	298.98	65.73	1.00	20.71	1.86	839.76	0.96	17.54	0.91	4.13	6.30	33.65	98.75	438.00	51.48	456.68	82.56
MIX S TRIAL 2.2	5.8	28.49	93.71	568.00	50.51	298.16	65.52	0.38	20.76	1.81	847.95	0.96	17.47	0.91	4.12	6.30	33.60	98.80	432.00	52.86	462.33	83.26
MIX S TRIAL 3.1	5.8	25.74	94.70	569.00	46.20	268.91	58.46	6.91	12.48	1.69	937.65	0.96	15.90	0.92	4.11	6.30	37.05	98.61	375.00	56.36	587.37	94.77
MIX S TRIAL 3.2	5.8	25.91	94.63	580.00	45.92	265.52	57.93	6.15	12.28	1.69	934.06	0.97	15.88	0.92	4.03	6.30	36.58	98.69	389.00	54.52	558.19	90.44

Table G1 (Continued)

st Sensitivity		quency and Orientation Selecti			formation Processing in the HV				Contrast	Visibility			Contrast Sensitivity				Frequency and Orientation Selectivity			Information Processing in the HVS			
UNIFORMITY RADIAL	UNIFORMITY ANGULAR	INCONSISTENCY COEFFICIENT	AVERAGE CENTROIDS DISTANCES	FORM FACTOR	AVERAGE COMPACTENESS PER REGION	SOLIDITY	ECCENTRICITY	PERCENT BINDER CONTENT	PERCENT AREA OF BLACK PIXELS	CONNECTIVITY OF BLACK PIXELS	NUMBER OF REGIONS	ORIENTATION	AREA OF REGIONS	AVERAGE PERIMETER PER REGION	UNIFORMITY RADIAL	UNIFORMITY ANGULAR	INCONSISTENCY COEFFICIENT	AVERAGE CENTROIDS DISTANCES	FORM FACTOR	AVERAGE COMPACTENESS PER REGION	SOLIDITY	ECCENTRICITY	Estimated Binder
5.98	11.11	1.86	896.07	0.83	21.84	0.89	9.11	6.30	61.45	92.58	101.00	51.38	3617.09	268.14	6.66	8.32	1.48	871.97	0.90	27.11	0.90	23.17	5.40
6.03	11.05	1.91	908.38	0.87	21.78	0.90	9.11	6.30	61.43	92.56	95.00	52.62	3843.80	284.42	6.75	8.36	1.48	873.86	0.84	28.20	0.89	24.63	5.50
1.34	10.51	1.85	910.62	0.83	22.52	0.89	9.87	6.30	61.66	92.96	100.00	48.67	3665.37	289.63	2.51	9.89	1.70	986.83	0.86	28.93	0.90	23.40	5.70
0.89	10.86	1.81	910.10	0.83	22.49	0.88	10.00	6.30	61.64	92.96	99.00	47.35	3701.24	293.21	2.61	9.64	1.70	985.44	0.88	29.25	0.89	23.64	5.40
10.91	14.25	2.28	847.85	0.79	25.14	0.88	17.08	6.30	70.32	92.73	47.00	49.27	8894.49	424.86	4.73	10.81	1.42	827.58	0.79	31.10	0.89	49.79	5.70
11.00	14.09	2.05	848.61	0.78	25.06	0.88	17.08	6.30	70.22	92.72	50.00	48.38	8348.70	396.79	4.86	10.84	1.41	836.16	0.88	28.96	0.90	46.80	5.50
6.40	12.88	1.78	846.26	0.92	21.83	0.90	9.71	6.30	58.51	92.61	155.00	51.93	2243.92	200.19	5.49	13.50	1.87	830.24	0.92	23.62	0.90	15.10	5.10
6.54	12.94	1.78	846.88	0.90	22.13	0.89	9.87	6.30	58.35	92.63	159.00	49.86	2181.65	197.74	5.34	13.46	1.88	824.85	0.94	23.65	0.90	14.72	5.10
5.33	13.80	1.79	891.10	0.95	22.87	0.90	13.85	6.30	71.46	92.80	60.00	52.37	7080.15	318.87	0.88	12.77	1.37	694.85	1.03	23.47	0.93	39.00	5.20
5.27	14.01	1.76	896.61	0.91	23.44	0.89	14.27	6.30	71.39	92.80	59.00	58.55	7198.49	304.12	0.88	12.84	1.37	682.20	0.98	22.89	0.92	39.66	5.20
2.16	20.26	1.67	736.97	0.94	25.49	0.91	16.14	6.30	71.71	92.37	46.00	47.85	9267.35	348.68	5.25	8.75	1.14	763.34	0.98	23.52	0.93	50.87	5.70
2.14	20.16	1.66	730.83	0.94	25.66	0.91	16.83	6.30	71.65	92.41	44.00	46.83	9680.55	368.39	5.25	8.78	1.05	752.93	1.00	23.47	0.94	53.18	5.70
3.64	12.15	1.41	806.30	0.89	26.43	0.90	18.28	6.30	68.10	92.83	92.00	51.21	4400.38	264.55	1.37	11.83	1.23	941.72	0.96	24.28	0.93	25.43	5.20
3.61	11.87	1.39	803.82	0.88	25.30	0.90	17.86	6.30	68.06	92.82	89.00	48.89	4546.03	283.99	1.75	11.89	1.40	960.41	0.93	26.08	0.92	26.29	5.20
7.63	15.44	1.50	997.19	0.90	24.98	0.92	19.83	6.30	74.48	93.01	39.00	48.96	11352.59	357.58	7.10	5.40	1.13	994.92	1.04	22.83	0.94	60.00	5.20
7.72	15.37	1.51	996.39	0.89	24.70	0.91	20.58	6.30	74.58	92.98	40.00	50.06	11076.15	368.45	7.05	5.39	1.13	974.58	1.02	23.62	0.94	58.50	5.20
5.99	14.68	1.68	800.26	0.90	27.30	0.90	16.36	6.30	68.44	93.16	59.00	48.20	6896.12	347.21	6.08	7.74	1.23	894.75	0.84	26.61	0.92	39.66	5.60
5.90	14.65	1.62	813.42	0.85	28.56	0.89	17.33	6.30	68.42	93.17	57.00	48.13	7135.96	358.55	6.09	7.69	1.13	881.48	0.85	26.95	0.92	41.05	5.60
2.02	7.92	1.39	881.76	0.99	24.95	0.92	25.43	6.30	69.77	92.77	54.00	48.49	7680.46	383.95	8.52	8.33	1.40	986.04	1.00	28.79	0.93	43.33	5.20
2.06	8.02	1.26	879.65	1.00	25.79	0.92	26.90	6.30	69.76	92.76	51.00	50.77	8131.35	443.02	8.55	8.25	1.39	985.24	0.97	33.01	0.93	45.88	5.20
3.54	11.26	1.55	836.46	0.95	29.09	0.90	28.19	6.30	71.23	92.71	47.00	45.70	9008.74	438.26	2.91	9.90	1.14	769.90	1.09	29.94	0.94	49.79	5.30
3.46	11.18	1.54	850.25	1.00	28.24	0.90	26.90	6.30	71.15	92.74	45.00	42.20	9398.78	455.41	2.93	9.98	1.19	765.62	1.03	30.64	0.94	52.00	5.30
5.18	16.43	1.64	794.23	0.92	27.34	0.89	19.83	6.30	76.24	92.52	38.00	58.60	11926.21	285.13	8.79	8.38	1.14	882.23	0.99	18.66	0.94	61.58	5.40
5.04	16.25	1.35	803.07	0.97	26.62	0.90	18.87	6.30	76.31	92.54	39.00	54.57	11631.64	276.33	8.72	8.40	1.14	904.65	1.04	18.04	0.94	60.00	5.40
4.96	10.28	1.50	854.39	0.93	23.17	0.90	10.31	6.30	58.81	92.33	156.00	48.67	2241.20	195.82	0.77	10.97	1.63	809.49	0.91	23.45	0.90	15.00	5.50
5.15	10.45	1.52	849.96	0.90	24.12	0.89	10.64	6.30	58.76	92.35	150.00	48.24	2328.81	202.95	0.76	11.02	1.60	807.20	0.88	23.96	0.90	15.60	5.50
16.29	13.48	1.78	878.61	0.88	22.14	0.90	9.29	6.30	54.46	92.57	170.00	51.90	1904.21	189.94	6.43	10.54	1.59	872.72	0.81	23.50	0.89	13.76	5.60
16.32	12.94	1.75	874.91	0.88	22.22	0.90	9.29	6.30	54.56	92.96	163.00	51.87	1989.85	198.29	6.50	10.59	1.58	869.71	0.80	24.14	0.88	14.36	5.60
16.32	12.94	1.75	874.91	0.88	22.22	0.90	9.29	6.30	54.56	92.96	163.00	51.87	1989.85	198.29	6.50	10.59	1.58	869.71	0.80	24.14	0.88	14.36	5.60
5.78	15.23	1.63	819.59	0.85	25.72	0.89	15.50	6.30	66.40	92.69	73.00	48.08	5406.85	239.86	0.55	9.32	1.20	912.41	1.02	21.05	0.93	32.05	5.60
3.01	10.27	1.73	851.21	0.87	23.11	0.90	11.41	6.30	75.00	92.57	25.00	51.61	17834.24	614.36	9.90	8.76	1.21	987.90	0.81	34.49	0.88	93.60	5.30
3.03	10.33	1.73	858.29	0.88	23.18	0.90	11.20	6.30	75.02	92.58	28.00	51.79	15926.43	548.64	9.86	8.75	1.21	975.51	0.90	30.87	0.89	83.57	5.30
0.42	12.43	1.81	937.41	0.83	23.47	0.88	10.54	6.30	62.71	92.55	86.00	52.29	4334.63	305.15	5.15	9.91	1.73	952.37	0.89	29.69	0.89	27.21	5.50
0.32	12.44	1.81	937.54	0.85	23.58	0.88	10.59	6.30	62.66	92.57	84.00	52.05	4434.14	315.43	5.16	9.86	1.73	956.76	0.89	30.38	0.89	27.86	5.50
8.77	12.21	1.90	915.13	0.85	23.93	0.89	13.68	6.30	56.54	92.77	146.00	47.03	2302.02	208.63	2.32	15.85	1.47	908.19	0.88	25.67	0.89	16.03	5.70
8.79	12.28	1.97	901.00	0.88	23.51	0.90	13.37	6.30	56.46	92.79	149.00	46.20	2252.72	208.28	2.34	15.96	1.47	906.44	0.90	24.98	0.90	15.70	5.70
1.80	13.82	1.83	888.72	0.85	20.77	0.90	9.14	6.30	65.10	92.81	81.00	44.91	4777.44	326.62	6.72	11.05	1.49	911.40	0.98	28.95	0.92	28.89	5.50
1.83	13.80	1.79	894.10	0.83	21.18	0.89	9.36	6.30	65.34	92.76	78.00	44.02	4979.72	340.18	6.72	11.05	1.40	901.72	0.93	30.07	0.92	30.00	5.50
12.37	17.70	2.01	836.44	0.84	21.26	0.90	10.54	6.30	62.77	93.10	96.00	55.11	3886.96	273.57	1.38	10.90	1.70	1015.67	0.84	26.24	0.89	24.38	5.50
11.99	17.56	2.01	833.74	0.85	21.19	0.90	10.26	6.30	62.84	93.09	99.00	54.82	3773.27	265.50	1.35	11.00	1.39	995.41	0.85	25.72	0.89	23.64	5.50
4.15	12.54	1.87	874.08	0.87	19.29	0.90	7.43	6.30	56.29	93.22	141.00	58.79	2373.22	215.46	7.70	9.29	1.82	860.11	0.88	24.42	0.90	16.60	5.50
4.31	12.80	1.92	876.55	0.88	19.33	0.90	7.52	6.30	56.20	93.22	141.00	55.91	2369.23	217.49	7.63	9.39	1.60	860.14	0.85	24.79	0.90	16.60	5.50
16.64	10.63	2.05	870.25	0.87	25.10	0.90	19.18	6.30	67.82	92.78	71.00	48.75	5678.39	272.17	10.98	10.87	1.23	805.70	1.08	21.61	0.94	32.96	5.70
16.51	10.15	2.07	888.44	0.88	25.33	0.90	19.18	6.30	67.64	92.83	70.00	50.93	5744.11	275.73	11.15	11.26	1.24	807.85	1.02	21.99	0.94	33.43	5.70
0.93	11.62	2.00	899.10	0.84	23.78	0.89	15.10	6.30	65.69	93.02	81.00	49.36	4821.32	277.45	4.40	10.98	1.38	901.49	0.95	24.57	0.93	28.89	5.70
0.94	11.67	1.99	897.44	0.80	25.20	0.89	16.14	6.30	65.56	93.08	86.00	47.29	4531.79	261.47	4.40	11.04	1.51	899.89	0.97	23.50	0.93	27.21	5.70
7.61	16.15	1.86	936.67	0.91	22.68	0.90	13.76	6.30	60.83	92.92	133.00	51.51	2719.05	189.87	6.11	16.94	1.50	927.33	0.91	21.46	0.91	17.59	5.80
7.64	16.03	1.90	935.55	0.90	22.44	0.90	13.93	6.30	60.75	92.92	141.00	52.62	2561.27	179.77	6.20	16.85	1.50	933.21	0.95	20.82	0.91	16.60	5.80
3.92	11.54	1.78	853.99	0.85	25.22	0.89	14.27	6.30	54.62	93.13	155.00	54.41	2094.96	189.89	6.46	15.23	1.73	957.74	0.90	22.77	0.91	15.10	5.30
3.96	11.68	1.77	872.68	0.88	24.85	0.89	13.85	6.30	54.35	93.19	154.00	56.36	2097.82	190.52	6.95	15.07	1.69	947.51	0.85	22.97	0.91	15.19	5.30
3.83	15.56	1.61	916.83	0.77	27.02	0.88	15.81	6.30	58.27	93.17	131.00	52.93	2644.41	196.14	10.06	16.41	1.93	952.36	0.86	21.88	0.91	17.86	5.40
4.07	15.60	1.60	916.59	0.79	26.49	0.88	15.50	6.30	58.34	93.16	137.00	52.05	2531.26	187.19	10.05	16.40	1.93	954.01	0.90	20.92	0.92	17.08	5.40
6.77	13.90	1.84	886.61	0.89	21.10	0.90	9.87	6.30	64.29	93.60	80.00	58.74	4777.41	287.20	6.09	18.04	1.58	884.54	0.94	26.03	0.92	29.25	5.60
6.61	13.87	1.84	888.17	0.86	21.46	0.89	9.96	6.30	64.25	93.60	86.00	52.95	4441.35	267.71	5.83	18.08	1.56	886.09	0.96	24.66	0.92	27.21	5.60
10.53	10.74	1.67	890.64	0.88	21.93	0.90	11.58	6.80	51.00	93.45	215.00	52.03	1410.25	144.64	7.99	6.70	1.71	883.77	0.92	19.87	0.91	10.88	5.70
10.49	10.71	1.65	896.95	0.87	21.70	0.90	11.41	6.80	50.98	93.46	216.00	51.76	1402.99	143.45	8.00	6.72	1.71	880.71	0.94	19.64	0.91	10.83	5.70
0.09	10.27	1.75	864.32	0.87	21.27	0.90	11.94	6.80	67.12	92.62	81.00	47.99	4925.86	301.34	8.22	8.53	1.46	806.44	0.95	26.15	0.91	28.89	5.70
0.09	10.27	1.75	864.32	0.87	21.27	0.90	11.94	6.80	67.24	92.62	75.00	48.52	5329.65	311.15	8.32	8.58	1.41	808.96	0.90	26.26	0.91	31.20	5.70
11.77	12.91	1.67	821.81	0.91	21.32	0.91	10.17	6.80	59.62	93.35	122.00	52.37	2904.98	232.51	2.36	8.96	1.92	856.37	0.89	24.08	0.91	19.18	5.70
11.87	13.51	1.66	824.55	0.91	21.28	0.91	10.04	6.80	59.62	93.35	122.00	52.37	2904.98	232.51	2.36	8.96	1.92	856.37	0.89	24.08	0.91	19.18	5.70
2.93	20.33	1.49	918.96	0.91	20.98	0.90	10.88	6.80	57.86	93.01	175.00	51.33	1965.55	170.72	0.18	15.44	1.35	870.13	0.98	20.75	0.93	13.37	5.80
2.80	20.28	1.50	915.35	0.90	20.93	0.90	10.88	6.80	57.76	93.08	174.00	51.90	1973.36	173.48	0.22	15.34	1.33	867.08	0.97	20.97	0.92	13.45	5.80
10.12	13.33	1.52	899.07	0.91	20.41	0.90	8.27	6.80	62.75	92.32	114.00	44.16	3272.23	272.27	1.48	6.68	1.87	902.57	0.88	27.86	0.90	20.53	5.08
10.58	13.36	1.53	901.32	0.90	20.49	0.90	8.45	6.80	62.56	92.37	110.00	44.44	3380.74	280.89	1.49	6.79	1.77	905.65	0.92	28.72	0.90	21.27	5.80
4.18	12.41	1.79	856.38	0.89	21.61	0.90	10.31	6.80	58.38	92.08	168.00	57.49	2065.61	206.15	5.01	7.33	1.68	829.02	0.83	25.35	0.90	13.93	5.90
4.24	12.61	1.82	855.10	0.88	21.38	0.90	10.31	6.80	58.38	92.01	170.00	56.82	2041.28	204.23	4.95	7.40	1.67	825.51	0.83	25.20	0.90	13.76	5.90
2.46	14.59	1.78	829.21	0.88	21.36	0.90	10.40	6.80	68.46	93.17	63.00	50.49	6459.52	359.01	0.91	15.15	1.67	846.38	0.94	27.68	0.92	37.14	5.80
2.34	14.62	1.79	830.51	0.91	20.82	0.90	10.00	6.80	68.45	93.17	62.00	50.74	6563.18	367.53	0.78	15.14	1.68	842.41	0.96	28.16	0.93	37.74	5.80
6.02	8.96	1.63	916.24	0.91	20.15	0.91	9.51	6.80	59.06	93.05	116.00	58.59	3026.81	234.71	10.50	13.81	1.42	878.71	0.87	24.30	0.90	20.17	6.00
5.91	8.81	1.68	913.52	0.88	20.54	0.91	9.92	6.80	58.98	93.04	119.00	58.68	2946.10	230.90	10.60	13.85	1.41	886.92	0.89	24.00	0.91	19.66	6.00
1.32	10.33	1.77	803.48	0.80	25.96	0.88	15.39	6.80	63.04	92.90	96.00	52.68	3903.42	269.41	3.89	9.69	1.78	835.03	0.87	26.52	0.90	24.38	6.10
1.43	10.60	1.75	806.58	0.83	26.00	0.89	15.29	6.80	63.14	92.87	102.00	50.86	3679.68	254.47	3.66	9.54	1.75	834.67	0.89	25.47	0.90	22.94	6.10
15.39	15.61	1.79	888.51	0.87	21.98	0.90	11.20	6.80	78.27	92.86	43.00	45.65	10820.98	362.07	3.64	12.74	1.56	682.99	0.82	27.24	0.91	54.42	5.60
15.30	15.73	1.79	881.30	0.88	21.78	0.90	11.04	6.80	77.92	92.91	42.00	48.65	11029.00	369.39	3.68	13.13	1.54	694.10	0.79	27.22	0.90	55.71	5.60
6.08	8.59	1.85	914.42	0.86	20.86	0.89	7.83	6.80	57.55	92.51	141.00	46.91	2426.48	227.93	0.51	8.28	1.81	928.57	0.91	27.10	0.90	16.60	5.70
6.04	8.66	1.77	913.06	0.85	20.93	0.89	7.85	6.80	57.76	92.48	139.00	46.11	2470.11	230.50	0.47	8.46	1.67	930.05	0.89	27.21	0.89	16.83	5.70
8.01	11.61	1.69	853.65	0.89	18.62	0.91	6.41	6.80	50.28	93.15	236.00	48.63	1266.48	140.32	3.27	14.82	1.84	881.35	0.91	20.48	0.90	9.92	5.80
7.89	11.96	1.71	853.15	0.90	18.45	0.91	6.41	6.80	50.28	93.13	242.00	47.36	1235.14	137.24	3.74	14.68	1.84	884.20	0.93	20.19	0.91	9.67	5.80
17.95	14.15	1.76	915.17	0.91	21.78	0.91	11.76	6.80	69.61	92.77	80.00	51.60	5172.61	258.90	7.20	9.62	1.41	987.44	0.94	21.85	0.92	29.25	6.00
18.05	14.14	1.73	913.95	0.91	22.16	0.91	11.94	6.80	69.54	92.78	76.00	51.37	5439.68	263.88	7.12	9.63	1.41	991.78	0.91	22.28	0.91	30.79	6.00
2.29	15.05	1.73	893.65	0.88	19.10	0.91	8.48	6.80	66.41	92.13	72.00	41.93	5482.94	325.22	1.24	9.96	1.46	926.54	0.93	27.96	0.91	32.50	6.10
2.31	15.39	1.75	900.10	0.89	19.38	0.91	8.45	6.80	66.22	92.09	72.00	43.77	5467.47	330.37	1.20	9.98	1.40	921.21	0.91	28.54	0.90	32.50	6.10
7.33	10.42	1.80	871.08	0.85	20.27	0.90	7.24	6.80	35.30	93.81	409.00	58.35	513.10	85.29	10.31	10.15	1.79	844.39	0.90	17.56	0.92	5.72	6.00
7.37	10.41	1.79	872.75	0.84	20.52	0.89	7.36	6.80	35.19	93.83	409.00	54.91	511.50	85.28	10.22	10.08	1.80	846.64	0.89	17.60	0.91	5.72	6.00
1.98	8.08	1.71	885.24	0.83	23.30	0.89	12.25	6.80	68.70	92.55	78.00	58.36	5235.53	308.34	3.70	8.30	1.26	901.54	1.02	25.86	0.93	30.00	5.80
1.95	7.95	1.73	884.97	0.81	23.86	0.89	12.72	6.80	68.97	92.47	77.00	57.22	5324.92	307.08	3.51	8.41	1.26	910.80	1.03	25.98	0.93	30.39	5.80
0.16	11.52	1.76	863.94	0.91	21.46	0.90	10.26	6.80	61.16	93.28	143.00	48.33	2542.58	187.12	9.32	9.94	1.59	873.67	1.02	20.25	0.93	16.36	5.90
0.10	11.54	1.78	876.35	0.90	20.89	0.90	9.92	6.80	61.12	93.27	142.00	46.33	2558.87	189.25	9.21	9.90	1.79	871.50	1.00	20.38	0.92	16.48	5.80
3.83	20.31	1.77	865.33	0.91	18.46	0.91	7.16	6.80	55.49	92.86	188.00	58.40	1754.56	172.10	7.07	10.87	1.87	958.11	0.86	22.31	0.90	12.45	5.80
4.02	20.43	1.75	868.48	0.89	18.83	0.91	7.29	6.80	55.44	92.84	190.00	58.46	1734.44	170.96	7.11	10.93	2.05	948.93	0.87	22.45	0.90	12.32	5.90
4.15	12.61	1.71	887.58	0.94	16.95	0.92	5.72	6.80	42.57	93.73	328.00	58.27	771.44	101.41	1.69	12.10	1.70	902.88	0.97	17.53	0.91	7.13	5.80
4.84	12.46	1.69	887.18	0.93	16.84	0.92	5.75	6.80	42.56	93.69	329.00	52.64	768.96	101.33	1.78	12.04	1.72	897.39	0.95	17.68	0.92	7.11	5.80
0.27	15.58	1.71	878.25	0.97	16.29	0.92	5.68	6.80	39.16	94.35	325.00	58.89	716.34	93.90	9.08	17.72	1.72	856.27	0.97	16.22	0.93	7.20	6.00
0.44	15.55	1.71	878.55	0.98	16.08	0.92	5.60	6.80	39.11	94.38	317.00	54.57	733.36	96.01	9.24	17.65	1.71	863.14	0.95	16.47	0.93	7.38	6.10
9.79	22.22	1.64	884.07	0.99	16.04	0.92	5.76	6.80	40.33	93.99	324.00	46.84	739.91	101.50	2.68	9.29	1.64	891.64	0.92	17.90	0.91	7.22	6.10
9.88	22.78	1.64	887.17	1.00	15.88	0.93	5.81	6.80	40.24	94.01	327.00	45.85	731.54	100.43	2.73	9.36	1.64	890.25	0.94	17.80	0.91	7.16	6.00
4.28	13.53	1.75	873.08	0.93	16.37	0.92	5.57	6.80	35.84	94.02	396.00	55.14	537.99	84.13	1.84	19.36	1.77	849.43	0.97	16.82	0.92	5.91	6.70
4.41	13.48	1.75	874.16	0.94	16.39	0.92	5.51	6.80	35.81	93.99	406.00	55.80	524.37	82.41	1.82	19.34	1.74	845.32	0.97	16.69	0.92	5.76	6.70
4.26	9.99	1.86	863.91	0.95	17.40	0.91	5.05	6.80	46.13	93.15	298.00	46.10	920.22	117.70	9.43	17.98	1.67	863.65	0.97	20.28	0.91	7.85	6.80
4.25	9.93	1.86	866.47	0.95	17.26	0.91	5.01	6.80	46.08	93.29	285.00	45.98	961.15	120.58	9.23	18.33	1.64	855.50	0.95	20.05	0.91	8.21	6.80
18.22	15.00	1.72	865.14	0.96	16.20	0.92	5.10	6.80	35.18	93.53	466.00	51.48	448.77	78.46	4.89	13.93	1.70	842.58	0.94	17.17	0.91	5.02	6.70
18.19	14.93	1.70	864.05	0.97	16.08	0.92	5.05	6.80	35.10	93.52	471.00	51.92	443.05	77.72	4.73	13.59	1.73	840.97	0.93	17.05	0.91	4.97	6.70
7.20	13.50	1.67	903.24	0.94	16.47	0.91	4.49	6.80	29.82	94.55	464.00	58.51	382.01	70.37	0.45	9.60	1.73	894.42	0.94	16.35	0.92	5.04	6.70
7.38	13.05	1.70	906.83	0.96	16.68	0.91	4.54	6.80	29.76	94.58	458.00	58.49	386.25	70.93	0.72	9.69	1.71	893.86	0.94	16.41	0.92	5.11	6.90
3.35	13.33	1.85	867.21	0.94	18.50	0.90	5.34	6.80	43.05	93.42	328.00	58.85	780.27	108.08	2.75	12.81	1.69	835.42	0.96	18.49	0.91	7.13	7.00
3.37	13.19	1.87	862.27	0.93	18.55	0.90	5.42	6.80	43.02	93.42	327.00	58.00	781.98	108.21	2.83	12.67	1.72	840.06	0.93	18.59	0.91	7.16	7.00
1.63	16.97	1.68	870.86	0.93	18.95	0.90	6.24	6.80	42.31	93.82	295.00	52.91	852.51	112.61	4.40	13.30	1.81	882.20	0.90	19.10	0.91	7.93	6.90
1.63	17.04	1.67	866.06	0.94	18.28	0.91	6.02	6.80	42.28	93.81	303.00	51.78	829.57	109.74	4.46	13.21	1.81	873.37	0.91	18.71	0.91	7.72	6.70

Table G2 Training, testing and predicting data base for the granitic and oolitic materials using GRNN model.

	Train-Test Report for Net Trained on Data Set #1				Train-Test Report for Net Trained on Data Set #1				Prediction Report: "Net Trained on Data Set #1	
Estimated Binder	Tag Used	Prediction	Good/Bad	Residual	Tag Used	Prediction	Good/Bad	Residual	Tag Used	Prediction
5.40	test	5.56	Good	-0.16	train				predict	5.60
5.50	test	5.55	Good	-0.05	train				predict	5.60
5.70	train				test	5.41	Good	0.29	predict	5.70
5.40	train				train				predict	5.70
5.70	train				train				predict	5.70
5.50	train				train				predict	5.50
5.10	test	5.10	Good	0.00	train				predict	5.10
5.10	train				train				predict	5.10
5.20	train				test	5.20	Good	0.00	predict	5.20
5.20	train				train				predict	5.20
5.70	test	5.60	Good	0.10	train				predict	5.70
5.70	test	5.60	Good	0.10	train				predict	5.70
5.20	train				test	5.21	Good	-0.01	predict	5.20
5.20	train				train				predict	5.20
5.20	train				train				predict	5.20
5.20	train				train				predict	5.20
5.60	train				train				predict	5.61
5.60	train				test	5.60	Good	0.00	predict	5.60
5.20	test	5.20	Good	0.00	train				predict	5.20
5.20	train				train				predict	5.20
5.30	train				train				predict	5.30
5.30	train				train				predict	5.30
5.40	test	5.40	Good	0.00	test	5.39	Good	0.01	predict	5.40
5.40	train				train				predict	5.40
5.50	train				train				predict	5.50
5.50	test	5.53	Good	-0.03	train				predict	5.50
5.60	train				train				predict	5.60
5.60	train				train				predict	5.60
5.60	train				test	5.60	Good	0.00	predict	5.60
5.60	train				test	5.67	Good	-0.07	predict	5.60
5.30	train				test	5.30	Good	0.00	predict	5.30

Table G2 (Continued)

	Train-Test Report for Net Trained on Data Set #1				Train-Test Report for Net Trained on Data Set #1				Prediction Report: "Net Trained on Data Set #1	
Estimated Binder	Tag Used	Prediction	Good/Bad	Residual	Tag Used	Prediction	Good/Bad	Residual	Tag Used	Prediction
5.30	train				test	5.30	Good	0.00	predict	5.30
5.30	train				train				predict	5.30
5.50	train				train				predict	5.50
5.50	train				train				predict	5.50
5.70	train				train				predict	5.70
5.70	train				test	5.70	Good	0.00	predict	5.70
5.50	train				train				predict	5.50
5.50	train				train				predict	5.50
5.50	train				train				predict	5.50
5.50	train				train				predict	5.50
5.50	test	5.51	Good	-0.01	train				predict	5.50
5.50	train				train				predict	5.50
5.70	train				train				predict	5.70
5.70	train				train				predict	5.70
5.70	train				test	5.80	Good	-0.10	predict	5.70
5.70	train				test	5.80	Good	-0.10	predict	5.70
5.80	train				train				predict	5.80
5.80	train				train				predict	5.80
5.30	train				train				predict	5.30
5.30	train				train				predict	5.30
5.40	train				test	5.40	Good	0.00	predict	5.40
5.40	train				train				predict	5.40
5.60	test	5.59	Good	0.01	train				predict	5.60
5.60	train				train				predict	5.60
5.70	train				train				predict	5.70
5.70	train				train				predict	5.70
5.70	train				train				predict	5.70
5.70	test	5.70	Good	0.00	train				predict	5.70
5.70	train				train				predict	5.70
5.70	train				train				predict	5.70
5.80	train				train				predict	5.80
5.80	test	5.80	Good	0.00	train				predict	5.80
5.08	train				train				predict	5.27
5.80	train				test	5.08	Good	0.72	predict	5.61
5.90	train				train				predict	5.90

Table G2 (Continued)

	Train-Test Report for Net Trained on Data Set #1				Train-Test Report for Net Trained on Data Set #1				Prediction Report: "Net Trained on Data Set #1	
Estimated Binder	Tag Used	Prediction	Good/Bad	Residual	Tag Used	Prediction	Good/Bad	Residual	Tag Used	Prediction
5.90	train				test	5.90	Good	0.00	predict	5.90
5.80	train				train				predict	5.80
5.80	train				train				predict	5.80
6.00	train				test	5.99	Good	0.01	predict	6.00
6.00	train				train				predict	6.00
6.10	train				train				predict	6.10
6.10	train				train				predict	6.10
5.60	train				train				predict	5.60
5.60	train				train				predict	5.60
5.70	train				train				predict	5.70
5.70	train				train				predict	5.70
5.80	test	5.80	Good	0.00	train				predict	5.80
5.80	train				test	5.80	Good	0.00	predict	5.80
6.00	train				test	6.00	Good	0.00	predict	6.00
6.00	train				train				predict	6.00
6.10	test	5.54	Good	0.56	train				predict	6.09
6.10	test	5.56	Good	0.54	train				predict	6.09
6.00	train				train				predict	6.00
6.00	train				train				predict	6.00
5.80	train				train				predict	5.80
5.80	train				train				predict	5.80
5.90	train				test	5.80	Good	0.10	predict	5.86
5.80	train				train				predict	5.84
5.80	test	5.91	Good	-0.11	train				predict	5.82
5.90	train				train				predict	5.88
5.80	train				test	5.80	Good	0.00	predict	5.81
5.80	train				train				predict	5.82
6.00	train				train				predict	6.10
6.10	test	6.00	Good	0.10	train				predict	6.10
6.10	test	6.01	Good	0.09	train				predict	6.00
6.00	test	6.08	Good	-0.08	test	6.10	Good	-0.10	predict	6.00
6.70	train				train				predict	6.70
6.70	train				train				predict	6.70
6.80	train				train				predict	6.59
6.80	train				train				predict	6.59
6.70	train				train				predict	6.70
6.70	train				train				predict	6.70
6.70	test	6.62	Good	0.08	train				predict	6.75
6.90	test	6.21	Good	0.69	train				predict	6.85
7.00	train				train				predict	7.00
7.00	train				test	6.99	Good	0.01	predict	7.00
6.90	test	6.70	Good	0.20	test	6.70	Good	0.20	predict	6.84
6.70	train				train				predict	6.74

APPENDIX H: STEPS FOR USING THE AUTOMATED OBC PREDICTION MODEL

STEPS FOR USING THE AUTOMATED OBC PREDICTION MODEL

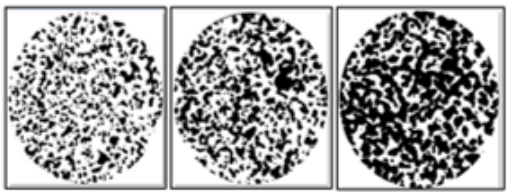

Mejias De Pernia, Yolibeth

May, 2015

Chapter 1: Getting Started

Introduction

The purpose of this guide is to illustrate the steps required in using the automated software package developed by the University of South Florida to predict the optimum binder content (OBC) of open graded friction course (OGFC) mixtures. The software package has been created using *Matlab* and *NeuralTools*. The general steps of the software package are shown in the following Figure C-1.

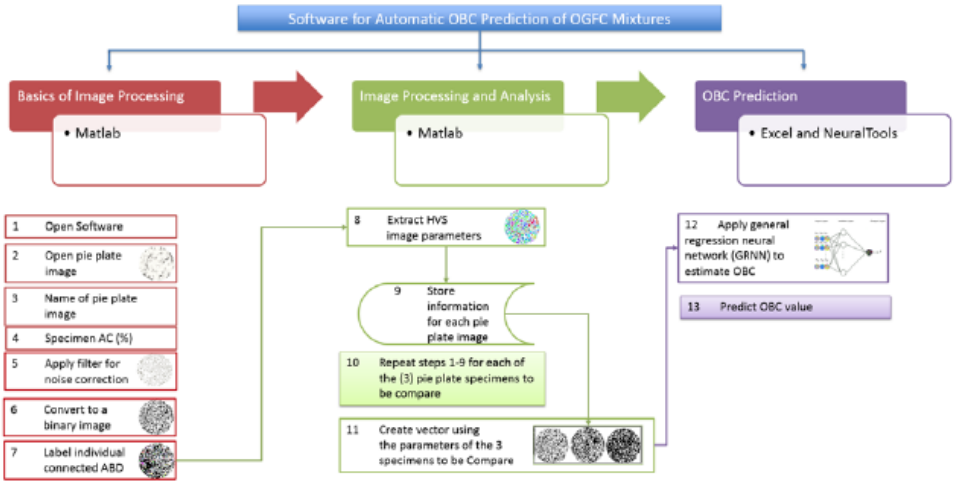

Figure C-1 Steps of the automatic OBC prediction of OGFC mixture software.

MATLAB was used to development an algorithm that measures and analyzes the digital images of the samples and acquire the human perception metrics considered to predict the OBC of a set of samples. The MATLAB algorithm can be run on your digital data, the charts from your analyses are created in MATLAB and the results report it is send automatically to a Microsoft Excel file.

NeuralTools was used to development of a general regression neural network (GRNN) to uncover the nonlinear correlation between the selected parameters of pie plate images, the corresponding asphalt binder contents and the visually estimated OBC. NeuralTools provides you with powerful neural network capabilities in an environment that you are familiar with - Microsoft Excel. NeuralTools procedures - such as defining data sets, training and testing neural networks and predicting values using trained networks- can be run on your data in Excel and the reports and charts from your analyses are created in Excel.

Checking your NeuralTools package

Your NeuralTools package should contain:

The NeuralTools or DecisionTools Suite CD-ROM including:

- *NeuralTools Program*
- *NeuralTools Tutorial*
- *The NeuralTools Users Guide in PDF format*

The NeuralTools Licensing Agreement

If your package is not complete, please call your NeuralTools dealer or supplier or contact Palisade Corporation directly at (607) 277-8000.

NeuralTools System requirements

System requirements for NeuralTools 5.0 for Microsoft Excel for Windows include:

- *Microsoft Windows 2000 SP4, Windows XP or higher.*
- *Microsoft Excel 2000 or higher.*

NeuralTools Installation and Activation Instructions

Download DecisionTools Suite 6.3 Industrial Student Edition:

http://download.palisade.com/D6/631/DTS63-Setup.exe (Figure C-2)

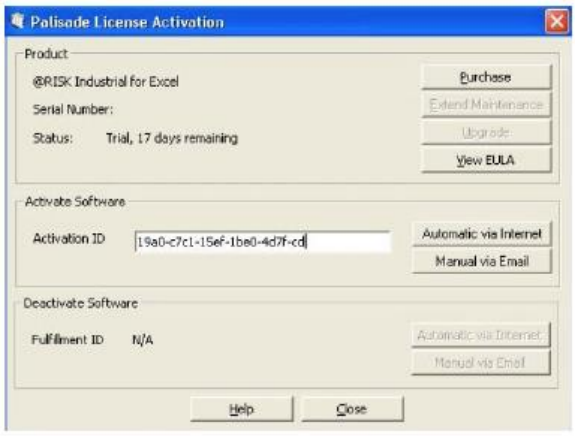

Figure C-2 Palisade license Activation.

Product ID: 1400-I-6004-EN

Serial Number: 6070370

Activation ID: DNE-6070370-C16D6B-ACB

Chapter 2: MATLAB

Data Sets and Data Set Manager

1. From the FDOT *labview* software you will get the following in a file (Figure C-3):

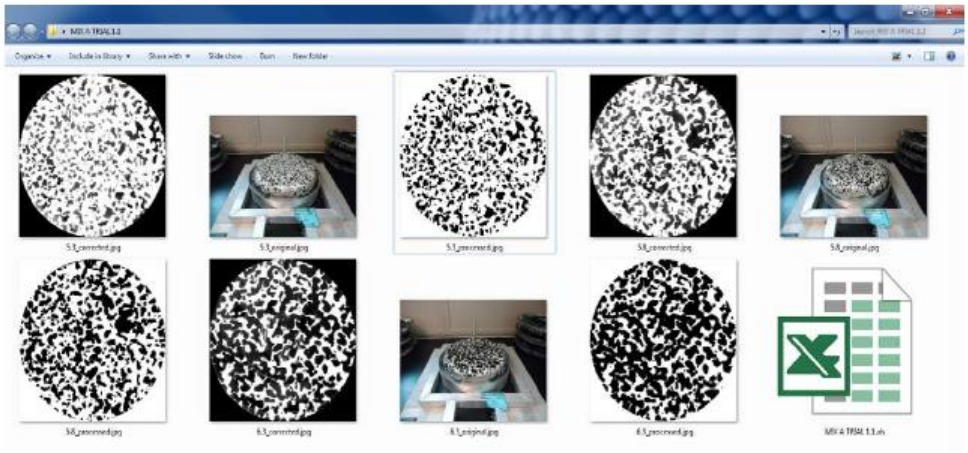

Figure C-3 Output files from FDOT *Labview* software.

2. Rename file and images with the following name convention:

   EXAMPLE

   a. File name : MIX name TRIAL number — MIX A TRIAL 1.1
   b. For each Image name: AC%_original.jpg — 5.3_original.jpg
   c. For each Image name: AC%_corrected.jpg — 5.3_corrected.jpg
   d. For each Image name: AC%_processed.jpg — 5.3_processed.jpg

3. Open Matlab file: NN.m

4. Write the following:

   a. name of the mixture — A
   b. trial number — 1.1

c. percent AC 5.3

5. Run the software

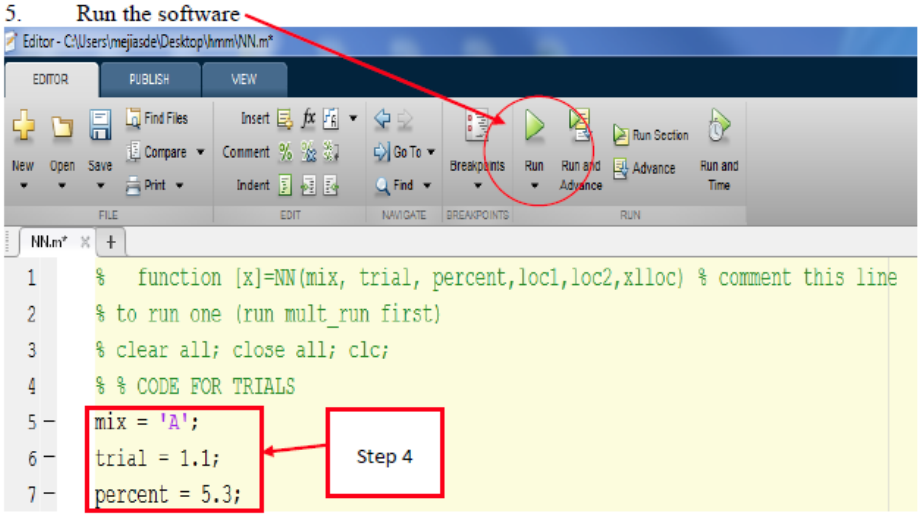

6. In a excel file: master.xlsx the parameters will be written automatically from Matlab in a tab call DATA

```
%% write important data to master excel file
% file = xlsread('C:\Users\mejiasde\Desktop\hmm\master.xlsx');
file = xlsread(xlloc);
nextRow = num2str(size(file,1)+3);
nextCell = strcat('A',nextRow);
img = strcat('MIX',{' '},mix,{' '},'TRIAL',{' '},trial,{' '}, {' '}, ...
    percent, ' %');
data_entry = [img,percent,PBP,PBPC,n, ORIENTATION, AreaComp,PERIMETER, ...
uniformity_radial,uniformity_angular,INCONSISTENCY,CENTROIDS,FORMFACTOR,...
COMPACTENESS,SOLIDITY,ECCENTRICITY];

xlswrite(xlloc,data_entry,'Data',nextRow);
```

Data Sets and Data Set Manager

7. Open the excel file: master
8. Open tab NeuralTools

a. First you must **define a data set** using the Data Set Manager.

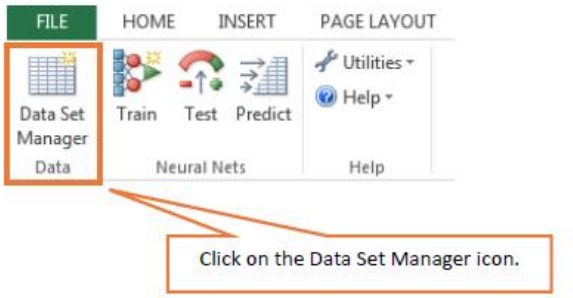

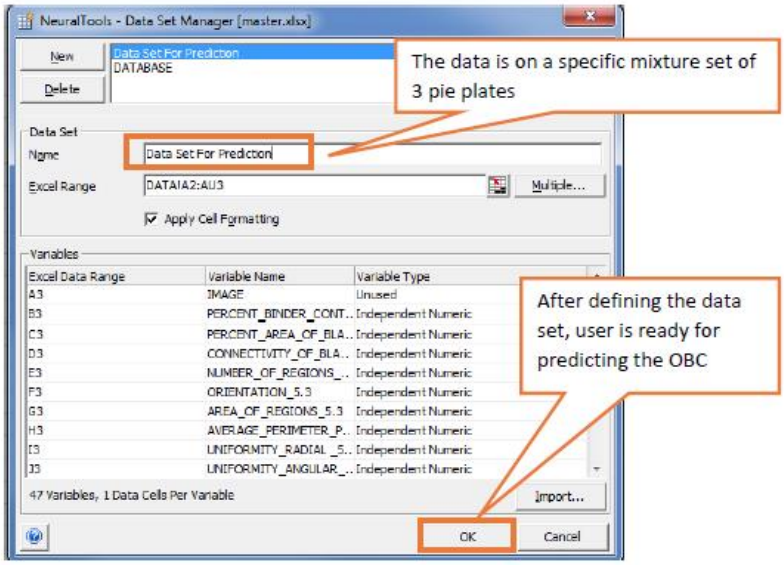

b. Next the user can use the Neural Tool to **train the data**. This must be done in the Train dialog.

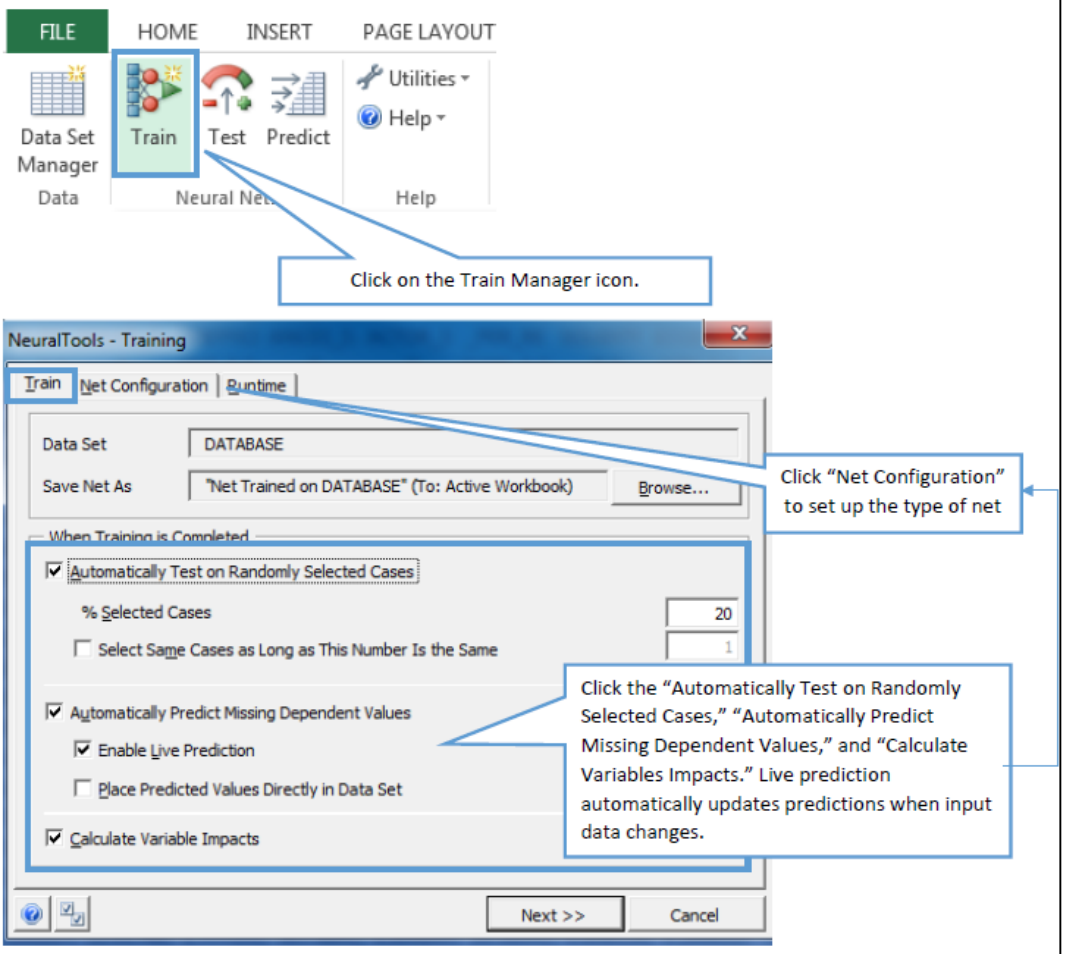

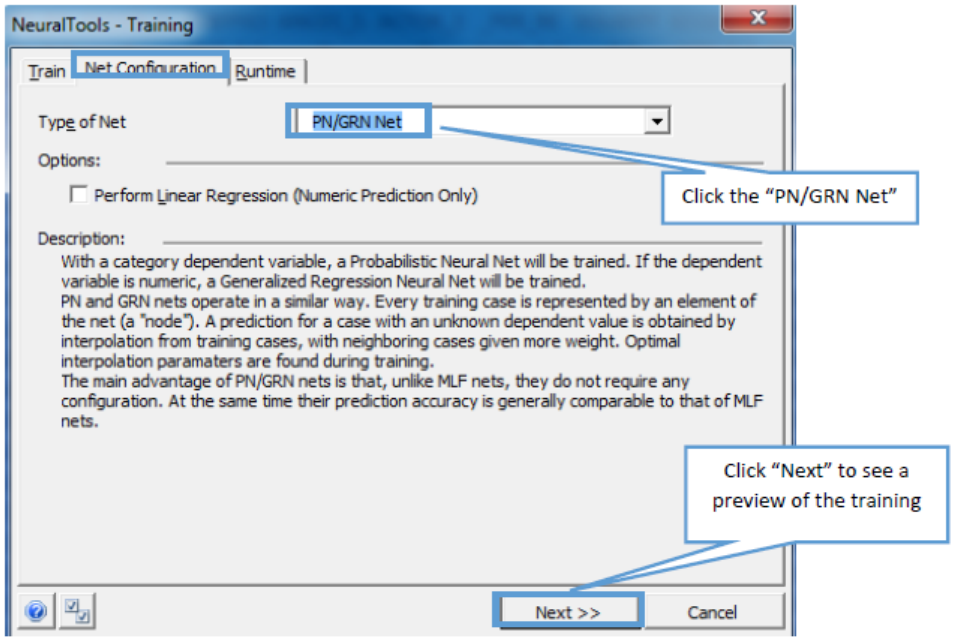

C | 8

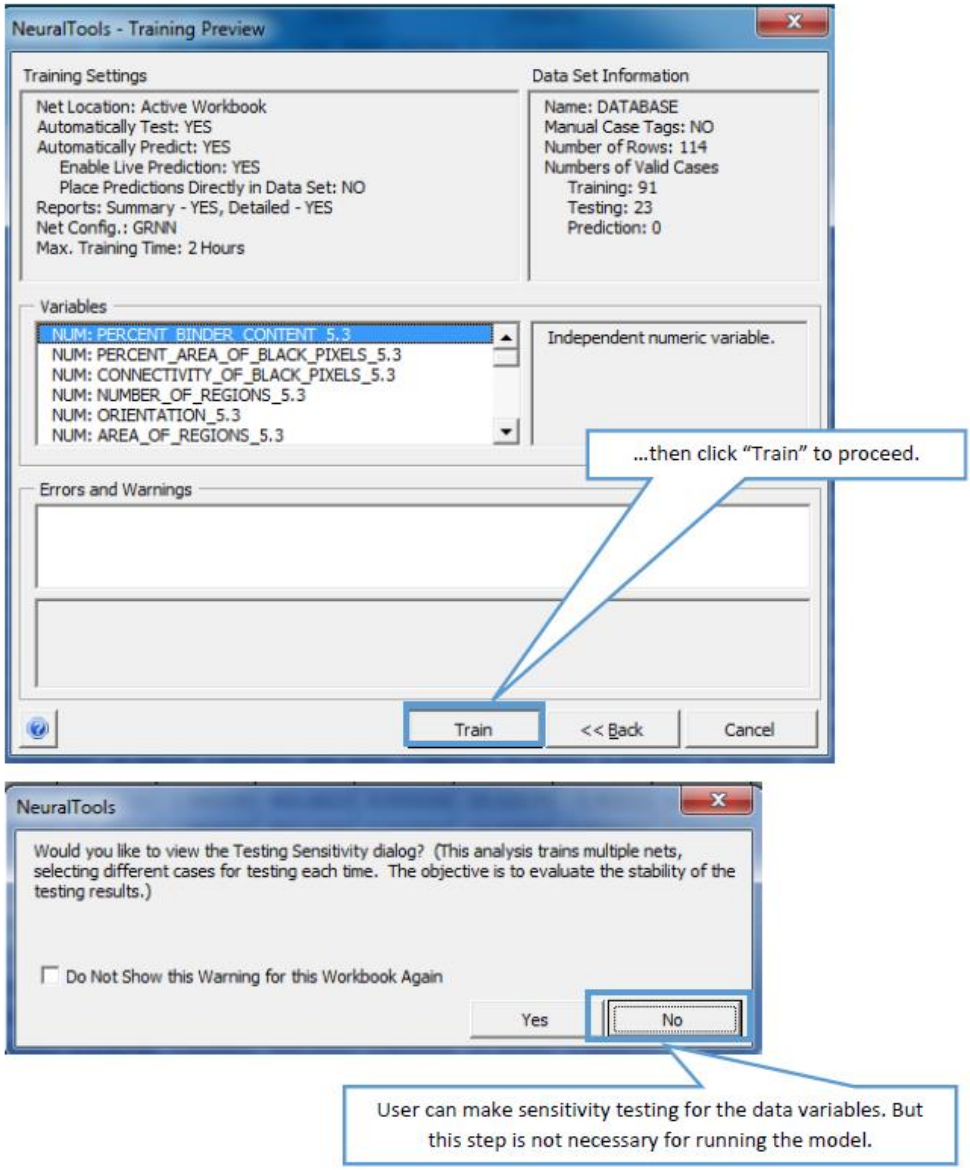

C | 9

c. Next the user can use the Neural Tool to **test the data.** This must be done in the Testing dialog.

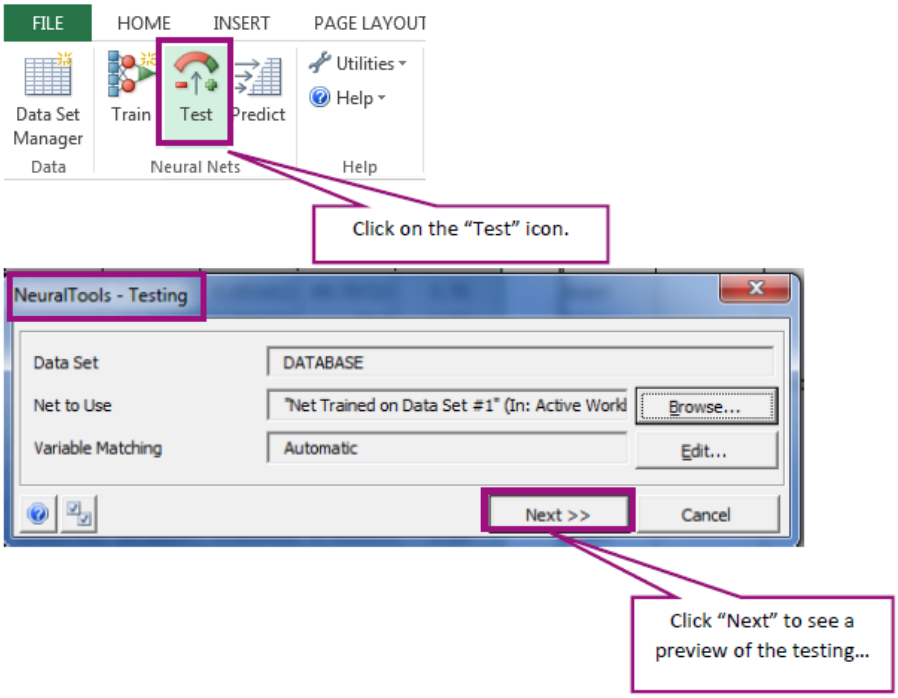

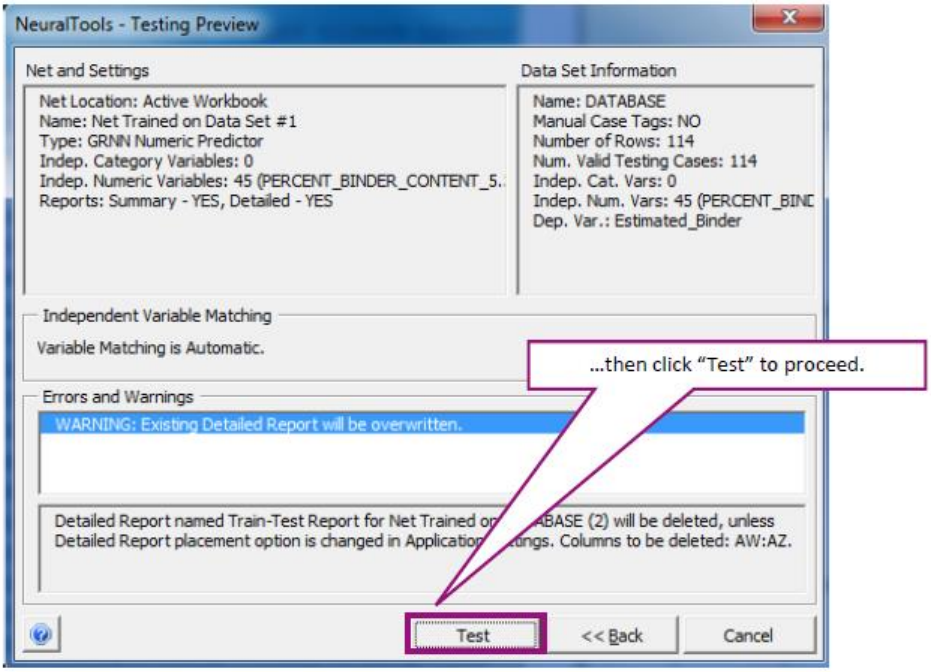

d. Next the user can use the Neural Tool to make **predictions** from new, incomplete data. This must be done in the Prediction dialog.

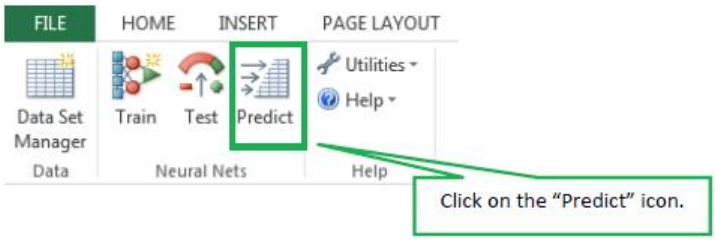

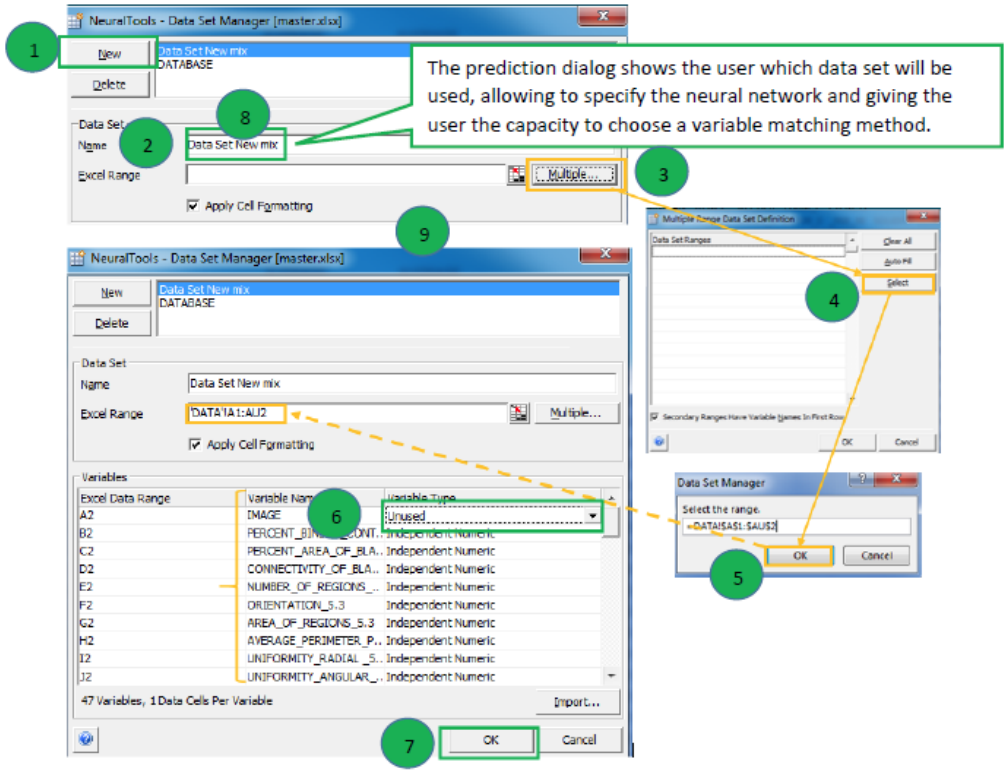

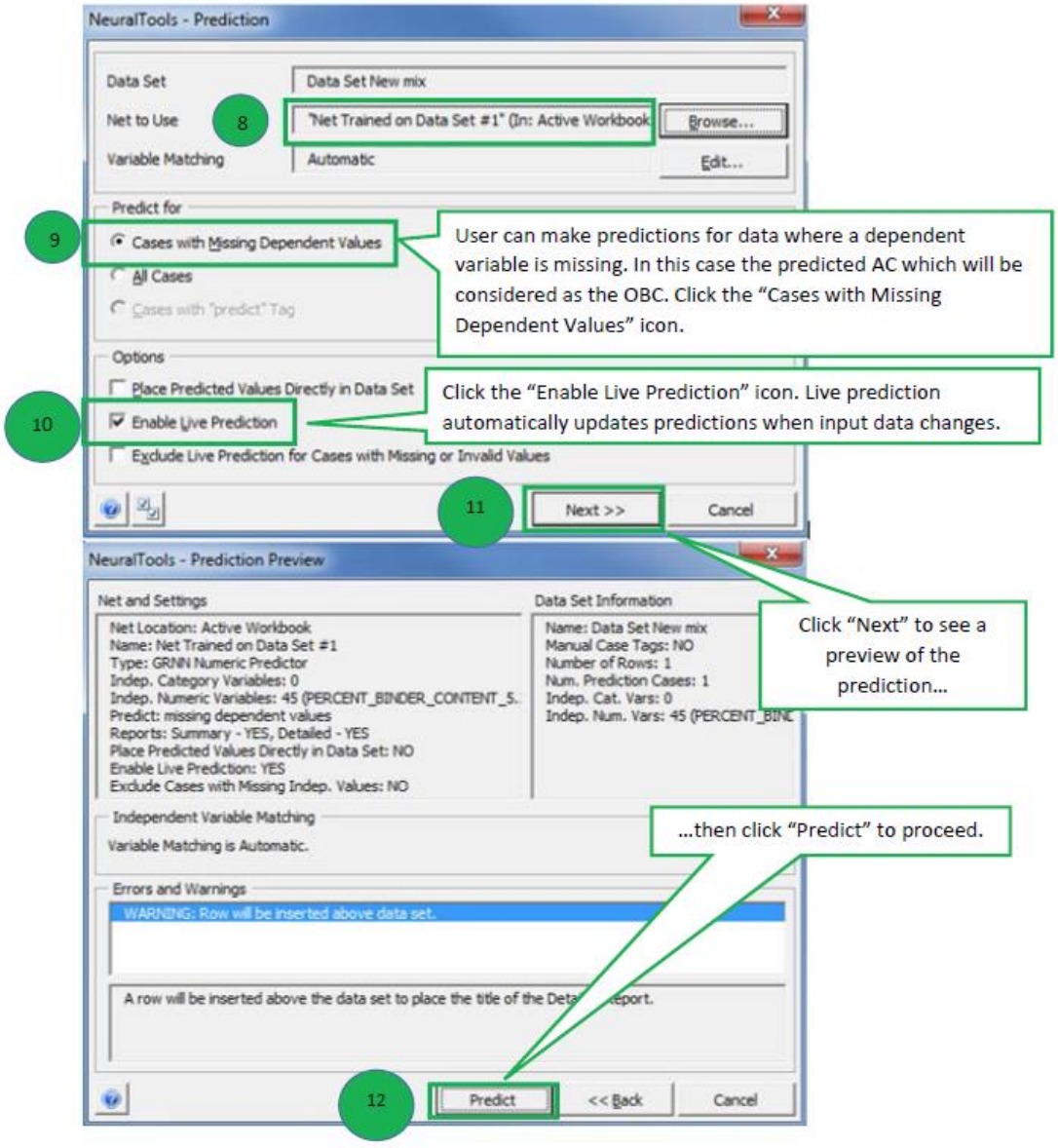

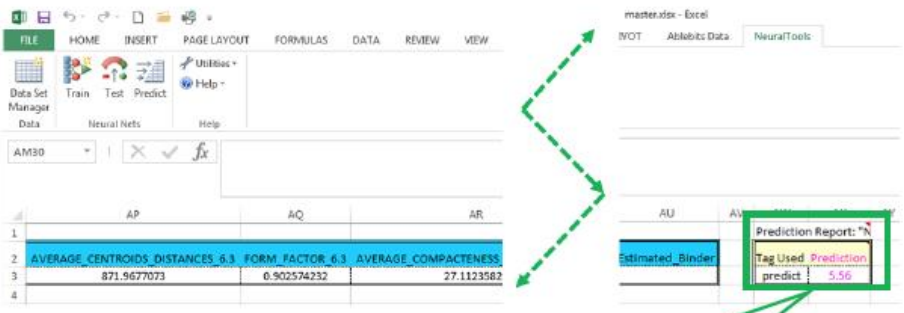

In this case, we have chosen to place the prediction next to the USF input data set. One can see the prediction of OBC here and next to it is the confidence level of the prediction.

C | 14

APPENDIX I: STATISTIC TABLES

Table I1 *t*-values for various values of *df* confidence intervals.

Table A2. t values for various values of df

	confidence interval						
	80%	90%	95%	98%	99%	99.8%	99.9%
	α level two-tailed test						
	0.2	0.1	0.05	0.02	0.01	0.002	0.001
	α level one-tailed test						
df	0.1	0.05	0.025	0.01	0.005	0.001	0.0005
1	3.078	6.314	12.706	31.821	63.657	318.313	636.589
2	1.886	2.920	4.303	6.965	9.925	22.327	31.598
3	1.638	2.353	3.182	4.541	5.841	10.215	12.924
4	1.533	2.132	2.776	3.747	4.604	7.173	8.610
5	1.476	2.015	2.571	3.365	4.032	5.893	6.869
6	1.440	1.943	2.447	3.143	3.707	5.208	5.959
7	1.415	1.895	2.365	2.998	3.499	4.785	5.408
8	1.397	1.860	2.306	2.896	3.355	4.501	5.041
9	1.383	1.833	2.262	2.821	3.250	4.297	4.781
10	1.372	1.812	2.228	2.764	3.169	4.144	4.587
11	1.363	1.796	2.201	2.718	3.106	4.025	4.437
12	1.356	1.782	2.179	2.681	3.055	3.930	4.318
13	1.350	1.771	2.160	2.650	3.012	3.852	4.221
14	1.345	1.761	2.145	2.624	2.977	3.787	4.140
15	1.341	1.753	2.131	2.602	2.947	3.733	4.073
16	1.337	1.746	2.120	2.583	2.921	3.686	4.015
17	1.333	1.740	2.110	2.567	2.898	3.646	3.965
18	1.330	1.734	2.101	2.552	2.878	3.610	3.922
19	1.328	1.729	2.093	2.539	2.861	3.579	3.883
20	1.325	1.725	2.086	2.528	2.845	3.552	3.849
21	1.323	1.721	2.080	2.518	2.831	3.527	3.819
22	1.321	1.717	2.074	2.508	2.819	3.505	3.792
23	1.319	1.714	2.069	2.500	2.807	3.485	3.768
24	1.318	1.711	2.064	2.492	2.797	3.467	3.745
25	1.316	1.708	2.060	2.485	2.787	3.450	3.725
26	1.315	1.706	2.056	2.479	2.779	3.435	3.707
27	1.314	1.703	2.052	2.473	2.771	3.421	3.690
28	1.313	1.701	2.048	2.467	2.763	3.408	3.674
29	1.311	1.699	2.045	2.462	2.756	3.396	3.659
30	1.310	1.697	2.042	2.457	2.750	3.385	3.646
40	1.303	1.684	2.021	2.423	2.704	3.307	3.551
60	1.296	1.671	2.000	2.390	2.660	3.232	3.460
120	1.289	1.658	1.980	2.358	2.617	3.160	3.373
∞ (σ known)	1.282	1.645	1.960	2.327	2.576	3.091	3.291

Table I2 T-test values for various spatial distribution values of *df* confidence intervals.

One-sample statistics

	N	Mean	Std. Deviation	Std. Error Mean
var001	12	8.3333	.78479	.22655
var002	12	8.3333	.92387	.26670
var003	12	8.3333	.69288	.20002
var004	12	8.3342	.77651	.22416
var005	12	8.3317	.92012	.26561
var006	12	8.3342	.69543	.20075
var007	12	8.3333	1.31646	.38003
var008	12	8.3350	.87515	.25263
var009	12	8.3333	.82490	.23813
var010	12	8.3325	1.30143	.37569
var011	12	8.3342	.90645	.26167
var012	12	8.3333	.80316	.23185
var013	12	8.3350	1.22799	.35449
var014	12	8.3317	1.18665	.34256
var015	12	8.3333	.89989	.25978
var016	12	8.3333	1.23038	.35518
var017	12	8.3342	1.17440	.33902
var018	12	8.3317	.90323	.26074
var019	12	8.3333	.74026	.21370
var020	12	8.3325	1.07336	.30985
var021	12	8.3333	1.12457	.32464
var022	12	8.3333	.73632	.21256
var023	12	8.3333	1.07828	.31127
var024	12	8.3333	1.12191	.32387
var025	12	8.3333	1.08718	.31384
var026	12	8.3350	1.14911	.33172
var027	12	8.3333	1.06444	.30728
var028	12	8.3342	1.10176	.31805
var029	12	8.3342	1.16601	.33660
var030	12	8.3333	1.07070	.30909
var031	12	8.3342	1.15220	.33261
var032	12	8.3342	1.68768	.48719
var033	12	8.3317	.72892	.21042
var034	12	8.3333	1.16613	.33663
var035	12	8.3342	1.67824	.48447

Table I2 (Continued)

One-sample statistics

	N	Mean	Std. Deviation	Std. Error Mean
var036	12	8.3342	.73071	.21094
var037	12	8.3342	1.18374	.34172
var038	12	8.3342	1.14393	.33022
var039	12	8.3325	.89879	.25946
var040	12	8.3342	1.14864	.33158
var041	12	8.3325	1.13913	.32884
var042	12	8.3333	.89828	.25931
var043	12	8.3325	.56120	.16201
var044	12	8.3325	1.49756	.43231
var045	12	8.3317	.79097	.22833
var046	12	8.3342	.56413	.16285
var047	12	8.3325	1.48781	.42949
var048	12	8.3333	.77919	.22493
var049	12	8.3342	.56413	.16285
var050	12	8.3325	1.48781	.42949
var051	12	8.3333	.77919	.22493
var052	12	8.3342	.56413	.16285
var053	12	8.3325	1.48781	.42949
var054	12	8.3333	.77919	.22493
var055	12	8.3342	1.00275	.28947
var056	12	8.3342	1.01268	.29234
var057	12	8.3342	.98650	.28478
var058	12	8.3325	.98665	.28482
var059	12	8.3325	.98790	.28518
var060	12	8.3333	.99225	.28644
var061	12	8.3333	1.19343	.34451
var062	12	8.3333	1.28597	.37123
var063	12	8.3342	.45077	.13012
var064	12	8.3342	1.16489	.33628
var065	12	8.3333	1.28119	.36985
var066	12	8.3333	.44945	.12975
var067	12	8.3333	1.14052	.32924
var068	12	8.3317	1.22246	.35289
var069	12	8.3333	.64456	.18607

Table I2 (Continued)

One-sample statistics

	N	Mean	Std. Deviation	Std. Error Mean
var070	12	8.3333	1.12797	.32562
var071	12	8.3342	1.22194	.35274
var072	12	8.3342	.63948	.18460
var073	12	8.3325	.95706	.27628
var074	12	8.3342	.65974	.19045
var075	12	8.3317	.69398	.20034
var076	12	8.3333	.92962	.26836
var077	12	8.3333	.66967	.19332
var078	12	8.3342	.68743	.19844
var079	12	8.3333	1.34522	.38833
var080	12	8.3333	.93922	.27113
var081	12	8.3350	.82410	.23790
var082	12	8.3333	1.35947	.39245
var083	12	8.3342	.93136	.26886
var084	12	8.3333	.83209	.24020
var085	12	8.3325	.93236	.26915
var086	12	8.3333	1.36820	.39497
var087	12	8.3333	.69803	.20150
var088	12	8.3350	.93499	.26991
var089	12	8.3325	1.35544	.39128
var090	12	8.3325	.70029	.20216
var091	12	8.3333	.96276	.27793
var092	12	8.3333	.85714	.24744
var093	12	8.3325	.91391	.26382
var094	12	8.3325	.95385	.27535
var095	12	8.3325	.86989	.25112
var096	12	8.3333	.91690	.26468
var097	12	8.3325	1.13063	.32639
var098	12	8.3333	1.12350	.32433
var099	12	8.3342	.87725	.25324
var100	12	8.3325	1.14462	.33042
var101	12	8.3325	1.07932	.31157
var102	12	8.3342	.88359	.25507
var103	12	8.3325	1.14462	.33042

Table I2 (Continued)

One-sample statistics

	N	Mean	Std. Deviation	Std. Error Mean
var104	12	8.3325	1.07932	.31157
var105	12	8.3342	.88359	.25507
var106	12	8.3342	1.08746	.31392
var107	12	8.3325	1.26949	.36647
var108	12	8.3342	.77575	.22394
var109	12	8.3325	1.89190	.54615
var110	12	8.3325	.85677	.24733
var111	12	8.3342	.73175	.21124
var112	12	8.3333	1.89763	.54780
var113	12	8.3342	.86013	.24830
var114	12	8.3342	.72884	.21040
var115	12	8.3350	1.16219	.33549
var116	12	8.3333	1.03522	.29884
var117	12	8.3350	.82589	.23841
var118	12	8.3342	1.17532	.33929
var119	12	8.3325	1.03497	.29877
var120	12	8.3325	.82317	.23763
var121	12	8.3342	1.02265	.29521
var122	12	8.3333	1.01783	.29382
var123	12	8.3325	1.32103	.38135
var124	12	8.3325	1.03966	.30012
var125	12	8.3333	1.02390	.29557
var126	12	8.3333	1.33151	.38437
var127	12	8.3342	1.10880	.32008
var128	12	8.3333	1.15120	.33232
var129	12	8.3342	.92066	.26577
var130	12	8.3325	1.10314	.31845
var131	12	8.3333	1.15035	.33208
var132	12	8.3333	.92135	.26597
var133	12	8.3333	.66591	.19223
var134	12	8.3333	1.47506	.42581
var135	12	8.3325	.90880	.26235
var136	12	8.3333	.71197	.20553
var137	12	8.3333	1.46294	.42232

Table I2 (Continued)

One-sample statistics

	N	Mean	Std. Deviation	Std. Error Mean
var138	12	8.3333	.91598	.26442
var139	12	8.3333	.97859	.28250
var140	12	8.3333	1.04522	.30173
var141	12	8.3342	.77336	.22325
var142	12	8.3342	.98783	.28516
var143	12	8.3325	1.06624	.30780
var144	12	8.3333	.78349	.22617
var145	12	8.3333	.89111	.25724
var146	12	8.3317	.88745	.25618
var147	12	8.3333	.90482	.26120
var148	12	8.3325	.89885	.25948
var149	12	8.3342	.84608	.24424
var150	12	8.3333	.93958	.27123
var151	12	8.3342	1.07146	.30930
var152	12	8.3333	.96863	.27962
var153	12	8.3325	.91392	.26383
var154	12	8.3325	1.07648	.31075
var155	12	8.3333	.97497	.28145
var156	12	8.3333	.91964	.26548
var157	12	8.3342	.73748	.21289
var158	12	8.3317	1.34703	.38885
var159	12	8.3317	1.41034	.40713
var160	12	8.3325	.72995	.21072
var161	12	8.3342	1.33525	.38545
var162	12	8.3333	1.40598	.40587
var163	12	8.3342	1.29308	.37328
var164	12	8.3325	.96181	.27765
var165	12	8.3333	1.26854	.36620
var166	12	8.3325	1.28895	.37209
var167	12	8.3342	.97246	.28073
var168	12	8.3333	1.25610	.36260
var169	12	8.3325	1.33652	.38582
var170	12	8.3342	1.29558	.37400

Table I2 (Continued)

One-sample statistics

	N	Mean	Std. Deviation	Std. Error Mean
var171	12	8.3333	1.36656	.39449
var172	12	8.3325	1.32851	.38351
var173	12	8.3333	1.29975	.37521
var174	12	8.3342	1.36714	.39466
var175	12	8.3333	1.07923	.31155
var176	12	8.3317	1.15801	.33429
var177	12	8.3342	1.50534	.43455
var178	12	8.3342	1.10237	.31823
var179	12	8.3333	1.15700	.33400
var180	12	8.3333	1.50669	.43494
var181	12	8.3342	.75278	.21731
var182	12	8.3325	.89535	.25847
var183	12	8.3350	.55757	.16096
var184	12	8.3325	.75341	.21749
var185	12	8.3317	.89097	.25720
var186	12	8.3325	.56073	.16187
var187	12	8.3342	1.54379	.44565
var188	12	8.3333	.85558	.24699
var189	12	8.3325	.71131	.20534
var190	12	8.3333	1.51280	.43671
var191	12	8.3333	.85558	.24699
var192	12	8.3325	.71328	.20591
var193	12	8.3325	1.04354	.30124
var194	12	8.3342	1.07585	.31057
var195	12	8.3333	.74798	.21592
var196	12	8.3342	1.07618	.31067
var197	12	8.3350	1.12589	.32502
var198	12	8.3333	.74798	.21592
var199	12	8.3342	1.14282	.32990
var200	12	8.3333	1.69616	.48964
var201	12	8.3342	1.28653	.37139
var202	12	8.3333	1.13304	.32708
var203	12	8.3333	1.69017	.48791
var204	12	8.3350	1.27827	.36900

Table I2 (Continued)

One-sample statistics

	N	Mean	Std. Deviation	Std. Error Mean
var205	12	8.3333	.75295	.21736
var206	12	8.3333	1.11177	.32094
var207	12	8.3333	.55610	.16053
var208	12	8.3325	.74711	.21567
var209	12	8.3333	1.11159	.32089
var210	12	8.3333	.56542	.16322
var211	12	8.3333	.80528	.23246
var212	12	8.3333	1.03497	.29877
var213	12	8.3317	.61207	.17669
var214	12	8.3342	.77420	.22349
var215	12	8.3317	1.05189	.30365
var216	12	8.3333	.61732	.17820
var217	12	8.3333	.94572	.27301
var218	12	8.3342	1.21557	.35090
var219	12	8.3325	1.26231	.36440
var220	12	8.3317	.93584	.27015
var221	12	8.3350	1.21932	.35199
var222	12	8.3333	1.26147	.36416
var223	12	8.3325	.70595	.20379
var224	12	8.3350	.74772	.21585
var225	12	8.3333	1.15134	.33236
var226	12	8.3333	.71567	.20660
var227	12	8.3333	.73351	.21175
var228	12	8.3342	1.15516	.33347
var229	12	8.3333	.70711	.20413
var230	12	8.3333	.86090	.24852
var231	12	8.3342	.80728	.23304
var232	12	8.3342	.72046	.20798
var233	12	8.3342	.88380	.25513
var234	12	8.3342	.79394	.22919
var235	12	8.3333	1.19240	.34421
var236	12	8.3333	1.30213	.37589
var237	12	8.3325	1.06108	.30631
var238	12	8.3333	1.17070	.33795

Table I2 (Continued)

One-sample statistics

	N	Mean	Std. Deviation	Std. Error Mean
var239	12	8.3342	1.30972	.37808
var240	12	8.3342	1.09475	.31603
var241	12	8.3333	1.37916	.39813
var242	12	8.3325	.71582	.20664
var243	12	8.3325	.68873	.19882
var244	12	8.3325	1.40262	.40490
var245	12	8.3342	.71985	.20780
var246	12	8.3342	.70526	.20359
var247	12	8.3317	1.13102	.32650
var248	12	8.3333	.96795	.27942
var249	12	8.3342	1.23513	.35655
var250	12	8.3317	1.13102	.32650
var251	12	8.3342	.99747	.28795
var252	12	8.3333	1.22284	.35300
var253	12	8.3333	1.29082	.37263
var254	12	8.3333	1.17796	.34005
var255	12	8.3342	.80223	.23158
var256	12	8.3350	1.28526	.37102
var257	12	8.3325	1.17695	.33976
var258	12	8.3308	.80293	.23179
var259	12	8.3333	1.33268	.38471
var260	12	8.3333	1.25518	.36234
var261	12	8.3325	.83028	.23968
var262	12	8.3325	1.31334	.37913
var263	12	8.3333	1.28428	.37074
var264	12	8.3333	.83164	.24007
var265	12	8.3325	1.34135	.38721
var266	12	8.3325	.86827	.25065
var267	12	8.3325	.84515	.24397
var268	12	8.3333	1.33141	.38434
var269	12	8.3350	.86696	.25027
var270	12	8.3333	.83697	.24161
var271	12	8.3317	1.19998	.34640
var272	12	8.3342	.67291	.19425

Table I2 (Continued)

One-sample statistics

	N	Mean	Std. Deviation	Std. Error Mean
var273	12	8.3333	.69243	.19989
var274	12	8.3325	1.19713	.34558
var275	12	8.3325	.66095	.19080
var276	12	8.3325	.70039	.20219
var277	12	8.3333	1.29529	.37392
var278	12	8.3333	.96008	.27715
var279	12	8.3325	.82864	.23921
var280	12	8.3325	1.30696	.37729
var281	12	8.3342	.96051	.27727
var282	12	8.3325	.82620	.23850
var283	12	8.3325	1.20462	.34774
var284	12	8.3342	1.69372	.48893
var285	12	8.3342	.90453	.26111
var286	12	8.3333	1.20581	.34809
var287	12	8.3333	1.70152	.49119
var288	12	8.3333	.91117	.26303
var289	12	8.3325	.72621	.20964
var290	12	8.3333	1.04956	.30298
var291	12	8.3333	1.00817	.29103
var292	12	8.3325	.72367	.20890
var293	12	8.3325	1.03804	.29966
var294	12	8.3325	1.00367	.28973
var295	12	8.3342	1.25859	.36332
var296	12	8.3342	1.29970	.37519
var297	12	8.3317	1.47551	.42594
var298	12	8.3342	1.27350	.36763
var299	12	8.3342	1.29479	.37377
var300	12	8.3333	1.47175	.42486
var301	12	8.3350	1.11038	.32054
var302	12	8.3325	1.85195	.53461
var303	12	8.3333	.77475	.22365
var304	12	8.3342	1.10929	.32022
var305	12	8.3325	1.89887	.54816
var306	12	8.3342	.77829	.22467

Table I2 (Continued)

One-sample statistics

	N	Mean	Std. Deviation	Std. Error Mean
var307	12	8.3325	1.03795	.29963
var308	12	8.3342	1.12847	.32576
var309	12	8.3342	1.61186	.46530
var310	12	8.3325	1.05583	.30479
var311	12	8.3333	1.12316	.32423
var312	12	8.3325	1.61205	.46536
var313	12	8.3325	1.32703	.38308
var314	12	8.3325	.83117	.23994
var315	12	8.3342	1.49705	.43216
var316	12	8.3333	1.32029	.38114
var317	12	8.3350	.82773	.23894
var318	12	8.3325	1.52778	.44103
var319	12	8.3325	1.20241	.34711
var320	12	8.3325	1.24885	.36051
var321	12	8.3325	1.16176	.33537
var322	12	8.3342	1.19562	.34514
var323	12	8.3317	1.24379	.35905
var324	12	8.3342	1.13414	.32740
var325	12	8.3333	1.24355	.35898
var326	12	8.3333	1.12625	.32512
var327	12	8.3325	.79930	.23074
var328	12	8.3350	1.19547	.34510
var329	12	8.3333	1.08688	.31376
var330	12	8.3333	.80683	.23291
var331	12	8.3333	1.72471	.49788
var332	12	8.3333	1.10985	.32039
var333	12	8.3325	1.06964	.30878
var334	12	8.3342	1.72956	.49928
var335	12	8.3342	1.10013	.31758
var336	12	8.3317	1.05381	.30421
var337	12	8.3342	1.03978	.30016
var338	12	8.3333	1.41369	.40810
var339	12	8.3325	1.10833	.31995

Table I2 (Continued)

One-sample statistics

	N	Mean	Std. Deviation	Std. Error Mean
var340	12	8.3317	1.02424	.29567
var341	12	8.3325	1.41938	.40974
var342	12	8.3325	1.10122	.31789

Table I3: One-sample test for various values of *df* confidence intervals.

One-Sample Test

	Test Value = 0					
					95% Confidence Interval of the Difference	
	t	df	Sig. (2-tailed)	Mean Difference	Lower	Upper
var001	36.784	11	.000	8.33333	7.8347	8.8320
var002	31.246	11	.000	8.33333	7.7463	8.9203
var003	41.663	11	.000	8.33333	7.8931	8.7736
var004	37.180	11	.000	8.33417	7.8408	8.8275
var005	31.367	11	.000	8.33167	7.7471	8.9163
var006	41.514	11	.000	8.33417	7.8923	8.7760
var007	21.928	11	.000	8.33333	7.4969	9.1698
var008	32.993	11	.000	8.33500	7.7790	8.8910
var009	34.995	11	.000	8.33333	7.8092	8.8575
var010	22.179	11	.000	8.33250	7.5056	9.1594
var011	31.850	11	.000	8.33417	7.7582	8.9101
var012	35.943	11	.000	8.33333	7.8230	8.8436
var013	23.513	11	.000	8.33500	7.5548	9.1152
var014	24.322	11	.000	8.33167	7.5777	9.0856
var015	32.079	11	.000	8.33333	7.7616	8.9051
var016	23.462	11	.000	8.33333	7.5516	9.1151
var017	24.583	11	.000	8.33417	7.5880	9.0803
var018	31.954	11	.000	8.33167	7.7578	8.9056
var019	38.996	11	.000	8.33333	7.8630	8.8037
var020	26.892	11	.000	8.33250	7.6505	9.0145
var021	25.670	11	.000	8.33333	7.6188	9.0479
var022	39.205	11	.000	8.33333	7.8655	8.8012
var023	26.772	11	.000	8.33333	7.6482	9.0184
var024	25.731	11	.000	8.33333	7.6205	9.0462
var025	26.553	11	.000	8.33333	7.6426	9.0241
var026	25.127	11	.000	8.33500	7.6049	9.0651
var027	27.120	11	.000	8.33333	7.6570	9.0096
var028	26.204	11	.000	8.33417	7.6341	9.0342
var029	24.760	11	.000	8.33417	7.5933	9.0750
var030	26.961	11	.000	8.33333	7.6530	9.0136
var031	25.057	11	.000	8.33417	7.6021	9.0662
var032	17.107	11	.000	8.33417	7.2619	9.4065

Table I3 (Continued)

One-Sample Test

	Test Value = 0					
					95% Confidence Interval of the Difference	
	t	df	Sig. (2-tailed)	Mean Difference	Lower	Upper
var033	39.595	11	.000	8.33167	7.8685	8.7948
var034	24.755	11	.000	8.33333	7.5924	9.0743
var035	17.203	11	.000	8.33417	7.2679	9.4005
var036	39.510	11	.000	8.33417	7.8699	8.7984
var037	24.389	11	.000	8.33417	7.5821	9.0863
var038	25.238	11	.000	8.33417	7.6073	9.0610
var039	32.115	11	.000	8.33250	7.7614	8.9036
var040	25.134	11	.000	8.33417	7.6044	9.0640
var041	25.339	11	.000	8.33250	7.6087	9.0563
var042	32.136	11	.000	8.33333	7.7626	8.9041
var043	51.434	11	.000	8.33250	7.9759	8.6891
var044	19.274	11	.000	8.33250	7.3810	9.2840
var045	36.489	11	.000	8.33167	7.8291	8.8342
var046	51.177	11	.000	8.33417	7.9757	8.6926
var047	19.401	11	.000	8.33250	7.3872	9.2778
var048	37.048	11	.000	8.33333	7.8383	8.8284
var049	51.177	11	.000	8.33417	7.9757	8.6926
var050	19.401	11	.000	8.33250	7.3872	9.2778
var051	37.048	11	.000	8.33333	7.8383	8.8284
var052	51.177	11	.000	8.33417	7.9757	8.6926
var053	19.401	11	.000	8.33250	7.3872	9.2778
var054	37.048	11	.000	8.33333	7.8383	8.8284
var055	28.791	11	.000	8.33417	7.6971	8.9713
var056	28.509	11	.000	8.33417	7.6907	8.9776
var057	29.265	11	.000	8.33417	7.7074	8.9610
var058	29.255	11	.000	8.33250	7.7056	8.9594
var059	29.218	11	.000	8.33250	7.7048	8.9602
var060	29.093	11	.000	8.33333	7.7029	8.9638
var061	24.189	11	.000	8.33333	7.5751	9.0916
var062	22.448	11	.000	8.33333	7.5163	9.1504
var063	64.047	11	.000	8.33417	8.0478	8.6206
var064	24.784	11	.000	8.33417	7.5940	9.0743

Table I3 (Continued)

One-Sample Test

	Test Value = 0					
					95% Confidence Interval of the Difference	
	t	df	Sig. (2-tailed)	Mean Difference	Lower	Upper
var065	22.532	11	.000	8.33333	7.5193	9.1474
var066	64.228	11	.000	8.33333	8.0478	8.6189
var067	25.311	11	.000	8.33333	7.6087	9.0580
var068	23.610	11	.000	8.33167	7.5550	9.1084
var069	44.786	11	.000	8.33333	7.9238	8.7429
var070	25.592	11	.000	8.33333	7.6167	9.0500
var071	23.627	11	.000	8.33417	7.5578	9.1105
var072	45.147	11	.000	8.33417	7.9279	8.7405
var073	30.160	11	.000	8.33250	7.7244	8.9406
var074	43.760	11	.000	8.33417	7.9150	8.7533
var075	41.588	11	.000	8.33167	7.8907	8.7726
var076	31.053	11	.000	8.33333	7.7427	8.9240
var077	43.107	11	.000	8.33333	7.9078	8.7588
var078	41.998	11	.000	8.33417	7.8974	8.7709
var079	21.459	11	.000	8.33333	7.4786	9.1880
var080	30.736	11	.000	8.33333	7.7366	8.9301
var081	35.036	11	.000	8.33500	7.8114	8.8586
var082	21.234	11	.000	8.33333	7.4696	9.1971
var083	30.998	11	.000	8.33417	7.7424	8.9259
var084	34.693	11	.000	8.33333	7.8047	8.8620
var085	30.959	11	.000	8.33250	7.7401	8.9249
var086	21.099	11	.000	8.33333	7.4640	9.2026
var087	41.356	11	.000	8.33333	7.8898	8.7768
var088	30.881	11	.000	8.33500	7.7409	8.9291
var089	21.295	11	.000	8.33250	7.4713	9.1937
var090	41.218	11	.000	8.33250	7.8876	8.7774
var091	29.984	11	.000	8.33333	7.7216	8.9450
var092	33.679	11	.000	8.33333	7.7887	8.8779
var093	31.584	11	.000	8.33250	7.7518	8.9132
var094	30.261	11	.000	8.33250	7.7265	8.9385
var095	33.182	11	.000	8.33250	7.7798	8.8852
var096	31.484	11	.000	8.33333	7.7508	8.9159

Table I3 (Continued)

One-Sample Test

	Test Value = 0					
					95% Confidence Interval of the Difference	
	t	df	Sig. (2-tailed)	Mean Difference	Lower	Upper
var097	25.530	11	.000	8.33250	7.6141	9.0509
var098	25.694	11	.000	8.33333	7.6195	9.0472
var099	32.910	11	.000	8.33417	7.7768	8.8915
var100	25.218	11	.000	8.33250	7.6052	9.0598
var101	26.743	11	.000	8.33250	7.6467	9.0183
var102	32.674	11	.000	8.33417	7.7728	8.8956
var103	25.218	11	.000	8.33250	7.6052	9.0598
var104	26.743	11	.000	8.33250	7.6467	9.0183
var105	32.674	11	.000	8.33417	7.7728	8.8956
var106	26.548	11	.000	8.33417	7.6432	9.0251
var107	22.737	11	.000	8.33250	7.5259	9.1391
var108	37.216	11	.000	8.33417	7.8413	8.8271
var109	15.257	11	.000	8.33250	7.1304	9.5346
var110	33.690	11	.000	8.33250	7.7881	8.8769
var111	39.454	11	.000	8.33417	7.8692	8.7991
var112	15.212	11	.000	8.33333	7.1276	9.5390
var113	33.565	11	.000	8.33417	7.7877	8.8807
var114	39.611	11	.000	8.33417	7.8711	8.7972
var115	24.844	11	.000	8.33500	7.5966	9.0734
var116	27.885	11	.000	8.33333	7.6756	8.9911
var117	34.960	11	.000	8.33500	7.8103	8.8597
var118	24.564	11	.000	8.33417	7.5874	9.0809
var119	27.889	11	.000	8.33250	7.6749	8.9901
var120	35.065	11	.000	8.33250	7.8095	8.8555
var121	28.231	11	.000	8.33417	7.6844	8.9839
var122	28.362	11	.000	8.33333	7.6866	8.9800
var123	21.850	11	.000	8.33250	7.4932	9.1718
var124	27.764	11	.000	8.33250	7.6719	8.9931
var125	28.194	11	.000	8.33333	7.6828	8.9839
var126	21.680	11	.000	8.33333	7.4873	9.1793
var127	26.037	11	.000	8.33417	7.6297	9.0387
var128	25.076	11	.000	8.33333	7.6019	9.0648

Table I3 (Continued)

One-Sample Test

	Test Value = 0					
					95% Confidence Interval of the Difference	
	t	df	Sig. (2-tailed)	Mean Difference	Lower	Upper
var129	31.358	11	.000	8.33417	7.7492	8.9191
var130	26.166	11	.000	8.33250	7.6316	9.0334
var131	25.094	11	.000	8.33333	7.6024	9.0642
var132	31.332	11	.000	8.33333	7.7479	8.9187
var133	43.350	11	.000	8.33333	7.9102	8.7564
var134	19.570	11	.000	8.33333	7.3961	9.2705
var135	31.761	11	.000	8.33250	7.7551	8.9099
var136	40.546	11	.000	8.33333	7.8810	8.7857
var137	19.732	11	.000	8.33333	7.4038	9.2628
var138	31.515	11	.000	8.33333	7.7513	8.9153
var139	29.499	11	.000	8.33333	7.7116	8.9551
var140	27.619	11	.000	8.33333	7.6692	8.9974
var141	37.331	11	.000	8.33417	7.8428	8.8255
var142	29.226	11	.000	8.33417	7.7065	8.9618
var143	27.071	11	.000	8.33250	7.6550	9.0100
var144	36.845	11	.000	8.33333	7.8355	8.8311
var145	32.395	11	.000	8.33333	7.7671	8.8995
var146	32.522	11	.000	8.33167	7.7678	8.8955
var147	31.904	11	.000	8.33333	7.7584	8.9082
var148	32.113	11	.000	8.33250	7.7614	8.9036
var149	34.123	11	.000	8.33417	7.7966	8.8717
var150	30.724	11	.000	8.33333	7.7364	8.9303
var151	26.945	11	.000	8.33417	7.6534	9.0149
var152	29.802	11	.000	8.33333	7.7179	8.9488
var153	31.583	11	.000	8.33250	7.7518	8.9132
var154	26.814	11	.000	8.33250	7.6485	9.0165
var155	29.609	11	.000	8.33333	7.7139	8.9528
var156	31.390	11	.000	8.33333	7.7490	8.9176
var157	39.147	11	.000	8.33417	7.8656	8.8027
var158	21.426	11	.000	8.33167	7.4758	9.1875
var159	20.464	11	.000	8.33167	7.4356	9.2278
var160	39.544	11	.000	8.33250	7.8687	8.7963

Table I3 (Continued)

One-Sample Test

	Test Value = 0					
					95% Confidence Interval of the Difference	
	t	df	Sig. (2-tailed)	Mean Difference	Lower	Upper
var161	21.622	11	.000	8.33417	7.4858	9.1825
var162	20.532	11	.000	8.33333	7.4400	9.2267
var163	22.327	11	.000	8.33417	7.5126	9.1557
var164	30.011	11	.000	8.33250	7.7214	8.9436
var165	22.756	11	.000	8.33333	7.5273	9.1393
var166	22.394	11	.000	8.33250	7.5135	9.1515
var167	29.688	11	.000	8.33417	7.7163	8.9520
var168	22.982	11	.000	8.33333	7.5352	9.1314
var169	21.597	11	.000	8.33250	7.4833	9.1817
var170	22.284	11	.000	8.33417	7.5110	9.1573
var171	21.124	11	.000	8.33333	7.4651	9.2016
var172	21.727	11	.000	8.33250	7.4884	9.1766
var173	22.210	11	.000	8.33333	7.5075	9.1592
var174	21.117	11	.000	8.33417	7.4655	9.2028
var175	26.748	11	.000	8.33333	7.6476	9.0190
var176	24.923	11	.000	8.33167	7.5959	9.0674
var177	19.179	11	.000	8.33417	7.3777	9.2906
var178	26.189	11	.000	8.33417	7.6338	9.0346
var179	24.950	11	.000	8.33333	7.5982	9.0685
var180	19.160	11	.000	8.33333	7.3760	9.2906
var181	38.352	11	.000	8.33417	7.8559	8.8125
var182	32.238	11	.000	8.33250	7.7636	8.9014
var183	51.784	11	.000	8.33500	7.9807	8.6893
var184	38.312	11	.000	8.33250	7.8538	8.8112
var185	32.393	11	.000	8.33167	7.7656	8.8978
var186	51.477	11	.000	8.33250	7.9762	8.6888
var187	18.701	11	.000	8.33417	7.3533	9.3150
var188	33.740	11	.000	8.33333	7.7897	8.8769
var189	40.579	11	.000	8.33250	7.8806	8.7844
var190	19.082	11	.000	8.33333	7.3721	9.2945
var191	33.740	11	.000	8.33333	7.7897	8.8769
var192	40.468	11	.000	8.33250	7.8793	8.7857

Table I3 (Continued)

One-Sample Test

	Test Value = 0					
					95% Confidence Interval of the Difference	
	t	df	Sig. (2-tailed)	Mean Difference	Lower	Upper
var193	27.660	11	.000	8.33250	7.6695	8.9955
var194	26.835	11	.000	8.33417	7.6506	9.0177
var195	38.594	11	.000	8.33333	7.8581	8.8086
var196	26.827	11	.000	8.33417	7.6504	9.0179
var197	25.645	11	.000	8.33500	7.6196	9.0504
var198	38.594	11	.000	8.33333	7.8581	8.8086
var199	25.262	11	.000	8.33417	7.6081	9.0603
var200	17.019	11	.000	8.33333	7.2556	9.4110
var201	22.440	11	.000	8.33417	7.5167	9.1516
var202	25.478	11	.000	8.33333	7.6134	9.0532
var203	17.080	11	.000	8.33333	7.2594	9.4072
var204	22.588	11	.000	8.33500	7.5228	9.1472
var205	38.339	11	.000	8.33333	7.8549	8.8117
var206	25.965	11	.000	8.33333	7.6270	9.0397
var207	51.911	11	.000	8.33333	7.9800	8.6867
var208	38.635	11	.000	8.33250	7.8578	8.8072
var209	25.969	11	.000	8.33333	7.6271	9.0396
var210	51.055	11	.000	8.33333	7.9741	8.6926
var211	35.848	11	.000	8.33333	7.8217	8.8450
var212	27.892	11	.000	8.33333	7.6757	8.9909
var213	47.154	11	.000	8.33167	7.9428	8.7206
var214	37.290	11	.000	8.33417	7.8423	8.8261
var215	27.438	11	.000	8.33167	7.6633	9.0000
var216	46.763	11	.000	8.33333	7.9411	8.7256
var217	30.524	11	.000	8.33333	7.7325	8.9342
var218	23.751	11	.000	8.33417	7.5618	9.1065
var219	22.867	11	.000	8.33250	7.5305	9.1345
var220	30.840	11	.000	8.33167	7.7371	8.9263
var221	23.680	11	.000	8.33500	7.5603	9.1097
var222	22.884	11	.000	8.33333	7.5318	9.1348
var223	40.888	11	.000	8.33250	7.8840	8.7810
var224	38.615	11	.000	8.33500	7.8599	8.8101

Table I3 (Continued)

One-Sample Test

	Test Value = 0					
					95% Confidence Interval of the Difference	
	t	df	Sig. (2-tailed)	Mean Difference	Lower	Upper
var225	25.073	11	.000	8.33333	7.6018	9.0649
var226	40.336	11	.000	8.33333	7.8786	8.7881
var227	39.355	11	.000	8.33333	7.8673	8.7994
var228	24.993	11	.000	8.33417	7.6002	9.0681
var229	40.825	11	.000	8.33333	7.8841	8.7826
var230	33.532	11	.000	8.33333	7.7863	8.8803
var231	35.763	11	.000	8.33417	7.8212	8.8471
var232	40.072	11	.000	8.33417	7.8764	8.7919
var233	32.666	11	.000	8.33417	7.7726	8.8957
var234	36.364	11	.000	8.33417	7.8297	8.8386
var235	24.210	11	.000	8.33333	7.5757	9.0909
var236	22.169	11	.000	8.33333	7.5060	9.1607
var237	27.203	11	.000	8.33250	7.6583	9.0067
var238	24.658	11	.000	8.33333	7.5895	9.0772
var239	22.043	11	.000	8.33417	7.5020	9.1663
var240	26.372	11	.000	8.33417	7.6386	9.0297
var241	20.931	11	.000	8.33333	7.4571	9.2096
var242	40.324	11	.000	8.33250	7.8777	8.7873
var243	41.910	11	.000	8.33250	7.8949	8.7701
var244	20.579	11	.000	8.33250	7.4413	9.2237
var245	40.106	11	.000	8.33417	7.8768	8.7915
var246	40.936	11	.000	8.33417	7.8861	8.7823
var247	25.518	11	.000	8.33167	7.6130	9.0503
var248	29.823	11	.000	8.33333	7.7183	8.9483
var249	23.374	11	.000	8.33417	7.5494	9.1189
var250	25.518	11	.000	8.33167	7.6130	9.0503
var251	28.944	11	.000	8.33417	7.7004	8.9679
var252	23.607	11	.000	8.33333	7.5564	9.1103
var253	22.364	11	.000	8.33333	7.5132	9.1535
var254	24.506	11	.000	8.33333	7.5849	9.0818
var255	35.988	11	.000	8.33417	7.8245	8.8439
var256	22.465	11	.000	8.33500	7.5184	9.1516

Table I3 (Continued)

One-Sample Test

	Test Value = 0					
					95% Confidence Interval of the Difference	
	t	df	Sig. (2-tailed)	Mean Difference	Lower	Upper
var257	24.525	11	.000	8.33250	7.5847	9.0803
var258	35.942	11	.000	8.33083	7.8207	8.8410
var259	21.661	11	.000	8.33333	7.4866	9.1801
var260	22.999	11	.000	8.33333	7.5358	9.1308
var261	34.765	11	.000	8.33250	7.8050	8.8600
var262	21.978	11	.000	8.33250	7.4980	9.1670
var263	22.478	11	.000	8.33333	7.5173	9.1493
var264	34.712	11	.000	8.33333	7.8049	8.8617
var265	21.519	11	.000	8.33250	7.4802	9.1848
var266	33.244	11	.000	8.33250	7.7808	8.8842
var267	34.153	11	.000	8.33250	7.7955	8.8695
var268	21.682	11	.000	8.33333	7.4874	9.1793
var269	33.304	11	.000	8.33500	7.7842	8.8858
var270	34.491	11	.000	8.33333	7.8015	8.8651
var271	24.052	11	.000	8.33167	7.5692	9.0941
var272	42.904	11	.000	8.33417	7.9066	8.7617
var273	41.690	11	.000	8.33333	7.8934	8.7733
var274	24.111	11	.000	8.33250	7.5719	9.0931
var275	43.671	11	.000	8.33250	7.9126	8.7524
var276	41.212	11	.000	8.33250	7.8875	8.7775
var277	22.287	11	.000	8.33333	7.5103	9.1563
var278	30.068	11	.000	8.33333	7.7233	8.9433
var279	34.834	11	.000	8.33250	7.8060	8.8590
var280	22.085	11	.000	8.33250	7.5021	9.1629
var281	30.057	11	.000	8.33417	7.7239	8.9444
var282	34.937	11	.000	8.33250	7.8076	8.8574
var283	23.962	11	.000	8.33250	7.5671	9.0979
var284	17.046	11	.000	8.33417	7.2580	9.4103
var285	31.918	11	.000	8.33417	7.7595	8.9089
var286	23.940	11	.000	8.33333	7.5672	9.0995
var287	16.966	11	.000	8.33333	7.2522	9.4144
var288	31.682	11	.000	8.33333	7.7544	8.9123

Table I3 (Continued)

One-Sample Test

	Test Value = 0					
					95% Confidence Interval of the Difference	
	t	df	Sig. (2-tailed)	Mean Difference	Lower	Upper
var289	39.747	11	.000	8.33250	7.8711	8.7939
var290	27.504	11	.000	8.33333	7.6665	9.0002
var291	28.634	11	.000	8.33333	7.6928	8.9739
var292	39.887	11	.000	8.33250	7.8727	8.7923
var293	27.807	11	.000	8.33250	7.6730	8.9920
var294	28.759	11	.000	8.33250	7.6948	8.9702
var295	22.939	11	.000	8.33417	7.5345	9.1338
var296	22.213	11	.000	8.33417	7.5084	9.1600
var297	19.560	11	.000	8.33167	7.3942	9.2692
var298	22.670	11	.000	8.33417	7.5250	9.1433
var299	22.297	11	.000	8.33417	7.5115	9.1568
var300	19.614	11	.000	8.33333	7.3982	9.2684
var301	26.003	11	.000	8.33500	7.6295	9.0405
var302	15.586	11	.000	8.33250	7.1558	9.5092
var303	37.260	11	.000	8.33333	7.8411	8.8256
var304	26.026	11	.000	8.33417	7.6294	9.0390
var305	15.201	11	.000	8.33250	7.1260	9.5390
var306	37.095	11	.000	8.33417	7.8397	8.8287
var307	27.809	11	.000	8.33250	7.6730	8.9920
var308	25.584	11	.000	8.33417	7.6172	9.0512
var309	17.911	11	.000	8.33417	7.3100	9.3583
var310	27.338	11	.000	8.33250	7.6617	9.0033
var311	25.702	11	.000	8.33333	7.6197	9.0470
var312	17.906	11	.000	8.33250	7.3083	9.3567
var313	21.751	11	.000	8.33250	7.4893	9.1757
var314	34.728	11	.000	8.33250	7.8044	8.8606
var315	19.285	11	.000	8.33417	7.3830	9.2853
var316	21.864	11	.000	8.33333	7.4945	9.1722
var317	34.883	11	.000	8.33500	7.8091	8.8609
var318	18.893	11	.000	8.33250	7.3618	9.3032
var319	24.006	11	.000	8.33250	7.5685	9.0965
var320	23.113	11	.000	8.33250	7.5390	9.1260

Table I3 (Continued)

One-Sample Test

	Test Value = 0					
					95% Confidence Interval of the Difference	
	t	df	Sig. (2-tailed)	Mean Difference	Lower	Upper
var321	24.846	11	.000	8.33250	7.5944	9.0706
var322	24.147	11	.000	8.33417	7.5745	9.0938
var323	23.205	11	.000	8.33167	7.5414	9.1219
var324	25.456	11	.000	8.33417	7.6136	9.0548
var325	23.214	11	.000	8.33333	7.5432	9.1234
var326	25.631	11	.000	8.33333	7.6177	9.0489
var327	36.113	11	.000	8.33250	7.8247	8.8403
var328	24.152	11	.000	8.33500	7.5754	9.0946
var329	26.560	11	.000	8.33333	7.6428	9.0239
var330	35.779	11	.000	8.33333	7.8207	8.8460
var331	16.738	11	.000	8.33333	7.2375	9.4292
var332	26.010	11	.000	8.33333	7.6282	9.0385
var333	26.985	11	.000	8.33250	7.6529	9.0121
var334	16.692	11	.000	8.33417	7.2353	9.4331
var335	26.243	11	.000	8.33417	7.6352	9.0332
var336	27.388	11	.000	8.33167	7.6621	9.0012
var337	27.766	11	.000	8.33417	7.6735	8.9948
var338	20.420	11	.000	8.33333	7.4351	9.2316
var339	26.043	11	.000	8.33250	7.6283	9.0367
var340	28.179	11	.000	8.33167	7.6809	8.9824
var341	20.336	11	.000	8.33250	7.4307	9.2343
var342	26.212	11	.000	8.33250	7.6328	9.0322

APPENDIX J: COPYRIGHT PERMISSIONS

Below is the permission for the use of materials in Chapter 7.

Barber, Phyllis <PBARBER@nas.edu> Jun 3

to me

Dear Mr. de Pernia,

Since this paper was not accepted for publication in the *Transportation Research Record* series, copyright belongs to the authors.

However, because the authors may have incorporated comments from the TRB peer review into this paper, we ask that as a professional courtesy you acknowledge that the paper was peer-reviewed by TRB and presented at the TRB Annual Meeting, Washington, D.C., January 2015.

Thank you for your request. Please let me know if you have any questions.

Sincerely,

Phyllis Barber-Gray
Publishing Services Manager
Transportation Research Board

Phyllis Barber
Transportation Research Board
Publications Office
202 334-2972 phone
202 334-3495 fax
pbarber@nas.edu

Below is the permission for the use of materials in Chapter 3, 4, and 5.

Musselman, Jim 1:03 PM (25 minutes ago)

to me, Tanya, Gunaratne

Yolibeth,

Yes, you have our permission to use any of the sections in our report in your Dissertation.

Good luck!

James A. Musselman, P.E.
State Bituminous Materials Engineer
Florida Department of Transportation
Office: (352) 955-2905
Cell: (352) 317-5989

From: Yolibeth Mejias De pernia [mailto:mejiasde@mail.usf.edu]
Sent: Thursday, May 28, 2015 11:39 AM
To: Nash, Tanya; Musselman, Jim
Cc: Gunaratne
Subject: Copyright permission

Hi,

I am including parts of the final reports for the BDV25, TWO # 820-1 and TWO # 820-2 in my PhD dissertation and I will like to have a copyright permission from FDOT as the sections on the Dissertation are identical as the report.

Thanks,
Yolibeth

Yolibeth Mejias de Pernia., MSc. Eng., P.Eng
Civil Engineering PhD. Candidate
University of South Florida
Yolibeth Mejias de Pernia., MSc. Eng., P.Eng
Civil Engineering PhD. Candidate
University of South Florida